

INTERFACIAL TENSIONS IN CARBON DIOXIDE +
HYDROCARBON SYSTEMS: EXPERIMENTAL
DATA AND CORRELATIONS

By

KENNETH B. DICKSON

Bachelor of Science in Chemical Engineering

New Mexico State University

Las Cruces, New Mexico

1978

Submitted to the Faculty of the Graduate College
of the Oklahoma State University
in partial fulfillment of the requirements
for the Degree of
MASTER OF SCIENCE
May, 1987

Thesis
1987
D5531
cop. 2



INTERFACIAL TENSIONS IN CARBON DIOXIDE +
HYDROCARBON SYSTEMS: EXPERIMENTAL
DATA AND CORRELATIONS

Thesis Approved:

Robert Robinson Jr.

Thesis Adviser

Lutz Weber

Albert H. Johannes

Norman N. Durham

Dean of the Graduate College

PREFACE

Interfacial tensions (IFTs), equilibrium phase compositions, and phase densities have been measured for the CO₂ + n-tetradecane system at 160°F and pressures from approximately 1000 psia to the critical point. The experimental data were smoothed using a multi-parameter function. The experimental data for the CO₂ + n-tetradecane plus four previously available binary systems containing CO₂ (CO₂ + n-butane, n-decane, benzene, and cyclohexane) were used to evaluate the frameworks and predictive capabilities of several IFT correlations. The Weinaug-Katz and Lee-Chien IFT correlations were evaluated by optimizing the parachors and critical exponent from regressions of the experimental data. The Hugill-Van Welsenens IFT correlation was evaluated in a similar manner except an additional parameter (binary interaction parameter) was determined for each binary system. Several parachor correlations were evaluated including: (1) Lee-Chien, (2) Hugill-Van Welsenens, and (3) a parachor correlation developed during this work.

To simply say thank you is not enough, but it is probably the most genuine and forthright expression of my gratitude for the guidance, assistance, and education given to me by Professor R. L. Robinson, Jr. The debt owed to Dr. Robinson can only be repaid by my diligent and dedicated work in my future endeavors in chemical engineering or in whatever career path I undertake.

Additional gratitude is due to my fellow coworkers on the IFT project, including Dr. Khaled A. M. Gasem, Peter B. Dulcamara, Jr.,

Jeff A. Graham, Anthony G. Lee, and Steven C. Nichols. I would like to express special thanks to Dr. Gasem for his invaluable instruction on the computer and his assistance in learning the experimental apparatus.

Finally, I would like to express my sincere appreciation to Dr. Billy L. Crynes for the financial support he secured for me during my graduate studies, especially the Dow Foundation Scholarship.

TABLE OF CONTENTS

Chapter	Page
I. INTRODUCTION	1
II. LITERATURE REVIEW.	3
IFT Correlations.	3
Previous Experimental Data.	10
III. EXPERIMENTAL APPARATUS AND OPERATING PROCEDURE	12
General Description of Apparatus.	12
IFT Cell.	14
Temperature Controlled Oven	15
Flow Patterns in the Apparatus.	17
Experimental Data Acquisition	17
Chemicals	25
IV. EXPERIMENTAL RESULTS AND SMOOTHED DATA	26
Experimental Data for CO ₂ + n-Tetradecane	26
Comparison of Experimental Results with Other Sources	50
Power Law (Scaling Behavior) Fit to Experimental Data.	53
V. INTERFACIAL TENSION CORRELATIONS	58
Weinaug-Katz Correlation Evaluation	60
Hugill-Van Welsenens Correlation Evaluation.	89
Lee-Chien Correlation Evaluation.	96
Parachor Correlations	103
Lee-Chien Parachor Correlation.	103
Hugill-Van Welsenens Parachor Correlation.	103
Parachor Correlations From The Present Work	104
Comparison of Predicted Parachors	104
IFT Correlation Predictions	108
VI. CONCLUSIONS AND RECOMMENDATIONS.	117
Conclusions	117
Recommendations	119
REFERENCES	120
APPENDICES	124

APPENDIX A - EXPERIMENTAL DATA	125
APPENDIX B - REDUCED PARACHORS FROM EQUATION E.15 FOR K = 3.55 AND K = 3.91	136
APPENDIX C - COMPARISON OF IFTS PREDICTED BY CORRELATIONS STUDIED IN THIS WORK.	141
APPENDIX D - NATIONAL BUREAU OF STANDARDS (NBS) DATA SET . .	177
APPENDIX E - PARACHOR CORRELATION FROM THE PRESENT WORK. . .	179

LIST OF TABLES

Table	Page
I. Available Sources for IFT, Phase Composition and Phase Density Data for CO ₂ + Hydrocarbon Systems	11
II. Phase Equilibria and Interfacial Tensions for CO ₂ + n-Tetradecane at 344.3 K (160°F)	27
III. Smoothed Phase Equilibria and Interfacial Tensions for CO ₂ + n-Tetradecane at 344.3 K (160°F)	32
IV. Comparisons of Experimental and Calculated (Equation 4.3) Phase Compositions for CO ₂ + n-Tetradecane at 344.3 K (160°F).	38
V. Comparisons of Experimental and Calculated (Equation 4.3) Phase Densities for CO ₂ + n-Tetradecane at 344.3 K (160°F).	39
VI. Comparisons of Experimental and Calculated (Equation 4.4) (IFT/Density Difference) for CO ₂ + n-Tetradecane at 344.3 (160°F)	40
VII. Parameters Used to Generate Smoothed Properties in Tables IV through VI.	49
VIII. Comparisons of Phase Density Measurements with Other Sources for CO ₂ + n-Tetradecane at 344.3 K (160°F)	51
IX. Comparisons of Liquid Phase Composition Measurements with Other Sources for CO ₂ + n-Tetradecane at 344.3 K (160°F).	53
X. Multicomponent IFT Correlation Parameters.	59
XI. IFT Correlation Parameters Optimized in Regression Analyses	61
XII. Evaluation of Weinaug-Katz Correlation for CO ₂ + n-Butane at 115, 160 and 220°F	65
XIII. Evaluation of Weinaug-Katz Correlation for CO ₂ + n-Decane at 160 and 220°F.	70
XIV. Evaluation of Weinaug-Katz Correlation for CO ₂ + n-Tetradecane at 160°F	74

Table	Page
XV. Evaluation of Weinaug-Katz Correlation for CO ₂ + Benzene and CO ₂ + Cyclohexane at 160°F	79
XVI. Evaluation of Weinaug-Katz Correlation for All Data.	87
XVII. Evaluation of Hugill-Van Welsenens Correlation for CO ₂ + n-Butane and CO ₂ + n-Decane.	91
XVIII. Evaluation of Hugill-Van Welsenens Correlation for CO ₂ + n-Tetradecane, CO ₂ + Benzene, and CO ₂ + Cyclohexane.	93
XIX. Evaluation of Hugill-Van Welsenens Correlation for All Data	94
XX. Evaluation of Lee-Chien Correlation for CO ₂ + n-Butane, CO ₂ + n-Decane, CO ₂ + n-tetradecane, CO ₂ + Benzene, and CO ₂ + Cyclohexane.	98
XXI. Evaluation of Lee-Chien Correlation for All Data	100
XXII. Comparison of Regressed Parachors.	101
XXIII. Comparison of IFT Correlations Accuracies.	101
XXIV. Comparison of Predicted Pure Component Parachors	106
XXV. Statistical Comparison of Predicted Parachors to W-K Regressed Parachors.	107
XXVI. Structural Contribution Parachors.	108
XXVII. Comparison of Interfacial Tensions Predicted by the Lee-Chien Correlation: Methane-Propane.	110
XXVIII. Comparison of Interfacial Tensions Predicted by the Lee-Chien Correlation: Methane-Pentane, Methane-Nonane, and Methane-Decane	112
XXIX. Predicted IFTs (W-K Model) for CO ₂ /n-Butane/n-Decane at 344.3 K (160°F).	114
XXX. Phase Equilibria and Interfacial Tensions for CO ₂ + n-Butane at 319.3 K (115°F).	126
XXXI. Phase Equilibria and Interfacial Tensions for CO ₂ + n-Butane at 344.3 K (160°F).	127
XXXII. Phase Equilibria and Interfacial Tensions for CO ₂ + n-Butane at 377.6 K (220°F).	128

Table	Page
XXXIII. Phase Equilibria and Interfacial Tensions for CO ₂ + n-Decane at 344.3 K (160°F)	129
XXXIV. Phase Equilibria and Interfacial Tensions for CO ₂ + n-Decane at 377.6 K (220°F)	130
XXXV. Phase Equilibria and Interfacial Tensions for CO ₂ + n-Tetradecane at 344.3 K (160°F)	132
XXXVI. Phase Equilibria and Interfacial Tensions for CO ₂ + Benzene at 344.3 K (160°F)	133
XXXVII. Phase Equilibria and Interfacial Tensions for CO ₂ + Cyclohexane at 344.3 K (160°F)	134
XXXVIII. Phase Equilibria and Interfacial Tensions for a 90% CO ₂ /6% n-Butane/4% n-Decane Mixture at 344.3 K (160°F)*	135
XXXIX. Present Work Reduced Parachors with k = 3.55	137
XL. Present Work Reduced Parachors with k = 3.91	138
XL I. Comparison of Predicted IFTs For CO ₂ + n-Butane at 319.3 K (115°F), k = 3.55, "This Work" Parachor Equation E.17.	144
XL II. Comparison of Predicted IFTs For CO ₂ + n-Butane at 344.3 K (160°F), k = 3.55, "This Work" Parachor Equation E.17.	145
XL III. Comparison of Predicted IFTs For CO ₂ + n-Butane at 377.6 K (220°F), k = 3.55, "This Work" Parachor Equation E.17.	146
XL IV. Comparison of Predicted IFTs For CO ₂ + n-Decane at 344.3 K (160°F), k = 3.55, "This Work" Parachor Equation E.17.	147
XL V. Comparison of Predicted IFTs For CO ₂ + n-Decane at 377.6 K (220°F), k = 3.55, "This Work" Parachor Equation E.17.	148
XL VI. Comparison of Predicted IFTs For CO ₂ + n-Tetradecane at 344.3 K (160°F), k = 3.55, "This Work" Parachor Equation E.17.	149
XL VII. Comparison of Predicted IFTs For CO ₂ + Benzene at 344.3 K (160°F), k = 3.55, "This Work" Parachor Equation E.17.	150

Table	Page
XLVIII. Comparison of Predicted IFTs For CO ₂ + Cyclohexane at 344.3 K (160°F), k = 3.55, "This Work" Parachor Equation E.17.	151
IL. Comparison of Predicted IFTs For CO ₂ + n-Butane at 319.3 K (115°F), k = 3.55, "This Work" Parachor Equation E.18.	152
L. Comparison of Predicted IFTs For CO ₂ + n-Butane at 344.3 K (160°F), k = 3.55, "This Work" Parachor Equation E.18.	153
LI. Comparison of Predicted IFTs For CO ₂ + n-Butane at 377.6 K (220°F), k = 3.55, "This Work" Parachor Equation E.18.	154
LII. Comparison of Predicted IFTs For CO ₂ + n-Decane at 344.3 K (160°F), k = 3.55, "This Work" Parachor Equation E.18.	155
LIII. Comparison of Predicted IFTs For CO ₂ + n-Decane at 377.6 K (220°F), k = 3.55, "This Work" Parachor Equation E.18.	156
LIV. Comparison of Predicted IFTs For CO ₂ + n-Tetradecane at 344.3 K (160°F), k = 3.55, "This Work" Parachor Equation E.18.	157
LV. Comparison of Predicted IFTs For CO ₂ + Benzene at 344.3 K (160°F), k = 3.55, "This Work" Parachor Equation E.18.	158
LVI. Comparison of Predicted IFTs For CO ₂ + Cyclohexane at 344.3 K (160°F), k = 3.55, "This Work" Parachor Equation E.18.	159
LVII. Comparison of Predicted IFTs For CO ₂ + n-Butane at 319.3 K (115°F), k = 3.91, "This Work" Parachor Equation E.19.	160
LVIII. Comparison of Predicted IFTs For CO ₂ + n-Butane at 344.3 K (160°F), k = 3.91, "This Work" Parachor Equation E.19.	161
LIX. Comparison of Predicted IFTs For CO ₂ + n-Butane at 377.6 K (220°F), k = 3.91, "This Work" Parachor Equation E.19.	162
LX. Comparison of Predicted IFTs For CO ₂ + n-Decane at 344.3 K (160°F), k = 3.91, "This Work" Parachor Equation E.19.	163

Table	Page
LXI. Comparison of Predicted IFTs For CO ₂ + n-Decane at 377.6 K (220°F), k = 3.91, "This Work" Parachor Equation E.19.	164
LXII. Comparison of Predicted IFTs For CO ₂ + n-Tetradecane at 344.3 K (160°F), k = 3.91, "This Work" Parachor Equation E.19.	165
LXIII. Comparison of Predicted IFTs For CO ₂ + Benzene at 344.3 K (160°F), k = 3.91, "This Work" Parachor Equation E.19.	166
LXIV. Comparison of Predicted IFTs For CO ₂ + Cyclohexane at 344.3 K (160°F), k = 3.91, "This Work" Parachor Equation E.19.	167
LXV. Comparison of Predicted IFTs For CO ₂ + n-Butane at 319.3 K (115°F), k = 3.91, "This Work" Parachor Equation E.20.	168
LXVI. Comparison of Predicted IFTs For CO ₂ + n-Butane at 344.3 K (160°F), k = 3.91, "This Work" Parachor Equation E.20.	169
LXVII. Comparison of Predicted IFTs For CO ₂ + n-Butane at 377.6 K (220°F), k = 3.91, "This Work" Parachor Equation E.20.	170
LXVIII. Comparison of Predicted IFTs For CO ₂ + n-Decane at 344.3 K (160°F), k = 3.91, "This Work" Parachor Equation E.20.	171
LXIX. Comparison of Predicted IFTs For CO ₂ + n-Decane at 377.6 K (220°F), k = 3.91, "This Work" Parachor Equation E.20.	172
LXX. Comparison of Predicted IFTs For CO ₂ + n-Tetradecane at 344.3 K (160°F), k = 3.91, "This Work" Parachor Equation E.20.	173
LXXI. Comparison of Predicted IFTs For CO ₂ + Benzene at 344.3 K (160°F), k = 3.91, "This Work" Parachor Equation E.20.	174
LXXII. Comparison of Predicted IFTs For CO ₂ + Cyclohexane at 344.3 K (160°F), k = 3.91, "This Work" Parachor Equation E.20.	175
LXXIII. Comparison of the Accuracy of Predicted IFTs Based on All Data Points.	176

Table	Page
LXXIV. Physical Property Data Set From the National Bureau of Standards.	178
LXXV. System Independent Constants for Equations E.3, E.4, E.6, E.7, E.9, E.10, and E.12	181

LIST OF FIGURES

Figure	Page
1. Schematic Diagram of Experimental Apparatus	13
2. Liquid Circulation Pattern in Experimental Apparatus.	18
3. Vapor Circulation Pattern in Experimental Apparatus	19
4. Measurements on Pendant Drop for IFT Calculation (Equation 3.2).	24
5. Effect of Pressure on Phase Density for CO ₂ + n-Tetradecane at 344.3 K (160°F).	29
6. Effect of Pressure on Phase Composition for CO ₂ + n-Tetradecane at 344.3 K (160°F).	30
7. Interfacial Tension - Phase Density Difference Ratios for CO ₂ + n-Tetradecane at 344.3 K (160°F).	31
8. Smoothing Function Fit to Composition Data (Weighted Deviations) for CO ₂ + n-Tetradecane at 344.3 K (160°F) . . .	41
9. Smoothing Function Fit to Density Data (Weighted Deviations) for CO ₂ + n-Tetradecane at 344.3 K (160°F).	42
10. Smoothing Function Fit to Pendant Drop Data (Weighted Deviations) for CO ₂ + n-Tetradecane at 344.3 K (160°F). . . .	43
11. Smoothing Function Fit to Composition Data (Deviations) for CO ₂ + n-Tetradecane at 344.3 K (160°F).	44
12. Smoothing Function Fit to Density Data (Deviations) for CO ₂ + n-Tetradecane at 344.3 K (160°F).	45
13. Smoothing Function Fit to Pendant Drop Data (Deviations) for CO ₂ + n-Tetradecane at 344.3 K (160°F).	46
14. Smoothing Function Fit to Density Data (Percent Deviations) for CO ₂ + n-Tetradecane at 344.3 K (160°F).	47
15. Smoothing Function Fit to Pendant Drop Data (Percent Deviations) for CO ₂ + n-Tetradecane at 344.3 K (160°F).	48
16. Comparison of Phase Density Data for CO ₂ + n-Tetradecane at 344.3 K (160°F).	52

Figure	Page
17. Comparison of Phase Composition Data for CO ₂ + n-Tetradecane at 344.3 K (160°F)	54
18. Power Law Fit to Pendant Drop Data for CO ₂ + n-Tetradecane at 344.3 K (160°F)	56
19. Power Law Fit to Smoothed Density Data for CO ₂ + n-Tetradecane at 344.3 K (160°F)	57
20. Comparison of Experimental IFTs to W-K Model for CO ₂ + n-Butane at 115, 160, and 220°F	66
21. Comparison of Experimental IFTs to W-K Model, (Percent Deviations) for CO ₂ + n-Butane at 115, 160, and 220°F	67
22. Comparison of Experimental IFTs to W-K Model, (Weighted Deviations) for CO ₂ + n-Butane at 115, 160, and 220°F	68
23. Comparison of Experimental IFTs to W-K Model for CO ₂ + n-Decane at 160 and 220°F	71
24. Comparison of Experimental IFTs to W-K Model, (Percent Deviations) for CO ₂ + n-Decane at 160 and 220°F	72
25. Comparison of Experimental IFTs to W-K Model, (Weighted Deviations) for CO ₂ + n-Decane at 160 and 220°F	73
26. Comparison of Experimental IFTs to W-K Model for CO ₂ + n-Tetradecane at 160°F	76
27. Comparison of Experimental IFTs to W-K Model, (Percent Deviations) for CO ₂ + n-Tetradecane at 160°F	77
28. Comparison of Experimental IFTs to W-K Model, (Weighted Deviations) for CO ₂ + n-Tetradecane at 160°F	78
29. Comparison of Experimental IFTs to W-K Model for CO ₂ + Benzene at 160°F	80
30. Comparison of Experimental IFTs to W-K Model, (Percent Deviations) for CO ₂ + Benzene at 160°F	81
31. Comparison of Experimental IFTs to W-K Model, (Weighted Deviations) for CO ₂ + Benzene at 160°F	82
32. Comparison of Experimental IFTs to W-K Model for CO ₂ + Cyclohexane at 160°F	84
33. Comparison of Experimental IFTs to W-K Model, (Percent Deviations) for CO ₂ + Cyclohexane at 160°F	85

Figure	Page
34. Comparison of Experimental IFTs to W-K Model, (Weighted Deviations) for CO ₂ + Cyclohexane at 160°F	86
35. Comparison of Experimental IFTs to W-K Model for CO ₂ /n-Butane/n-Decane at 160°F	116

CHAPTER I

INTRODUCTION

Enhanced Oil Recovery (EOR) refers to the processes to recover oil after all primary or secondary operations, such as water flooding, have been completed. CO₂ miscible flooding on a large scale is a relatively recent EOR technique. The technique of flooding a reservoir with CO₂ is sufficiently promising that both laboratory and field studies are being conducted. The laboratory studies are devised to discover the exact mechanisms by which CO₂ flooding increases oil recovery, while the field studies are designed to assess the applicability under actual operating conditions.

The various mechanisms by which CO₂ flooding can act include: (1) solution gas drive, (2) hydrocarbon vaporization, (3) miscible CO₂ drive, and (4) immiscible CO₂ drive (43). Immiscible CO₂ flooding is not as well understood as the other methods. In immiscible displacements, the efficiency of the recovery process can be affected by the interfacial tension (IFT) between the CO₂ and the reservoir fluids (44). In order to model the IFT of CO₂ + reservoir fluid systems, predictive correlations are needed.

In this work, several IFT correlations were evaluated including: (1) Weinaug-Katz (11), (2) Hugill-Van Welsenes (13), (3) Lee-Chien (29), and (4) an IFT correlation developed during this work. (These correlations are described in detail in Chapter II and V). To evaluate

the various correlations, accurate experimental data are needed. IFT data on CO₂ + hydrocarbon systems are extremely scarce; therefore, one of the major objectives of this work was to obtain additional IFT data, along with equilibrium phase densities and compositions, on CO₂ + hydrocarbon systems. Experimental data were obtained for the binary system CO₂ + n-tetradecane.

CHAPTER II

LITERATURE REVIEW

A literature review was made to reexamine previous work on interfacial tension (IFT) correlations and experimental IFT data for mixtures. A brief review of previous interfacial tension correlations, starting with van der Waals work and leading to the current efforts, is given. The majority of the attention is focused on work that leads to IFT correlations for mixtures. A survey of experimental IFT data for CO₂ + hydrocarbon systems is also included.

IFT Correlations

J. D. van der Waals (1) suggested two correlations for the surface tension of pure substances as functions of critical constants and reduced temperature. Surface tension is a measure of the specific free energy between two phases having the same composition (e.g., between a pure liquid and its vapor) (36). Interfacial tension is a measure of the surface free energy between phases having different composition (e.g., liquid-liquid and gas-liquid interfaces of multicomponent systems) (36). Hereafter, surface tension will be referred to as IFT since mixtures will be the major focus of this work. The van der Waals' equations may be written as:

$$\gamma = K_1 T_c V_c^{-2/3} (1 - Tr)^n \quad (2.1)$$

$$\gamma = K_2 T_c^{1/3} P_c^{2/3} (1 - Tr)^n \quad (2.2)$$

γ = interfacial tension

K_1, K_2, n = universal constants

T_c, V_c, P_c = critical temperature, volume, pressure

Tr = reduced temperature (T/T_c)

The van der Waals correlation was rewritten by Sugden (2) as

$$\gamma = \gamma_\theta (1 - Tr)^{1.20} \quad (2.3)$$

where

$$\gamma_\theta = K_1 T_c V_c^{-2/3} = K_2 T_c^{1/3} P_c^{2/3}$$

Ferguson (3) derived the following correlation in 1922:

$$\gamma^{1/4} = C \Delta\rho \quad (2.4)$$

C = a constant over a large temperature range

$\Delta\rho$ = density difference ($\rho^L - \rho^V$), gm/cc

The same equation was reported in 1923 by Macleod (4) on a strictly empirical basis. Macleod states, "The magnitude of the surface tension of a liquid is a function of the distance between the molecules and is therefore dependent on the density."

When both sides of equation 2.4 are multiplied by the molecular weight, the widely recognized correlation for the Parachor (5) results:

$$[P] = M\gamma^{1/4}/\Delta\rho \quad (2.5)$$

[P] = parachor

M = molecular weight

$\Delta\rho = (\rho^L - \rho^V)$, gm/cc

The parachor is an additive and constitutive secondary physical property of organic and inorganic compounds. Studies have shown (5, 6) that the parachor is essentially independent of temperature, although a small temperature dependence can be observed over a wide temperature range (7). There have been many correlations for predicting the parachor (8, 9, 10), including one which will be presented in this work. The parachor is important in the present work because it is the fundamental building block for the Weinaug-Katz IFT correlation for mixtures.

In 1943, Weinaug and Katz (11) presented the following correlation for the IFT of mixtures which can be viewed as an empirical extension of Equation 2.5 to mixtures:

$$\begin{aligned} \gamma^{1/4} = & [P]_1 (\rho^L x_1 - \rho^V y_1) + \\ & [P]_2 (\rho^L x_2 - \rho^V y_2) + \dots \end{aligned} \quad (2.6)$$

Equation 2.6 can be rewritten in a more general form as:

$$\gamma^{1/4} = \sum_i \{ [P]_i (\rho^L x_i - \rho^V y_i) \} \quad (2.7)$$

where

$[P]_i$ = parachor of component i

ρ^L, ρ^V = liquid and vapor molar densities, gm-moles/cc

x_i, y_i = liquid and vapor mole fractions of component i

Equation 2.7 expresses the interfacial tension to the one-fourth power as the summation over all components of the parachor of the component multiplied by the difference in the molar concentrations of the component in the liquid and vapor phases.

The Weinaug-Katz (W-K) correlation was originally developed with an exponent of 1/4, but other exponents have been suggested. Hough and Warren (12) found that an exponent of 1/3.667 gave better results when comparing calculated and experimental IFTs. Porteous (19) proposed the following modification of the W-K correlation:

$$\gamma = \left[\sum_i \epsilon_i \{ [P]_i | \rho^L x_i - \rho^V y_i | \}^{k_i/k} \right]^k \quad (2.8)$$

where

$$\begin{aligned} \epsilon_i &= +1 \text{ if } (\rho^L x_i - \rho^V y_i) > 0 \\ &= -1 \text{ if } (\rho^L x_i - \rho^V y_i) < 0 \\ k &= \text{constant} \end{aligned}$$

The k_i and $[P]_i$ values are determined by fitting pure component data "i" to a modified Macleod-Sugden equation

$$\gamma_i = \{ [P]_i (\rho^L - \rho^V) \}^{k_i} \quad (2.9)$$

Porteous reported values of k_i for several compounds, ranging from 3.6 to 4.4 from fits to pure alkane IFT data.

Recently, Hugill and Van Welsenes (13) proposed a modification to the W-K correlation which incorporates adjustable binary interaction

parameters in the parachor "mixing rules". The W-K correlation may be rewritten as follows:

$$\gamma^{1/4} = \rho^L \left(\sum_i x_i [P]_i \right) - \rho^V \left(\sum_i y_i [P]_i \right) \quad (2.10)$$

$$\gamma^{1/4} = \rho^L [P]_L - \rho^V [P]_V \quad (2.11)$$

where

$$[P]_{L,V} = \sum_i z_i [P]_i \quad (2.12)$$

z_i = mole fraction in liquid ($z=x$) or vapor ($z=y$)

Hugill and Van Welsenens (H-VW) proposed that the parachors $[P]_L$ and $[P]_V$ of the liquid and vapor phases be determined by the following quadratic mixing rules:

$$[P]_{L,V} = \sum_i \sum_j z_i z_j [P]_{ij} \quad (2.13)$$

where

$$[P]_{ij} = 1/2 ([P]_i + [P]_j) \lambda_{ij} \quad (2.14)$$

λ_{ij} = binary interaction parameter where $\lambda_{ij} = \lambda_{ji}$ and $\lambda_{ii} = 1$

If all λ_{ij} are taken as 1, Equation 2.11 reduces to the original W-K correlation. Hugill and Van Welsenens found that the binary interaction parameter, λ_{ij} , exhibits a temperature dependence, but this dependence appears to be linear. Hugill and Van Welsenens also presented a new correlation based on the acentric factor for predicting pure component

parachors; however, their correlation was presented only in graphical form. An analytical representation of their graphical results is presented in Chapter V.

Another multicomponent interfacial tension correlation based on scaling theory was presented in 1984 by Lee and Chien (29). Their correlation contained two major features: (1) a method to predict pure component parachors in the framework of corresponding states and (2) a correlation for predicting IFTs of mixtures based on "mixed" parachors. Lee and Chien's correlation incorporates the same framework as Equation 2.11 to determine the IFT of multicomponent systems,

$$\gamma^{1/k} = \rho^L [P]_L - \rho^V [P]_V \quad (2.15)$$

k = exponent set by "scaling theory"; $k = 3.91$

but differs from W-K and H-VW in the method used to determine the mixed liquid and vapor parachors ($[P]_L$, $[P]_V$) and in the exponent to which the IFT is raised. Lee and Chien proposed the following correlation for the pure component parachor:

$$[P]_i = A_{ci}^{\beta/\theta} v_{ci}/B_i \quad (2.16)$$

where

$$A_{ci} = P_{ci}^{2/3} T_{ci}^{1/3} (0.133 \alpha_{ci} - 0.281)$$

$$\alpha_{ci} = 0.9076 (1 + (Tbr_i \ln P_{ci}) / (1 - Tbr_i))$$

Tbr_i = reduced boiling-point temperature

$$\beta = 5/16, \theta = 11/9$$

V_{ci} = critical volume

B_i = component specific parameter of the correlation

Using the principle of corresponding states, Lee and Chien extended Equation 2.16 to mixtures utilizing the following equations:

$$[P]_{L,V} = A_{cL,V}^{(\beta/\theta)} V_{cL,V}/B_{L,V} \quad (2.17)$$

where

$$A_{cL,V} = P_{cL,V}^{2/3} T_{cL,V}^{1/3} (0.133 \alpha_{cL,V} - 0.281)$$

$$P_{cL,V} = \sum_i z_i P_{ci}$$

$$T_{cL,V} = \sum_i z_i T_{ci}$$

$$\alpha_{cL,V} = \sum_i z_i \alpha_{ci}$$

$$V_{cL,V} = \sum_i z_i V_{ci}$$

$$B_{L,V} = \sum_i z_i B_i$$

z_i = mole fraction in liquid ($z=x$) or vapor ($z=y$)

L,V - refer to either the liquid (L) or vapor (V) phase

Equation 2.17 gives the "mixed" liquid and vapor parachors based on linear mixing rules for V_{ci} , B_i , P_{ci} , T_{ci} , and α_{ci} . The mixing parachors ($[P]_L$, $[P]_V$) are then used in Equation 2.15 to calculate the IFT of the mixture.

Sahimi, Davis, and Scriven (14) have proposed a much more theoretically-based method for calculating the IFT of multicomponent systems based on the gradient theory of fluid interfaces (GTFI). The inputs to the theory include the equation of state (EOS) of homogeneous fluid and the influence parameters of inhomogeneous fluid. Gupta and Robinson

(47) found the GTFI model, in combination with a classical EOS, predicts "classical" scaling behavior in the near-critical region for both pure substances and mixtures. This scaling behavior is in conflict with experimentally observed IFTs for mixtures in the near critical, low IFT region. However, the GTFI model does a good job at high IFTs.

The IFT correlations which will be studied further in this work are the W-K, H-VW, and L-C correlations. These correlations were chosen because they demonstrated their suitability in previous tests on hydrocarbon systems and their ease of application. The input variables required for these correlations are obtainable through familiar sources, (e.g., EOS, established data bases). The simple frameworks of the correlations are well suited for computer applications. The GTFI model was not studied because of its complexity and improper scaling at low IFTs.

Previous Experimental Data

A literature survey for experimental data concentrated on CO_2 + hydrocarbon systems. Since the main area of interest is the interfacial tension of CO_2 + hydrocarbon systems, only those systems with experimental data on interfacial tension plus phase composition and density have been reported. There are additional data on the phase compositions and densities of other CO_2 + hydrocarbon systems (e.g., CO_2 + propane), but since no IFT data are available, they will not be considered. Very limited interfacial tension data are available, especially data for which phase density and phase composition data are also available. Except for the work of Simon, Rosman, and Zana (39), no studies other than those performed at Oklahoma State University have

obtained phase density and phase composition data in the same experiment as the interfacial tension data. The table below lists the data available and their references.

TABLE I
AVAILABLE SOURCES FOR IFT, PHASE COMPOSITION AND PHASE
DENSITY DATA FOR CO₂ + HYDROCARBON SYSTEMS

System	Reference Number	
	IFT	Phase Composition and Density
CO ₂ + butane	38,15	40,15
CO ₂ + n-decane	26	26
CO ₂ + n-tetradecane	28	28
CO ₂ + cyclohexane	34	34
CO ₂ + benzene	35	35
CO ₂ /n-butane/n-decane	33	33
CO ₂ + recombined reservoir oil	37,39,41,42	37,39,41,42

As the table above shows, only two studies (CO₂ + n-butane and CO₂ + reservoir oil), other than the Oklahoma State University data, have been presented for CO₂ + hydrocarbon systems.

CHAPTER III

EXPERIMENTAL APPARATUS AND OPERATING PROCEDURE

The experimental equipment used in this study was assembled and constructed by Dr. J. C. Hsu under the guidance of Professor R. L. Robinson (15, 26, 28). It has undergone several modifications by Drs. N. Nagarajan and K. A. M. Gasem. The experimental facility was designed for the measurement of interfacial tensions (IFTs), equilibrium phase compositions, and phase densities in multicomponent systems at reservoir conditions (to 3000 psia and 300°F). The specific emphasis of the present work deals with CO₂ + n-tetradecane, but other binary and ternary systems of light solute gases and hydrocarbon solvents have been studied and will be studied in the future. In the present work, the apparatus was utilized as originally constructed except for the following changes: (1) a second vibrating U-tube densitometer was installed so separate measurements of vapor and liquid densities could be obtained and (2) several needles in the IFT cell were replaced with smaller diameter wires for better measurement of low IFTs.

General Description of Apparatus

The experimental apparatus is illustrated in Figure 1. The individual pieces of equipment (including model numbers and manufacturers) in the apparatus were detailed by Nagarajan and Robinson (15, 48). The apparatus is a semi-automatic facility utilizing a computer programmed gas chromatograph (GC) for phase compositions,

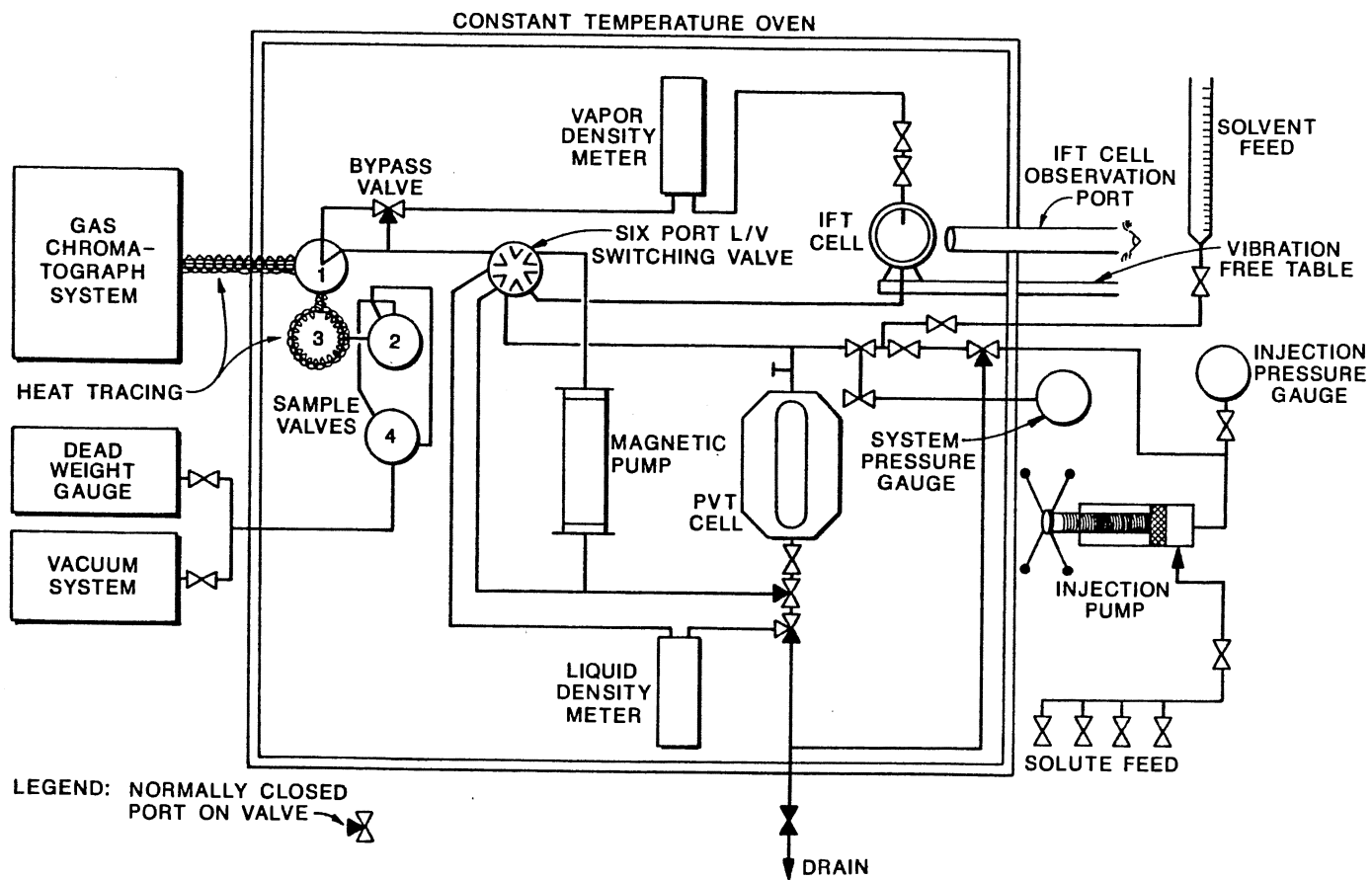


Figure 1. Schematic Diagram of Experimental Apparatus

vibrating U-tube densitometers for continuous on-line density measurements and a pendant drop IFT cell for direct measurement of the IFT to density difference ratio, $\gamma/\Delta\rho$.

The pendant drop method is an absolute method; that is, it has been subjected to a complete mathematical analysis which shows that the $\gamma/\Delta\rho$ value can be calculated directly from measurements of the pendant drop dimensions. Thus, pendant drop measurements are free of any empirical correction or adjustment ("calibrations") and are directly convertible by analytical means to interfacial tension values. The pendant drop method is adaptable to measurements under high pressures and wide ranges of temperature. In addition, the photograph of the drop provides a permanent record of the data that can be referred to at any future time.

IFT Cell

The IFT cell used in the present work is based on Jennings' (16) design and was fabricated by Temco, Inc. of Tulsa. The cell utilizes the pendant drop technique described by Bashforth and Adams (17) and Jennings (18). The cell consists of a stainless steel containment vessel with high pressure viewing windows on both ends of the horizontal cylindrical vessel. In the middle of the cell is a revolving turret with five needles and wires projecting in a pentagonal manner toward the center of the turret. The needles range in size from 0.0185 inches to 0.0035 inches O.D. The turret can be rotated in the cell under operating conditions, enabling an operator to position the desired needle at the top of the cell, which aligns the needle with the inlet flow line. The ability to select different O.D. needles allows the operator to obtain $\gamma/\Delta\rho$ data over a wide range. As the critical state

of the system is approached, the IFT value decreases, and a smaller O.D. needle is required to sustain a pendant drop. The pendant drop method permits IFT measurements from approximately 20 to 0.005 mN/m.

Temperature Controlled Oven

To assure precise temperature control for the required constant temperature equilibrium condition, the main equipment items were housed in a commercial air oven. The original oven temperature controller was replaced by Precision Scientific Thermotrol temperature controller to maintain the necessary system temperature. The required heat input comes from an ordinary 100 watt incandescent light bulb mounted within the oven and controlled by the Thermotrol. The equipment housed within the oven includes the high pressure see-through IFT cell, vapor and liquid densitometers, see-through PVT cell, magnetic positive displacement circulating pump, pneumatically actuated GC sampling valves, platinum resistance thermometer probe, and various piping and valves for the closed loop circulating system.

Outside the temperature controlled oven is the GC equipment, including the Varian 3700 chromatograph and Varian CDS-111 integrator with chart recorder. For the CO₂ + n-tetradecane system studied in this work, the gas chromatographic analyses were performed at the following conditions:

Columns	Temperatures	
3.7 ft Porapak Q®	Column	- 260°C
5.7 ft OV-101	Injector	- 300°C
(columns in series)	Thermal Conductivity Detector	- 300°C
	Filament	- 350°C

Helium

Carrier - 25 psig

Reference - 15 psig

Rate - 30 cc/min

Also outside the oven is the Mettler/Parr digital density indicator, working in conjunction with the vibrating U-tubes housed within the oven, the Minco platinum resistance thermometer read-out, the Heise digital pressure indicator read-out, and Wild zoom stereo microscope for photographing the pendant drops from outside the oven. Various ancillary equipment is also located outside the oven and consists of: (1) the equipment for charging chemicals into the system, (2) the oven temperature controller, (3) the automatic valve sequencer which pneumatically operates the GC sampling valves, (4) the fiber optic light for viewing the contents within the IFT cell, (5) the electric motor which drives the magnetic circulating pump, and (6) the Doric digital temperature indicator for the various temperature probes within the oven.

The arrangement of the above equipment is designed for continuous operation. Once the desired compounds have been charged into the system and equilibrium conditions have been reached, the experimental data can be obtained in one continuous effort without altering anything within the system except the circulation pattern, either liquid or vapor. The facilities allow the experimenter to obtain the equilibrium phase densities, mole fractions and IFTs all in the same data run.

Flow Patterns in the Apparatus

As shown in Figure 1, the apparatus is a closed loop continuous circulating system. When the system under study is in the two-phase state, the desired circulation pattern, either liquid or vapor, is selected by the six port liquid/vapor circulation (L/V) valve shown in Figure 1. The liquid and vapor circulation patterns are shown in Figures 2 and 3, respectively. In liquid circulation, liquid flows from the bottom of the PVT cell through the liquid densitometer, through the six port L/V valve into the inlet of the circulating pump. From the circulating pump discharge, liquid flows through a different port in the six port L/V valve, to the GC sampling valve, then through the vapor densitometer, the IFT cell where pendant drop pictures can be taken, and again through the six port L/V valve into the windowed PVT cell, which completes the closed loop circulation pattern. The GC sampling valve can be by-passed when phase composition data are not required. By-passing the GC sampling valve reduces flow restrictions and allows the system to reach equilibrium faster. The liquid flow pattern assures that liquid is flowing down into the IFT cell, the PVT cell and liquid densitometer. The vapor circulation pattern is essentially the reverse of the liquid pattern with the vapor flowing upward through the IFT cell, the PVT cell and the vapor densitometer (Figure 3).

Experimental Data Acquisition

The acquisition of experimental data consists of three separate measurements, including phase densities, phase compositions and the pendant drop IFT data. Before the start of any data run, several system checks and calibrations are made. These include leak testing the entire

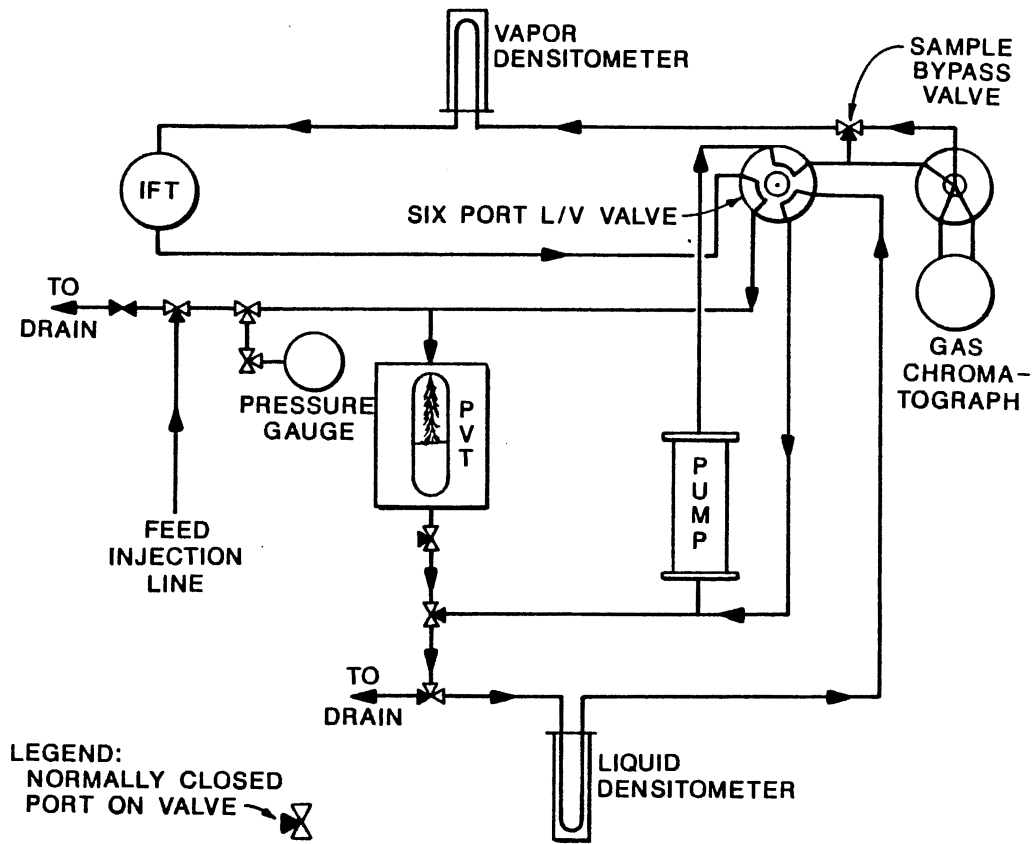


Figure 2. Liquid Circulation Pattern in Experimental Apparatus

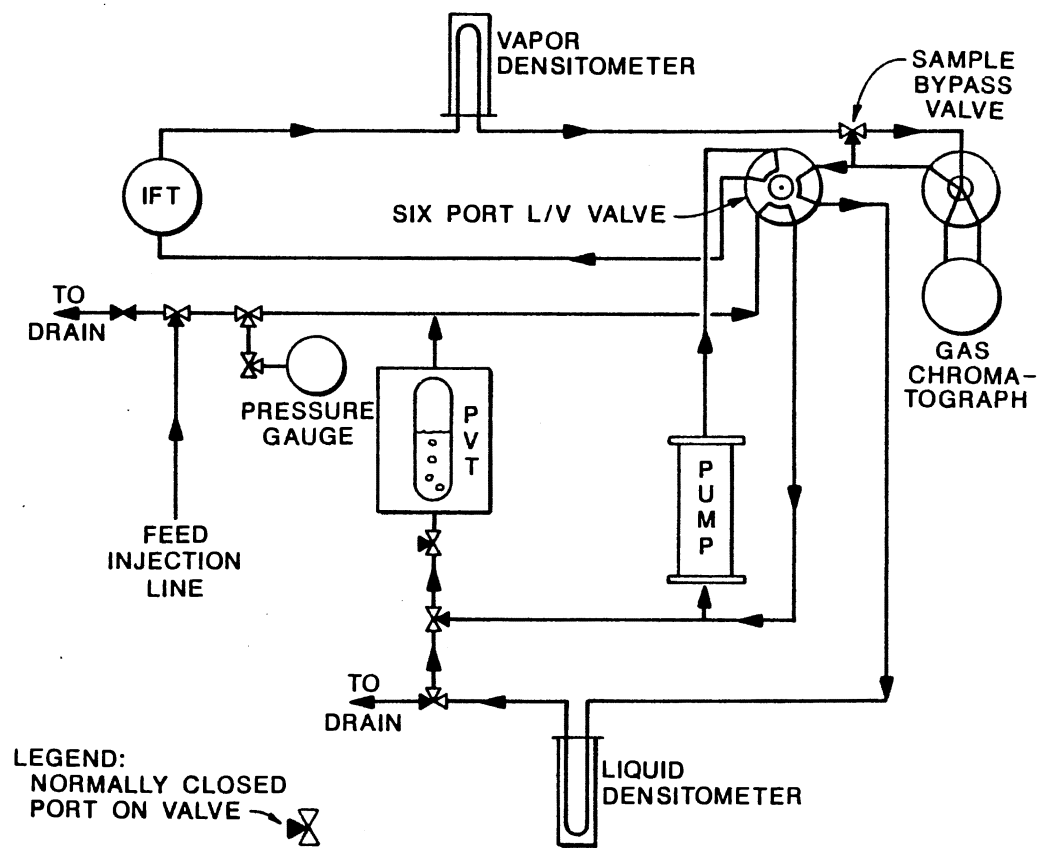


Figure 3. Vapor Circulation Pattern in Experimental Apparatus

system with helium to approximately 10% above the maximum expected operating pressure. The Heise digital pressure gauge is calibrated against a precision dead weight gauge using nitrogen as the working fluid in the calibration. The densitometers are calibrated using compounds (water, air, and CO₂) with very well known physical properties. These compounds also cover the density range expected during data acquisition. Next, the chromatograph thermal conductivity response factor for the particular system under study is determined. The response factor is the ratio of the moles of the solvent (e.g., n-tetradecane) to the moles of the solute (e.g., CO₂) times the GC detector area ratio of solute to solvent, Equation 3.1.

$$RF = a N_2/N_1 \quad (3.1)$$

where a = GC detector area ratio of solute to solvent

N_1 = moles of solute in calibration mixture

N_2 = moles of solvent in calibration mixture

To determine the response factor, known amounts of solute (N_1) and solvent (N_2) are injected into the system and maintained above the critical pressure (single phase region). While in the single phase region, the calibration mixture is sampled and analyzed by the GC. The thermal conductivity detector area ratio is measured by the GC and in conjunction with the known amounts of solute and solvent is used in Equation 3.1 to calculate the response factor. After repeating the above procedure several times, an average response factor of 0.26 was determined for the CO₂ + n-tetradecane system studied in this work.

Once the response factor was determined, compositions in the two phase (sub-critical region) could be obtained by using the response factor and the GC detector area ratio.

After the equipment has been calibrated, the system is thoroughly cleaned and prepared for the injection of the compounds to be studied. The system is cleaned with a mixture of solvent (pentane) and solute (e.g., CO₂). The mixture is circulated through the system for approximately one hour, the system is drained and then placed under a vacuum for approximately one hour. This procedure is repeated three times. After the final washing, the system is filled with the solute (e.g., CO₂) and allowed to circulate another hour before the final vacuum is placed on the system. The system remains under a vacuum until the compounds to be studied are injected. The air oven is heated up to the temperature at which data will be obtained and is maintained at this temperature throughout the experiment. A sufficient quantity of hydrocarbon solvent (e.g., n-tetradecane) is degassed by slightly heating the solvent in a container which is under vacuum. The degassed solvent is then transferred to an evacuated graduated burette where it is metered into the system. Generally, a pure component density of the solvent is obtained at this time for comparison with literature data. The solute (e.g., CO₂) is injected into the closed system by a Ruska hand operated positive displacement metering pump. To measure the amount of solute injected into the system, the injection header (a piping arrangement immediately outside the closed system which includes the metering pump) is filled with liquid solute by compressing the vapor solute with the metering pump. The liquid solute is allowed to stabilize in the injection header after which the temperature and

pressure of the solute and pump volume are recorded. The liquid solute is released into the system until the desired system pressure is reached. The closed loop equilibrium system is then isolated from the solute injection header and allowed to circulate until equilibrium conditions are obtained. The remaining solute in the injection header is recompressed to the initial pressure and temperature in the injection header prior to injection. The resulting pump volume is recorded and subtracted from the initial pump volume to determine the cubic centimeters of liquid solute injected. Now that the volume, temperature, and pressure of the solute are known, the amount of solute injected can be determined from known physical property information on the pure component solute. The apparatus is placed in the desired circulation pattern (liquid or vapor) and the components are allowed to circulate until equilibrium is reached. The system is considered to be at equilibrium when the densitometer readings remain consistent with time (approximately two hours) and the system pressure stabilizes.

The current arrangement of the experimental apparatus permits good vapor/liquid circulation at pressures as low as 300 to 400 psia, though this minimum pressure varies from system to system. Data are gathered at the lowest possible pressure so the most complete density and composition envelope can be obtained. Once the lowest pressure is obtained, liquid and vapor density measurements are generally taken first. The circulating pump is turned off and the system is allowed to remain in a static condition for approximately 15 minutes to relieve any minor pressure head within the system. The operator notes the circulation pattern (liquid or vapor) that the apparatus is in and checks to see that the Mettler/Parr densitometer indicator is switched

to indicate the corresponding liquid or vapor U-tube densitometer. This is important because both the liquid and vapor densitometers use the same indicating instrument, but each densitometer has a separate calibration. The densitometer reading is observed until consistent readings are obtained. Once it stabilizes, the densitometer reading is recorded along with the system temperature and pressure. After obtaining both vapor and liquid densities, the GC is started and phase composition data are obtained. The vapor and liquid samples are obtained automatically by the pneumatically-operated, one microliter sampling valve inside the oven. The sample is flushed from the sampling valve by helium carrier gas and flows to the columns in the GC. At least four consistent chromatograms are taken in both the liquid and vapor phases and the average of the four is reported. An effort to obtain the densities and phase compositions at precisely the same pressure is not made; therefore, any pressure changes in the system between individual measurements are indicated in the raw data (usually <5 psi from nominal measurement pressure).

The next experimental datum obtained is the photograph of the pendant drop. The system is placed in liquid circulation and the liquid level in the IFT cell is lowered so a liquid drop can be seen on the end of the selected needle. Good liquid circulation is obtained through the desired needle or down the outside of the selected wire. The circulation is stopped and a small amount of liquid is trapped above the needle by closing a block valve located upstream of the needle. A regulating valve, located between the block valve and the needle, is partially closed, squeezing liquid from the end of the needle and forming the pendant drop. The drop is then photographed and appropriate

measurements are made from the photograph. (The drop measurements are performed after completion of the experimental measurements described here).

The required measurements on each pendant drop are indicated below in Figure 4. Interfacial tension is calculated from the measured diameters X_{DE} (maximum or equatorial diameter) and X_{DS} (diameter a distance X_{DE} from the bottom of the drop). The IFT is calculated using Equation 3.2 (45).

$$\frac{\gamma}{\Delta\rho} = \frac{g X_{DE}^2}{H} \quad (3.2)$$

where

$1/H =$ function of S

$S = X_{DS}/X_{DE}$; X_{DS} and X_{DE} , cm

$g =$ acceleration due to gravity = 980.665 cm/sec^2

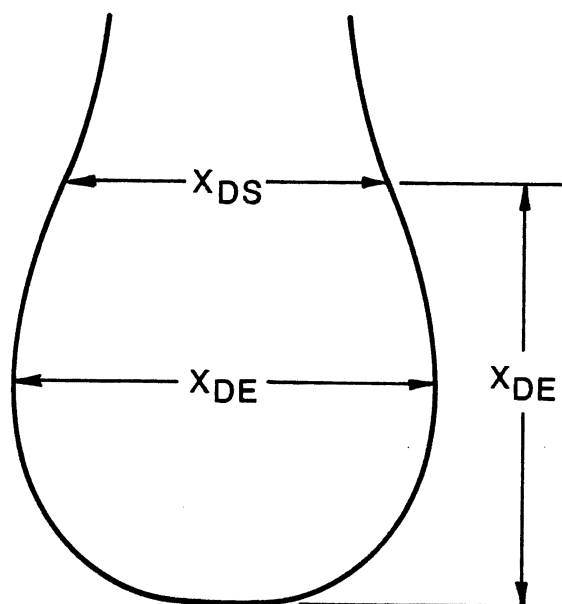


Figure 4. Measurements on Pendant Drop for IFT Calculation (Equation 3.2)

Calculations of interfacial tension from Equation 3.2 requires a relationship between the shape parameter, H , and the shape factor, S . Tabular values of the relationship between H and S (20) are utilized.

After all required data has been gathered at the current pressure, additional solute is injected into the system until the next desired pressure is obtained. Once equilibrium has been reached, the data acquisition procedure is repeated and is continued until the pressure envelope is completed up to the critical pressure. As the critical pressure is approached, the distinction between the vapor and liquid phases diminishes. The visual interface in the PVT cell becomes harder to distinguish, and IFT data are more difficult to obtain. Great care is exercised in this region because of the sensitivity the system exhibits. A visual observation of the critical pressure is made. The critical condition can be distinguished by the bright burst of orangish-red color in the system. The critical point is very easy to miss by visual observation; therefore, more credence is placed on the value obtained by scaling law analyses of the phase density-pressure data at pressures near the critical. This application of scaling law analyses to the experimental data is discussed in Chapter IV.

Chemicals

The CO_2 used in these studies was obtained from Union Carbide Linde Division and had a stated purity of 99.99 mole%. The n -tetradecane was obtained from Alpha Products with a stated purity of 99 mole%. These chemicals were used without further purification.

CHAPTER IV

EXPERIMENTAL RESULTS AND SMOOTHED DATA

Experimental data on the interfacial tension γ , equilibrium phase compositions (x, y) , and phase densities, (ρ^L, ρ^V) of the $\text{CO}_2 + n$ -tetradecane system were measured at 160°F . The measurements cover the pressure range from slightly over 1000 psia to the critical point. The experimental apparatus and procedures used to obtain this information were described in detail in Chapter III.

Experimental Data for $\text{CO}_2 + n$ -Tetradecane

The raw experimental data, including the ratio of interfacial tension to density difference $(\gamma/\Delta\rho)$, equilibrium phase compositions (x, y) , and phase densities (ρ^L, ρ^V) for $\text{CO}_2 + n$ -tetradecane, are shown in Table II. The values of $\gamma/\Delta\rho$ are reported in Table II instead of γ because $\gamma/\Delta\rho$ is determined directly from the pendant drop photographs, (Equation 3.2). The estimated accuracy of the experimental data is:

Composition (x, y) , mole fraction:	± 0.003
Densities (ρ^L, ρ^V) , gm/cc:	± 0.001
IFT (γ) , mN/m:	$\pm 0.04 \gamma^{0.08}$
Pressure (P) , psi:	± 2.0
Temperature (T) , $^\circ\text{F}$:	± 0.1

The estimated accuracies are from the works of Robinson and Nagarajan (15,48). For the IFT accuracy, multiple "readings" on each pendant drop photograph, plus multiple photographs were used to calculate the maximum

TABLE II

PHASE EQUILIBRIA AND INTERFACIAL TENSIONS FOR CO₂ + N-TETRADECANE AT 344.3 K (160°F)

Phase Compositions, Mole Fraction CO ₂				Phase Densities, (kg/m ³) x 10 ⁻³				IFT-Density Difference Ratio	
Liquid Phase		Vapor Phase		Liquid Phase		Vapor Phase		Pressure, psia	$\gamma/\Delta\rho \times 10^3$ (mN/m)/(kg/m ³)
Pressure, psia	Composition, x	Pressure, psia	Composition, y	Pressure, psia	Density, ρ^L	Pressure, psia	Density, ρ^V		
		1027	0.989			1029	0.1466		
		1204	0.989			1204	0.1827		
		1307	0.988			1306	0.2076		
		1506	0.991			1504	0.2640		
1606	0.685	1603	0.992	1601	0.7508	1602	0.2966	1602	8.95
1694	0.711	1696	0.991	1694	0.7514	1695	0.3324	1693	7.85
1787	0.738	1788	0.992	1787	0.7525	1787	0.3708	1787	6.48
1902	0.769	1900	0.988	1900	0.7545	1899	0.4251	1901	5.48
2025	0.797	2017	0.987	2025	0.7551	2017	0.4861	2022	4.00
2025	0.797	2017	0.987	2025	0.7551	2017	0.4861	2022	4.26
2111	0.819	2102	0.984	2101	0.7546	2101	0.5303	2106	3.22
2153	0.827	2145	0.983	2153	0.7541	2144	0.5532	2148	2.93
2194	0.839	2197	0.983	2190	0.7528	2190	0.5766	2188	2.32
2256	0.857	2256	0.976	2255	0.7523	2256	0.6102	2256	1.43
2276	0.862	2274	0.976	2275	0.7504	2273	0.6165	2272	1.22
2309	0.870	2296	0.971	2307	0.7486	2307	0.6321	2307	0.790
2325	0.877	2315	0.968	2324	0.7458	2324	0.6411	2324	0.700
2341	0.885	2340	0.965	2342	0.7442	2342	0.6544	2342	0.445
2353	0.887	2346	0.964	2354	0.7409	2354	0.6598	2354	0.296
2363	0.893	2360	0.960	2360	0.7388	2360	0.6659	2361	0.195
2364	0.895	2364	0.958	2361	0.7373	2361	0.6670	2365	0.173
2372	0.899	2365	0.955	2365	0.7365	2365	0.6705		

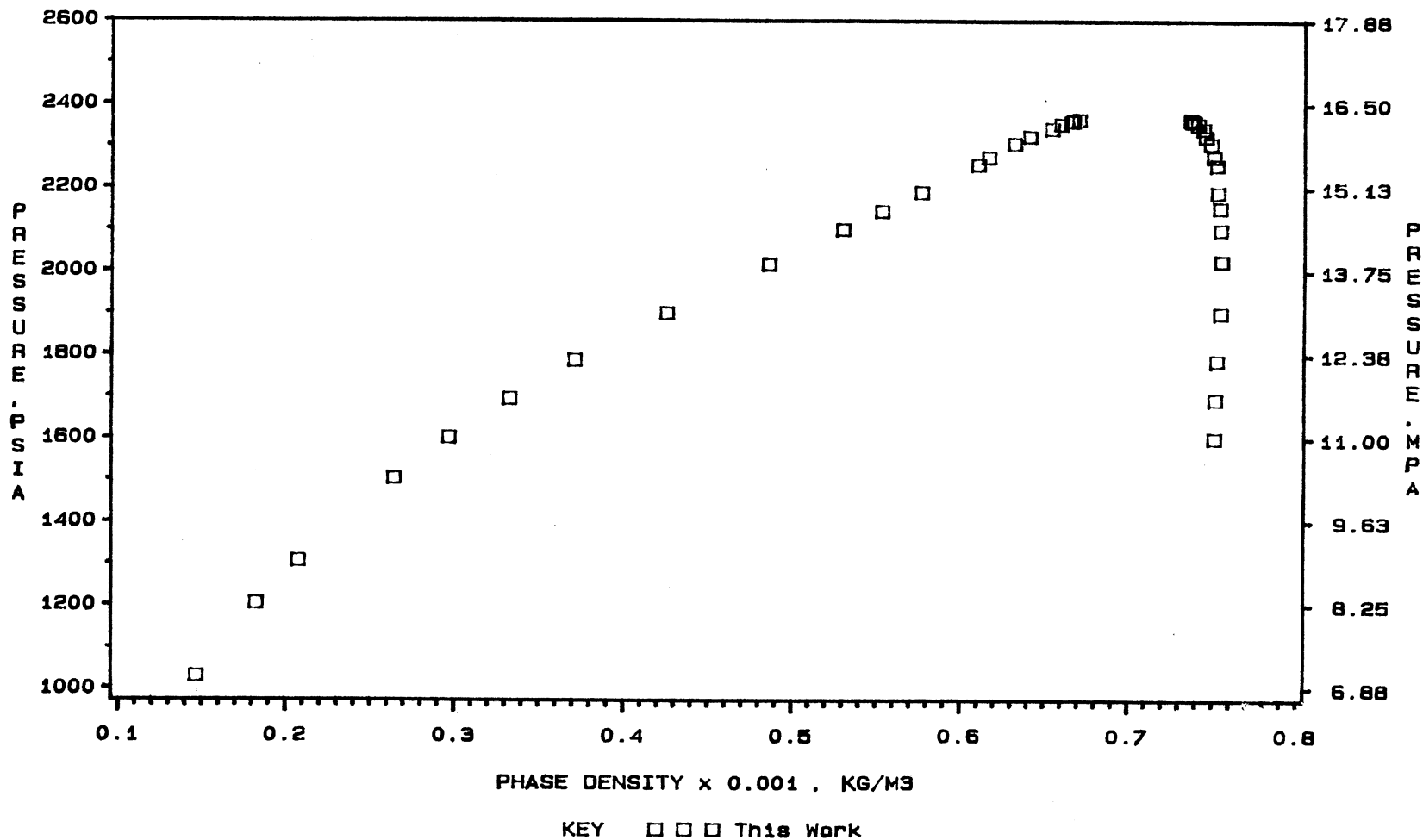
deviations from the mean value of IFT for each IFT data point. These deviations are represented reasonably well by the above relationship.

Table II shows that no values for the liquid phase composition and density and $\gamma/\Delta\rho$ were reported from approximately 1000 to 1600 psia. Good liquid circulation was not established over this pressure range, therefore no data were taken. However, over the same pressure range, good vapor circulation was obtained and experimental data are reported. As mentioned in Chapter III, the lowest pressure at which experimental data are obtained varies from system to system, and good vapor circulation is always obtained before liquid circulation.

The experimental phase densities, phase compositions, and $\gamma/\Delta\rho$ values are illustrated in Figures 5-7, respectively. The $\gamma/\Delta\rho$ values are plotted as a function of "scaled" pressure because: (a) this conveniently expands the near-critical, low-IFT region and (b) "scaling laws" require that this relationship becomes linear (log-log) as the critical pressure is approached and that the slope should be a specific, universal value (independent of the substances studied).

As shown in Table II, the experimental data (x , y , ρ^L , ρ^V , $\gamma/\Delta\rho$) were not measured at precisely the same pressure. To facilitate better use of the data, smoothed and interpolated results are presented in Table III. The smoothed data retain the same accuracy as stated earlier for the raw data.

Table III contains smoothed data covering the same pressure range as the raw experimental data plus extrapolated values from the highest measured pressures to the estimated critical point. The estimated critical point ($P_c = 2376$ psia) compares favorably with visual observations in the equilibrium cell ($P_c = 2374 \pm 2$ psi). The estimated



**Figure 5. Effect of Pressure on Phase Density for
 CO₂ + n-Tetradecane at 344.3 K (160 °F)**

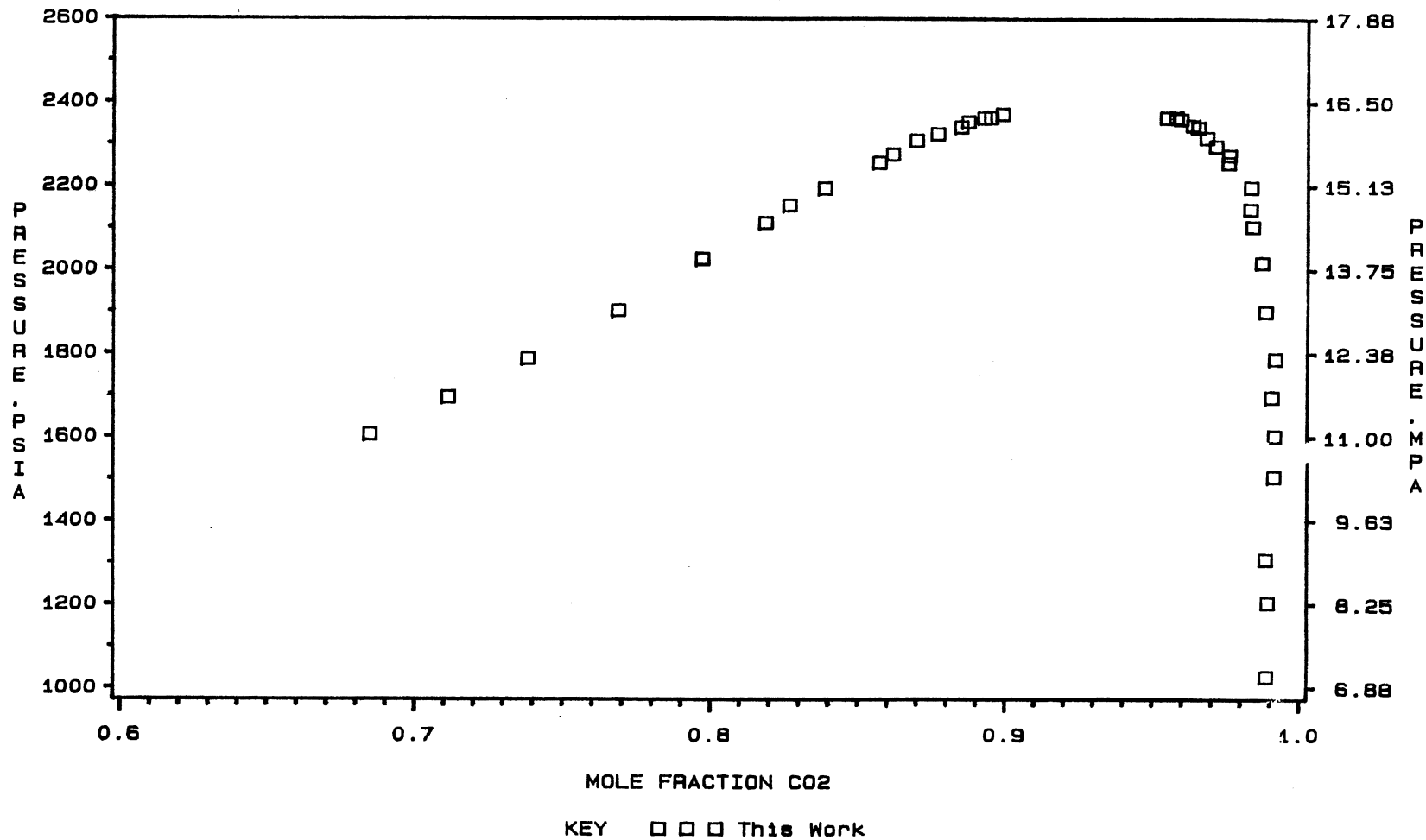


Figure 6. Effect of Pressure on Phase Composition for CO₂ + n-Tetradecane at 344.3 K (160 °F)

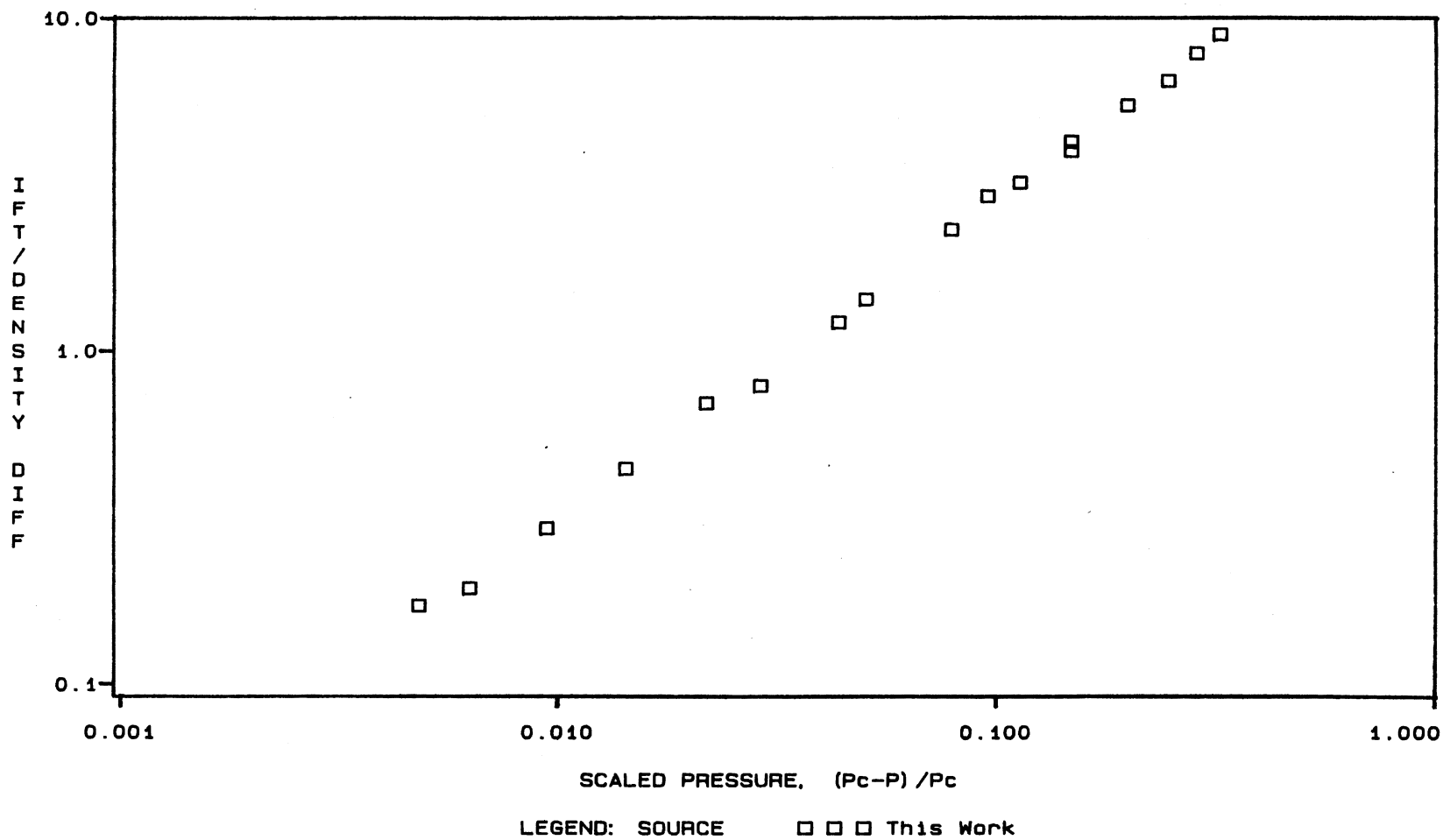


Figure 7. Interfacial Tension - Phase Density Difference Ratios for CO₂ + n-Tetradecane at 344.3 K (160 °F)

TABLE III
SMOOTHED PHASE EQUILIBRIA AND INTERFACIAL TENSIONS
FOR CO₂ + N-TETRADECANE AT 344.3 K (160°F)

Pressure		Phase Compositions, Mole Fraction CO ₂		Phase Densities, (kg/m ³) x 10 ⁻³		Interfacial Tension, mN/m
kPa	psia	Liquid	Vapor	Liquid	Vapor	
6895	1000		0.989		0.1417	
7585	1100		0.988		0.1600	
8275	1200		0.988		0.1818	
8963	1300		0.989		0.2061	
9650	1400		0.990		0.2328	
10340	1500		0.991		0.2626	
11030	1600	0.683	0.991	0.7508	0.2961	4.03
11270	1700	0.713	0.991	0.7415	0.3342	3.23
12410	1800	0.742	0.990	0.7529	0.3772	2.49
13100	1900	0.768	0.989	0.7542	0.4252	1.81
13790	2000	0.792	0.987	0.7550	0.4769	1.22
14480	2100	0.815	0.985	0.7548	0.5303	0.728
15170	2200	0.840	0.981	0.7531	0.5818	0.360
15860	2300	0.869	0.972	0.7489	0.6294	0.113
15925	2310	0.873	0.970	0.7481	0.6342	0.094
15995	2320	0.876	0.969	0.7471	0.6392	0.077
16065	2330	0.879	0.967	0.7459	0.6445	0.060
16135	2340	0.883	0.965	0.7443	0.6504	0.044
16200	2350	0.887	0.962	0.7420	0.6572	0.029
16215	2352	0.888	0.962	0.7414	0.6587	0.026
16230	2354	0.888	0.961	0.7408	0.6603	0.024
16245	2356	0.889	0.960	0.7401	0.6620	0.021
16255	2358	0.890	0.960	0.7394	0.6638	0.018
16270	2360	0.891	0.959	0.7385	0.6657	0.016
16285	2362	0.892	0.958	(0.7375)*	(0.6678)	(0.013)
16300	2364	0.893	0.957	(0.7364)	(0.6701)	(0.011)
16315	2366	0.894	(0.955)	(0.7351)	(0.6727)	(0.009)
16325	2368	0.896	(0.954)	(0.7336)	(0.6755)	(0.007)
16340	2370	0.898	(0.952)	(0.7316)	(0.6789)	(0.005)
16355	2372	0.900	(0.949)	(0.7291)	(0.6831)	(0.003)
16370	2374	(0.903)	(0.945)	(0.7252)	(0.6889)	(0.001)
16380**	2376	(0.924)	(0.924)	(0.7085)	(0.7085)	(0.000)

* Numbers in parenthesis are extrapolations beyond highest measured pressures

** Estimated critical point (visual observation gave 2374 ± 2 psia)

critical point is the value which produced the optimum fit of the smoothing function to the experimental data. The smoothing procedure is outlined below.

In order to facilitate convenient use of the experimental results, the data were smoothed using a function of the type presented by Kobayashi (23) and Charoensombutamom (24). The function is based on the renormalized group theory (RGT) which states that systems, defined by spatial and order parameters in the same universality class, exhibit the same critical exponents in the near-critical region. The function employed is of the type shown below:

$$\phi_+ - \phi_- = \sum_{i=0}^N B_i (P^*)^{\beta+i\Delta} \quad (4.1)$$

The function represents the difference between the order parameter, ϕ , in two equilibrium phases (denoted by "+" and "-"). The lead term represents the near critical "power law" scaling behavior. The additional terms are corrections to scaling behavior suggested by Wegner (25); $\Delta = 0.5$ is the "gap exponent", which is the same for all systems in the same universality class.

The average value of ϕ is determined by the following equation for the "rectilinear diameter":

$$(\phi_+ + \phi_-)/2 = \phi_c + A_0 (P^*)^{1-\alpha} + \sum_{j=1}^M A_j (P^*)^j \quad (4.2)$$

Combining Equations 4.1 and 4.2 results in an equation for the individual values of ϕ_+ and ϕ_-

$$\phi_{\pm} = \phi_c + A_0 (P^*)^{1-\alpha} + \sum_{j=1}^M A_j (P^*)^j \pm \frac{1}{2} \sum_{i=0}^N B_i (P^*)^{\beta+i\Delta} \quad (4.3)$$

where

P^* = scaled pressure, $(P_c - P)/P_c$

P = equilibrium pressure

P_c = critical pressure

ϕ_c = critical order parameter

A_i, B_i = regressed parameters in Equations 4.1-4.2

α, Δ, β = scaling law exponents

Equation 4.3 was used to represent the experimental results of equilibrium phase compositions and phase densities with:

For P - x, y : ϕ_c = critical composition, z_c

$\phi_+ = y, \phi_- = x, M = 5, N = 5$

For P - ρ^L, ρ^V : ϕ_c = critical density

$\phi_+ = \rho^L, \phi_- = \rho^V, M = 5, N = 5$

The values of $\gamma/\Delta\rho$ were fitted to the following expression:

$$\gamma/\Delta\rho = \sum_{k=0}^L G_k (P^*)^{2\nu-\beta+k\Delta} \quad (4.4)$$

For P - $\gamma/\Delta\rho$: $L = 1$

where the lead term represents the limiting "power law" behavior with the critical exponent of $2\nu-\beta$ and the succeeding terms are Wegner corrections to scaling law.

The parameters A_i , B_i , G_i and the number of expansion terms M , N , L were determined by nonlinear regressions using the Statistical Analysis System (SAS). The criterion used to determine the best fit of the equations to the experimental data was to minimize the sum of the squares (SS) of the weighted residuals (27) where:

$$SS = \sum_{i=1}^K [(Y^{\text{exp}} - Y^{\text{calc}})/\sigma_Y]_i^2 = \sum_{i=1}^K (\Delta Y/\sigma_Y)_i^2 \quad (4.5)$$

where K is the number of experimental data points, Y represents either the phase compositions (x , y), the densities (ρ^L , ρ^V), or the IFT to density difference ratio $\gamma/\Delta\rho$, and σ is the fully propagated error term used to weight the individual residuals. The value of σ is defined as:

$$\sigma_Y^2 = \varepsilon_Y^2 + (\partial Y/\partial P)^2 \varepsilon_P^2 \quad (4.6)$$

ε_Y represents the experimental uncertainty (standard deviation) of the variables measured during data acquisition and are estimated to be:

$$\varepsilon_x = \varepsilon_y = 0.001 \text{ (mole fraction)}$$

$$\varepsilon_{\rho^L} = \varepsilon_{\rho^V} = 0.0004 \text{ gm/cc}$$

$$\varepsilon_{(\gamma/\Delta\rho)} = 0.04 (\gamma/\Delta\rho)^{0.08} \text{ mN/m}$$

$$\epsilon_p = 1.0 \text{ psi}$$

These experimental uncertainties are taken from the experimental studies of Robinson and Nagarajan (15, 26). They reflect the precision of the measurements and not the accuracy of the data. The estimated accuracy of the data was reported earlier in this chapter.

The minimum number of terms (L, M, N) necessary for Equations 4.3 and 4.4 to represent the experimental data adequately was determined by repeating SAS regressions varying the values of L, M, N. These regressions were made with all experimental data points. The values of $L = 1$, $M = 5$, $N = 5$ were found to provide acceptable results. The values of the critical pressure (P_c) and the critical exponents (α , β , and ν) also were allowed to vary during the regressions. The critical exponents were varied over generally acceptable ranges (27), but the regressions appeared relatively insensitive to changes in the critical exponents. This lack of sensitivity permitted the use of the simple values of ($\alpha = 1/8$), ($\beta = 1/3$), and ($\nu = 0.63$) in subsequent regressions. The regressions were sensitive to the value of the critical pressure (P_c). The optimum (integer) value of P_c was found to be 2376 psia. Individual regressions (e.g., density, composition, or $\gamma/\Delta\rho$) gave slightly different optimum values of P_c , but the best overall fit of the experimental data (x , y , ρ^L , ρ^V , $\gamma/\Delta\rho$) using Equations 4.3 and 4.4 was given by $P_c = 2376$ psia. The regressed value of P_c is in good agreement with the experimentally determined value of $P_c = 2374 \pm 2$ psi which was obtained by visual observations.

After the first round of regressions were made and the values of (L, M, and N), (α , β and ν), and P_c were determined, the individual data

points were reviewed. Data points with weighted deviations greater than 2.5 were (somewhat arbitrarily) discarded, where the weighted deviations are defined as:

$$(Y^{\text{exp}} - Y^{\text{calc}})/\sigma_Y \quad (4.7)$$

and σ_Y is defined by Equation 4.6 above. Only the vapor density datum at $P = 2342$ psia was discarded by this criterion. The final regressions were made on the reduced data set. The results of these regressions are shown in Tables IV through VI for phase composition, phase density, and $\gamma/\Delta\rho$, respectively. The residuals in Tables IV, V, and VI show no systematic behavior and the magnitudes of these residuals are generally within the experimental expectations. The results presented in these tables carry more significant figures than the experimental data justify. The number of significant figures justified were indicated earlier by the estimated accuracy of the experimental data. Figures 8 through 10 show the weighted deviations as a function of scaled pressure for phase composition, phase density, and $\gamma/\Delta\rho$. Figures 11 through 13 illustrate these deviations, expressed as $Y^{\text{exp}} - Y^{\text{calc}}$. The final Figures 14 and 15 illustrate percent deviations for phase density and $\gamma/\Delta\rho$. The regressed parameters for Equations 4.3 and 4.4 appear in Table VII.

An indication that the regressions are acceptable can be found in the weighted root mean square deviations (WRMS). If the experimental uncertainties selected for the fully propagated weighted term σ_Y are correct, the WRMS should be near 1.0. For the $\text{CO}_2 + n\text{-tetradecane}$ system, the WRMS values were 0.97 for x , y , 0.96 for ρ^L , ρ^V , and 1.09

TABLE IV

COMPARISONS OF EXPERIMENTAL AND CALCULATED (EQUATION 4.3)
 PHASE COMPOSITIONS FOR CO₂ + N-TETRADECANE
 AT 344.3 K (160°F)

Pressure, psia	Scaled Press., (P _c -P)/P _c	Mole Fraction CO ₂ Expt'l.	Mole Fraction CO ₂ Calc'd.	Error in Calculated Composition Mole Frn.	% Wtd. Error	Weighting Factor, Mol Frn.
-----Liquid Phase-----						
1606.0	0.324074	0.684848	0.684874	-0.0000258	-0.00377	0.00104578
1694.0	0.287037	0.711432	0.711506	-0.0000739	-0.01039	0.00104319
1787.0	0.247896	0.738431	0.738255	0.0001754	0.02375	0.00103765
1902.0	0.199495	0.768683	0.768445	0.0002382	0.03098	0.00103042
2025.0	0.147727	0.797192	0.797679	-0.0004874	-0.06114	0.00102625
2025.0	0.147727	0.797192	0.797679	-0.0004874	-0.06114	0.00102625
2111.0	0.111532	0.818689	0.817631	0.0010576	0.12918	0.00102762
2153.0	0.093855	0.826782	0.827776	-0.0009943	-0.12026	0.00103015
2194.0	0.076599	0.838710	0.838230	0.0004796	0.05718	0.00103412
2256.0	0.050505	0.857143	0.855565	0.0015783	0.18414	0.00104330
2276.0	0.042088	0.861702	0.861640	0.0000618	0.00717	0.00104702
2309.0	0.028199	0.869739	0.872243	-0.0025038	-0.28788	0.00105391
2325.0	0.021465	0.876894	0.877668	-0.0007741	-0.08827	0.00105815
2341.0	0.014731	0.884956	0.883359	0.0015964	0.18039	0.00106571
2353.0	0.009680	0.887348	0.888001	-0.0006525	-0.07353	0.00108201
2363.0	0.005471	0.892828	0.892641	0.0001864	0.02088	0.00113886
2364.0	0.005051	0.894992	0.893200	0.0017919	0.20022	0.00115263
2372.0	0.001684	0.898951	0.899828	-0.0008778	-0.09765	0.00169841
-----Vapor Phase-----						
1027.0	0.567761	0.988686	0.988832	-0.0001465	-0.01482	0.00100020
1204.0	0.493266	0.989212	0.988347	0.0008643	0.08737	0.00100004
1307.0	0.449916	0.988485	0.989457	-0.0009720	-0.09833	0.00100007
1506.0	0.366162	0.991322	0.991264	0.0000574	0.00579	0.00100001
1603.0	0.325337	0.991594	0.991434	0.0001597	0.01610	0.00100000
1696.0	0.286195	0.990597	0.991110	-0.0005129	-0.05178	0.00100002
1787.5	0.247685	0.991785	0.990400	0.0013855	0.13969	0.00100005
1900.0	0.200337	0.988408	0.989100	-0.0006920	-0.07001	0.00100009
2017.0	0.151094	0.987078	0.987160	-0.0000820	-0.00831	0.00100021
2017.0	0.151094	0.987078	0.987160	-0.0000820	-0.00831	0.00100021
2102.0	0.115320	0.983941	0.984987	-0.0010462	-0.10633	0.00100051
2145.0	0.097222	0.983051	0.983418	-0.0003671	-0.03734	0.00100087
2197.0	0.075337	0.983290	0.980833	0.0024579	0.24997	0.00100174
2256.0	0.050505	0.975610	0.976494	-0.0008840	-0.09061	0.00100412
2274.0	0.042929	0.975836	0.974737	0.0010999	0.11271	0.00100548
2296.0	0.033670	0.971302	0.972197	-0.0008948	-0.09213	0.00100805
2315.5	0.025463	0.968215	0.969457	-0.0012415	-0.12822	0.00101209
2340.0	0.015152	0.965379	0.964897	0.0004826	0.04999	0.00102558
2346.0	0.012626	0.963585	0.963434	0.0001514	0.01571	0.00103378
2360.0	0.006734	0.959502	0.958749	0.0007523	0.07840	0.00109484
2364.0	0.005051	0.954783	0.956727	-0.0019447	-0.20368	0.00115494
2364.5	0.004840	0.957929	0.956433	0.0014961	0.15618	0.00116656

TABLE V
 COMPARISONS OF EXPERIMENTAL AND CALCULATED (EQUATION 4.3)
 PHASE DENSITIES FOR CO₂ + N-TETRADECANE
 AT 344.3 K (160°F)

Pressure, psia	Scaled Press., (P _c -P)/P _c	Phase Density, gm/cc		Error in Calculated Density			Weighting Factor, gm/cc
		Expt'l.	Calc'd.	gm/cc	%	Wtd. Error	
-----Liquid Phase-----							
1601.0	0.326178	0.7508	0.750767	0.00003272	0.00436	0.0818	0.00040000
1694.0	0.287037	0.7514	0.751415	-0.00001512	-0.00201	-0.0378	0.00040017
1787.0	0.247896	0.7525	0.752683	-0.00018329	-0.02436	-0.4579	0.00040027
1900.0	0.200337	0.7545	0.754230	0.00026988	0.03577	0.6744	0.00040016
2025.0	0.147727	0.7551	0.755059	0.00004084	0.00541	0.1021	0.00040000
2025.0	0.147727	0.7551	0.755059	0.00004084	0.00541	0.1021	0.00040000
2101.0	0.115741	0.7546	0.754763	-0.00016324	-0.02163	-0.4080	0.00040010
2153.0	0.093855	0.7541	0.754108	-0.00007988	-0.00106	-0.0199	0.00040034
2190.0	0.078283	0.7528	0.753377	-0.00057671	-0.07661	-1.4394	0.00040067
2255.0	0.050926	0.7523	0.751362	0.00093801	0.12468	2.3327	0.00040211
2275.0	0.042508	0.7504	0.750442	-0.00004193	-0.00559	-0.1040	0.00040331
2307.0	0.029040	0.7486	0.748354	0.00024632	0.03290	0.6028	0.00040866
2324.0	0.021886	0.7458	0.746654	-0.00085428	-0.11455	-2.0456	0.00041761
2342.0	0.014310	0.7442	0.743868	0.00033238	0.04466	0.7422	0.00044780
2353.5	0.009470	0.7409	0.740962	-0.00006208	-0.00838	-0.1213	0.00051179
2360.0	0.006734	0.7388	0.738487	0.00030286	0.04099	0.5013	0.00060416
2361.0	0.006313	0.7373	0.738030	-0.00072986	-0.09899	-1.1648	0.00062661
2364.5	0.004840	0.7365	0.736119	0.00038110	0.05174	0.5163	0.00073806
-----Vapor Phase-----							
1029.0	0.566919	0.1466	0.146599	0.00000099	0.00067	0.0023	0.00043639
1204.0	0.493266	0.1827	0.182709	-0.00000878	-0.00480	-0.0190	0.00046236
1306.0	0.450337	0.2076	0.207608	-0.00000833	-0.00401	-0.0175	0.00047508
1504.0	0.367003	0.2640	0.263856	0.00014448	0.05473	0.2833	0.00051001
1602.0	0.325758	0.2966	0.296816	-0.00021631	-0.07293	-0.4032	0.00053651
1695.0	0.286616	0.3324	0.332131	0.00026881	0.08087	0.4736	0.00056756
1787.0	0.247896	0.3708	0.371328	-0.00052839	-0.14250	-0.8782	0.00060165
1899.0	0.200758	0.4251	0.424651	0.00044881	0.10558	0.7003	0.00064092
2017.0	0.151094	0.4861	0.485951	0.00014891	0.03063	0.2235	0.00066624
2017.0	0.151094	0.4861	0.485951	0.00014891	0.03063	0.2235	0.00066624
2101.0	0.115741	0.5303	0.530796	-0.00049569	-0.09347	-0.7459	0.00066458
2144.0	0.097643	0.5532	0.553398	-0.00019848	-0.03588	-0.3028	0.00065555
2190.0	0.078283	0.5766	0.576866	-0.00026603	-0.04614	-0.4155	0.00064020
2256.0	0.050505	0.6102	0.608774	0.00142570	0.23365	2.3138	0.00061617
2273.0	0.043350	0.6165	0.616708	-0.00020777	-0.03370	-0.3385	0.00061371
2307.0	0.029040	0.6321	0.632723	-0.00062272	-0.09852	-0.9902	0.00062891
2324.0	0.021886	0.6411	0.641283	-0.00018331	-0.02859	-0.2767	0.00066243
2353.5	0.009470	0.6598	0.659881	-0.00008098	-0.01227	-0.0894	0.00090590
2360.0	0.006734	0.6659	0.665724	0.00017613	0.02645	0.1630	0.00108043
2361.0	0.006313	0.6670	0.666748	0.00025205	0.03779	0.2252	0.00111916
2364.5	0.004840	0.6705	0.670716	-0.00021611	-0.03223	-0.1663	0.00129927

TABLE VI

COMPARISONS OF EXPERIMENTAL AND CALCULATED (EQUATION 4.4) (IFT/DENSITY DIFFERENCE)
FOR CO₂ + N-TETRADECANE AT 344.3 K (160°F)

Pressure, psia	Scaled Press., (P _c -P)/P _c	γ/Δρ (mN/m)/(gm/cc)		Error in Calculated γ/Δρ (mN/m) (gm/cc)			Weighting Factor, (mN/m)/(gm/cc)
		Expt'l.	Calc'd.	%	Wtd. Error		
1602.0	0.325758	8.945	8.84565	0.09935	1.1107	0.4206	0.236230
1693.0	0.287458	7.850	7.82132	0.02868	0.3653	0.1349	0.212576
1787.0	0.247896	6.483	6.76429	-0.28129	-4.3388	-1.5443	0.182149
1901.0	0.199916	5.478	5.48284	-0.00484	-0.0883	-0.0304	0.159013
2022.0	0.148990	4.001	4.12116	-0.12016	-3.0031	-0.9730	0.123490
2022.0	0.148990	4.259	4.12116	0.13784	3.2365	1.0616	0.129850
2106.0	0.113636	3.218	3.17267	0.04533	1.4085	0.4371	0.103707
2148.0	0.095960	2.930	2.69650	0.23350	7.9694	2.4267	0.096221
2188.0	0.079125	2.320	2.24109	0.07891	3.4013	0.9875	0.079907
2256.0	0.050505	1.434	1.46001	-0.02601	-1.8136	-0.4746	0.054800
2272.0	0.043771	1.222	1.27428	-0.05228	-4.2780	-1.0785	0.048471
2307.0	0.029040	0.790	0.86372	-0.07372	-9.3311	-2.0999	0.035104
2324.0	0.021886	0.700	0.66120	0.03880	5.5431	1.2022	0.032275
2342.0	0.014310	0.445	0.44315	0.00185	0.4161	0.0768	0.024108
2353.5	0.009470	0.296	0.30074	-0.00474	-1.6011	-0.2432	0.019488
2361.0	0.006313	0.195	0.20570	-0.01070	-5.4872	-0.6418	0.016671
2364.5	0.004840	0.173	0.16044	0.01256	7.2594	0.7739	0.016227

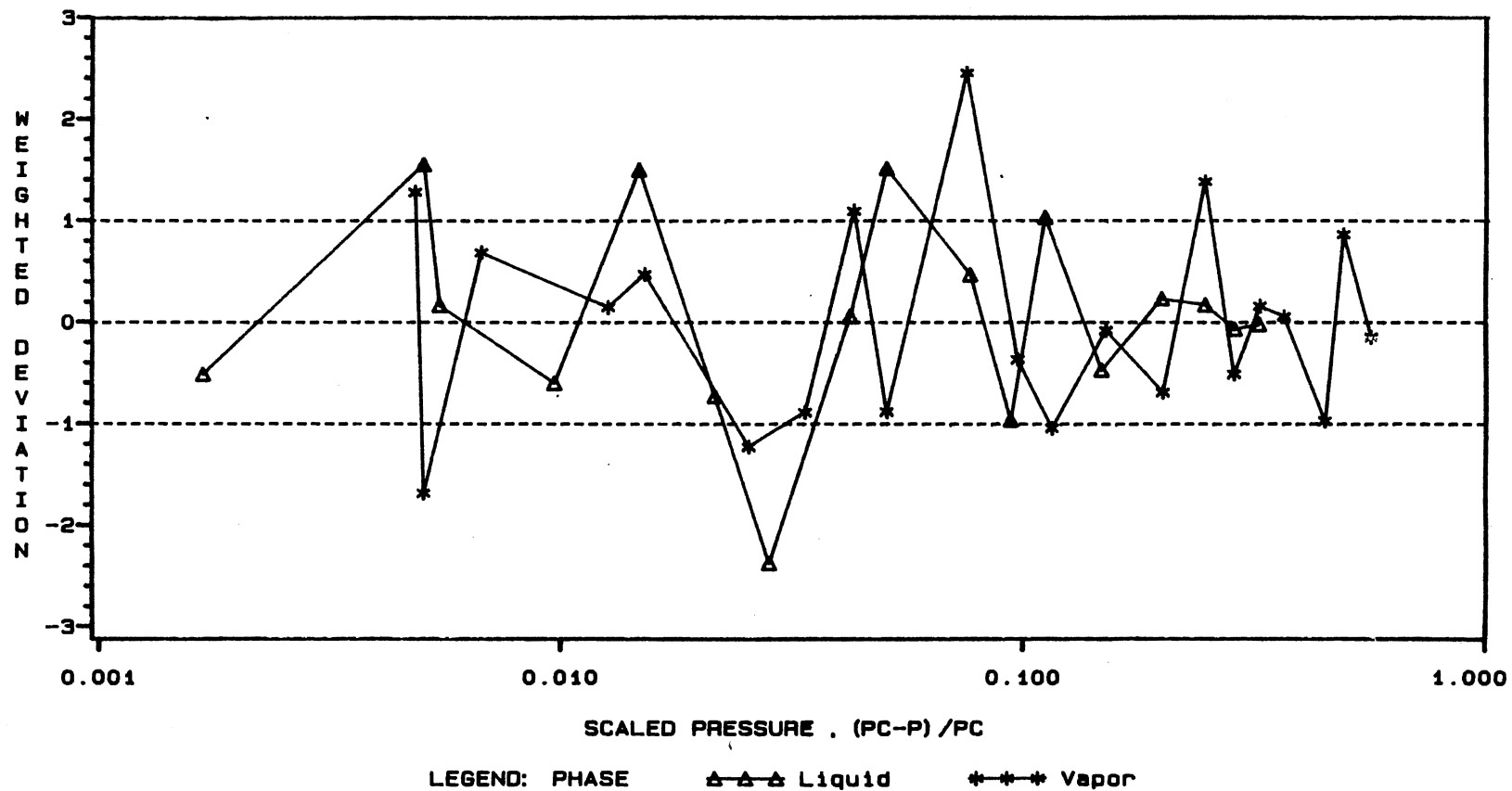


Figure 8. Smoothing Function Fit To Composition Data (Weighted Deviations) for CO₂ + n-Tetradecane at 344.3 K (160 °F)

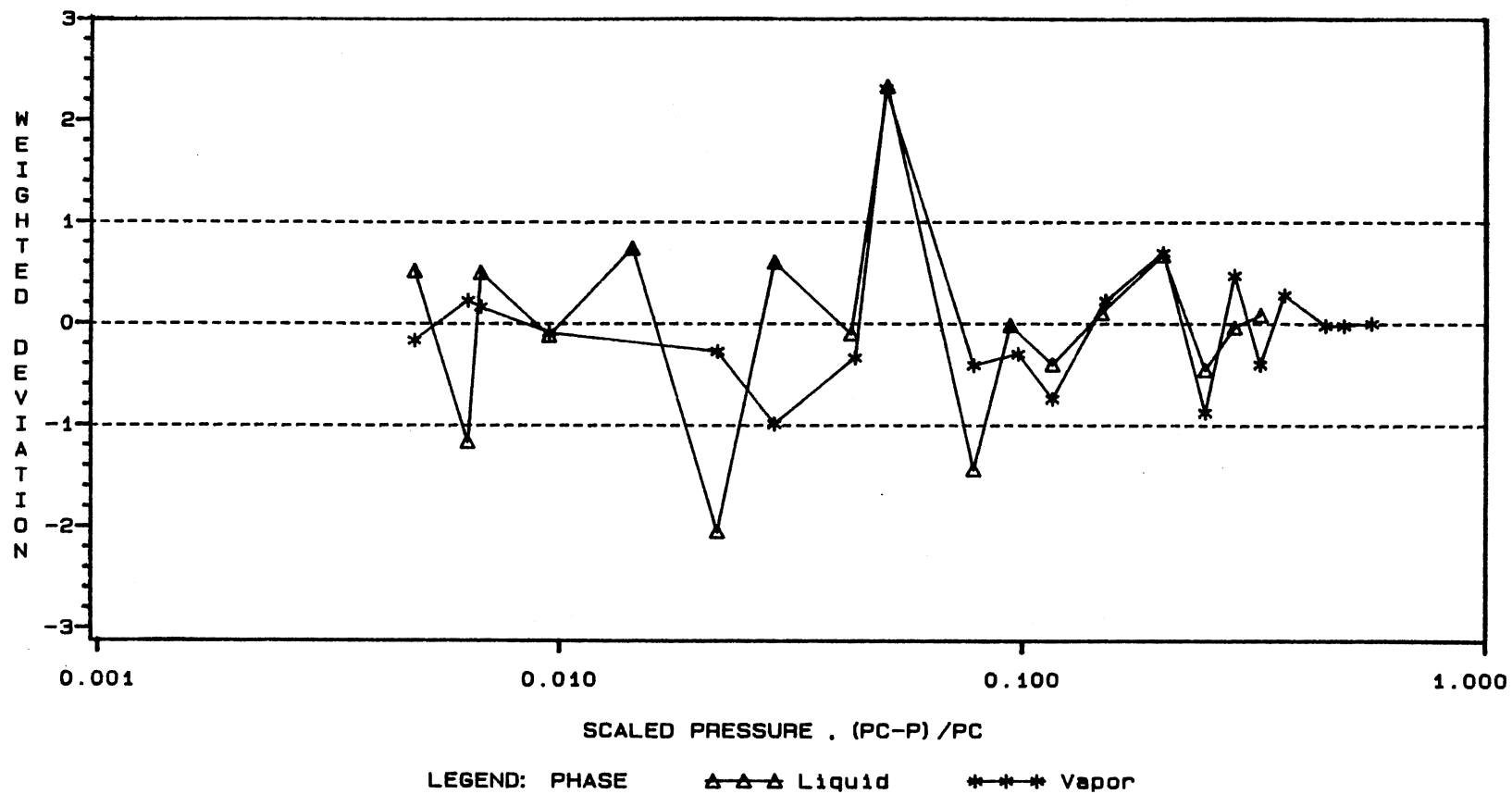


Figure 9. Smoothing Function Fit To Density Data (Weighted Deviations) for CO₂ + n-Tetradecane at 344.3 K (160 °F)

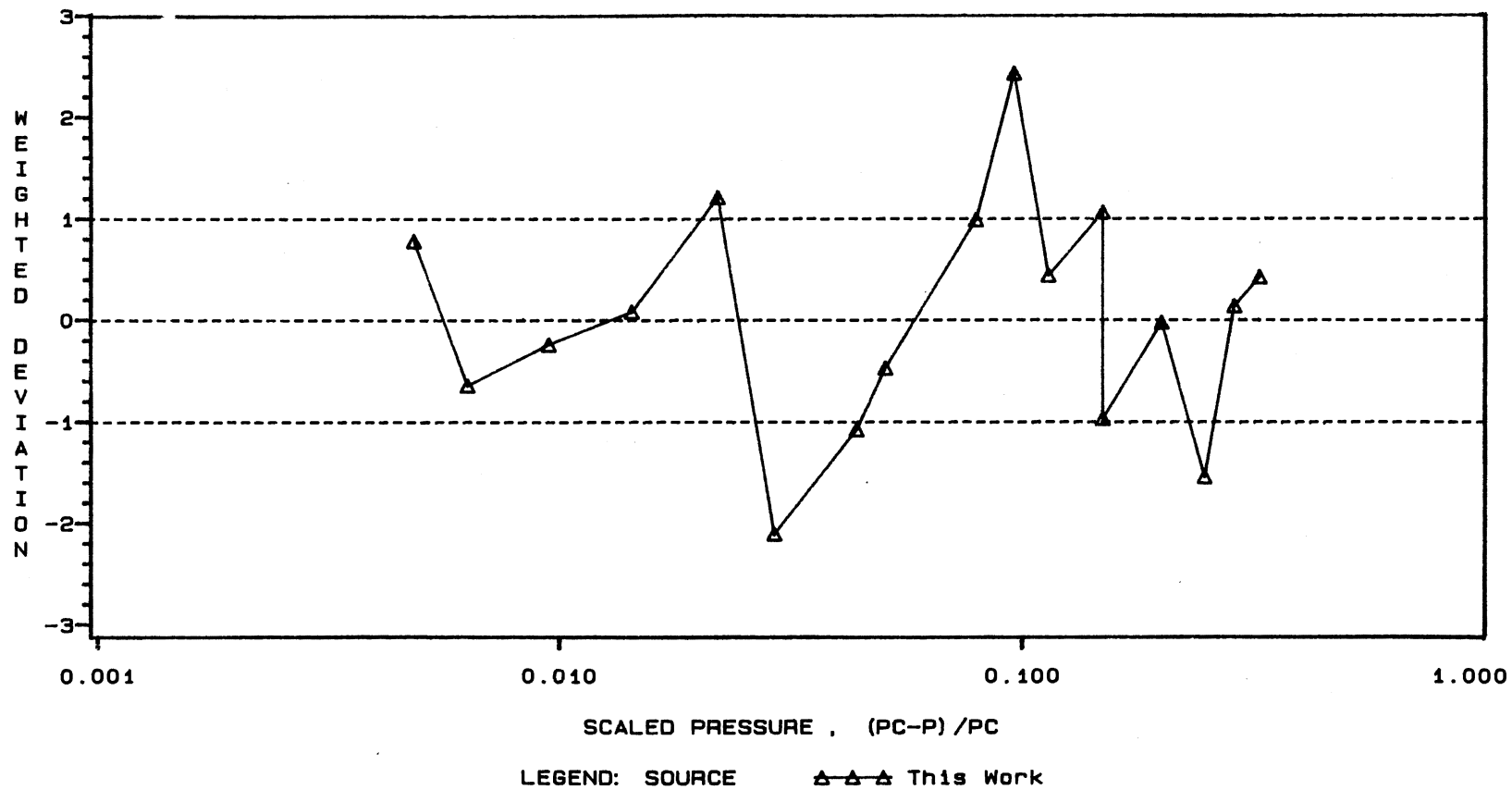


Figure 10. Smoothing Function Fit to Pendant Drop Data (Weighted Deviations) for CO₂ + n-Tetradecane at 344.3 K (160 °F)

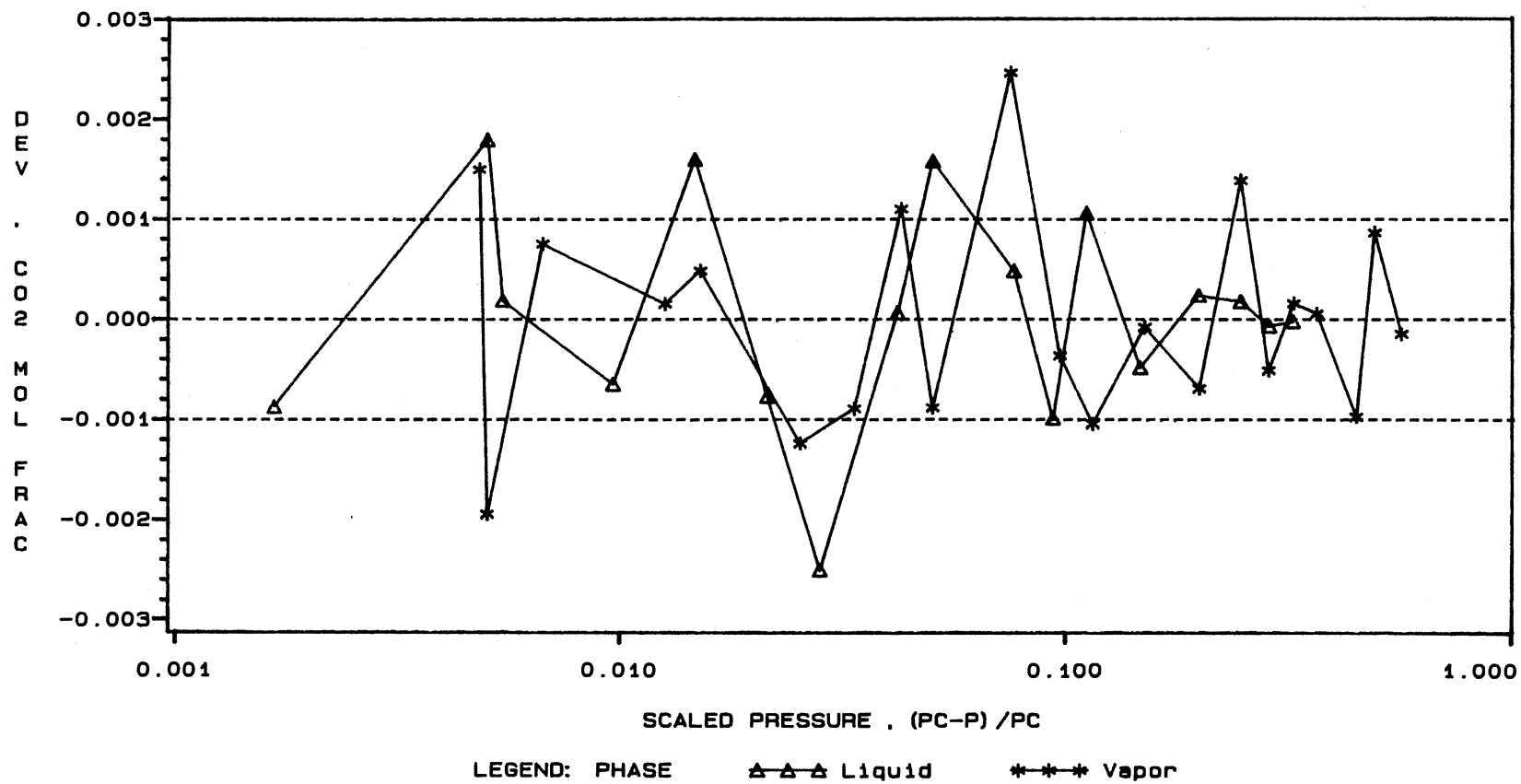


Figure 11. Smoothing Function Fit To Composition Data (Deviations) for CO₂ + n-Tetradecane at 344.3 K (160 °F)

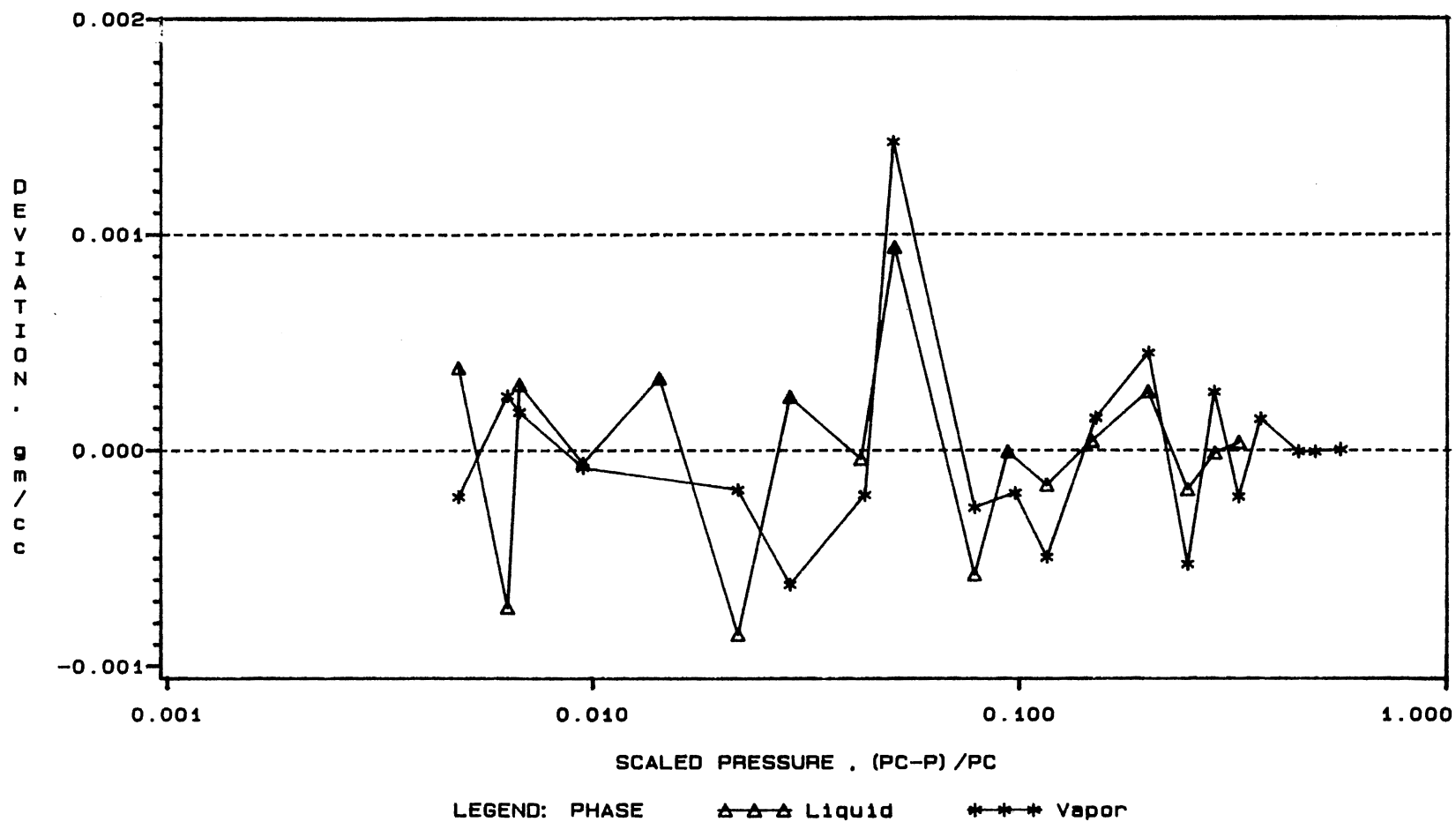


Figure 12. Smoothing Function Fit To Density Data (Deviations)
for CO₂ + n-Tetradecane at 344.3 K (160 °F)

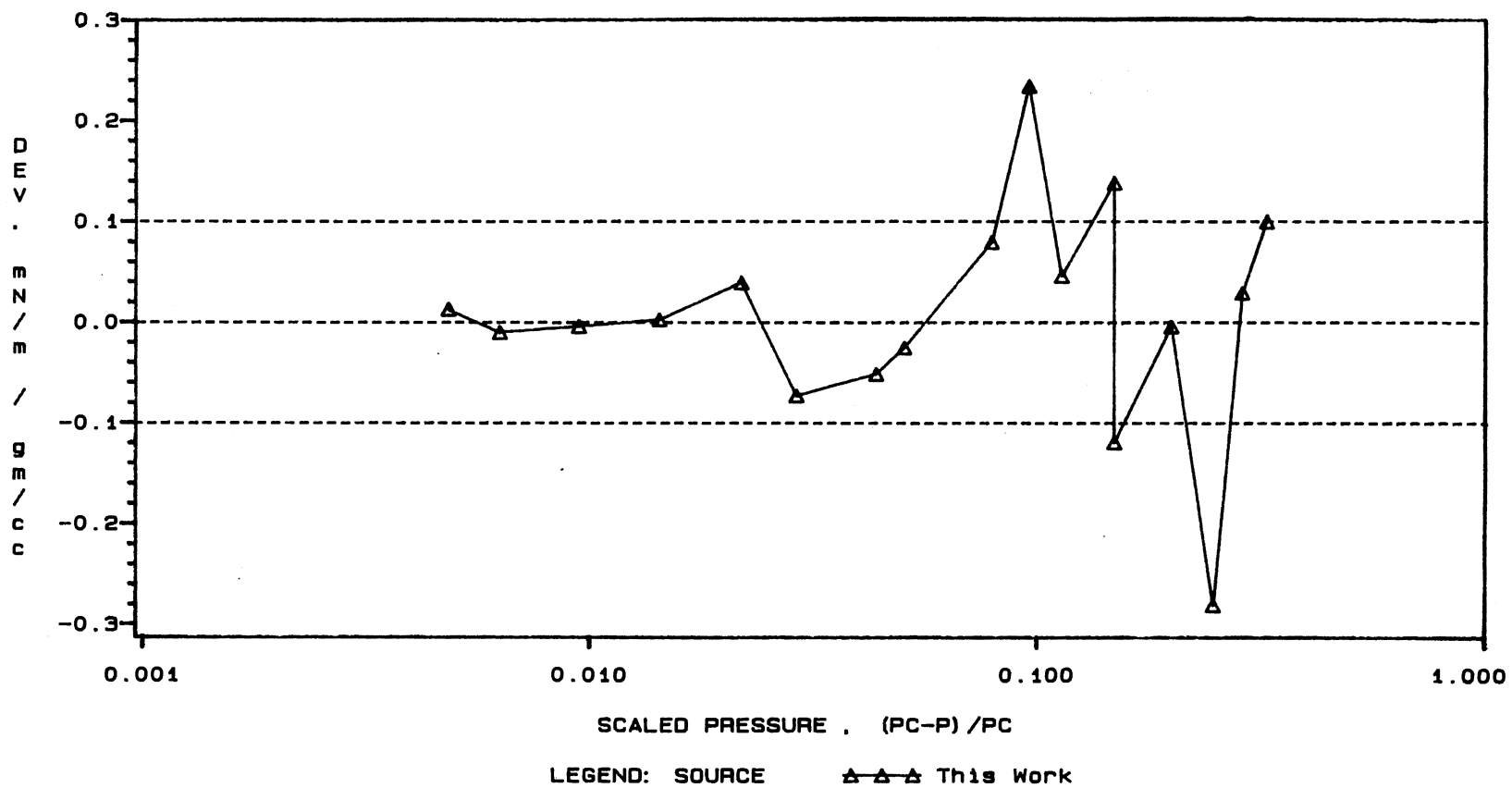


Figure 13. Smoothing Function Fit to Pendant Drop Data (Deviations) for CO₂ + n-Tetradecane at 344.3 K (160 °F)

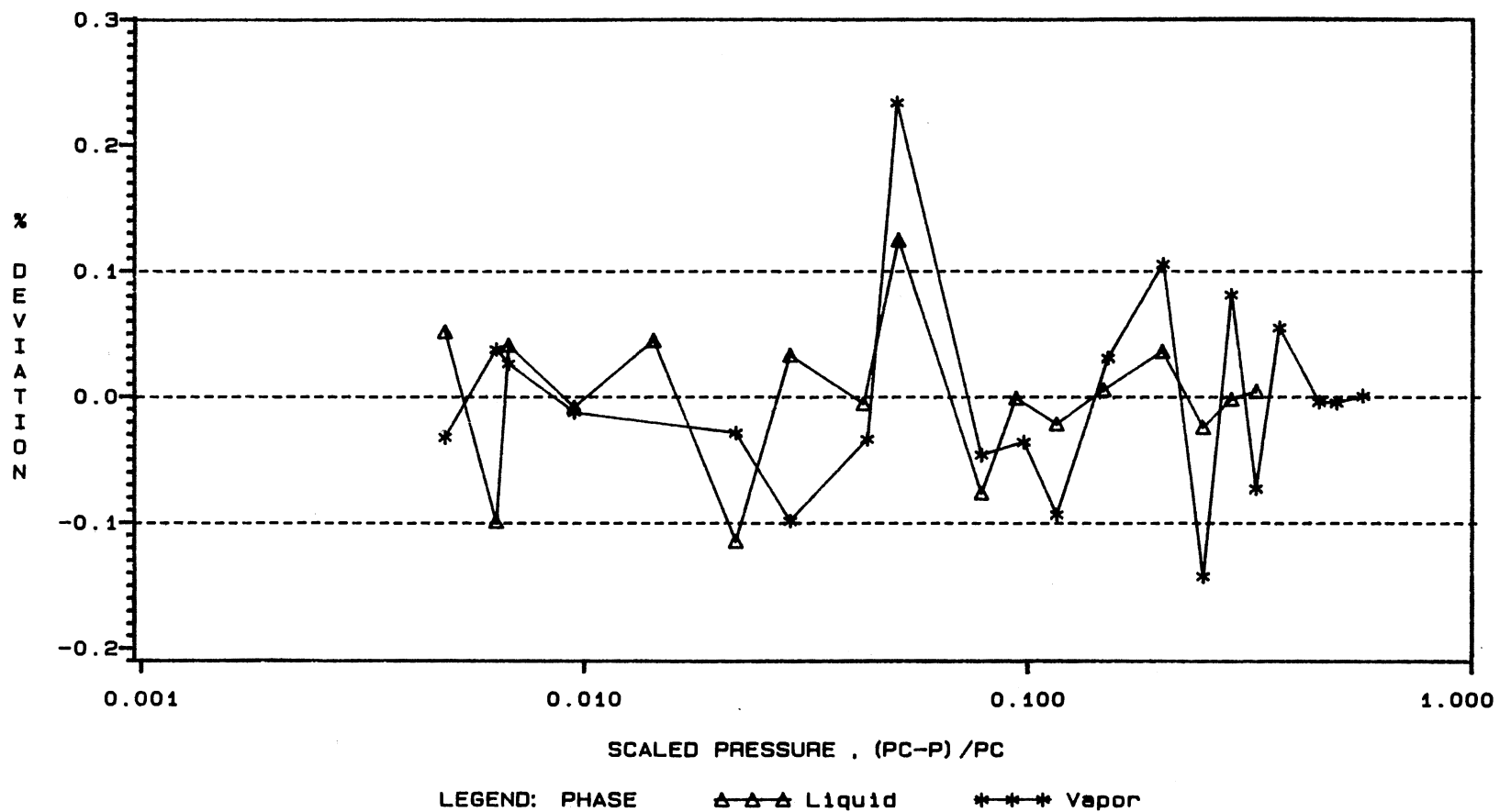


Figure 14. Smoothing Function Fit To Density Data (Percent Deviations) for CO₂ + n-Tetradecane at 344.3 K (160 °F)

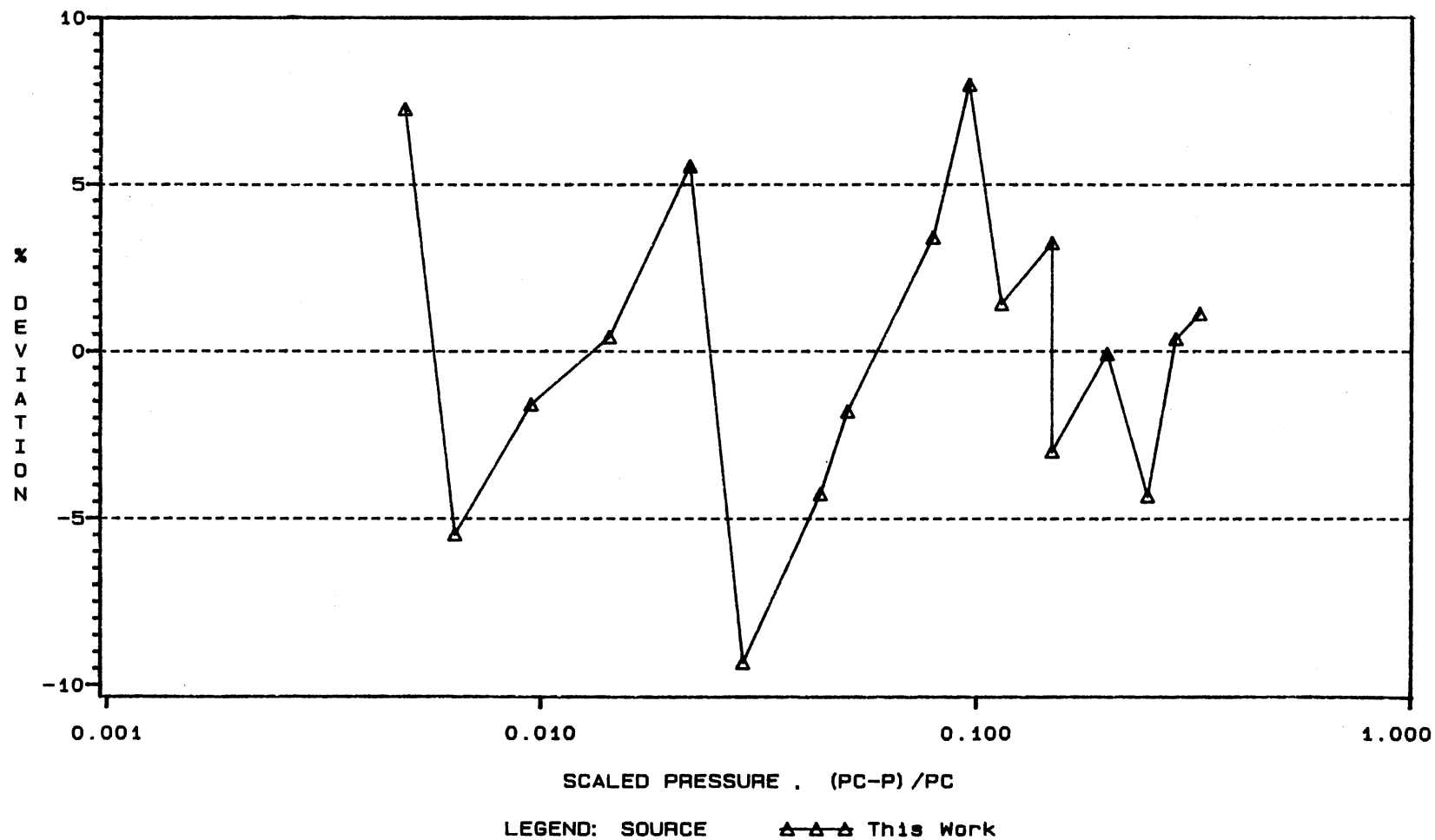


Figure 15. Smoothing Function Fit to Pendant Drop Data (Percent Deviations) for CO₂ + n-Tetradecane at 344.3 K (160 °F)

TABLE VII
PARAMETERS USED TO GENERATE SMOOTHED PROPERTIES IN
TABLES IV THROUGH VI

Phase Compositions (Equation 4.3)		Phase Densities (Equation 4.3)	
Units: Mole Fraction CO ₂		Units: (kg/m ³)10 ⁻³ or (gm/cc)	
PARAMETER	ESTIMATE	PARAMETER	ESTIMATE
ZC	0.92379386	RHOC	0.70849223
AO	0.98113728	AO	-1.40792517
A1	-1.68021254	A1	1.71919772
A2	2.32344137	A2	-5.51169409
A3	-6.54541147	A3	17.24483888
A4	6.41370932	A4	-25.37807471
A5	0.23375371	A5	15.66613172
BO	0.52509289	BO	0.37080281
B1	-3.39718892	B1	0.69566641
B2	21.02370193	B2	-9.38000350
B3	-60.24133169	B3	42.69697460
B4	83.20339046	B4	-67.99571566
B5	-43.19772693	B5	36.72891374

IFT-Density Difference Ratio
(Equation 4.4)

Units: [(mN/m)/(kg/m³)]10³ or [(mN/m)/(gm/cc)]

PARAMETER	ESTIMATE
GO	22.06349213
G1	5.16256039

for $\gamma/\Delta\rho$. These values were determined using all experimental data points. If the ρ^V at $P = 2342$ psia data point is deleted, the density WRMS reduces to 0.80. The unweighted deviations, root mean square (RMS), for the reduced data set are 0.001 mole fraction CO_2 for phase composition, 0.00041 gm/cc or 0.07% for phase density, and 0.108 (mN/m)/(gm/cc) or 3.6% for $\gamma/\Delta\rho$.

The parameters listed in Table VII were used in Equations 4.3 and 4.4 to calculate the smoothed values presented in Table III. The values shown in parentheses in Table III are extrapolated beyond the highest measured experimental pressure. They are considered accurate since they are in the near-critical asymptotic region where scaling law behavior holds. However extrapolations below the lowest measured experimental pressure may not be accurate and such extrapolations should not be attempted.

Comparisons of Experimental Results with Other Sources

There are no published data on the $\text{CO}_2 + n$ -tetradecane system, but several data sets have been made available from private communications. Table VIII compares the density data of Creek (42) with the present smoothed results for the $\text{CO}_2 + n$ -tetradecane system. The estimated uncertainty of the Creek data is 0.001, provided by the investigator. For the liquid densities, the data typically scatter by less than 0.4% for the mean value (i.e., ~ 0.003 gm/cc). For the vapor densities, the data typically scatter by less than 0.7% from the mean value (i.e., ~ 0.004 gm/cc). For both the liquid and vapor densities, the agreement with Creek is better above 2285 psia. Figure 16

TABLE VIII
 COMPARISONS OF PHASE DENSITY MEASUREMENTS WITH OTHER SOURCES
 FOR CO₂ + N-TETRADECANE AT 344.3 K (160°F)

Pressure, psia	Phase Density, (kg/m ³) x 10 ⁻³	
	This work (Smoothed)	Creek (42)
-----Liquid Phase-----		
2110	0.7547	0.759 (0.6%)*
2200	0.7531	0.758 (0.7%)
2285	0.7499	0.752 (0.3%)
2348	0.7425	0.743 (0.1%)
-----Vapor Phase-----		
2110	0.5355	0.529 (-1.2%)
2200	0.5818	0.574 (-1.3%)
2285	0.6223	0.622 (0.0%)
2348	0.6557	0.658 (0.4%)

*Numbers in parentheses are percentage deviations from values of the present work.

illustrates the comparisons of the experimental phase densities as a function of system pressure. Probably the major conclusion to be drawn from the above analyses is that the phase densities are consistent to no better than about 1%. These comparisons appear to confirm the accuracy of the present results to about that level.

For phase compositions, Bufkin (22) has made measurements of the solubility of CO₂ in n-tetradecane at 160°F. A comparison of these data appears in Table IX.

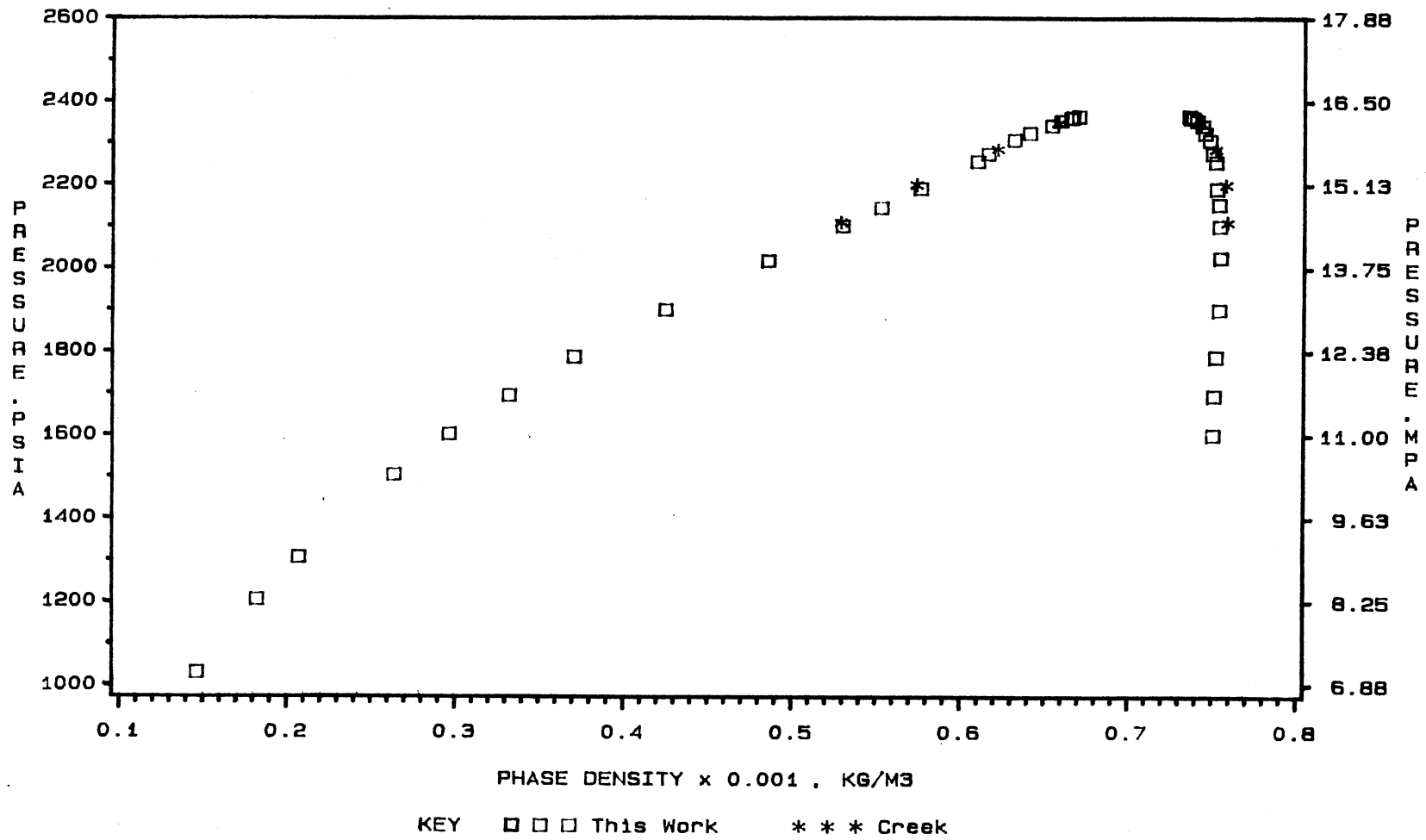


Figure 16. Comparison of Phase Density Data
 for CO₂ + n-Tetradecane at 344.3 K (160 °F)

TABLE IX

COMPARISONS OF LIQUID PHASE COMPOSITION MEASUREMENTS WITH OTHER SOURCES FOR CO₂ + N-TETRADECANE AT 344.3 K (160°F)

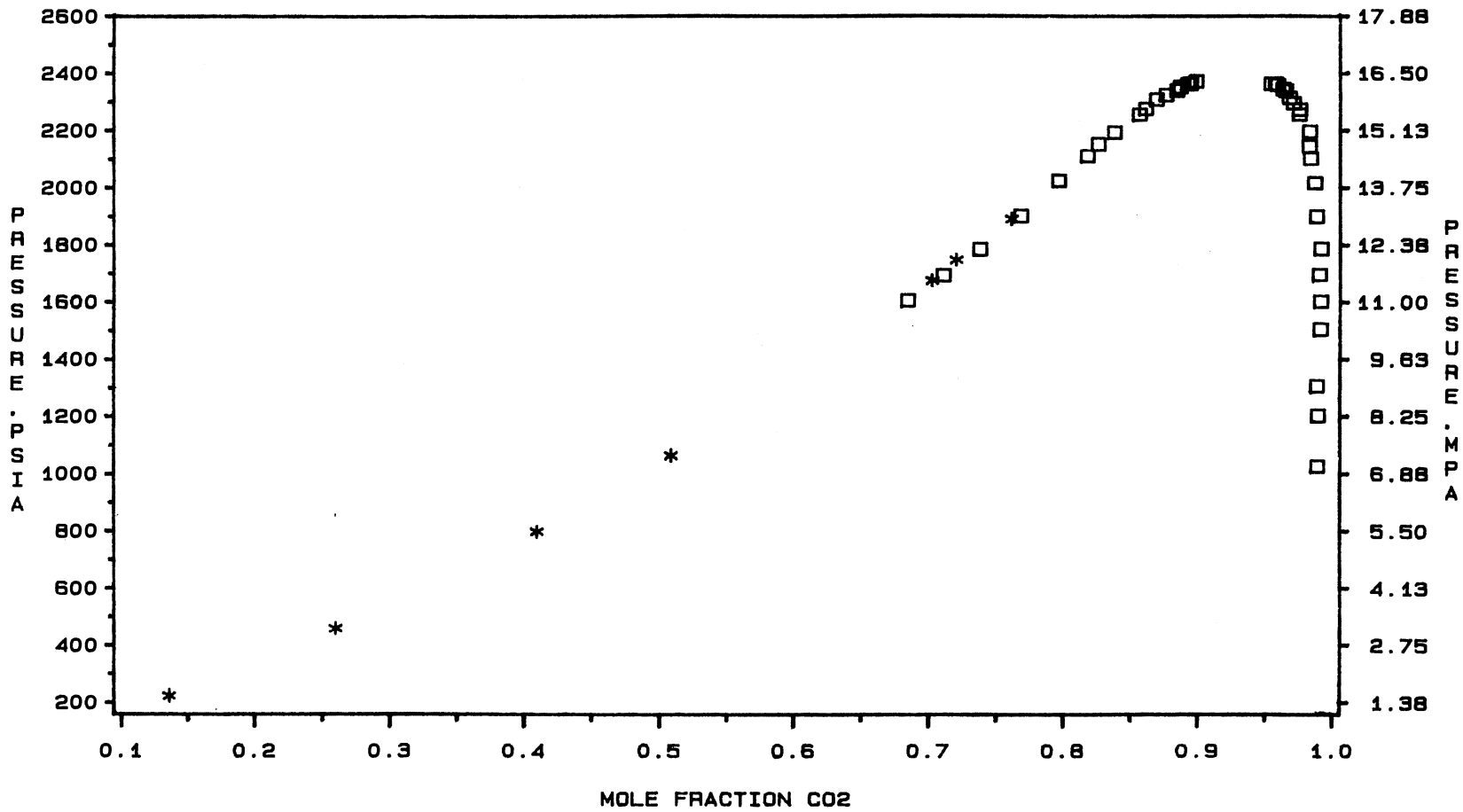
Pressure, psia	Liquid Mole Fraction CO ₂	
	This work (Smoothed)	Bufkin (22)
224.5		0.136
460.0		0.260
800.0		0.410
1065.0		0.509
1677.0	0.706	0.703 (-0.003)*
1748.5	0.727	0.721 (-0.006)
1832.0	0.766	0.762 (-0.004)

*Numbers in parentheses are deviations (mole fraction) from values of the present work.

Over the narrow pressure range in which the two data sets overlap, the differences in compositions are essentially within the combined experimental uncertainties in the data. This offers good confirmation of the composition data, since the two sets of measurements are based on very different experimental techniques. The Bufkin data can be used with confidence to extend the present liquid composition measurements to lower pressures. Figure 17 illustrates the comparisons of the experimental phase compositions as a function of system pressure.

Power Law (Scaling Behavior) Fit
to Experimental Data

Theoretical and experimental results confirm that fluids obey what has been termed "universal" scaling behavior as the fluids approach the



KEY □ □ □ This Work * * * Bufkin

Figure 17. Comparison of Phase Composition Data for CO₂ + n-Tetradecane at 344.3 K (160 °F)

critical point (46). This behavior implies that all fluid systems (pure components and mixtures) obey certain general relationships in the near-critical region, and some of the parameters in these relationships are independent of the particular system of interest. The following relationships for $\gamma/\Delta\rho$ and density difference are suggested by "power laws" for the near-critical region:

$$\gamma/\Delta\rho = A(P^*)^{2\nu-\beta} \quad (4.8)$$

$$\Delta\rho = B(P^*)^\beta \quad (4.9)$$

where A and B are constants for the specific system of interest and ν and β are system independent universal scaling exponents ($\nu = 0.630$ and $\beta = 0.32$ (21)). Figure 18 illustrates $\gamma/\Delta\rho$ as a function of scaled pressure on a log-log plot. This type of plot expands the near critical, low IFT region and illustrates the linear behavior required by "power law" scaling behavior as the critical point is approached. The slope of the line should be a specific, system independent universal value of $2\nu-\beta = 0.93$, dictated by theory (21). The present data show good agreement with scaling law over the entire pressure range covered. Figure 19 plots density difference as a function of scaled pressure on a log-log plot. The liquid and vapor density values are smoothed data predicted at the liquid density pressure points. Figure 19 illustrates the range over which the smoothed data follow simple scaling behavior.

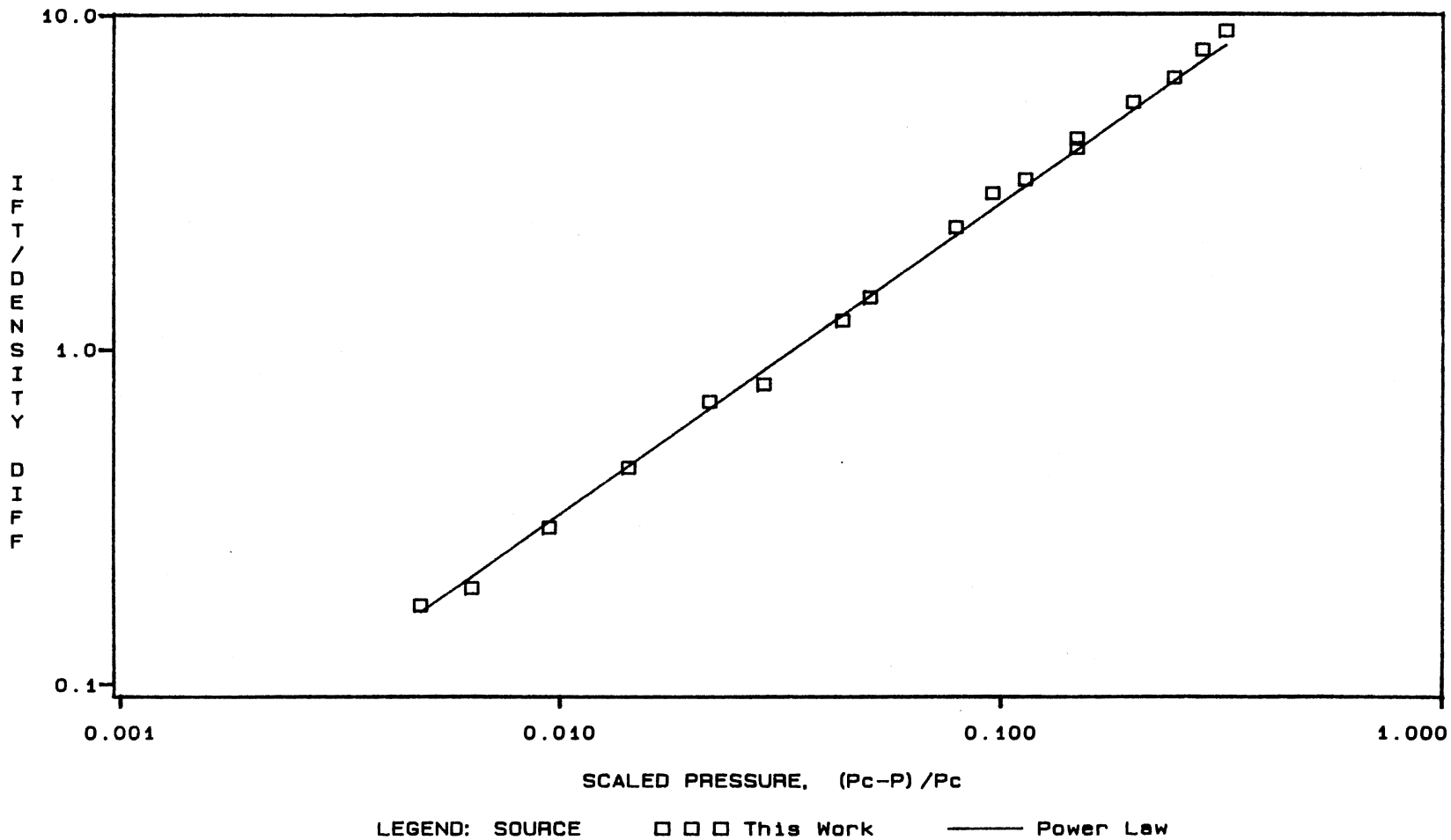
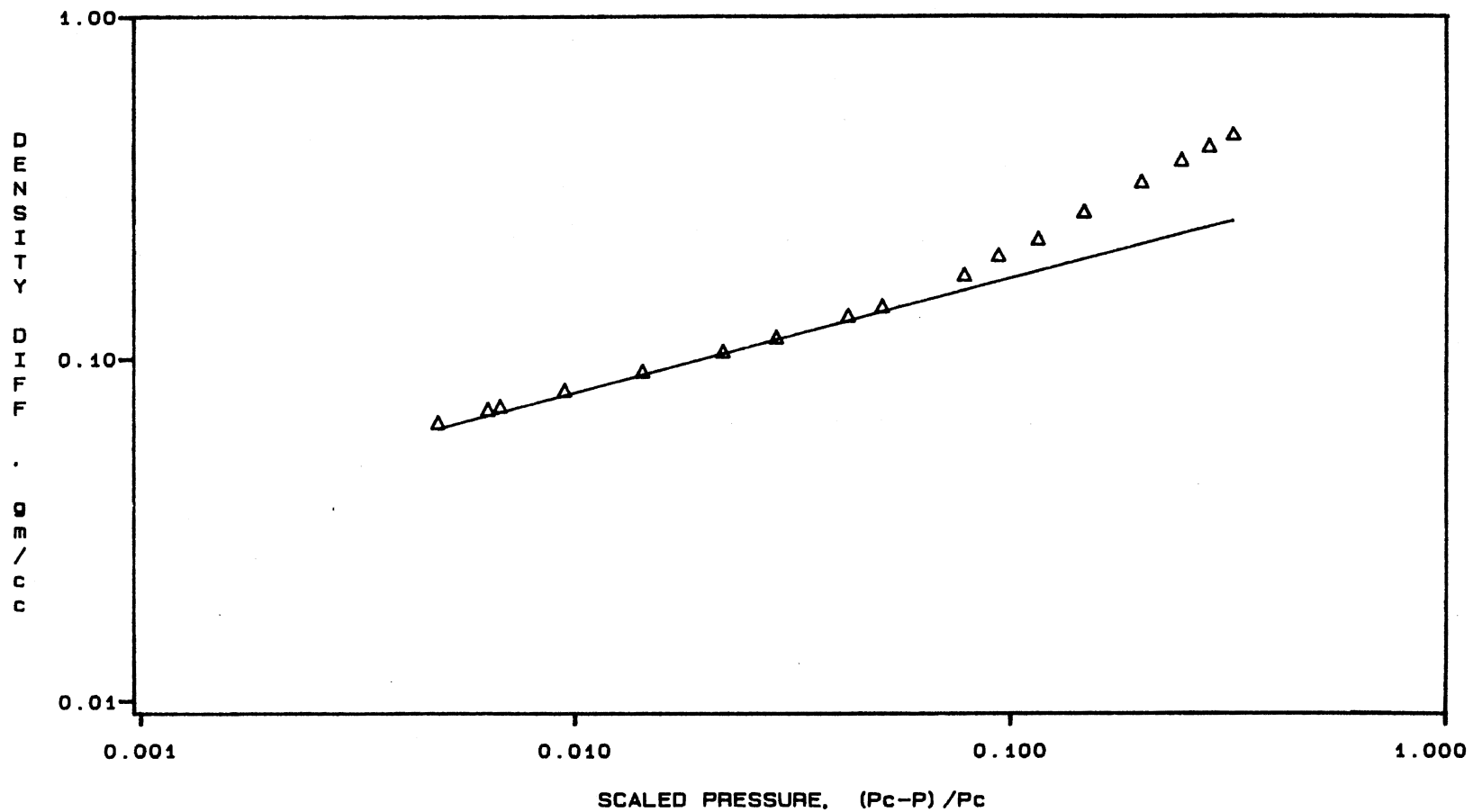


Figure 18. Power Law Fit To Pendant Drop Data for CO₂ + n-Tetradecane at 344.3 K (160 °F)



LEGEND: SOURCE Δ Δ Δ SMOOTHED DATA ——— POWER LAW

Figure 19. Power Law Fit To Smoothed Density Data for CO₂ + n-Tetradecane at 344.3 K (160 °F)

CHAPTER V

INTERFACIAL TENSION CORRELATIONS

Four interfacial tension correlations were evaluated in the present work. The four correlations are (1) the Weinaug-Katz (W-K) correlation (Equation 2.7), (2) the Hugill-Van Welsenes (H-VW) modified form of the W-K correlation (Equation 2.11), (3) the Lee-Chien (L-C) mixed parachor correlation (Equation 2.15), and (4) a correlation developed in the present work (discussed in more detail later in this chapter).

As mentioned in Chapter II, the W-K, H-VW, and L-C correlations were chosen because of their ease of application. The input variables required for these correlations are available through widely known data bases (e.g., National Bureau of Standards) or predictive equations (e.g., Peng-Robinson EOS). Their simplicity makes the correlations well suited for computer applications such as petroleum reservoir simulators. Table X lists the various input parameters required by the three correlations.

The equilibrium phase compositions and densities and the pure component physical properties can be obtained from available data bases or predicted by appropriate correlations. In the following correlation evaluations, experimental phase compositions and densities were used. The experimental data for the five CO₂ + hydrocarbon binary systems used to evaluate the correlations are presented in Appendix A. Physical properties for the pure substances were obtained from National Bureau of Standards (NBS) publications and are presented in Appendix D. The

TABLE X
MULTICOMPONENT IFT CORRELATION PARAMETERS

Input Parameter	W-K	H-VW	L-C
1. Equilibrium phase Compositions	yes	yes	yes
Densities	yes	yes	yes
2. Parachor - mixed or pure component	yes	yes	yes
3. Binary interaction IFT parameter	no	yes	no
4. B - parachor correlation parameter	no	no	yes
5. Individual pure component physical properties, (e.g., P_c , V_c , T_c , etc.)	no	yes	yes

parameters specific to the individual correlations (e.g., binary interaction parameter and L-C B parameter) were evaluated in the present work. The parachor, which is required in all three correlations, can be obtained from published tables (6) or predicted by various correlations. The evaluation of several parachor correlations is presented later in this chapter.

The W-K, H-VW, and L-C IFT correlations were evaluated by performing regressions to optimize various parameters in the correlations. This type of evaluation tested the frameworks of the correlations and their ability to predict IFT. Several parachor correlations were also evaluated and their results were used in the various IFT correlations. A new parachor correlation developed in the present work is presented and evaluated with the other parachor correlations. After establishing the suitability of the IFT correlation frameworks, the correlations were compared using predicted input parameters such as parachors and L-C B parachor correlating parameters.

Regression analysis was used to optimize various parameters in the W-K, H-VW, and L-C IFT correlations. Table XI lists the various parameters optimized in the correlations. The numbers shown are for the complete data set of five binary systems.

Weinaug-Katz Correlation Evaluation

The W-K correlation (Equation 2.7) requires phase compositions, phase densities, and pure component parachors as input data. In applications of the W-K correlation, the phase compositions and densities are often calculated from equations of state (EOS) and the

TABLE XI
IFT CORRELATION PARAMETERS OPTIMIZED IN REGRESSION ANALYSES

Parameter	Number of parameters		
	W-K	H-VW	L-C
Pure component parachors - $[P]_i$	6	6	-
Scaling exponent - k	1	1	1
Binary interaction IFT parameter - λ_{ij}	-	*5(8)	-
B - parachor correlating parameter	-	-	6
Total parameters	7	12 (15)	7

* The binary interaction IFT parameter was evaluated in two ways one per system (total of five) and one per data isotherm (total of eight).

parachors from structural contribution methods like those proposed by Quayle (6). As mentioned earlier, the correlation was evaluated by performing regressions using experimental data to determine the optimum values for the individual component parachors and the scaling exponent (k). The experimental data used to evaluate the W-K correlation were obtained at Oklahoma State University using the experimental apparatus described in Chapter III. The data includes five binary systems of CO₂ with n-butane, n-decane, n-tetradecane, benzene, and cyclohexane, respectively. The experimental data are shown in Tables XXX through XXXVII, Appendix A.

The objective function, SS, in the non-linear regressions is indicated below:

$$SS = \sum_{i=1}^K [(Y^{\text{calc}} - Y^{\text{exp}})/W]_i^2$$

where i is from 1 to K , the number of experimental observations.

The regression program determined the parameters (listed in Table XI) in the correlation (model) which minimized the value of the function SS. Here, Y is the calculated (calculated from model equation, e.g., W-K, H-VW) or experimental value of the interfacial tension and W is the weighting factor. Three different weighting factors were used in the W-K correlation regressions. They include:

$$W_1 = Y^{\text{exp}} ; \text{ this minimizes the fractional (\%)} \\ \text{errors in the predictions}$$

$$W_2 = \epsilon_Y ; \text{ the expected uncertainty in the regressed variable } Y$$

$W_3 = \sigma_Y$; the fully propagated error

where

$$\sigma_Y^2 = \epsilon_Y^2 + \sum_{i=1}^N \left(\frac{\partial Y}{\partial X_i} \right)^2 \epsilon_{X_i}^2$$

and

$N = 1$ number of independent variables

ϵ_X = expected uncertainty (standard deviation) in the independent variable, X .

$X = (x, y, \rho^L, \rho^V)$

The specified values of ϵ employed were as follows:

$$\epsilon_\gamma = \epsilon_{(\gamma/\Delta\rho)} = 0.04 (\gamma^{\text{exp}})^{0.08} \text{ mN/m}$$

$$\epsilon_x = \epsilon_y = 0.002 \text{ (mole fraction)}$$

$$\epsilon_{\rho^L} = \epsilon_{\rho^V} = 0.0005 \text{ gm/cc}$$

The fully propagated weighting factor (if properly evaluated) results in the most accurate regressed parameters because it accounts for the effects of uncertainties in all variables used in the W-K correlation.

The five binary systems mentioned above were evaluated: (1) on an isotherm-by-isotherm basis, (2) on a system-by-system basis which included all isotherms in a particular system, and (3) with all data from the five systems lumped together. The number of parameters regressed depends on whether the regression is on a single isotherm (k and two parachors regressed), a complete system (k and two parachors but

larger data set), or all data (k and six parachors). Table XII through XVI present the results of the regressions. In most cases, the different weighting factors had little effect on the regressed results. In the discussion that follows, all references concerning regression results refer to results for fully propagated weighting factors (W_3).

Table XII presents results of $\text{CO}_2 + n\text{-butane}$ at 115, 160, and 220°F. The complete experimental data set, with no deletions, was used in the regressions. The CO_2 parachor shows considerable variation among isotherms (67 - 124), but the $n\text{-butane}$ parachor remains fairly constant at 191 - 206. The variation in the CO_2 parachor indicates the lower correlating value of the CO_2 parachor. This result was substantiated because wide variation in the CO_2 parachor value had only small effects on k , the $n\text{-butane}$ parachor, and the errors in predicted (γ). The regressions made with the combined data set yields more accurate results of the scaling exponent (k) and two parachors because the number of experimental data points increases, which lowers the standard error of the regressed parameters. The average absolute percent deviations (AAPD) increased from 2% to 3% for the individual isotherms up to 5.4% for the combined data regression, still a very acceptable number. The regressed scaling exponent (k) for the combined data set is $k = 3.52$ which is in good agreement with the accepted experimental value of 3.55 (27). Figures 20 through 22 are plots of the regression results for the $\text{CO}_2 + n\text{-butane}$ system. Figure 20 illustrates the accuracy of the W-K predicted IFT values at 115, 160, and 220°F. Figure 21 shows percent deviations in the IFTs and Figure 22 shows fully propagated weighted deviations. The lines in Figure 20 (as well as in Figures 23, 26, 29,

TABLE XII
EVALUATION OF WEINAUG-KATZ CORRELATION FOR
CO₂ + N-BUTANE AT 115, 160 AND 220°F

No. of Data Pts.	Weighting Factor	Regressed Parameter			Error in Predicted IFTs	
		Parachors		Critical Exponent, k	RMSE mN/m	AAPD %
		CO ₂	C ₄			
-----CO ₂ + n-butane at 115°F-----						
18	W ₁	88	192	3.52	0.054	2.7
18	W ₂	89	191	3.54	0.057	2.7
18	W ₃	89	191	3.54	0.057	2.7
-----CO ₂ + n-butane at 160°F-----						
12	W ₁	68	205	3.48	0.027	2.3
12	W ₂	67	206	3.48	0.026	2.3
12	W ₃	67	206	3.48	0.026	2.3
-----CO ₂ + n-butane at 220°F-----						
12	W ₁	123	194	3.86	0.019	2.1
12	W ₂	124	194	3.87	0.019	2.1
12	W ₃	124	194	3.86	0.019	2.1
-----CO ₂ + n-butane at 115, 160, and 220°F-----						
42	W ₁	87	195	3.56	0.144	5.1
42	W ₂	85	197	3.52	0.123	5.4
42	W ₃	85	197	3.52	0.128	5.4

Note: Regressions included all experimental data points

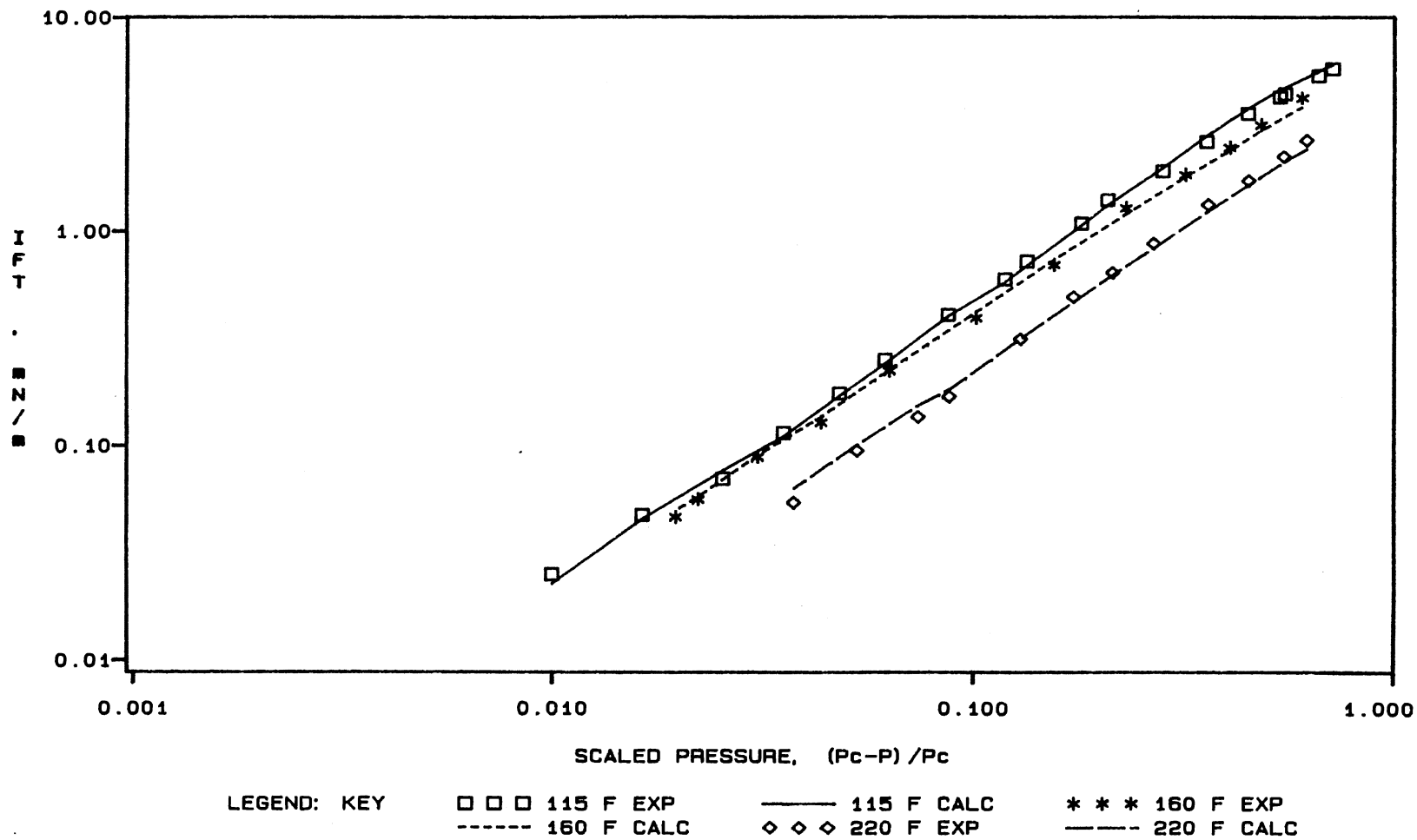


Figure 20. Comparison of Experimental IFTs to W-K Model for CO₂ + n-Butane at 115, 160, and 220 °F

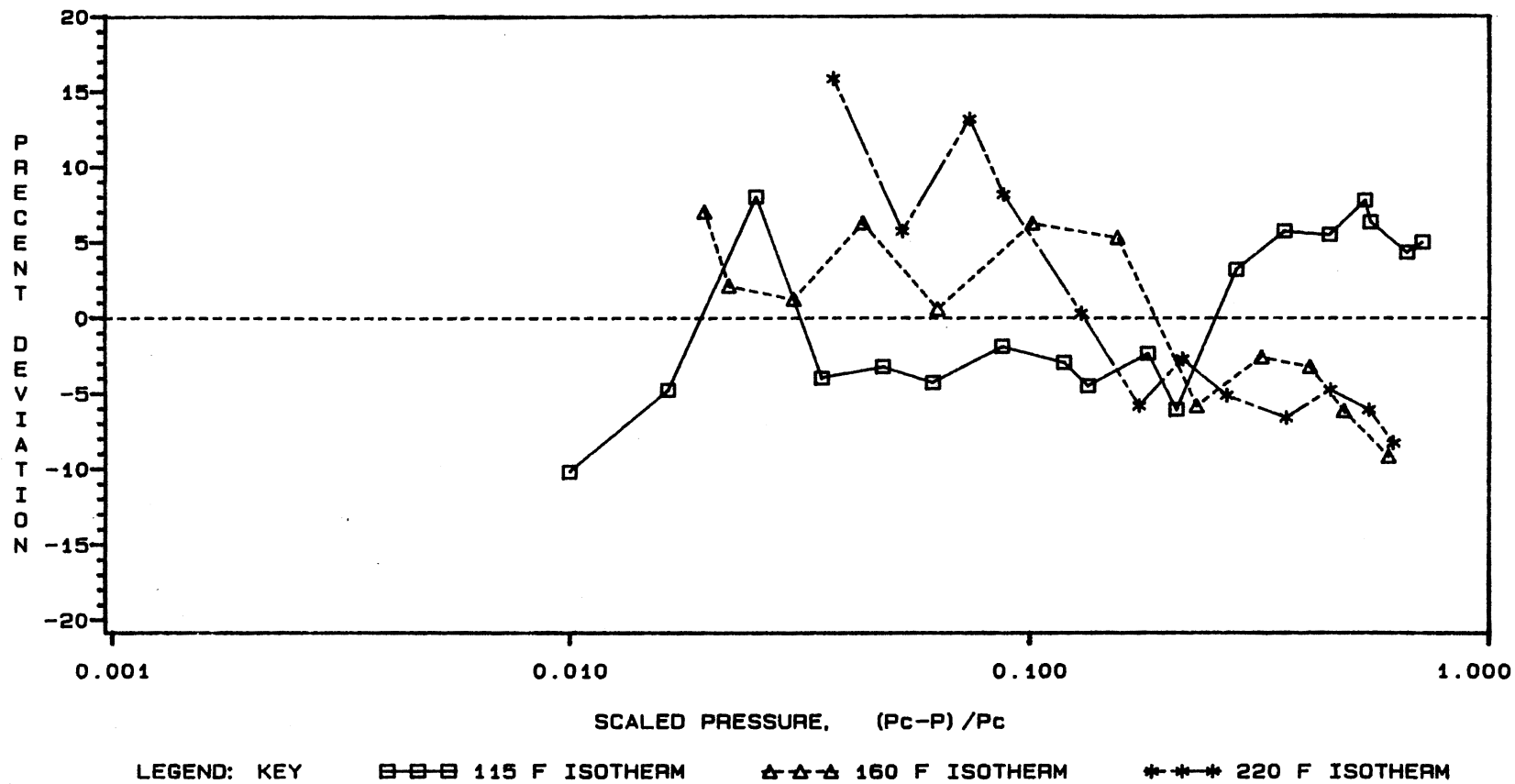


Figure 21. Comparison of Experimental IFTs to W-K Model, (Percent Deviations) for CO₂ + n-Butane at 115, 160, and 220 °F

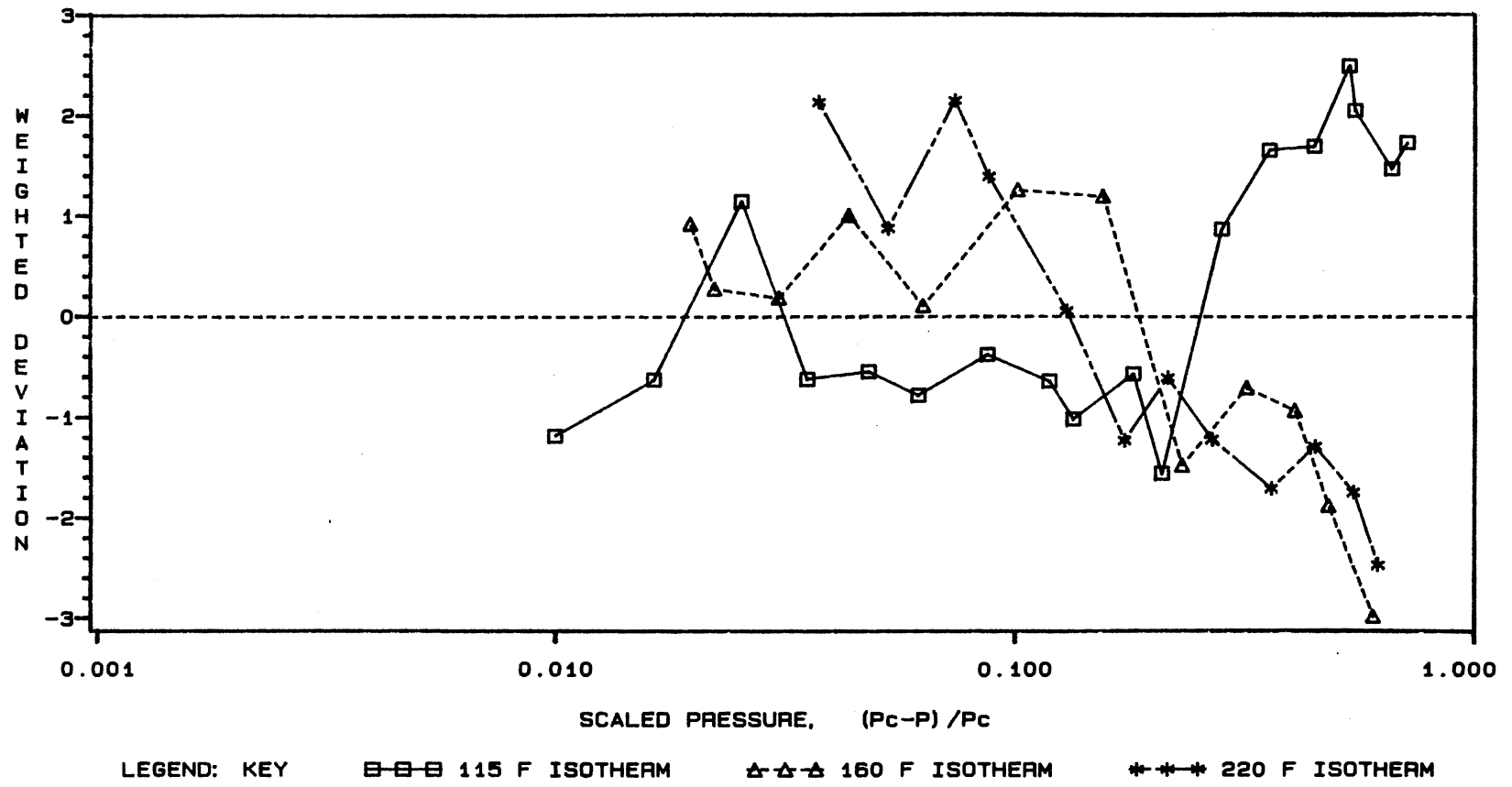


Figure 22. Comparison of Experimental IFTs to W-K Model, (Weighted Deviations) for CO₂ + n-Butane at 115, 160, and 220 °F

32, and 35 presented later) are not smooth curves; they are point-to-point connections in predicted IFTs. They show scatter as a result of the uncertainties associated with the input variables from the predicted values (ρ^L , ρ^V , x , y).

Table XIII presents results of the W-K regressions for the CO₂ + n-decane system at 160 and 220°F. The regressions were made in a manner analogous to those for CO₂ + n-butane. Again, the CO₂ parachor shows considerable variation, but the n-decane parachor is more constant at values near 450. The AAPD for the combined data set was 5.7% and the scaling exponent was $k = 3.62$. Figures 23 through 25 contain the regression results for CO₂ + n-decane. Figure 23 presents the W-K predicted IFT values in graphical form at 160 and 220°F. Figure 24 shows percent deviations in the IFTs and Figure 25 shows fully propagated weighted deviations.

The regressions for CO₂ + n-tetradecane were performed on two different data sets. Since the experimental phase densities, phase compositions, and $\gamma/\Delta\rho$ data were not always taken at the same pressure, the raw data were interpolated to give phase densities and compositions at the experimental $\gamma/\Delta\rho$ data pressures. These regressions are indicated under the raw data heading in Table XIV. Regressions were also made on a smoothed data set covering the same pressure range as the raw data and are shown in Table XIV under the heading of smoothed data. The smoothed data were calculated by the smoothing functions discussed in Chapter IV. Regressions were performed where all three parameters (two parachors and k) were treated as variables. These regressions produced unrealistic values of the CO₂ parachor, $[P]_{\text{CO}_2} = 2.41$ and the scaling exponent, $k = 4.68$. Next, regressions were made

TABLE XIII
EVALUATION OF WEINAUG-KATZ CORRELATION FOR
CO₂ + N-DECANE AT 160 AND 220°F

No. of Data Pts.	Weighting Factor	Regressed Parameter			Error in Predicted IFTs	
		Parachors		Critical Exponent, k	RMSE mN/m	AAPD %
		CO ₂	C ₁₀			
-----CO ₂ + n-decane at 160°F-----						
18	W ₁	99	431	3.67	0.237	5.8
18	W ₂	74	440	3.66	0.153	6.2
18	W ₃	64	444	3.61	0.139	6.4
-----CO ₂ + n-decane at 220°F-----						
23	W ₁	105	457	3.64	0.061	4.8
23	W ₂	114	456	3.57	0.025	4.1
23	W ₃	88	455	3.61	0.033	4.2
*21	W ₃	80	454	3.58	0.021	2.2
-----CO ₂ + n-decane at 160 and 220°F-----						
41	W ₁	59	449	3.66	0.088	6.2
41	W ₂	49	450	3.62	0.074	5.7
41	W ₃	55	450	3.62	0.079	5.7

* Dropped the two highest pressure (P = 2381 and 2386 psia) - lowest IFT data points. Unless noted, regressions included all experimental data.

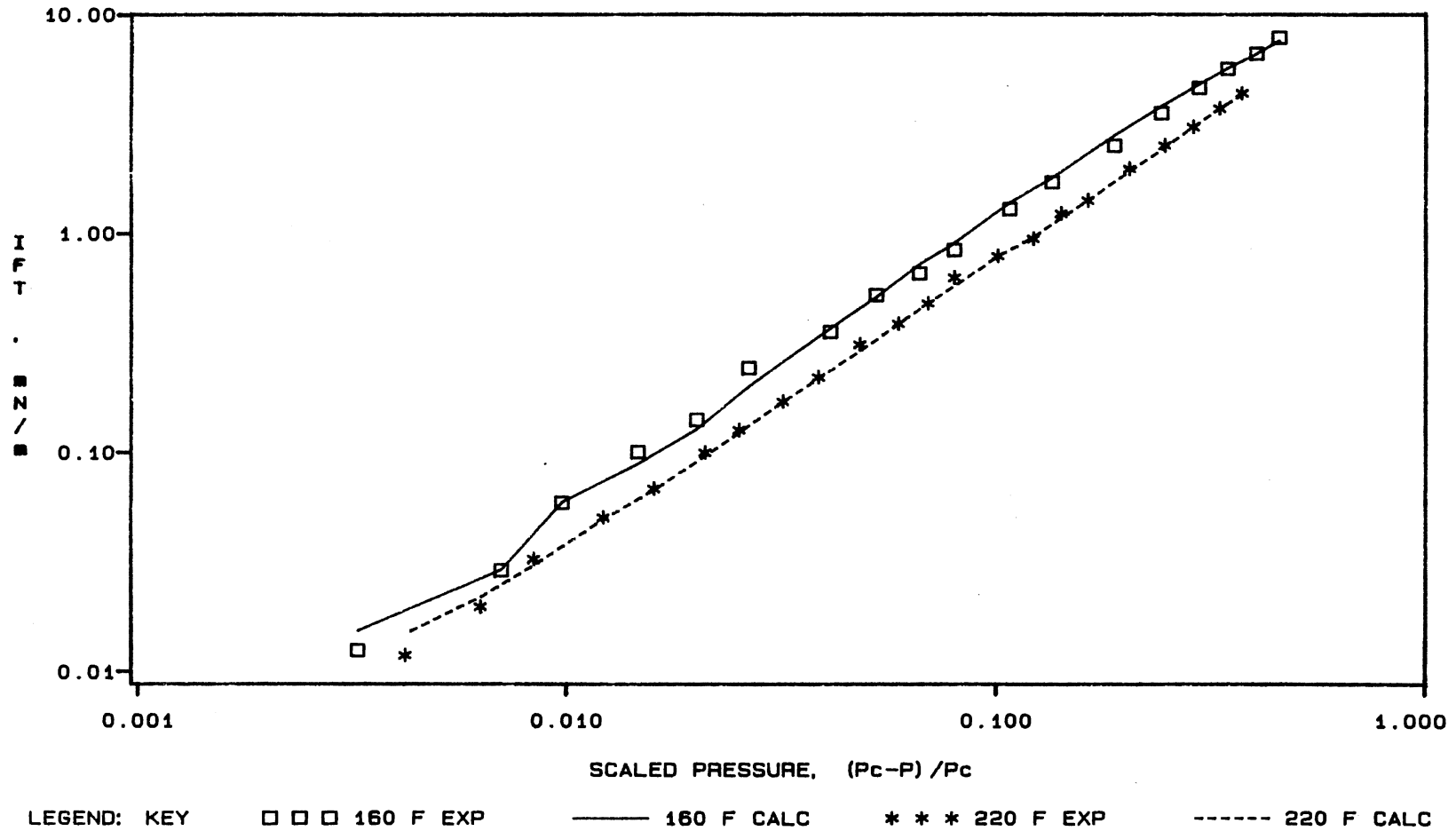
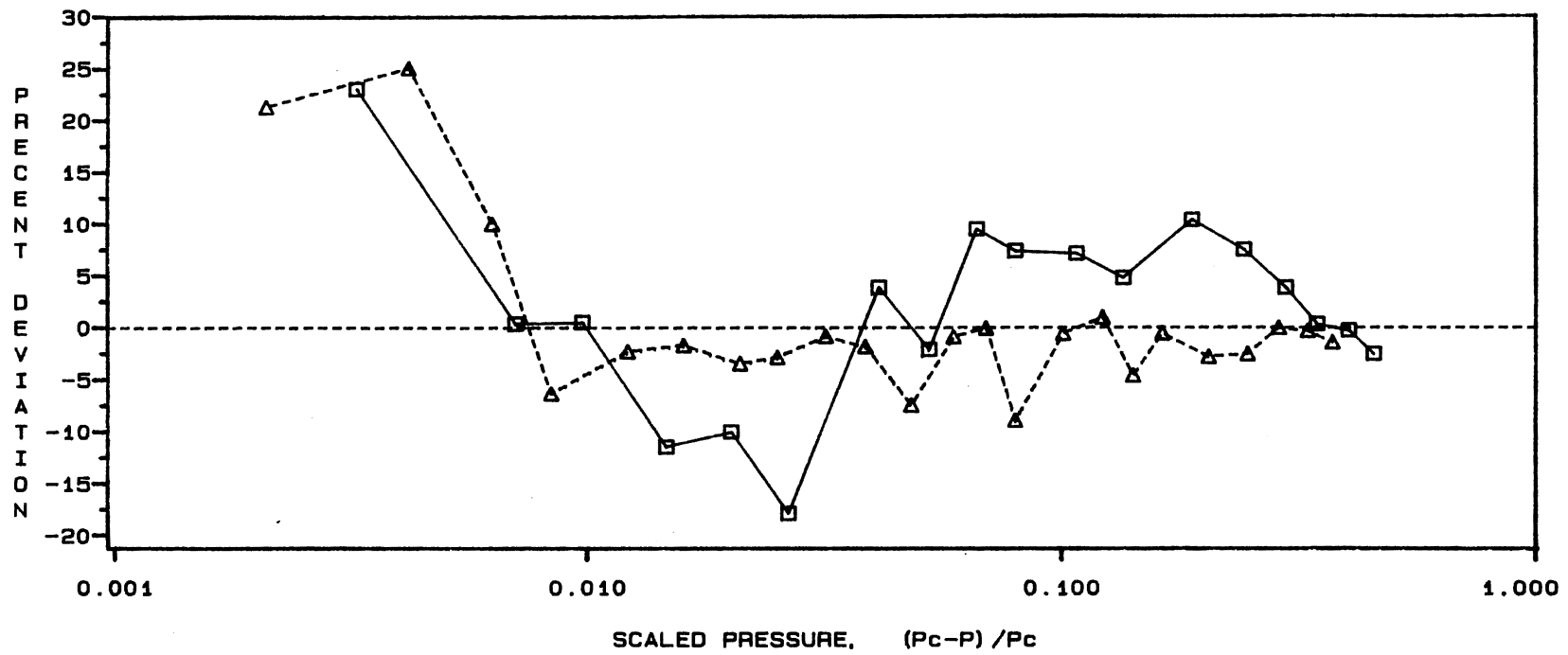
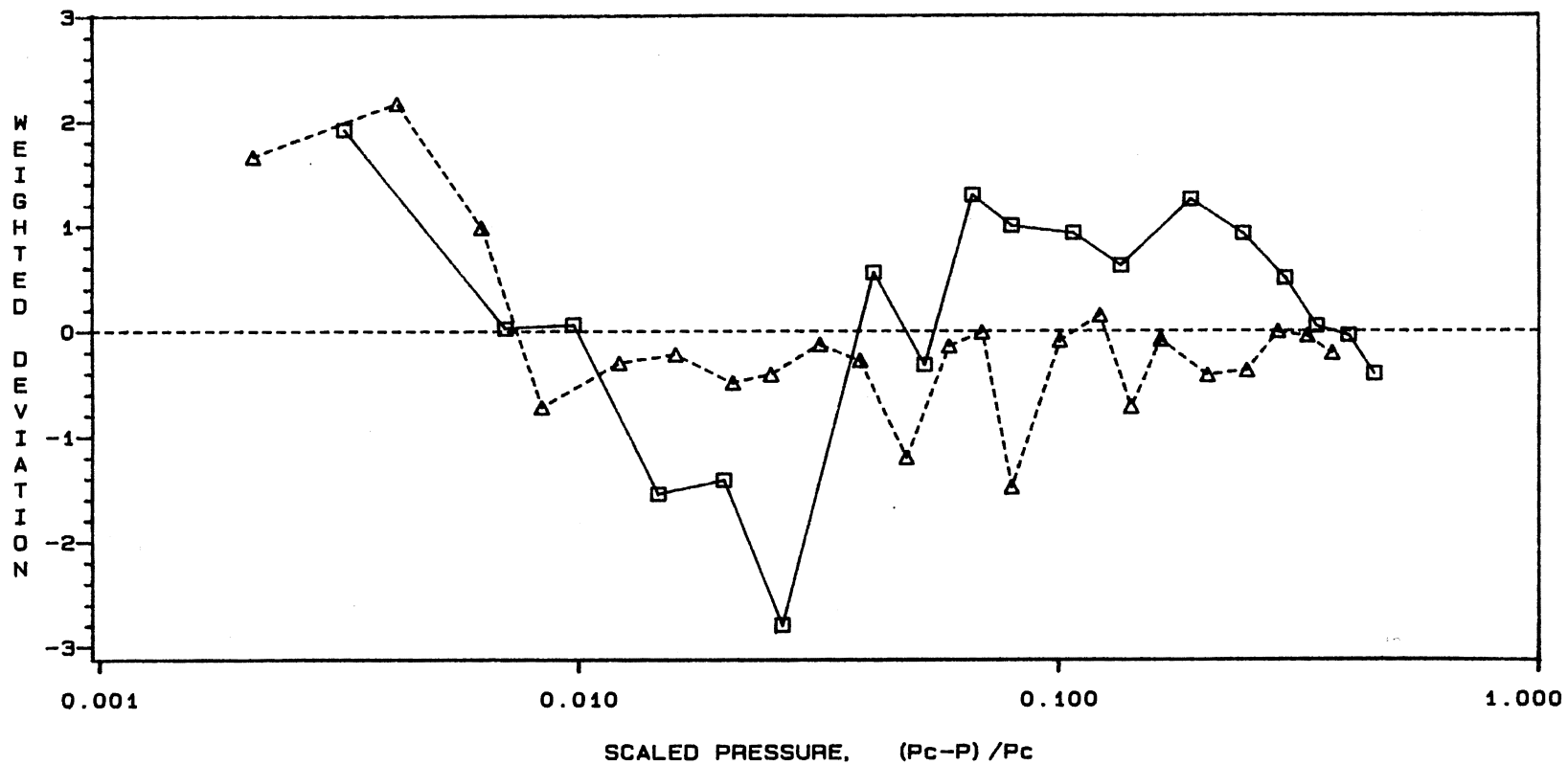


Figure 23. Comparison of Experimental IFTs to W-K Model for CO₂ + n-Decane at 160 and 220 °F



LEGEND: KEY □-□-□ 160 F ISOTHERM △-△-△ 220 F ISOTHERM

Figure 24. Comparison of Experimental IFTs to W-K Model, (Percent Deviations) for CO₂ + n-Decane at 160 and 220 °F



LEGEND: KEY □-□-□ 160 F ISOTHERM ▲-▲-▲ 220 F ISOTHERM

Figure 25. Comparison of Experimental IFTs to W-K Model, (Weighted Deviations) for CO₂ + n-Decane at 160 and 220 °F

TABLE XIV
EVALUATION OF WEINAUG-KATZ CORRELATION FOR
CO₂ + N-TETRADECANE AT 160°F

No. of Data Pts.	Weighting Factor	Regressed Parameter			Error in Predicted IFTs	
		Parachors		Critical Exponent, k	RMSE mN/m	AAPD %
		CO ₂	C ₁₄			
-----Raw Data-----						
17	W ₁	54	601	*4.00	0.131	9.8
17	W ₁	97	653	*3.55	0.196	14.5
17	W ₂	44	590	*4.00	0.065	9.2
17	W ₃	56	610	*4.00	0.218	9.8
17	W ₃	88	646	*3.55	0.162	14.0
17	W ₃	2.41	541	4.68	0.027	3.9
-----Smoothed Data-----						
18	W ₁	54	599	*4.00	0.110	8.2
18	W ₁	96	648	*3.55	0.151	11.3
18	W ₂	48	592	*4.00	0.072	8.4
18	W ₃	55	605	*4.00	0.154	8.2
18	W ₃	92	647	*3.55	0.148	11.8
18	W ₃	-5.26	534	4.78	0.030	4.0

* Parameters fixed at listed values

Note: The smoothed data set covers only the pressure range where both liquid and vapor raw data exist

restricting the scaling exponent to $k = 4.00$. These regressions produced more reasonable results. The raw data regression gave a CO_2 parachor of 56 and AAPD of 9.8% for $k = 4.00$. The smoothed data regression gave a CO_2 parachor of 55 and AAPD of 8.2% for $k = 4.00$. The last regressions made restricted the scaling exponent to $k = 3.55$. These regressions also produced reasonable values of the parachors, $\text{CO}_2 = 88$ and $C_{14} = 646$ for the raw data, and $\text{CO}_2 = 92$ and $C_{14} = 647$ for the smoothed data, but the AAPD increased from 9.8% to 14.0% for the smoothed data and from 8.2% to 11.8% for the raw data. The smoothed data regressions might be viewed as more valid because the vapor and liquid data are at the same pressure in the smoothed data set; whereas, in the raw data set the liquid and vapor data are interpolated at a common pressure between the liquid and vapor experimental pressure. Figures 26 through 28 are plots of the regression results for the $\text{CO}_2 + n$ -tetradecane system. Figure 26 illustrates the accuracy of the W-K predicted IFT values at 160°F . Figure 27 shows percent deviations in the IFTs and Figure 28 shows fully propagated weighted deviations.

Table XV presents the regression results for the $\text{CO}_2 + \text{benzene}$ and $\text{CO}_2 + \text{cyclohexane}$ systems. In these regressions, all parameters (two parachors and k) were regressed. In both the benzene and cyclohexane regressions, the scaling exponents ($k_{\text{benzene}} = 3.40$ and $k_{\text{cyclohexane}} = 3.47$) are in agreement with the accepted experimental value of 3.55. The AAPD of 5.3% for benzene and 4.7% for cyclohexane are again reasonable values. Figures 29 through 31 are plots of the regression results for the $\text{CO}_2 + \text{benzene}$ system. Figure 29 illustrates the accuracy of the W-K predicted IFT values at 160°F . Figure 30 shows percent deviations in the IFTs and Figure 31 shows fully propagated

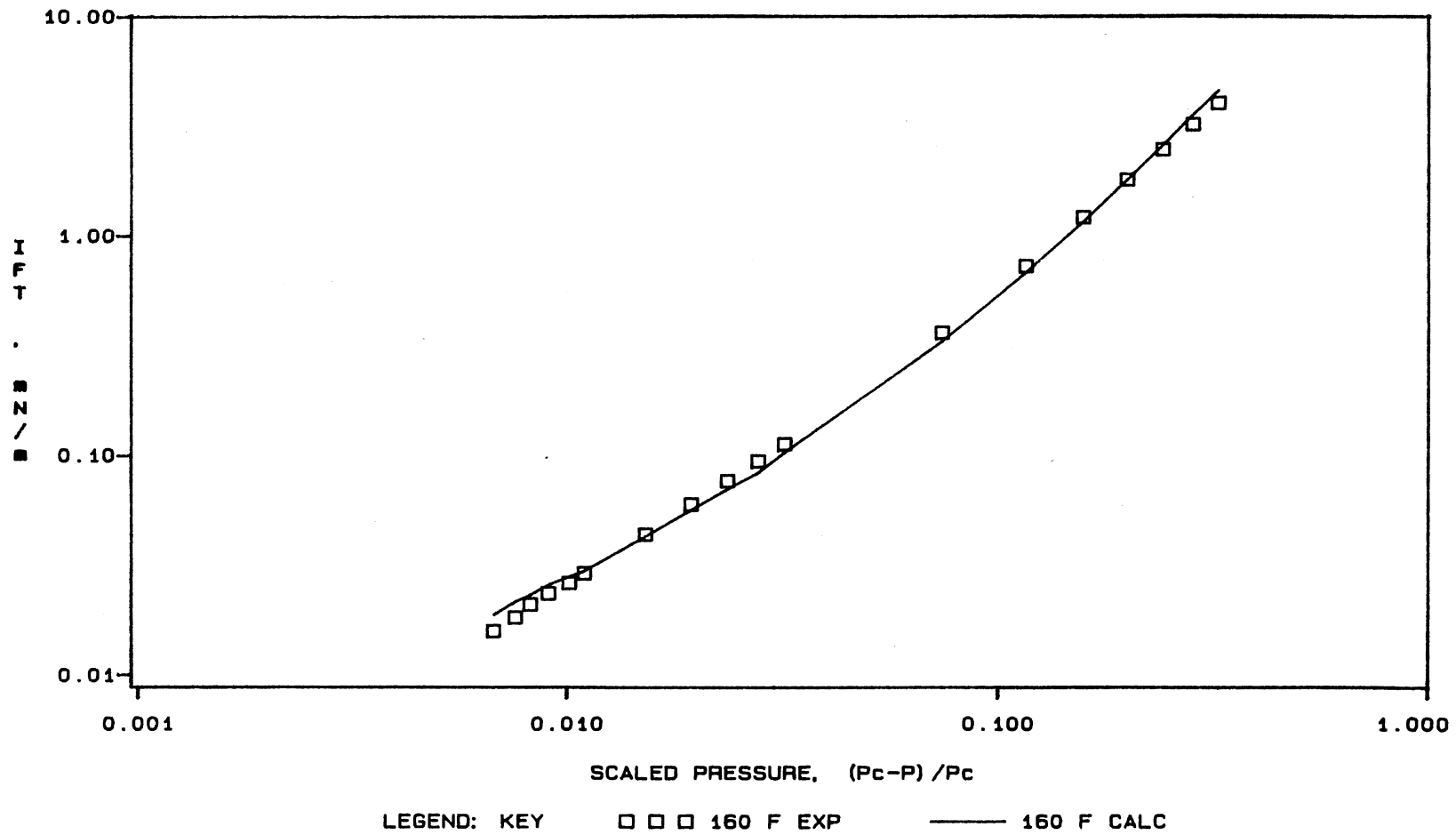


Figure 26. Comparison of Experimental IFTs to W-K Model for CO₂ + n-Tetradecane at 160 °F

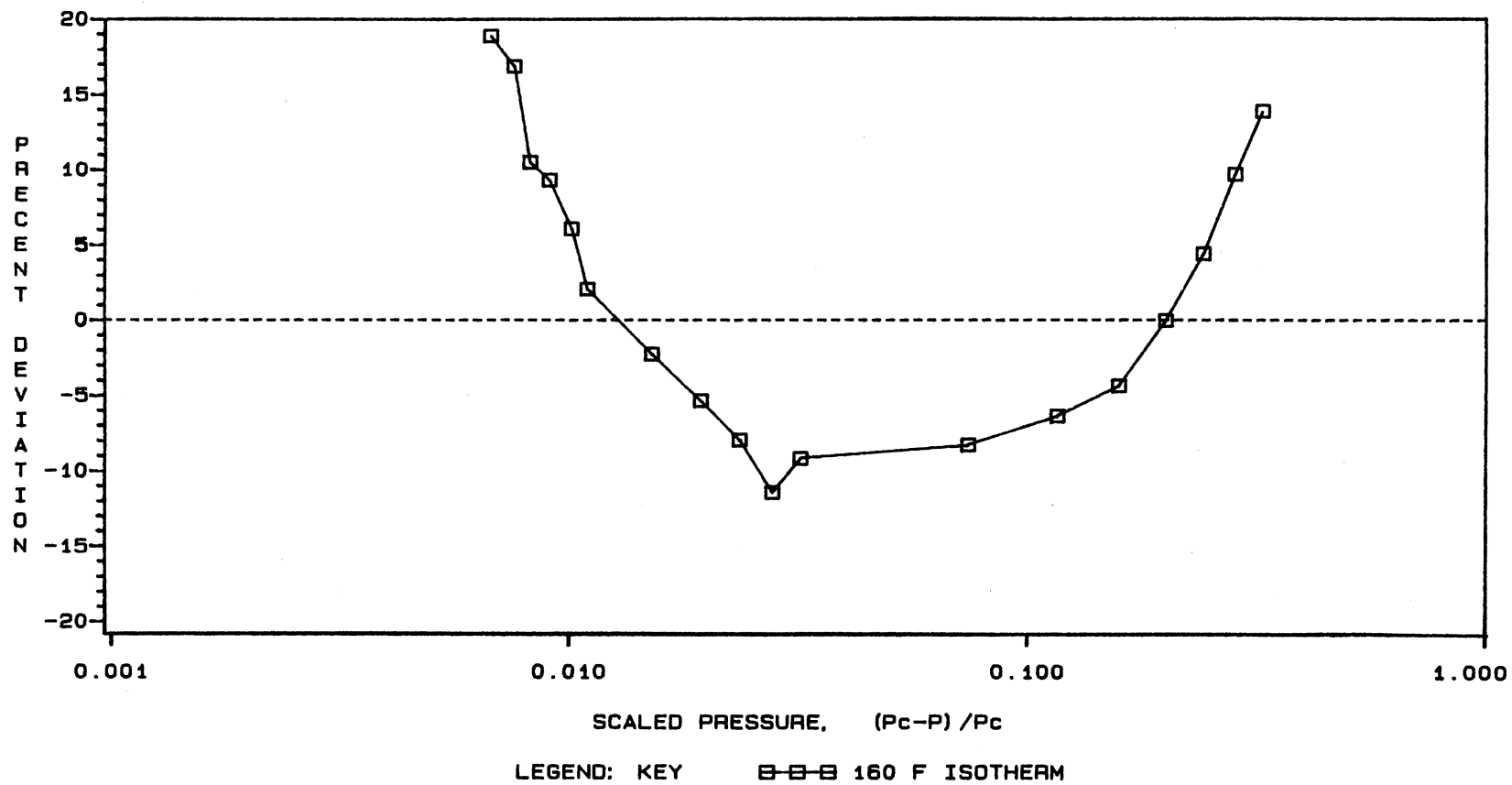


Figure 27. Comparison of Experimental IFTs to W-K Model, (Percent Deviations) for CO₂ + n-Tetradecane at 160 °F

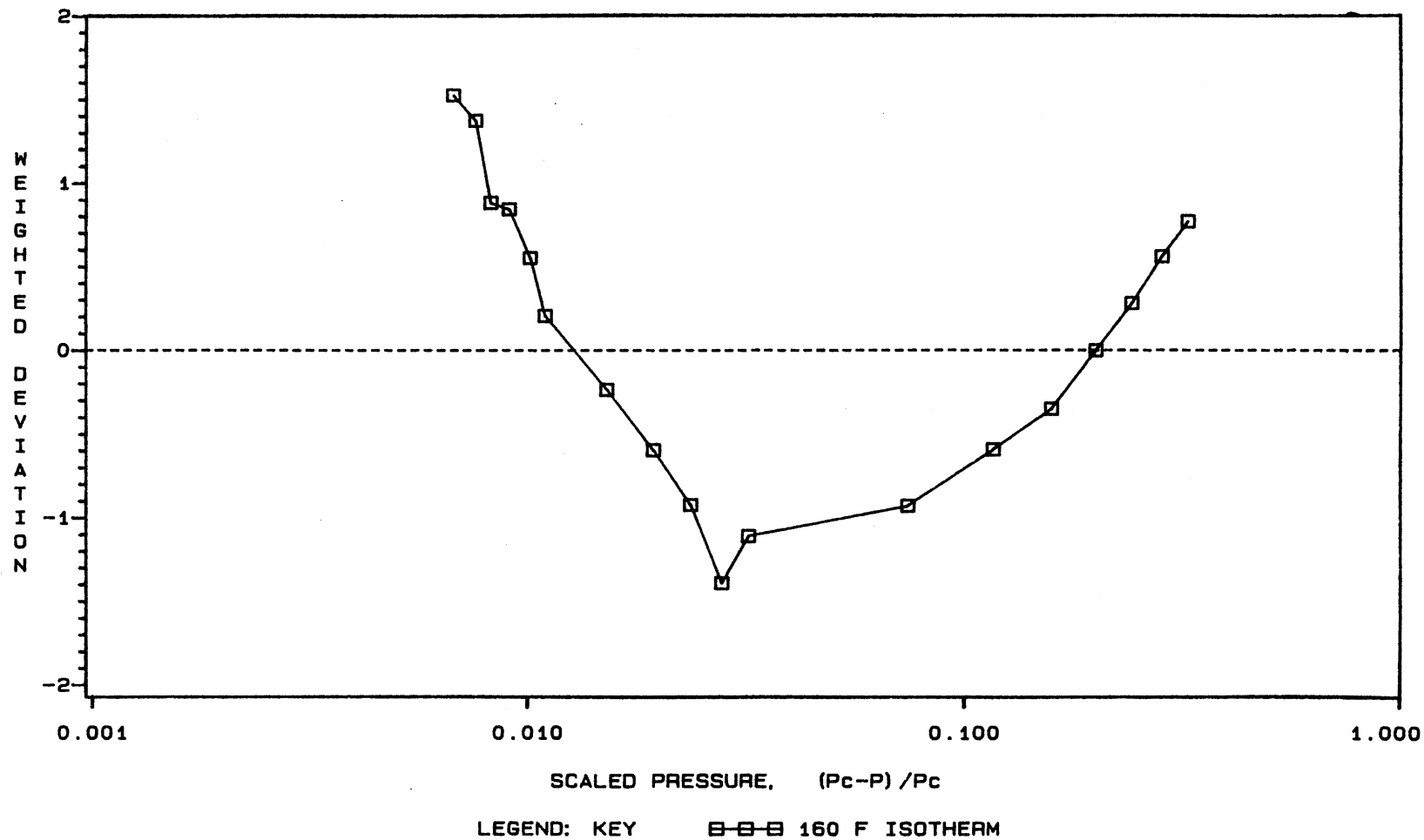


Figure 28. Comparison of Experimental IFTs to W-K Model, (Weighted Deviations) for CO₂ + n-Tetradecane at 160 °F

TABLE XV
 EVALUATION OF WEINAUG-KATZ CORRELATION FOR CO₂ + BENZENE
 AND CO₂ + CYCLOHEXANE AT 160°F

No. of Data Pts.	Weighting Factor	Regressed Parameter			Error in Predicted IFTs		
		Parachors		Critical	RMSE	AAPD	
		CO ₂	Benzene	Cyclohexane	Exponent, k	mN/m	%
-----CO ₂ + benzene at 160°F-----							
15	W ₁	68	212		3.55	0.172	4.9
15	W ₂	53	228		3.39	0.101	5.4
15	W ₃	54	226		3.40	0.108	5.3
-----CO ₂ + cyclohexane at 160°F-----							
14	W ₁	66		251	3.58	0.124	4.3
14	W ₂	49		263	3.45	0.070	4.8
14	W ₃	52		261	3.47	0.079	4.7

Note: Regressions included all experimental data points

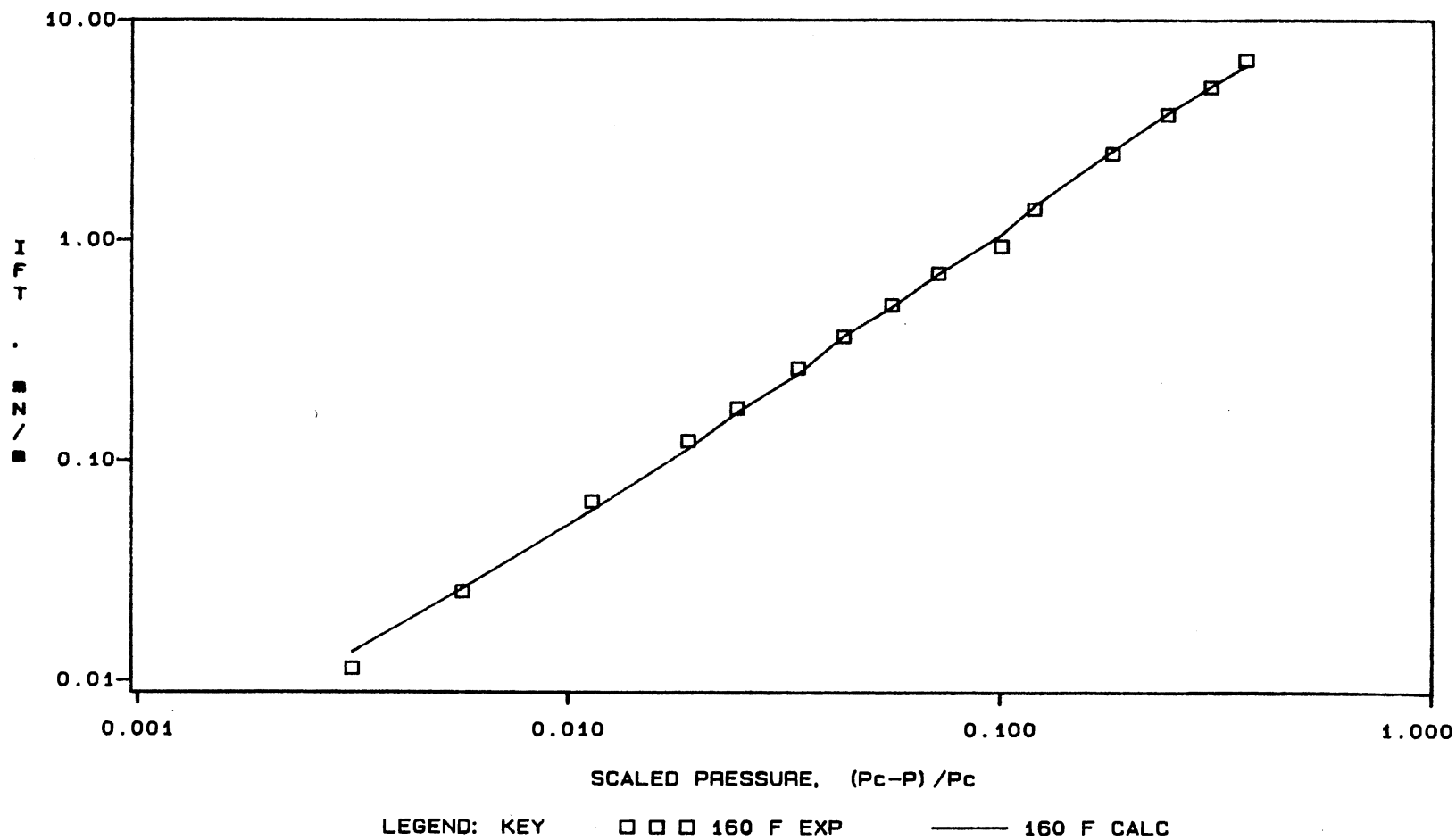


Figure 29. Comparison of Experimental IFTs to W-K Model for CO₂ + Benzene at 160 °F

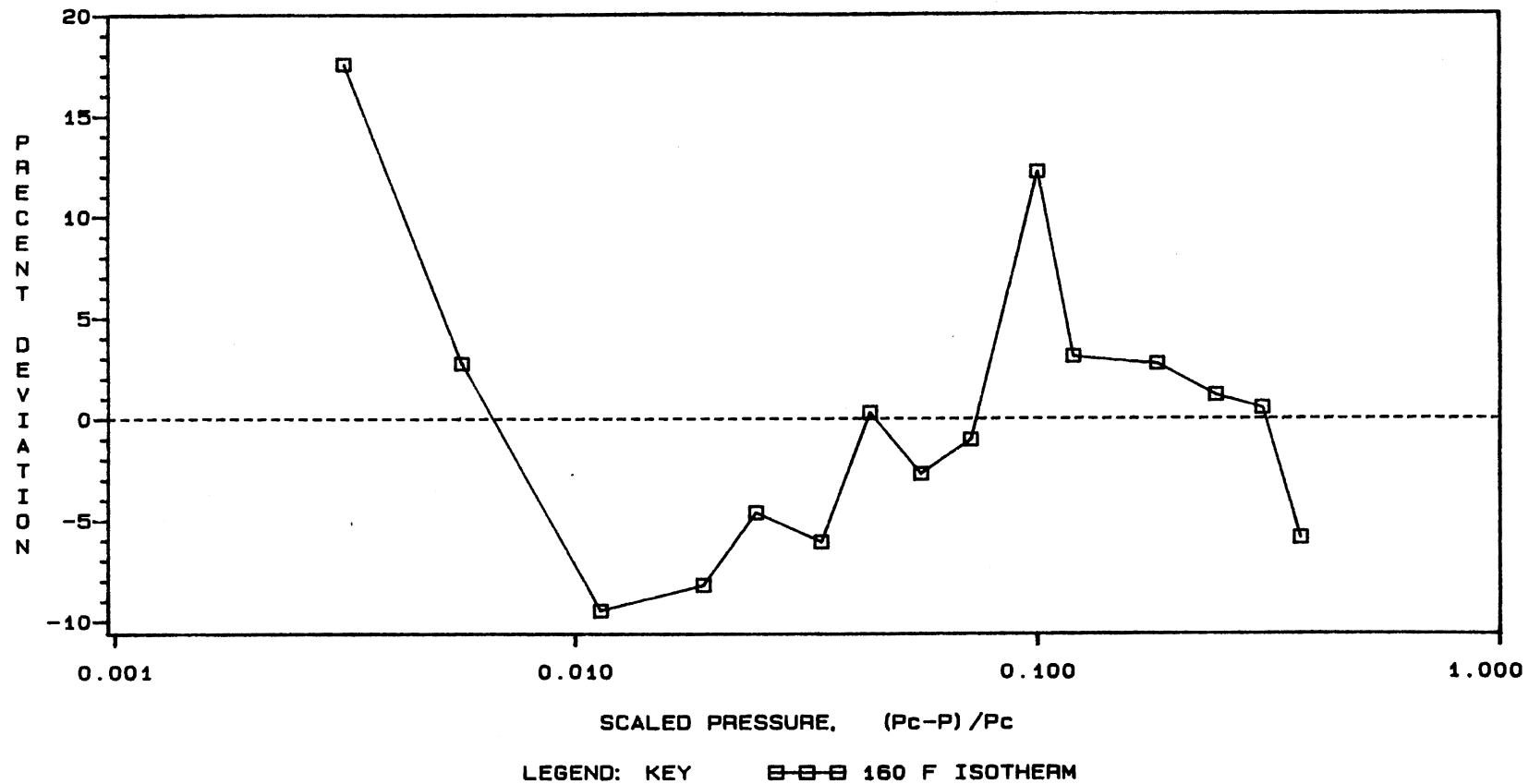


Figure 30. Comparison of Experimental IFTs to W-K Model, (Percent Deviations) for CO₂ + Benzene at 160 °F

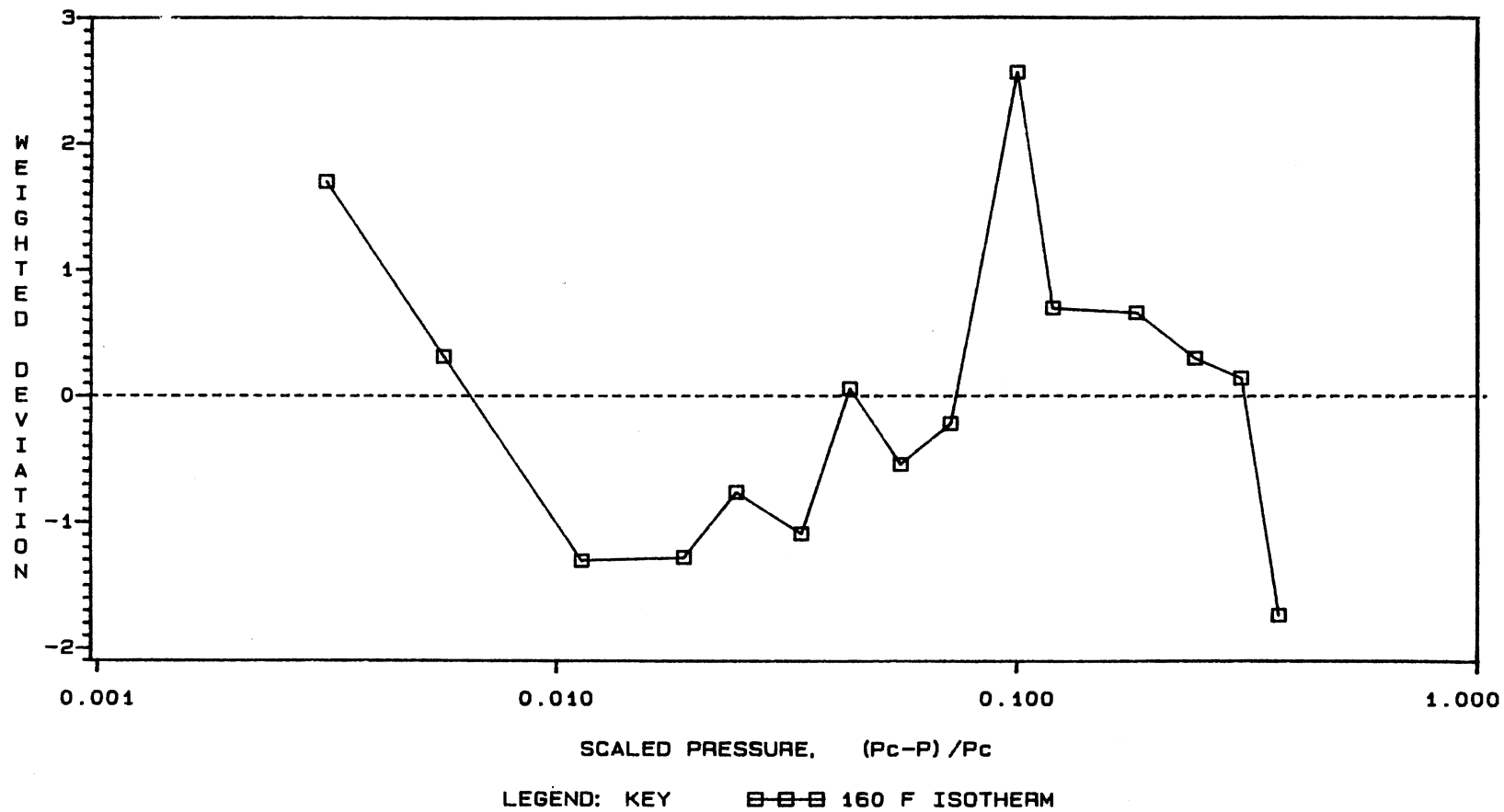


Figure 31. Comparison of Experimental IFTs to W-K Model, (Weighted Deviations) for CO₂ + Benzene at 160 °F

weighted deviations. Figures 32 through 34 are plots of the regression results for the CO₂ + cyclohexane system. Figure 32 illustrates the accuracy of the W-K predicted IFT values at 160°F. Figure 33 shows percent deviations in the IFTs and Figure 34 shows fully propagated weighted deviations.

The final W-K regressions were made on a combined data set which included all five binary systems. In these regressions, the data base is increased significantly to 130 data points. Because of the larger sample size and greater degrees of freedom in the regressions, the regression results provide greater precision in the regressed parameters. These regressions produce seven parameters, k , the scaling exponent plus six individual component parachors. Table XVI presents the results of these regressions plus those on several modified combined data sets.

The regressions made on the combined data set with 130 data points produced very reasonable values for the parachors and the scaling exponent. The scaling exponent value of 3.61 is in very good agreement with the accepted experimental value near 3.55. Four additional regressions were made on modified combined data sets. The first modified data set included all the binary system data at 160°F. The second modified data set included those data points from the main combined data set regression with weighted deviations less than 2.50. The third modified data set included data points from the main data set regression with percent deviations less than 10%. The fourth modified data set is based on experimental data points with interfacial tensions less than or equal to 1.0 mN/m. The purpose of analyzing these various subsets of the total data set was to investigate the effect they had on

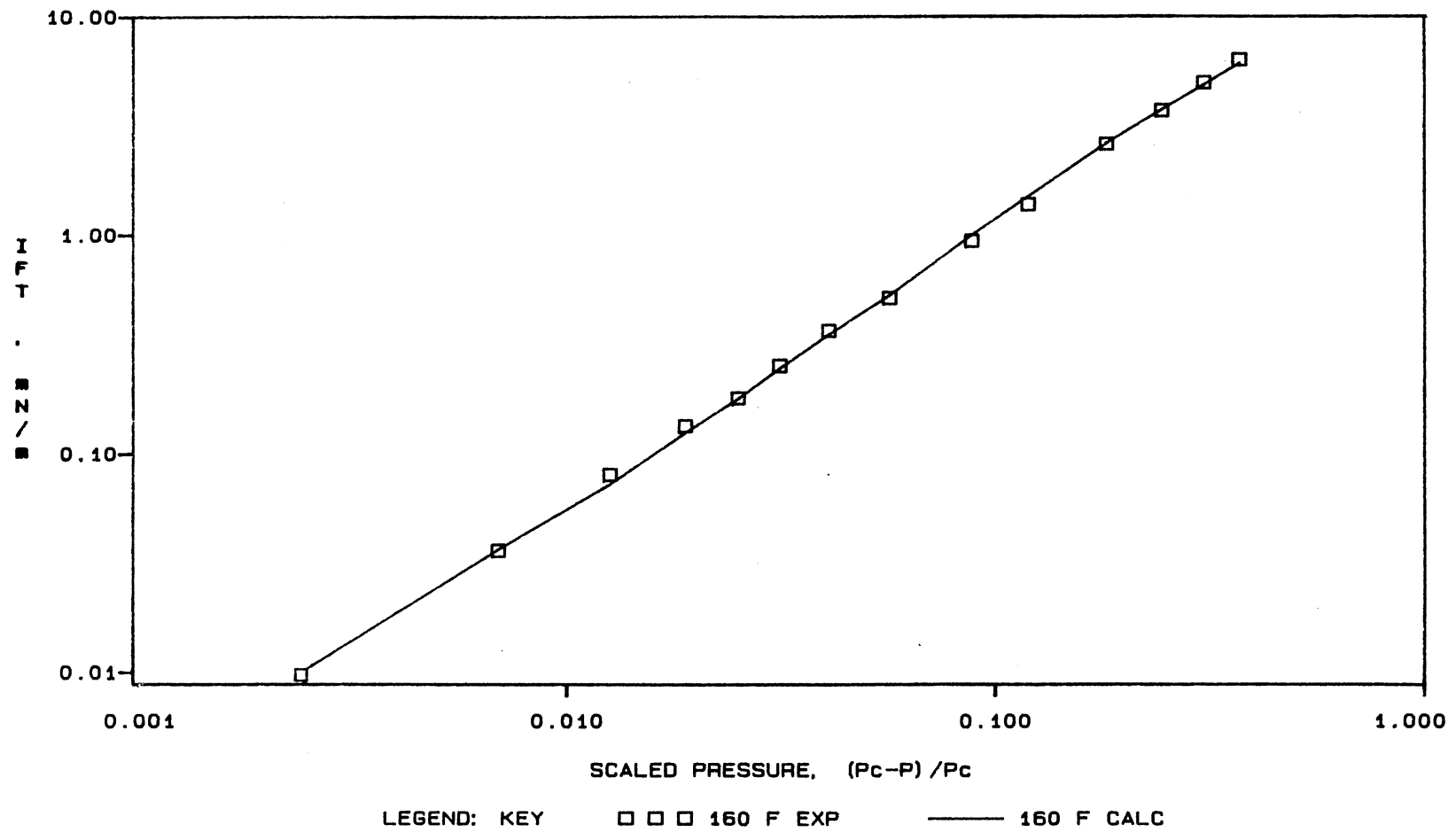


Figure 32. Comparison of Experimental IFTs to W-K Model for CO₂ + Cyclohexane at 160 °F

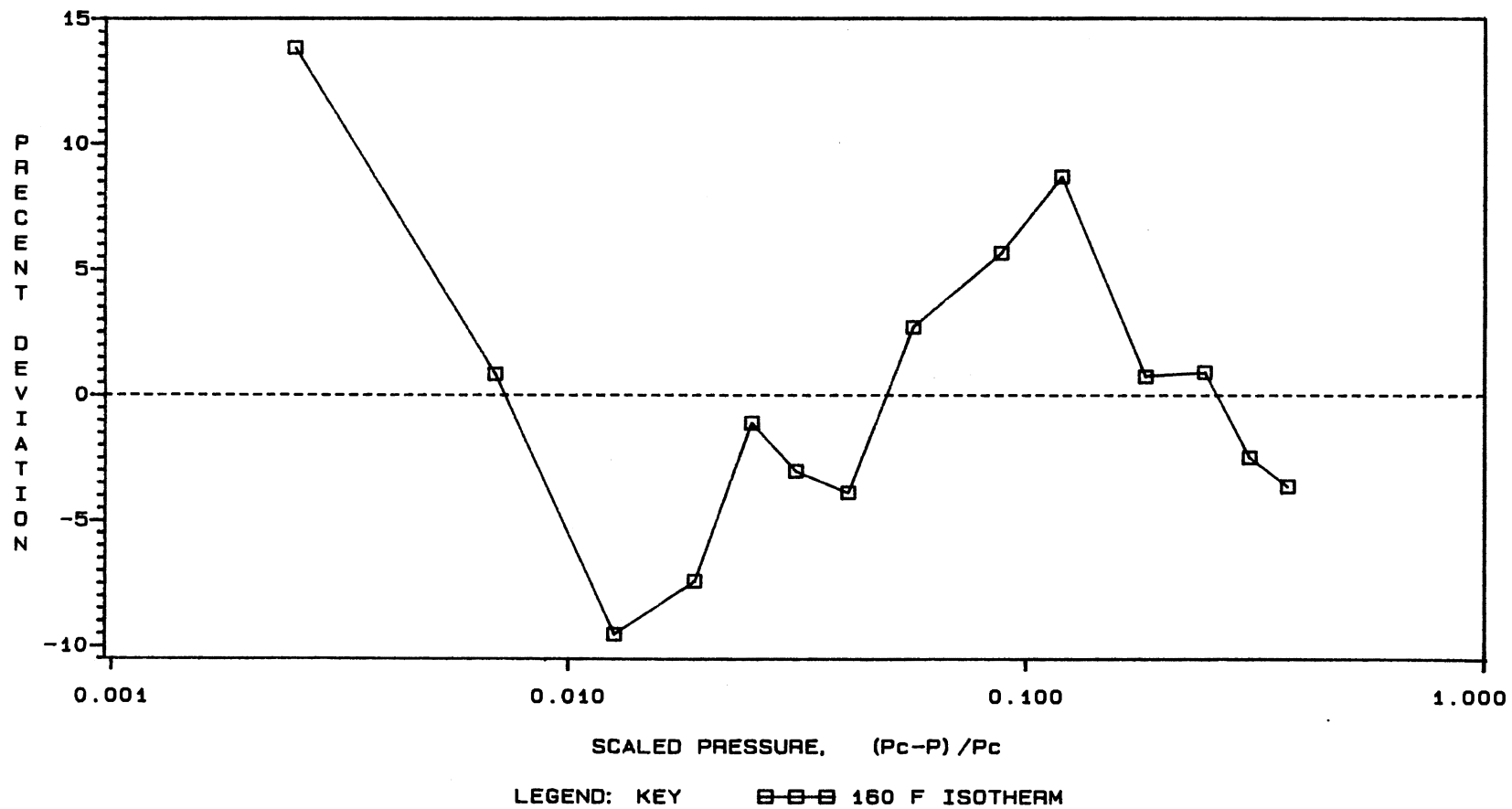


Figure 33. Comparison of Experimental IFTs to W-K Model, (Percent Deviations) for CO₂ + Cyclohexane at 160 °F

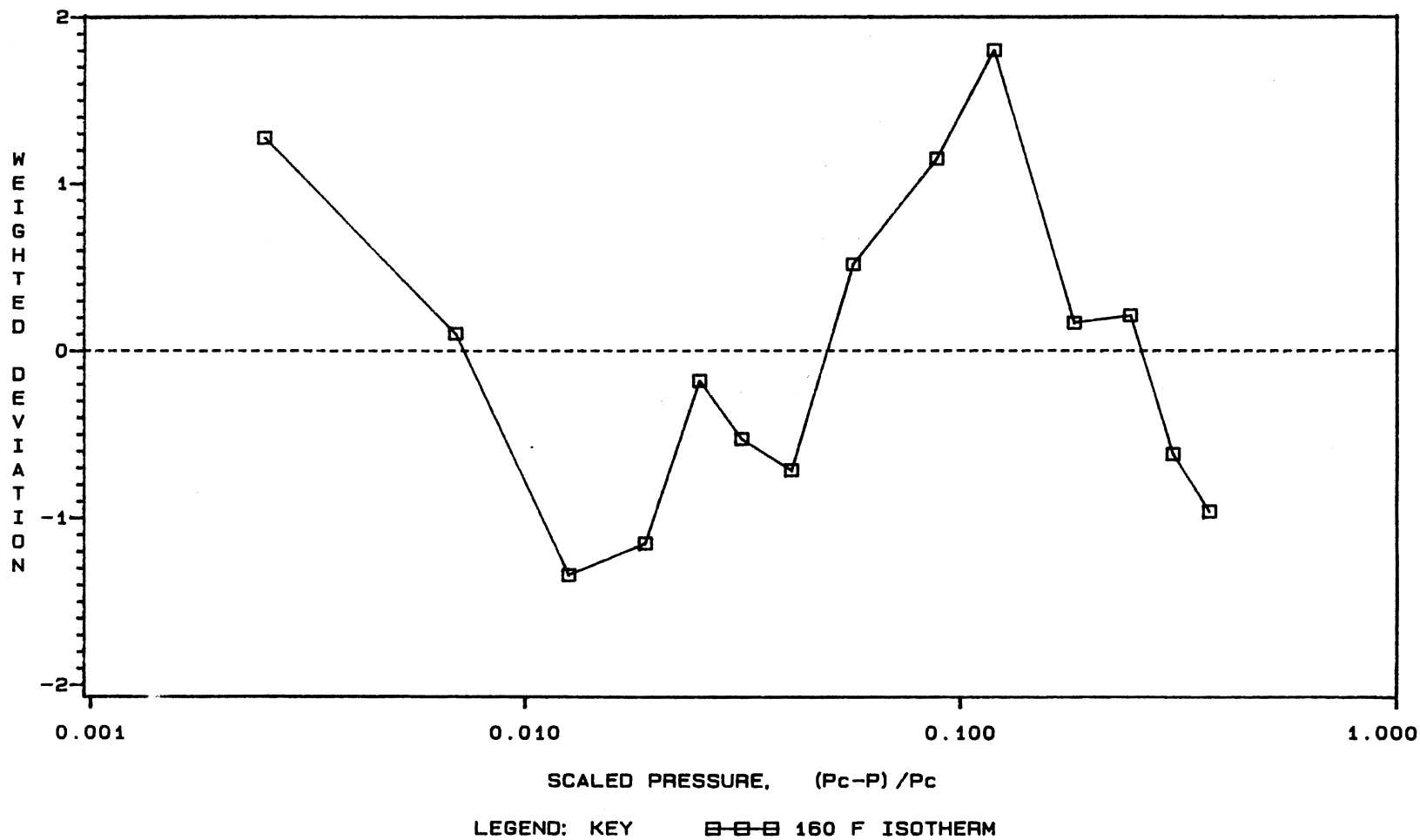


Figure 34. Comparison of Experimental IFTs to W-K Model, (Weighted Deviations) for CO₂ + Cyclohexane at 160 °F

TABLE XVI
EVALUATION OF WEINAUG-KATZ CORRELATION FOR ALL DATA

No. of Data Pts.	Weighting Factor	Regressed Parameters						Error in Predicted IFTs			
		Parachors						Critical Exponent, k	RMSE mN/m	AAPD %	
		CO ₂	C ₄	C ₁₀	C ₁₄	Benzene	Cyclohexane				
-----All Data-----											
130	W ₁	85	197	446	634	194		235	3.64	0.231	7.6
130	W ₂	81	198	446	629	202		242	3.61	0.175	8.1
130	W ₃	81	197	448	630	201		241	3.61	0.179	8.1
-----All Data at 160°F only-----											
77	W ₁	82	200	438	630	199		239	3.68	0.186	6.6
77	W ₂	75	202	440	622	207		245	3.67	0.127	6.9
77	W ₃	74	202	441	619	207		245	3.65	0.130	6.8
-----All Data with Weighted Deviations < 2.50-----											
118	W ₁	85	198	446	633	195		235	3.65	0.142	6.6
118	W ₂	81	199	446	629	200		239	3.62	0.115	7.0
118	W ₃	83	199	447	632	199		238	3.63	0.122	6.8
-----All Data with Percent Deviations < 10%-----											
92	W ₁	80	199	451	626	202		240	3.61	0.177	4.7
92	W ₂	77	199	450	624	206		245	3.59	0.142	4.8
92	W ₃	78	199	451	624	205		244	3.60	0.149	4.8

TABLE XVI (CONTINUED)

No. of Data Pts.	Weighting Factor	Regressed Parameters							Error in Predicted IFTs		
		Parachors						Critical Exponent, k	RMSE mN/m	AAPD %	
		CO ₂	C ₄	C ₁₀	C ₁₄	Benzene	Cyclohexane				
-----All Data with IFTs < 1.0 mN/m-----											
82	W ₁	89	197	449	647	186		229	3.67	0.034	6.9
82	W ₂	87	197	447	646	187		229	3.64	0.031	7.1
82	W ₃	87	197	449	644	187		228	3.63	0.032	7.1

the regressed parameters and the accuracy of the correlations at low IFTs.

Hugill-Van Welsenens Correlation Evaluation

The second correlation evaluated was the Hugill-Van Welsenens (H-VW) modified form of the W-K correlation (Equation 2.11). If all binary interaction parameters λ_{ij} are taken as one, Equation 2.11 reduces to the original W-K correlation. The binary interaction parameter λ_{ij} exhibits a temperature dependence, but this dependence appears to be linear (13). Like the original W-K correlations, the H-VW correlation requires phase compositions, phase densities, and pure component parachors. In addition, a binary interaction parameter is required. As with the W-K correlation, the phase densities and compositions can be predicted from an equation of state (EOS) for process applications. The pure component parachors could be predicted from structural contribution methods like those proposed by Quayle (6). At the present time, however, there is no useful method to predict the binary interaction parameter. The interaction parameter must be determined from experimental data, but only limited data are available for this purpose. The H-VW correlation was evaluated by performing regressions using experimental data to determine the optimum values for the individual component parachors, the scaling exponent (k), the binary interaction IFT parameters (λ_{ij}). The experimental data used in the regressions included the same five binary systems used with the W-K regressions. The objective function of the regressions was the same as the W-K regressions, except only fractional (%) errors (W_1) were used in

the H-VW regressions. The results appear to have the same accuracy as the fully propagated weighting for the W-K regressions.

The regressions for the CO_2 + n-butane and CO_2 + n-decane are shown in Table XVII. The regressions were made on a system-by-system basis with no experimental data points excluded. The regressions were conducted in two different ways. First, interaction parameters were regressed for each isotherm in the system. Second, an interaction parameter was regressed for each of the five binary systems. In the first regression for the CO_2 + n-butane system, all parameters were allowed to vary without restriction. The value of the CO_2 parachor varies by 17 units from the value regressed in the W-K correlation (H-VW = 104 vs. W-K = 87), but the n-butane parachor is approximately the same, (H-VW = 198 vs. W-K = 197). As in the W-K regression, the CO_2 parachor has less influence in the regression compared to the n-butane parachor, thus the CO_2 parachor is determined with less accuracy. The scaling exponent is $k = 3.67$, again an acceptable value. The interaction parameters (λ) for the 115, 160, and 220°F isotherms are 0.856, 0.929, and 0.957, respectively. The interaction parameters follow the temperature dependence indicated by Hugill-Van Welsenens (13). The AAPD is approximately 2% less than the W-K regression (H-VW = 3.3% vs. W-K = 5.4%), however, the H-VW correlation should do at least as well as W-K (H-VW reduces to the W-K when $\lambda_{ij} = 1$) and should be better if the binary interaction parameter has a significant effect. The second type of regression on the CO_2 + n-butane system calculated only one interaction parameter per system (not one for each isotherm in a system, as above). The results are in good agreement with the first regression, but since the interaction parameter clearly shows a

TABLE XVII
EVALUATION OF HUGILL-VAN WELSENES CORRELATION FOR
CO₂ + N-BUTANE AND CO₂ + N-DECANE

No. of Data Pts.	Regressed Parameters					Error in Predicted IFTs		
	Parachors		Binary Interaction Parameters			Critical Exponent, k	RMSE mN/m	AAPD %
-----CO ₂ (1) + n-butane (2) at 115, 160, and 220°F-----								
	CO ₂	C ₄	λ ₁₂ (115°F)	λ ₁₂ (160°F)	λ ₁₂ (220°F)			
42	104	198	0.856	0.929	0.957	3.67	0.083	3.3
42	*85	*197	0.998	0.991	0.969	*3.52	0.139	5.3
			λ ₁₂ (all T's)					
42	93	200		0.927		3.55	0.136	4.3
42	*85	*197		0.992		*3.52	0.125	5.4
-----CO ₂ (1) + n-decane (3) at 160 and 220°F-----								
	CO ₂	C ₁₀	λ ₁₃ (160°F)	λ ₁₃ (220°F)				
41	118	463	0.908	0.988		3.62	0.128	4.8
41	*85	*450	0.966	1.012		3.62	0.089	8.5
			λ ₁₃ (All T's)					
41	54	423		1.080		3.70	0.106	6.2
41	*85	*450		0.988		3.62	0.119	8.5

* Parameters fixed at listed values. Values chosen for their realistic magnitudes (near W-K values).
Note: All regressions were performed with weighting factor W₁

temperature dependence, the first regression is more significant. Several other regressions were made where some of the parameters were specified. These results are also indicated in Table XVII. Similar regression results for the CO_2 + n-decane, CO_2 + n-tetradecane, CO_2 + benzene, and CO_2 + cyclohexane systems are shown in Tables XVII and XVIII. The CO_2 + n-tetradecane regression did not produce very realistic results for the parameters. The parachors ($\text{CO}_2 = 39$ and $C_{14} = 297$) and $k = 4.55$ are unrealistic values. When the parachors were fixed at more reasonable values ($\text{CO}_2 = 85$ and $C_{14} = 620$), the regression indicated no improvement over the W-K regression when comparing AAPD, (H-VW = 10.1% vs. W-K = 8.4-11.8%). The CO_2 + benzene and CO_2 + cyclohexane systems produced better results than the CO_2 + n-tetradecane, but the values of the regressed parachors were higher than expected. The value of the scaling exponents $k_{\text{benzene}} = 3.76$ and $k_{\text{cyclohexane}} = 3.61$ are in reasonable agreement with experimental values. The wide variation in the parachors was probably caused by the fact that four parameters (two parachors, one interaction parameter, and scaling exponent) are too many variables to accurately fix by one isotherm of data.

The next regressions made on the Hugill-Van Welsenes correlation were with a combined data set including all data from the five binary systems. The results of these regressions are shown in Table XIX. The first regression included all 130 data points and regressed interaction parameters for each isotherm. The regressed parachors compare favorably with the W-K parachors from Table XVI except for n-tetradecane which was 383 for H-VW and 630 for W-K. The scaling exponent, $k = 3.69$, is reasonable. The AAPD is approximately half the value obtained from the

TABLE XVIII

EVALUATION OF HUGILL-VAN WELSENES CORRELATION FOR CO₂ + N-TETRADECANE,
CO₂+ BENZENE AND CO₂ + CYCLOHEXANE

No. of Data Pts.	Regressed Parameters			Critical Exponent, k	Error in Predicted IFTs		
	Parachors	Binary Interaction Parameters			RMSE mN/m	AAPD %	
-----CO ₂ (1) + n-tetradecane (4) at 160°F - Smoothed Data-----							
	CO ₂	C ₁₄	λ ₁₄ (160°F)				
18	39	297	2.122	4.55	0.039	3.6	
18	*85	*580	1.116	3.76	0.172	9.7	
18	*85	*620	1.035	3.72	0.184	10.1	
-----CO ₂ (1) + benzene (5) at 160°F-----							
	CO ₂	benzene	λ ₁₅ (160°F)				
15	131	272	0.521	3.76	0.048	2.4	
15	*85	*200	0.975	3.70	0.287	5.5	
15	*85	*240	0.786	3.57	0.071	3.6	
-----CO ₂ (1) + cyclohexane (6) at 160°F-----							
	CO ₂	cyclohexane	λ ₁₆ (160°F)				
14	111	302	0.670	3.61	0.070	2.7	
14	*85	*210	1.144	3.82	0.400	8.3	
14	*85	*240	0.983	3.71	0.228	5.4	

* Parameters fixed at listed values. Values chosen for their realistic magnitudes (near W-K values).
Note: All regressions were performed with weighting factor - W₁

TABLE XIX
EVALUATION OF HUGILL-VAN WELSENES CORRELATION FOR ALL DATA

No. of Data Pts.	Regressed Parameters						Critical Exponent, k	Error in Predicted IFTs	
								RMSE mN/m	AAPD %
	Parachors								
	CO ₂	C ₄	C ₁₀	C ₁₄	Benzene	Cyclohexane			
	-----All Data-----								
130	108	198	432	383	250	284	3.69	0.106	4.6
	-----All Data Except n-Tetradecane-----								
112	104	199	449	-	252	287	3.65	0.095	3.8
	-----All Data with IFTs < 1.0 mN/m-----								
83	115	195	170	717	155	159	3.80	0.017	4.3
	All Data Except n-Tetradecane with IFTs < 1.0 mN/m								
70	110	199	243	-	170	181	3.75	0.016	3.6
	Binary Interaction Parameters								
	$\lambda_{12}(115^\circ\text{F})$	$\lambda_{12}(160^\circ\text{F})$	$\lambda_{12}(220^\circ\text{F})$	$\lambda_{13}(160^\circ\text{F})$	$\lambda_{13}(220^\circ\text{F})$	$\lambda_{14}(160^\circ\text{F})$	$\lambda_{15}(160^\circ\text{F})$	$\lambda_{16}(160^\circ\text{F})$	
	-----All Data-----								
130	0.825	0.911	0.943	0.989	1.067	1.743	0.662	0.739	
	-----All Data Except n-Tetradecane-----								
112	0.844	0.914	0.930	0.952	1.020	-	0.665	0.734	
	-----All Data with IFTs < 1.0 mN/m-----								
83	0.792	0.922	0.999	2.100	2.366	1.00	0.996	1.229	
	-----All Data Except n-Tetradecane with IFTs < 1.0 mN/m-----								
70	0.806	0.905	0.943	1.632	1.815	-	0.948	1.128	

TABLE XIX (CONTINUED)

No. of Data Pts.	Regressed Parameters						Critical Exponent, k	Error in Predicted IFTs	
								RMSE mN/m	AAPD %
	Parachors								
	CO ₂	C ₄	C ₁₀	C ₁₄	Benzene	Cyclohexane			
	-----All Data-----								
130	89	198	486	666	245	285	3.57	0.128	6.6
	-----All Data with IFTs < 1.0 mN/m-----								
83	91	198	637	1372	188	231	3.61	0.028	5.9
	All Data Except n-Tetradecane with IFTs < 1.0 mN/m								
70	90	197	643	-	199	243	3.59	0.028	5.3
	Binary Interaction Parameters								
	$\lambda_{12}(160^\circ\text{F})$	$\lambda_{13}(160^\circ\text{F})$	$\lambda_{14}(160^\circ\text{F})$	$\lambda_{15}(160^\circ\text{F})$	$\lambda_{16}(160^\circ\text{F})$				
	-----All Data-----								
130	0.968	0.901	0.969	0.748	0.779				
	-----All Data with IFTs < 1.0 mN/m-----								
83	0.967	0.669	0.407	0.968	0.970				
	-----All Data Except n-Tetradecane with IFTs < 1.0 mN/m-----								
70	0.970	0.658	-	0.916	0.919				

Note: All regressions were performed with weighting factor - W_1

W-K regression ($H-VW = 4.6\%$ vs. $W-K = 8.1\%$). This result is not as significant as it may appear since the regressed parachors have greater deviations from values calculated from structural contribution methods.

The final regressions calculated one interaction parameter for each system. This regression produced parachors which compare quite favorably with the W-K parachors in Table XVI, including the n-tetradecane. The interaction parameters appear reasonable. The H-VW regression, with one interaction parameter per system, resulted in an AAPD of 6.6% compared with 8.1% for the W-K regression. The improved accuracy of the H-VW correlation was not significantly greater than the W-K correlation, especially considering the amount of additional effort required to obtain binary interaction parameters. The improved fit can be attributed to the interaction parameter, again recognizing the fact that the H-VW correlation reduces to the W-K correlation if the interaction parameters are set equal to one. The scaling exponent, $k = 3.57$, is reasonable. The results of several other regressions are shown in Table XIX for completeness.

Lee-Chien Correlation Evaluation

The third correlation evaluated was the Lee-Chien (L-C) multi-component interfacial tension correlation based on scaling theory. Their work contained two major features: (1) a method to predict pure component parachors which is consistent with the theory of corresponding states and (2) a correlation for predicting the IFTs of mixtures based on "mixed" parachors. The L-C correlations (Equation 2.15) is the same basic equation as W-K (Equation 2.7) and H-VW (Equation 2.11) except for

the method used to calculate the mixed liquid and vapor parachors.

Equation 2.15 was used in the regressions that follow.

Like the W-K and the H-VW correlations, the L-C correlation requires phase compositions and phase densities. L-C also requires pure component physical properties (e.g., P_c , T_c , etc.) and the pure component parachor correlating parameter, B_1 . As with the two previous correlations, the phase densities and compositions can be predicted from an equation of state (EOS) for process applications.

The L-C correlation was evaluated by performing regressions using experimental data to determine the optimum values for the pure component parachor correlating parameter, B_1 and the scaling exponent (k). The parachor correlating parameter can be used in Equation 2.16 to calculate the pure component parachor (which corresponds to optimizing the parachor in the previous correlation evaluations). The experimental data used in the regressions included the same five binary systems used previously. The objective function of the regressions was the same as the W-K regressions except only fractional (%) errors (W_1) were used. The L-C regressions, using fractional (%) error, appear to have the same accuracy as regressions using fully propagated weighting.

The regression results for the CO_2 + n-butane, CO_2 + n-decane, CO_2 + n-tetradecane, CO_2 + benzene, and CO_2 + cyclohexane on a system-by-system basis are shown in Table XX. The regressions were made using all experimental data points in each system; no data points were excluded. The optimum parachor correlating parameters were converted to pure component parachors by Equation 2.16 which are also shown in Table XX. The discussions which follow refer to the optimum parachor not the correlating parameter. In the first regression for the CO_2 + n-butane

TABLE XX

EVALUATION OF LEE-CHIEN CORRELATION FOR CO₂ + N-BUTANE,
 CO₂ + N-DECANE, CO₂ + N-TETRADECANE, CO₂ + BENZENE,
 AND CO₂ + CYCLOHEXANE

No. of Data Pts.	Regressed Parameters			Error in Predicted IFTs	
	Parachor B (Parachor)*	Correlating Parameters	Critical Exponent, k	RMSE mN/m	AAPD %
-----CO ₂ + n-butane at 115, 160, and 220°F-----					
	CO ₂	C ₄			
42	3.704 (80)	3.703 (190)	3.56	0.164	6.6
-----CO ₂ + n-decane at 160 and 220°F-----					
	CO ₂	C ₁₀			
41	4.406 (68)	3.870 (430)	3.63	0.096	6.6
-----CO ₂ + n-tetradecane at 160°F-----					
	CO ₂	C ₁₄			
18	2.842 (105)	5.861 (382)	3.88	0.094	7.5
-----CO ₂ + benzene at 160°F-----					
	CO ₂	Benzene			
15	4.279 (70)	3.382 (226)	3.52	0.111	4.3
-----CO ₂ + cyclohexane at 160°F-----					
	CO ₂	Cyclohexane			
14	4.316 (69)	3.301 (267)	3.55	0.061	3.7

* Parachor value calculated by Equation 2.16 using optimum parachor correlating parameter

system, all parameters (e.g., scaling exponent - k and two parachor correlating parameters) were allowed to vary without restriction. The value of the CO_2 parachor ($[P]_{\text{CO}_2} = 80$) varies by 7 units from the value regressed in the W-K correlation (W-K = 87), but by 24 units from the H-VW parachor (H-VW = 104). The n-butane parachor is closer to the W-K and H-VW parachors (L-C = 190, H-VW = 198, and W-K = 197). As in the W-K regression, the CO_2 parachor has less significance in the outcome of the regression when compared to the n-butane parachor. The scaling exponent is $k = 3.56$, again an acceptable value. The AAPD is higher than the W-K and H-VW (L-C = 6.6%, H-VW = 3.3%, and W-K = 5.4%). Similar regression results for the CO_2 + n-decane, CO_2 + n-tetradecane, CO_2 + benzene, and CO_2 + cyclohexane systems are shown in Table XX. The CO_2 + n-tetradecane regression produced a most unrealistic result for the n-tetradecane parachor ($[P]_{\text{C}_{14}} = 382$). The scaling exponents obtained from all regressions were acceptable.

The final regression performed used the combined data set including all 130 data points. The results of this regression are shown in Table XXI. The optimum parachors for n-decane and n-tetradecane show large deviations from the values obtained from the W-K and H-VW regressions. The AAPD of 9.2% was higher than the comparable W-K and H-VW regressions. The scaling exponent, $k = 3.71$, was reasonable.

These evaluations of the W-K, H-VW, and L-C correlations, as mentioned earlier, tested the frameworks of the three multicomponent IFT correlations and established the relative accuracy of the three correlations in predicting IFTs. The three correlations have several common regression parameters (e.g., parachors and scaling exponent) which are shown in Table XXII for comparison. All values shown in Table

TABLE XXI

EVALUATION OF LEE-CHIEN CORRELATION FOR ALL DATA

No. of Data Pts.	Regressed Parameters						Critical Exponent, k	Error in Predicted IFTs	
	Parachor Correlating Parameters B (Parachor)*							RMSE mN/m	AAPD %
	All Data								
	CO ₂	C ₄	C ₁₀	C ₁₄	Benzene	Cyclohexane			
130	3.802 (78)	3.647 (193)	4.785 (347)	5.038 (444)	3.989 (192)	3.885 (226)	3.71	0.278	9.2

* Parachor value calculated by Equation 2.16 using optimum parachor correlating parameter

TABLE XXII
COMPARISON OF REGRESSED PARACHORS

Substance	Literature Values (6)	Parachors		
		Optimum Values		
		W-K	H-VW	L-C
CO ₂	78	81	89	78*
n-Butane	190	197	198	193*
n-Decane	431	448*	486	347
n-Tetradecane	592	630*	656	444
Benzene	205	201*	245	192
Cyclohexane	242	241*	285	226
Critical Exponent, k	4.00	3.61	3.57	3.71

* Value nearest the pure-component parachors reported in the literature (6)

TABLE XXIII
COMPARISON OF IFT CORRELATIONS ACCURACIES

System	Average Absolute Percent Deviation (AAPD) in IFT		
	W-K	H-VW	L-C
CO ₂ + n-Butane	7.2	4.8	9.3
CO ₂ + n-Decane	7.9	8.7	10.2
CO ₂ + n-Tetradecane	11.5	11.2	11.9
CO ₂ + n-Benzene	7.1	3.4	6.2
CO ₂ + Cyclohexane	7.5	3.0	5.9
All Systems	8.1	6.6	9.2

XXII were calculated from the combined data set with 130 data points. The H-VW data was from the regression which calculated one interaction parameter per binary system. The L-C parachors were obtained from Equation 2.16 using the optimized parachor correlation parameter, B. The parachor values of Quayle (6) are also shown for comparison with the regressed parachors.

The W-K parachors deviate the least from the literature values of Quayle, but when making comparisons with Quayle, one must remember that Quayle calculated his parachors with a scaling exponent of $k = 4.0$, whereas the parachors shown in Table XXII have different scaling exponents (e.g., $k_{W-K} = 3.61$). The scaling exponents shown for the three correlations are all acceptable. A comparison of the accuracy of the three correlations is shown in Table XXIII based on the same regressions in Table XXII above. The H-VW correlation had the lowest AAPD of the three correlations, with an AAPD of 6.6%. The W-K was slightly higher at AAPD = 8.1% and the L-C was highest with an AAPD = 9.2%. The H-VW correlation was expected to be at least as accurate as the W-K correlation considering they are the same when the binary interaction parameters are equal to one. The shortcoming of the H-VW correlation is in obtaining values of the binary interaction parameter, which have to be obtained from limited experimental data. In light of this shortcoming, the W-K correlation is recommended for the prediction of IFTs in CO_2 + hydrocarbon systems especially if there are no binary interaction parameters available.

Parachor Correlations

The ability to predict parachors accurately permits the use of the IFT correlations discussed above in a predictive fashion. Parachor correlations proposed in the works by L-C and H-VW were evaluated, as is a correlation developed in the present work.

Lee-Chien Parachor Correlation

The L-C parachor correlation (Equation 2.16) was used to reproduce the pure component parachors shown in the Lee-Chien article (29). The values predicted were identical to their results. This confirmed that the correct pure component physical properties (P_c , T_c , V_c , T_{br}) and computer coding were being used. The B parameters used in the calculations above were from the Lee-Chien article, where they were obtained from regressions of pure component density data. Once the interpretation of the L-C correlation was confirmed, the correlation was used to predict the pure component parachors of the six compounds under study in the present work. (The results are shown after the other parachor correlations have been discussed.)

Hugill-Van Welsenens Parachor Correlation

Hugill-Van Welsenens also proposed a graphical relationship for a reduced parachor as a function of Pitzer's acentric factor. Their graph indicated a linear relationship between the reduced parachor and the acentric factor. A curve fit to their graph resulted in the following equation for the reduced parachor.

$$[P_r] = 0.151 - 0.04636\omega \quad (5.1)$$

where ω = Pitzer acentric factor. The parachor is obtained with the following conversion.

$$[P] = 39.6431 [P_r] T_c^{13/12} / (P_c^{5/6}) \quad (5.2)$$

where

$[P]$ = pure component parachor, $(\text{cm}^3 \text{ mol}^{-1}) (\text{mN m}^{-1})^{1/4}$

T_c = critical temperature, K

P_c = critical pressure, bars

Parachor Correlations From The Present Work

A parachor correlation was developed as part of the present work and is discussed in detail in Appendix E. Four reduced parachor correlations were developed. Equation E.17 calculates the reduced parachor with a scaling exponent of $k = 3.55$ and a function of reduced acentric factor. Equation E.18 calculates the reduced parachor with a scaling exponent of 3.55 and a function of reduced acentric factor and reduced temperature. Equation E.19 calculates the reduced parachor with a scaling exponent of $k = 3.91$ and a function of reduced acentric factor. Equation E.20 calculates the reduced parachor with a scaling exponent of $k = 3.91$ and a function of reduced acentric factor and reduced temperature. The reduced parachors calculated by Equations E.17-E.20 are converted to parachors by Equation E.15.

Comparison of Predicted Parachors

The three parachor correlations presented above (L-C, H-VW, and present work) were used to predict the pure component parachors of the

six compounds under study. Table XXIV shows the results of the three correlations plus the optimum parachors from the W-K regressions and the parachors of Quayle (6).

The pure component parachors predicted by the L-C correlation (Equation 2.16) were predicted using B parameters calculated from the following correlation proposed by Lee-Chien (29).

$$B = 1.854426 Z_c^{-0.52402} \quad (5.3)$$

where

Z_c = critical compressibility factor

Lee-Chien chose to report predicted parachors using B parameters regressed from pure component density data. Parachors predicted from regressed B parameters reported by L-C are slightly different than the values shown in Table XXIV, but having to obtain regressed B parameters limits the predictive ability of their correlation to components with experimental density data versus temperature. Such experimental data are in limited supply for heavier hydrocarbons which are of interest in enhanced oil recovery by CO₂ injection. To incorporate the true predictive nature of their correlation, the parachors indicated in Table XXIV use the L-C B parameter correlation, shown above.

Based strictly on the results above, the H-VW parachor correlation would appear to give the best results for pure component parachors using the parachors regressed from the W-K correlation optimization as a basis of reference. The physical properties (e.g., P_c , T_c , ω , etc.), used in the predictions, were taken from the National Bureau of Standards (NBS)

TABLE XXIV
COMPARISON OF PREDICTED PURE COMPONENT PARACHORS

Component	Parachors											
	Quayle (6) k = 4.00	W-K Optimized			"This Work" Parachor							
		Parachors, k = 3.61	L-C, k = 3.91	H-VW, k = 4.00	[P] ~ f (ω)		[P] ~ (ω, T)					
					k = 3.55	k = 3.91	k = 3.55			k = 3.91		
						115°F	160°F	220°F	115°F	160°F	220°F	
CO ₂	78	81	81	77	90	85	93	92	90	83	83	82
n-Butane	190	197	192	196	203	196	221	219	217	195	195	194
n-Decane	431	448	428	445	443	431	487	481	473	446	443	439
n-Tetradecane	592	630	547	612	599	589	674	665	652	623	619	613
Benzene	205	201	206	213	225	214	249	247	245	216	216	215
Cyclohexane	242	241	238	245	247	237	272	271	269	239	238	237

and are indicated in Appendix D. The W-K pure component parachors were compared to parachors predicted from the L-C, H-VW, "This Work" ($k = 3.55$), and "This Work" ($k = 3.91$) parachor correlations. The "This Work" parachors were obtained from Equation E.17 and E.19 which are a function of acentric factor only. The results are presented in Table XXV below:

TABLE XXV
STATISTICAL COMPARISON OF PREDICTED PARACHORS TO
W-K REGRESSED PARACHORS

	L-C	H-VW	This Work $k = 3.55$	This Work $k = 3.91$
AAPD	4.0	2.8	5.8	4.0
RMSE*	35.0	9.2	16.9	19.0

*RMSE = $[(\text{mN/m})^{1/k}/(\text{mol/cm}^3)]$, $k = \text{scaling exponent}$

Again the Hugill-Van Welsenens parachor correlation resulted in the best results (AAPD = 2.8% and RMSE = 9.2). Based on the current results, the Hugill-Van Welsenens pure component parachor correlation, in conjunction with the Weinaug-Katz correlation, is recommended for the prediction of the interfacial tension of multicomponent systems.

Structural contribution methods have been used successfully to predict parachor values, especially the n-paraffin hydrocarbons. Structural contributions determined from a linear least squares fit of

the parachors predicted by the four correlations plus the W-K regressed parachors are shown in Table XXVI below:

TABLE XXVI
STRUCTURAL CONTRIBUTION PARACHORS

	L-C	H-VW	This Work k = 3.55	This Work k = 3.91	W-K Regressed
-CH ₃	63.2	56.3	62.9	58.6	54.2
-CH ₂ -	35.8	41.6	39.6	39.3	43.2
CO ₂	81.0	77.0	90.0	85.0	81.0

The W-K structural contribution parachors are recommended because they resulted from the optimum fit of the W-K IFT correlation to the experimental data. The next important thing to consider when using the W-K correlation is the selection of the scaling exponent, k . Considering the results of the W-K optimizations of the experimental data for the five binary systems, a scaling exponent of $k = 3.61$ is recommended. This value is in good agreement with previous experimental values. It appears to work well for the range of IFTs covered by the experimental data (IFT 0.008 - 7.8 mN/m).

IFT Correlation Predictions

In addition to optimizing the various parameters in the IFT correlations, tests were also conducted on their abilities in a direct

predictive mode. The W-K correlation, using the L-C, H-WV, and "this work" predictive parachor correlations outlined in Appendix E, was used to calculate the IFTs of the five binary systems under study. Also the L-C multicomponent IFT correlation (Equation 2.15), in conjunction with mixed parachors calculated by Equation 2.17, was used to predict IFTs of the five binary systems. The last predictive method utilizes the parachor correlations developed in this work to calculate mixed parachors which are used in an equation of the same form as 2.15, which is discussed later in this chapter.

Lee-Chien proposed a correlation, derived from the Weinaug-Katz correlation, for the prediction of interfacial tension of multicomponent systems (Equation 2.15). The liquid and vapor mixed parachors are calculated by Equation 2.17 using linear mixing rules. The mixed parachors, along with the liquid and vapor phase densities, are used in Equation 2.15 to predict the interfacial tension of multicomponent systems.

To check the accuracy of the L-C correlation, attempts were made to reproduce the results obtained by L-C for four binary systems studied in their manuscript. The first system tested was the methane-propane system. The experimental data used to test the correlation was from Weinaug-Katz (11). This probably provided the most accurate comparison with Lee-Chien's results because Weinaug-Katz reported all necessary experimental data for the correlation (e.g., IFTs, phase compositions, and densities). The results obtained from Equation 2.15 did not agree with the values reported by Lee-Chien. The comparison is shown in Table XXVII. The only variable that could be different from L-C was their B parameter. The B parameter was varied from the tabular values reported

TABLE XXVII

COMPARISON OF INTERFACIAL TENSIONS PREDICTED BY
THE LEE-CHIEN CORRELATION: METHANE-PROPANE

Temperature °F	Pressure psia	Experimental IFT, mN/m	L-C	"This Work"*
-----Methane - Propane-----				
86.0	1039.0	0.82	0.835	0.809
	982.0	1.11	1.097	1.065
	948.0	1.30	1.463	1.420
	858.0	1.73	1.731	1.695
	808.0	2.14	1.998	1.964
	744.0	2.34	2.388	2.356
	583.0	3.37	3.432	3.415
	510.0	3.83	3.939	3.936
	419.0	4.43	4.607	4.624
	311.0	5.25	5.397	5.448
	220.0	5.91	6.093	6.177
	163.0	6.39	6.466	6.592
113.0	982.0	0.64	0.647	0.634
	893.0	0.97	0.977	0.962
	872.0	1.06	1.059	1.044
	821.0	1.30	1.281	1.266
	733.0	1.68	1.693	1.682
	728.0	1.70	1.721	1.710
	692.0	1.87	1.902	1.892
	623.0	2.23	2.279	2.275
	619.0	2.30	2.298	2.295
	518.0	2.79	2.880	2.891
	348.0	3.78	3.918	3.966
222.0	4.58	4.719	4.825	
149.0	830.0	0.54	0.520	0.519
	718.0	0.87	0.908	0.912
	615.0	1.28	1.345	1.356
	480.0	1.87	1.961	1.986
	435.0	2.05	2.188	2.219
	340.0	2.57	2.686	2.790

* B parameter is calculated from Equation 5.3

by L-C to the ones calculated by Equation 5.3 above. The predicted IFTs reported in Table XXVII were calculated with B values calculated by Equation 5.3. The results were always less accurate than the ones reported by L-C. A similar study was made on the three other binary systems, methane-pentane, methane-decane, and methane-nonane. A comparison of the interfacial tensions predicted for these systems are shown in Table XXVIII. The accuracy of the experimental data is somewhat in question since on all three systems the IFT data and phase equilibrium data were not from the same source. Also some values had to be interpreted so that all data were at the same temperature and pressure. The predicted results of these systems indicated the same kind of deviations from the L-C results as did the methane-propane system. Though the deviation between Lee-Chien's results and the ones presented in this work could not be explained, the application of the L-C correlation appeared correct. The authors of the correlation were contacted in an effort to resolve the discrepancies. Repeated attempts to obtain information from the authors proved fruitless. Since the framework of the correlation was being applied correctly, as demonstrated by the predicted pure component parachors, evaluation of the correlation with the five binary systems under study proceeded. Speculation on the discrepancy between the results obtained by Lee-Chien and the present work indicate the differences lie in the B parameter used or the experimental equilibrium data. The L-C correlation was used to predict the IFTs of the five binary systems under study. The results of these predictions are discussed in Appendix C.

The Hugill-Van Welsenens correlation was not used in a predictive manner because of the inability to predict the binary interaction

TABLE XXVIII

COMPARISON OF INTERFACIAL TENSIONS PREDICTED BY THE
LEE-CHIEN CORRELATION: METHANE-PENTANE,
METHANE-NONANE, AND METHANE-DECANE

Temperature °F	Pressure psia	Experimental IFT, mN/m	L-C	"This Work"*
-----Methane - Pentane-----				
100.0	600.0	9.02	8.620	7.546
100.0	1250.0	4.59	4.273	3.698
220.0	600.0	4.62	4.449	3.916
220.0	1250.0	1.98	1.754	1.530
-----Methane - Nonane-----				
30.0	300.0	19.27	18.77	22.146
30.0	600.0	16.28	16.15	18.944
30.0	900.0	13.68	13.10	15.386
30.0	1175.0	10.48	10.80	12.500
30.0	1315.0	9.30	9.52	11.167
30.0	1475.0	8.26	8.53	9.8251
-----Methane - Decane-----				
100.0	2000.0	7.35	7.498	6.984
100.0	3500.0	2.40	1.948	1.782
280.0	1000.0	9.13	9.175	8.770
460.0	1000.0	3.30	3.677	3.523

* B parameter is calculated from Equation 5.3

parameter. Hugill-Van Welsenes did not propose a method for the prediction of the binary interaction parameter or report values for various systems.

The parachor equations developed in this work (Equations E.17 - E.20) can be extended to mixtures in the same manner as the L-C parachor correlation. Using linear mixing rules, mixed liquid and vapor critical properties can be obtained and used in the parachor correlations to predict mixed liquid and vapor parachors. The mixed liquid and vapor parachors are used in Equation 5.4 below to predict the multicomponent IFTs. Equation 5.4 is the same IFT equation proposed by W-K (Equation 2.7), H-VW (Equation 2.11), and L-C (Equation 2.15) except the mixed liquid and vapor parachors are obtained from different methods.

$$\gamma^{1/k} = \rho^L [P]_L - \rho^V [P]_V \quad (5.4)$$

The IFTs predicted for the five CO₂ + hydrocarbon binary systems by Equation 5.4, using Equations E.17 - E.20, are shown in Appendix C.

The results in Appendix C include IFTs predicted by the W-K correlation using the three pure component parachor correlations (Equations 2.16, 5.2 and E.17 - E.20), IFTs predicted by the L-C mixed parachor approach (Equation 2.15), and IFTs predicted by Equation 5.4 using mixed parachors predicted by the correlations proposed in this work.

The general result of these evaluations is that the W-K correlation using the H-VW parachor correlation resulted in the best overall fit to the experimental data for the five binary systems. The accuracy of the various correlation evaluations is indicated in Table LXXIII, Appendix C.

All of the predicted IFTs in Appendix C were for binary systems, (e.g., CO₂ + hydrocarbon). To further test the predictive ability of the W-K correlation, the IFTs of the CO₂/n-butane/n-decane ternary system (33) were calculated. The experimental data for the CO₂/n-butane/n-decane ternary system are shown in Table XXXVIII, Appendix A. The IFTs were predicted using the W-K correlation with a scaling exponent of $k = 3.61$ and the W-K regressed pure parachors indicated in Table XXIV. The experimental phase densities and phase compositions were used in the calculations. The results are indicated in Table XXIX below.

TABLE XXIX
PREDICTED IFTS (W-K MODEL) FOR CO₂/N-BUTANE/N-DECANE
AT 344.3 K (160°F)

Pressure psia	Experimental IFT, mN/n	Calculated IFT, mN/m	Percent Error exp-calc
1351	2.43	2.53	-4.1
1400	1.77	2.06	-16.4
1451	1.34	1.59	-18.7
1501	0.94	1.162	-23.6
1524	0.76	0.949	-24.9
1553	0.545	0.692	-26.9
1580	0.405	0.431	-6.4
1601	0.295	0.333	-12.9
1621	0.200	0.207	-3.5
1640	0.115	0.119	-3.5
1651	0.064	0.066	-3.1
1661	0.033	0.032	3.0

Note: RMSE = 0.1487 mN/m AAPD = 12.3%

The IFTs predicted for the CO₂/n-butane/n-decane system resulted in an AAPD = 12.3%. This value compares favorably with the AAPD = 8.1% indicated in Table XXIII for the W-K regression using all 130 data points. Figure 35 illustrates the accuracy of the predicted IFTs for the CO₂/n-butane/n-decane system at 160°F. From the results shown above, the W-K correlation can be extended to multicomponent systems other than binaries and with a relative accuracy on the same magnitude as the binary systems.

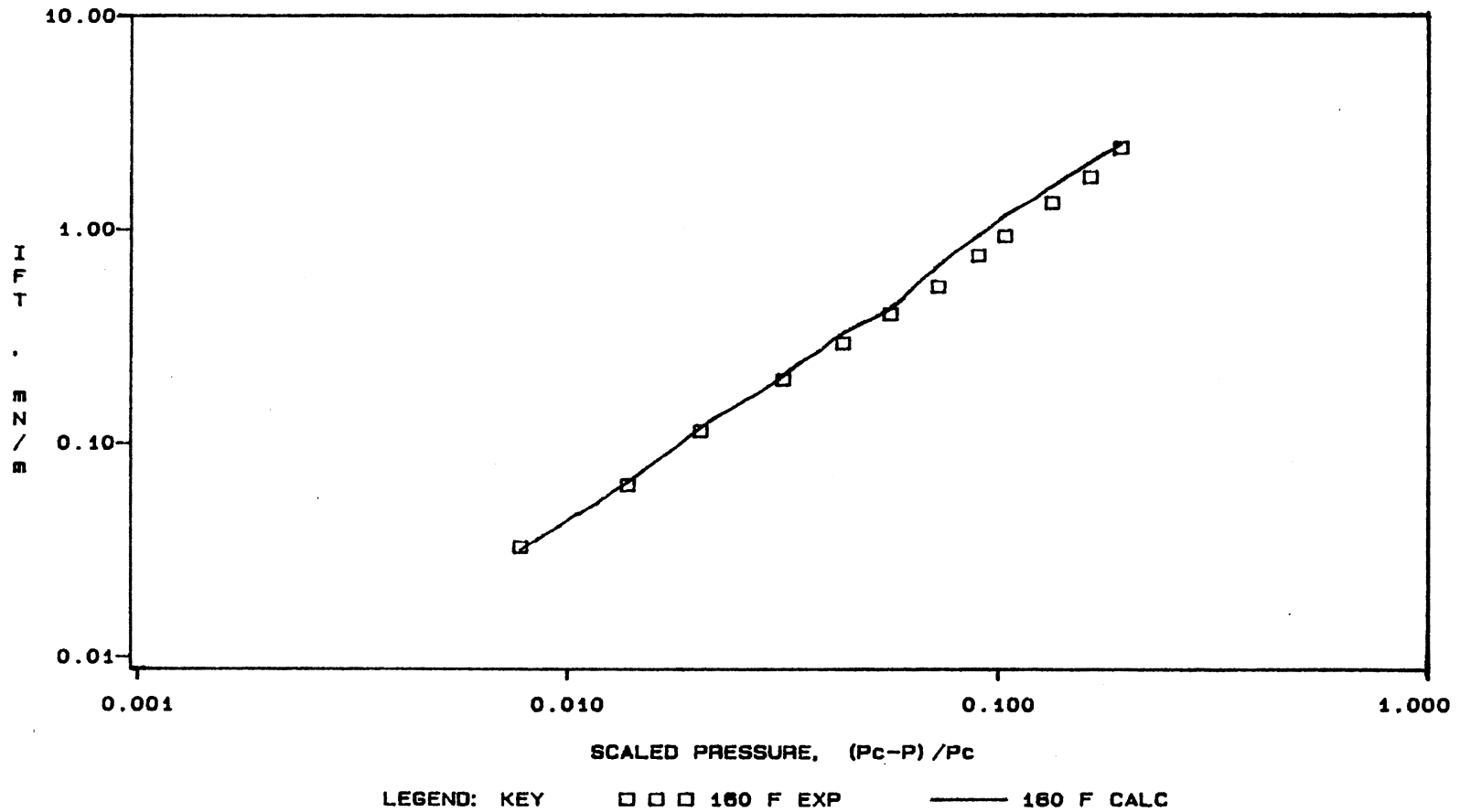


Figure 35. Comparison of Experimental IFTs to W-K Model for CO₂/n-Butane/n-Decane at 160 °F

CHAPTER VI

CONCLUSIONS AND RECOMMENDATIONS

Conclusions

1. The experimental data for CO_2 + n-tetradecane obtained during this investigation represent a consistent data set for the evaluation of IFT correlations. The experimental accuracy is comparable to previous studies (26,38,33-37). The consistency of these data lies in the fact that all properties, $(\gamma/\Delta\rho, \rho^L, \rho^V, x, y)$ were obtained essentially simultaneously in an experimental apparatus utilizing the same equilibrium mixture of components.

2. The CO_2 + n-tetradecane data $(\gamma, \rho^L, \rho^V, x, y)$ are represented adequately by functions based on the renormalized group theory (RGT), originally presented by Kobayashi and Charoensombut-amon (23,24).

3. The Weinaug-Katz correlation is the preferred IFT correlation based on the results of the evaluations in this work. The W-K correlation requires fewer input parameters than the H-VW correlation and the parameters are more easily obtained by the method outlined in Chapter V. The W-K correlations provided a better fit (lower AAPD) to the experimental data than the L-C correlation. For these reasons, and because of its simplicity and ease of application, the W-K correlation is recommended. It requires only the following input parameters; $\rho^L, \rho^V, x, y, \text{parachors}$.

4. The Huggill-Van Welsenens IFT correlation can predict multicomponent system IFTs slightly better than W-K, but the necessity of the binary interaction parameter makes the H-VW correlation more difficult to apply.

5. The Lee-Chien correlation is not as accurate for CO₂ systems as it was for the hydrocarbon systems studied by its authors. This lower accuracy appears to arise from the correlation presented for their B parameter.

6. An appropriate value of the scaling exponent in the W-K correlation is $k = 3.61$, (not the original $k = 4.0$ proposed by Weinaug-Katz). The value of $k = 3.61$ compares favorably with the experimental value ($k = 2\nu/\beta = 3.55$) suggested by Sengers, Greer, and Sengers (46).

7. The parachors for the heavier components in a system have the greatest effect on the predicted IFTs for the system when using the W-K correlation.

8. The parachor correlation proposed by Huggill-Van Welsenens predicts parachors in good agreement with the optimum parachors from the regressions on the W-K correlation. The W-K correlation using the H-VW parachors resulted in the most accurate predictions of the IFTs compared to the experimental data.

9. The parachor correlation developed in this work offers reasonable results but does not exhibit the same accuracy as the Huggill-Van Welsenens parachor correlation (when compared to parachors optimized from the W-K correlation).

Recommendations

1. The Weinaug-Katz correlation is recommended for the prediction of multicomponent IFTs in CO_2 + hydrocarbon systems.
2. The recommended structural contribution parachors for n-paraffins are $-\text{CH}_3 = 54.2$, $-\text{CH}_2- = 43.2$, and $\text{CO}_2 = 81$. These parachors are well suited for use in the W-K correlation with scaling exponent of $k = 3.61$.
3. Additional experimental data should be obtained with the experimental apparatus so the type of evaluations performed in this work can be extended to multi-ring naphthenic and aromatic systems.
4. To further evaluate the IFT correlations reviewed in this work, it is recommended that equilibrium phase densities and compositions predicted by an equation of state be used in the correlations along with parachors predicted by the correlations evaluated in this work. This type of evaluation will assess the true predictive ability of the IFT correlations.

REFERENCES

1. Van der Waals, J. D., "Thermodynamische Theorie der Kapillarität," *Zeitschrift für Physikalische Chemie*, 13 (1894), p. 617.
2. Sugden, S., "The Variation of Surface Tension with Temperature and Some Related Functions," *J. Chem. Soc.*, (1924), p. 32-41.
3. Ferguson, A., Dowson, P. E., "Studies in Capillarity," *Faraday Society Transactions*, Vol. 17, (1922).
4. Macleod, D. B., "On a Relation Between Surface Tension and Density," *Faraday Society Transactions*, Vol. 19, (1922), p. 38-43.
5. Sugden, S., "The Parachor and Valency," George Routledge and Sons, Ltd., London, (1930).
6. Quayle, O. R., "The Parachors of Organic Compounds," *Chem. Review*, Vol. 53, (1953), p. 439-586.
7. Paquette, L. J., Goldsack, D. E., "An Anisotropic Surface Model for the Parachor," *J. Colloid Int. Sci.*, Vol. 92, (1983), p. 154-160.
8. Ferguson, A., Kennedy, S. J., "Free and Total Surface Energies and Related Quantities," *Faraday Society Transactions*, Vol. 32, (1936), p. 1474.
9. Lennard-Jones, J. E., Corner, J., "The Calculation of Surface Tension from Intermolecular Forces," *Faraday Society Transactions*, Vol. 36, (1940), p. 1156.
10. Goldsack, D. E., Paquette, L. J., M.Sc. Thesis, Laurentian University, 1982.
11. Weinaug, C. F., Katz, D. L., "Surface Tensions of Methane-Propane Mixtures," *Ind. and Eng. Chem.*, Vol. 35, no. 2, (1943), p. 239-246.
12. Hough, E. W., Warren, H. G., "Correlation of Interfacial Tension of Hydrocarbons," *Soc. Pet. Eng. J.*, (Dec. 1966), p. 345-348.
13. Hugill, J. A., Van Welsenens, A. J., "Surface Tension: A Simple Correlation for Natural Gas + Condensate Systems," presented Fourth Int. Conf. of Fluid Properties and Phase Equilibria for Chemical Process Design, Helsingor, 11-16 May, 1986.

14. Sahimi, M., Davis, H. T., Scriven, L. E., "Thermodynamic Modeling of Phase and Tension Behavior of CO₂/Hydrocarbon Systems," Soc. Pet. Eng. J., (April, 1985), p. 235-254.
15. Nagarajan, N., Robinson, R. L., Jr., "Interfacial Tensions in Carbon Dioxide-Hydrocarbon Systems: Development of Experimental Facilities and Acquisition of Experimental Data," Third Annual Progress Report, submitted to Amoco Production Co. (March, 1983).
16. Schoettle, V., Jennings, H. Y., "High-Pressure High-Temperature Visual Cell for Interfacial Tension Measurements," Rev. Sci. Instrum., Vol. 39, (1968), p. 386.
17. Bashforth, S., Adams, J. C., "An Attempt to Test the Theories of Capillary Action," Part 1, Cambridge: Cambridge University Press, 1883.
18. Jennings, H. Y., "Apparatus for Measuring Very Low Interfacial Tensions," Rev. Sci. Instrum., Vol. 28, (1957), p. 774.
19. Porteous, W., "Calculating Surface Tension of Light Hydrocarbons and Their Mixtures," J. Chem. Eng. Data, Vol. 20, (1975), p. 339.
20. Mills, O. S., "Tables for Use in Measurement of Interfacial Tension Between Liquids with Small Density Differences," British Journal of Applied Physics, Vol. 4, (1953).
21. Le Guillou, J. C., Zinn-Justin, J., "Critical Exponents from Field Theory," Phys. Rev. B 21, (1980), p. 3976.
22. Bufkin, B. L. M.S. Thesis, Oklahoma State University, (1986).
23. Wichterle, I., Chappellear, P. S., Kobayashi, R., "Determination of Critical Exponents from Measurements of Binary Vapor-Liquid Equilibrium in the Neighborhood of the Critical Line," J. Computational Phys., Vol. 7, (1971), p. 606.
24. Charoensomsbut-amon, T., Ph.D. Dissertation, Rice University, 1985.
25. Wegner, F. J., "Corrections to Scaling Laws," Phys. Rec., Vol. B 5 (1972), p. 4529.
26. Nagarajan, N., Robinson, R. L., Jr., "Interfacial Tensions in Carbon Dioxide-Hydrocarbon Systems: Development of Experimental Facilities and Acquisitions of Experimental Data, Experimental Data for CO₂ + n-Decane," Technical Progress Report to Amoco Production Co., May, 1983.
27. Robinson, R. L., Jr., Personal Communication, Oklahoma State University, Stillwater, Oklahoma, September, 1986.

28. Gasem, K. A. M., Dickson, K. B., Dulcamara, P. B., Robinson, R. L., Jr., "Interfacial Tensions in Carbon Dioxide-Hydrocarbon Systems: Development of Experimental Facilities and Acquisition of Experimental Data for CO₂ + n-Tetradecane," Technical Progress Report to Amoco Production Co., September 20, 1985.
29. Lee, S. T., Chien, M. C. H., "A New Multicomponent Surface Tension Correlation Based on Scaling Theory," paper 12643 presented at SPE/DOE Fourth Symposium on EOR, Tulsa, Oklahoma, April 15-18, (1984).
30. Pitzer, K. S., Lippmann, D. Z., Curl, R. F., Haggins, C. M., Peterson, D. E., "The Volumetric and Thermodynamic Properties of Fluids. II. Compressibility Factor, Vapor Pressure, and Entropy of Vaporization," Volumetric and Thermodynamic Properties of Fluids, Vol. 77, July 5, (1955), p. 3433-3440.
31. Sivaraman, A., Zega, J., Kobayashi, R., "Correlation for Prediction of Interfacial Tensions of Pure Alkane, Naphthenic and Aromatic Compounds Between Their Freezing and Critical Points," Fluid Phase Equilibria, Vol. 18, (1984), p. 225-235.
32. Sivaraman, A., Kobayashi, R., "Correlation for Prediction of Saturated Liquid Density of Pure Components Incorporating Renormalization Group Formulations with Corresponding-States Principle," paper submitted to Fluid Phase Equilibria, August (1984).
33. Nagaragan, N., Robinson, R. L., Jr., "Interfacial Tensions in Carbon-Dioxide-Hydrocarbon Systems: Development of Experimental Facilities and Acquisition of Experimental Data. Experimental Data for CO₂/n-Butane/n-Decane Ternary System," Technical Progress Report to Amoco Production Co., January, (1984).
34. Nagarajan, N., Chen, Y.-K., and Robinson, R. L., Jr., "Interfacial Tensions in Carbon Dioxide-Hydrocarbon Systems: Development of Experimental Facilities and Acquisition of Experimental Data. Experimental Data for CO₂ + Cyclohexane," Technical Progress Report submitted to Amoco Production Co., May, (1984).
35. Nagarajan, N., Chen, Y.-K., and Robinson, R. L., Jr., "Interfacial Tensions in Carbon Dioxide-Hydrocarbon Systems: Development of Experimental Facilities and Acquisition of Experimental Data. Experimental Data for CO₂ + Benzene," Technical Progress Report submitted to Amoco Production Co., June 14, (1984).
36. Hough, E. W., Wood, B. B., Rzasas, M. J., "Adsorption at Water-Helium, -Methane and -Nitrogen Interfaces at Pressures to 15,000 P.S.I.A.," J. Phys. Chem., Vol. 56, (1952), p. 996.

37. Gasem, K. A. M., Dickson, K. B., Robinson, R. L., Jr., "Interfacial Tensions in Carbon Dioxide-Hydrocarbon Systems: Development of Experimental Facilities and Acquisition of Experimental Data for CO₂ + A Recombined Reservoir Oil," Technical Progress Report submitted to Amoco Production Co., March 28, (1986).
38. Brauer, E. B., and Hough, E. W., "Interfacial Tension of the Normal Butane-Carbon Dioxide System," *Prod. Monthly*, (1965), 29, 13.
39. Simon, R., Rosman, A., and Zana, E., "Phase-Behavior Properties of CO₂ - Reservoir Oil Systems," *Soc. Pet. Eng. J.*, 20 (Feb., 1978).
40. Olds, R. H., Reamer, H. H., Sage, B. H., Lacey, W. N., "Phase Equilibria in Hydrocarbon Systems, the n-Butane - Carbon Dioxide System," *Ind. Eng. Chem.*, Vol. 41, (1949), p. 475.
41. Creek, J. L., Personal Communication with R. L. Robinson, Jr., Chevron Oil Field Research Company, La Habra, California, (September 28, 1983).
42. Creek, J. L., Personal Communication with R. L. Robinson, Jr., Chevron Oil Field Research Company, La Habra, California, (February 28, 1986).
43. Holm, L. W., and Josendal, V. A., "Mechanisms of Oil Displacement by Carbon Dioxide," *J. Pet. Tech.*, (Dec., 1974), p. 1427-1438; *Trans., AIME*, 257.
44. Emmanuel, A. S., Behrens, R. A., and McMillen, T. J., "A Generalized Method for Predicting Gas/Oil Miscibility," *SPE Res. Eng.*, (Sept., 1986), p. 463-473.
45. Deam, J. R., Maddox, R. N., "Interfacial Tension in Hydrocarbon Systems," *J. Chem. Engr.*, Vol. 15, No. 2, (1970).
46. Levelt-Sengers, J. M. H., Greer, W. L., Sengers, J. V., "Scaled Equations of State Parameters for Gases in the Critical Region," *J. Phys. Chem. Ref. Data*, Vol. 5, No. 1, (1976).
47. Robinson, R. L., Jr., Personal Communication, Oklahoma State University, (August, 1986).
48. Hsu, J. J.-C., Nagarajan, N., Robinson, R. L., Jr., "Equilibrium Phase Compositions, Phase Densities, and Interfacial Tensions for CO₂ + Hydrocarbon Systems. 1. CO₂ + n-Butane," *J. Chem. Eng. Data*, Vol. 30, (1985), p. 485-491.

APPENDICES

APPENDIX A

EXPERIMENTAL DATA

The experimental data for the CO_2 + n-butane, CO_2 + n-decane, CO_2 + n-tetradecane, CO_2 + benzene, and CO_2 + cyclohexane binary systems are shown in Tables XXX through XXXVIII. The experimental data for the ternary system CO_2 /n-butane/n-decane are shown in Table XXVII. The experimental data include IFTs, equilibrium phase compositions, and equilibrium phase densities at various temperatures and pressures. The experimental data were used in the evaluations of the IFT correlations studied in this work. All data were obtained at Oklahoma State University using the experimental apparatus described in Chapter III. The specific sources of the data were listed in Table I, Chapter II. The CO_2 + n-tetradecane data shown in Table XXXV is the same as that shown in Table II, Chapter IV, but was included here for completeness.

TABLE XXX
 PHASE EQUILIBRIA AND INTERFACIAL TENSIONS FOR
 CO₂ + N-BUTANE AT 319.3 K (115°F)

Pressure		Phase Compositions, Mole Fraction CO ₂		Phase Densities, (kg/m ³) x 10 ⁻³		Interfacial Tension, mN/m
kPa	psia	Liquid	Vapor	Liquid	Vapor	
2180	316	0.188	0.745	0.5634	0.0501	5.75
2585	375	0.232	0.778	0.5677	0.0592	5.37
3425	497	0.335	0.826	0.5767	0.0760	4.41
3545	514	0.346	0.830	0.5779	0.0779	4.27
4205	610	0.428	0.856	0.5849	0.0992	3.55
4895	710	0.515	0.873	0.5869	0.1244	2.63
5475	794	0.592	0.885	0.5835	0.1472	1.93
6035	875	0.665	0.893	0.5767	0.1713	1.42
6245	906	0.692	0.893	0.5731	0.1858	1.10
6605	958	0.735	0.896	0.5629	0.2114	0.729
6720	975	0.750	0.898	0.5573	0.2204	0.598
6965	1010	0.778	0.898	0.5495	0.2393	0.412
7155	1038	0.800	0.899	0.5320	0.2596	0.255
7260	1053	0.811	0.898	0.5212	0.2732	0.177
7355	1067	0.824	0.897	0.5103	0.2891	0.116
7435	1078	0.835	0.896	0.5015	0.3002	0.071
7500	1088	0.842	0.893	0.4919	0.3175	0.048
7550	1095	0.850	0.893	0.4782	0.3349	0.026
7585	1100	0.855	0.888	0.4700	0.3559	-----
7620	1105	0.864	0.882	0.4450	0.3835	-----
+7640	1108	0.873	0.876	0.4194	0.4101	-----
*7625	1106	- 0.875 -		- 0.4060 -		-----

* Estimated critical point
 + Suspect data point

TABLE XXXI
 PHASE EQUILIBRIA AND INTERFACIAL TENSIONS FOR
 CO₂ + N-BUTANE AT 344.3 K (160°F)

Pressure		Phase Compositions, Mole Fraction CO ₂		Phase Densities, (kg/m ³) x 10 ⁻³		Interfacial Tension, mN/m
kPa	psia	Liquid	Vapor	Liquid	Vapor	
3205	465	0.208	0.682	0.5201	0.0691	4.22
4205	610	0.297	0.740	0.5233	0.0946	3.16
4820	699	0.353	0.761	0.5229	0.1132	2.48
5530	802	0.418	0.777	0.5209	0.1352	1.85
6245	906	0.486	0.788	0.5159	0.1637	1.28
6860	995	0.545	0.791	0.5061	0.1932	0.703
7300	1059	0.590	0.788	0.4926	0.2216	0.397
7610	1104	0.623	0.783	0.4783	0.2487	0.226
7770	1127	0.641	0.778	0.4670	0.2674	0.129
7865	1142	0.653	0.773	0.4595	0.2814	0.090
7945	1152	0.663	0.768	0.4493	0.2922	0.057
7965	1155	0.666	0.767	0.4473	0.2965	0.047
8055	1168	0.682	0.757	0.4290	0.3159	-----
8065	1170	0.685	0.755	0.4249	0.3192	-----
8080	1173	0.691	0.750	0.4170	0.3284	-----
*8120	1178	- 0.720 -		- 0.3735 -		-----

* Estimated critical point

TABLE XXXII
 PHASE EQUILIBRIA AND INTERFACIAL TENSIONS FOR
 CO₂ + N-BUTANE AT 377.6 K (220°F)

Pressure		Phase Compositions, Mole Fraction CO ₂		Phase Densities, (kg/m ³) x 10 ⁻³		Interfacial Tension, mN/m
kPa	psia	Liquid	Vapor	Liquid	Vapor	
2880	418	0.088	0.340	0.4565	0.0714	2.67
3435	498	0.129	0.414	0.4552	0.0836	2.24
4165	604	0.181	0.481	0.4521	0.1025	1.73
4840	702	0.230	0.525	0.4474	0.1218	1.33
5545	804	0.284	0.556	0.4399	0.1460	0.887
5950	863	0.315	0.565	0.4340	0.1617	0.646
6265	909	0.341	0.571	0.4274	0.1761	0.496
6600	957	0.368	0.575	0.4187	0.1928	0.316
6915	1003	0.398	0.573	0.4072	0.2125	0.170
7020	1018	0.406	0.572	0.4044	0.2186	0.138
7175	1041	0.423	0.569	0.3961	0.2313	0.096
7295	1058	0.434	0.565	0.3877	0.2436	0.054
7425	1077	0.452	0.554	0.3745	0.2604	-----
7530	1092	0.473	0.539	0.3551	0.2824	-----
7565	1097	0.485	0.527	0.3415	0.2967	-----
*7580	1099	- 0.510 -		- 0.3195 -		-----

TABLE XXXIII
 PHASE EQUILIBRIA AND INTERFACIAL TENSIONS FOR
 CO₂ + N-DECANE AT 344.3 K (160°F)

Pressure		Phase Compositions, Mole Fraction CO ₂		Phase Densities, (kg/m ³) × 10 ⁻³		Interfacial Tension, mN/m
kPa	psia	Liquid	Vapor	Liquid	Vapor	
6385	926	0.457	0.995	0.7081	0.1303	-----
6940	1007	0.489	0.995	0.7099	0.1456	7.81
7610	1104	0.535	0.995	0.7111	0.1630	6.65
8340	1210	0.575	0.995	0.7140	0.1885	5.67
8960	1300	0.615	0.994	0.7154	0.2119	4.61
9650	1400	0.657	0.993	0.7164	0.2418	3.54
10340	1500	0.702	0.990	0.7166	0.2770	2.53
11020	1599	0.753	0.987	0.7146	0.3194	1.71
11380	1650	0.775	0.986	0.7120	0.3429	1.29
11730	1701	0.804	0.983	0.7074	0.3755	0.848
11900	1726	0.815	0.981	0.7043	0.3930	0.665
12070	1751	0.834	0.979	0.6995	0.4122	0.529
12220	1772	0.847	0.976	0.6944	0.4306	0.356
12400	1799	0.866	0.971	0.6840	0.4595	0.245
12490	1811	0.877	0.968	0.6763	0.4758	0.142
12550	1821	0.883	0.965	0.6708	0.4899	0.101
12620	1830	0.886	0.960	0.6627	0.5039	0.059
12670	1835	0.893	0.955	0.6511	0.5230	0.029
12700	1842	0.897	0.953	0.6379	0.5358	0.0125
12730	1847	0.918	0.935	0.6191	0.5853	-----
+12760	1850	0.925	0.931	0.6128	0.6025	-----
*12740	1848	- 0.930 -		- 0.5905 -		-----

* Estimated critical point
 + Suspect data point

TABLE XXXIV
 PHASE EQUILIBRIA AND INTERFACIAL TENSIONS FOR
 CO₂ + N-DECANE AT 377.6 K (220°F)

Pressure		Phase Compositions, Mole Fraction CO ₂		Phase Densities, (kg/m ³) x 10 ⁻³		Interfacial Tension, mN/m
kPa	psia	Liquid	Vapor	Liquid	Vapor	
10340	1500	0.565	0.987	0.6762	0.2051	4.39
11040	1601	0.595	0.985	0.6760	0.2241	3.73
11750	1705	0.626	0.984	0.6742	0.2469	3.08
12420	1801	0.656	0.981	0.6716	0.2688	2.54
13120	1903	0.689	0.978	0.6709	0.2939	1.98
13800	2001	0.719	0.975	0.6677	0.3221	1.42
14150	2053	0.734	0.973	0.6652	0.3366	1.24
14480	2100	0.746	0.970	0.6604	0.3521	0.950
14830	2151	0.757	0.968	0.6587	0.3696	0.792
15170	2201	0.776	0.964	0.6539	0.3886	0.634
15350	2226	0.784	0.962	0.6509	0.3997	0.482
15510	2250	0.794	0.959	0.6472	0.4104	0.390
15690	2276	0.806	0.957	0.6432	0.4241	0.314
15850	2299	0.816	0.953	0.6380	0.4357	0.221
15960	2315	0.821	0.950	0.6336	0.4460	0.171
16070	2331	0.829	0.946	0.6288	0.4573	0.127
16140	2341	0.836	0.944	0.6249	0.4638	0.100
16220	2353	0.842	0.940	0.6195	0.4741	0.069
16280	2362	0.846	0.937	0.6133	0.4814	0.051
16350	2371	0.854	0.933	0.6075	0.4916	0.033

TABLE XXXIV (CONTINUED)

Pressure		Phase Compositions, Mole Fraction CO ₂		Phase Densities, (kg/m ³) x 10 ⁻³		Interfacial Tension, mN/m
kPa	psia	Liquid	Vapor	Liquid	Vapor	
16380	2376	0.856	0.930	0.6027	0.5000	0.020
16410	2381	0.860	0.926	0.5990	0.5061	0.012
16450	2386	0.865	0.922	0.5940	0.5099	0.008
16460	2388	0.870	0.916	0.5845	0.5199	-----
+16490	2392	-----	-----	0.5632	0.5527	-----
*16480	2391	- 0.895 -		- 0.5535 -		-----

* Estimated critical point

+ Suspect data point

TABLE XXXV

PHASE EQUILIBRIA AND INTERFACIAL TENSIONS FOR CO₂ + N-TETRADECANE AT 344.3 K (160°F)

Phase Compositions, Mole Fraction CO ₂				Phase Densities, (kg/m ³) x 10 ⁻³				IFT-Density Difference Ratio	
Liquid Phase		Vapor Phase		Liquid Phase		Vapor Phase		Pressure, psia	$\gamma/\Delta\rho \times 10^3$ (mN/m)/(kg/m ³)
Pressure, psia	Composition, x	Pressure, psia	Composition, y	Pressure, psia	Density, ρ^L	Pressure, psia	Density, ρ^V		
		1027	0.989			1029	0.1466		
		1204	0.989			1204	0.1827		
		1307	0.988			1306	0.2076		
		1506	0.991			1504	0.2640		
1606	0.685	1603	0.992	1601	0.7508	1602	0.2966	1602	8.95
1694	0.711	1696	0.991	1694	0.7514	1695	0.3324	1693	7.85
1787	0.738	1788	0.992	1787	0.7525	1787	0.3708	1787	6.48
1902	0.769	1900	0.988	1900	0.7545	1899	0.4251	1901	5.48
2025	0.797	2017	0.987	2025	0.7551	2017	0.4861	2022	4.00
2025	0.797	2017	0.987	2025	0.7551	2017	0.4861	2022	4.26
2111	0.819	2102	0.984	2101	0.7546	2101	0.5303	2106	3.22
2153	0.827	2145	0.983	2153	0.7541	2144	0.5532	2148	2.93
2194	0.839	2197	0.983	2190	0.7528	2190	0.5766	2188	2.32
2256	0.857	2256	0.976	2255	0.7523	2256	0.6102	2256	1.43
2276	0.862	2274	0.976	2275	0.7504	2273	0.6165	2272	1.22
2309	0.870	2296	0.971	2307	0.7486	2307	0.6321	2307	0.790
2325	0.877	2315	0.968	2324	0.7458	2324	0.6411	2324	0.700
2341	0.885	2340	0.965	2342	0.7442	2342	0.6544	2342	0.445
2353	0.887	2346	0.964	2354	0.7409	2354	0.6598	2354	0.296
2363	0.893	2360	0.960	2360	0.7388	2360	0.6659	2361	0.195
2364	0.895	2364	0.958	2361	0.7373	2361	0.6670	2365	0.173
2372	0.899	2365	0.955	2365	0.7365	2365	0.6705		

TABLE XXXVI
 PHASE EQUILIBRIA AND INTERFACIAL TENSIONS FOR
 CO₂ + BENZENE AT 344.3 K (160°F)

Pressure		Phase Compositions, Mole Fraction CO ₂		Phase Densities, (kg/m ³) x 10 ⁻³		Interfacial Tension, mN/m
kPa	psia	Liquid	Vapor	Liquid	Vapor	
6895	1000	0.453	0.932	0.8150	0.1560	6.60
7590	1101	0.507	0.937	0.8095	0.1775	4.96
8280	1201	0.564	0.941	0.8012	0.2048	3.72
8960	1300	0.625	0.940	0.7875	0.2374	2.48
9645	1399	0.692	0.936	0.7636	0.2786	1.39
9855	1430	0.712	0.934	0.7503	0.2952	1.10
9995	1450	0.726	0.932	0.7403	0.3061	0.917
10170	1475	0.745	0.929	0.7312	0.3223	0.709
10340	1500	0.763	0.925	0.7141	0.3413	0.508
10480	1520	0.779	0.924	0.6977	0.3577	0.363
10580	1535	0.793	0.919	0.6853	0.3744	0.262
10690	1550	0.805	0.916	0.6692	0.3910	0.172
10750	1559	0.815	0.912	0.6578	0.4064	0.123
10830	1571	0.828	0.907	0.6376	0.4275	0.065
10890	1580	0.841	0.902	0.6167	0.4500	0.026
10920	1584	0.846	0.898	0.5996	0.4642	0.011
†10960	1589	0.875	0.877	0.5455	0.5455	-----
*10960	1589	- 0.875 -		- 0.5330 -		

* Estimated critical point

† Suspect data point

TABLE XXXVII

 PHASE EQUILIBRIA AND INTERFACIAL TENSIONS FOR
 CO₂ + CYCLOHEXANE AT 344.3 K (160°F)

Pressure		Phase Compositions, Mole Fraction CO ₂		Phase Densities, (kg/m ³) x 10 ⁻³		Interfacial Tension, mN/m
kPa	psia	Liquid	Vapor	Liquid	Vapor	
6870	997	0.426	0.952	0.7348	0.1493	6.35
7590	1101	0.481	0.947	0.7336	0.1760	4.98
8270	1200	0.534	0.949	0.7309	0.2054	3.71
8960	1300	0.596	0.946	0.7248	0.2341	2.62
9650	1400	0.665	0.940	0.7119	0.2785	1.39
9995	1450	0.704	0.935	0.7005	0.3044	0.947
10340	1500	0.747	0.927	0.6796	0.3375	0.519
10510	1525	0.766	0.923	0.6658	0.3592	0.365
10620	1540	0.781	0.920	0.6553	0.3756	0.254
10690	1550	0.792	0.916	0.6451	0.3876	0.180
10760	1560	0.803	0.913	0.6353	0.4011	0.135
10820	1570	0.815	0.908	0.6198	0.4170	0.081
10890	1579	0.826	0.901	0.6058	0.4396	0.036
10930	1586	0.840	0.896	0.5822	0.4680	0.009
†10960	1589	0.848	0.883	0.5683	0.4987	-----
*10970	1590	- 0.880 -		- 0.5250 -		

* Estimated critical point

† Suspect data point

TABLE XXXVIII

PHASE EQUILIBRIA AND INTERFACIAL TENSIONS FOR A 90% CO₂/6%
N-BUTANE/4% N-DECANE MIXTURE AT 344.3 K (160°F)*

Pressure,		Phase Compositions, Mole Fractions				Phase Densities, (kg/m ³) x 10 ⁻³		Interfacial Tension
MPa	psia	Liquid		Vapor		Liquid	Vapor	mN/m
		CO ₂	nC ₄	CO ₂	nC ₄			
9.03	1310	0.637	0.157	0.948	0.029	0.6822	0.2348	----
9.31	1351	0.643	0.150	0.949	0.032	0.6812	0.2498	2.43
9.65	1400	0.671	0.139	0.949	0.031	0.6793	0.2686	1.77
10.00	1451	0.704	0.129	0.948	0.034	0.6763	0.2887	1.34
10.35	1501	0.732	0.116	0.945	0.036	0.6717	0.3137	0.94
10.51	1524	0.744	0.114	0.943	0.038	0.6661	0.3269	0.76
10.71	1553	0.767	0.106	0.942	0.039	0.6611	0.3473	0.545
10.89	1580	0.802	0.098	0.941	0.039	0.6556	0.3667	0.405
11.04	1601	0.809	0.093	0.938	0.042	0.6483	0.3845	0.295
11.17	1621	0.826	0.087	0.934	0.044	0.6388	0.4046	0.200
11.30	1640	0.838	0.082	0.932	0.045	0.6276	0.4283	0.115
11.38	1651	0.852	0.078	0.927	0.048	0.6181	0.4454	0.064
11.45	1661	0.861	0.075	0.919	0.051	0.6070	0.4638	0.033
11.51	1670	0.874	0.070	0.911	0.054	0.5890	0.4915	-----
11.57	#1678	0.902	0.058	0.903	0.058	0.5253	0.5213	-----

* Exact overall compositions in 90.2% CO₂/5.9 C₄/3.9% C₁₀

Suspect data point

APPENDIX B

REDUCED PARACHORS FROM EQUATION E.15

FOR $k = 3.55$ AND $k = 3.91$

Tables XXXIX and XL show the reduced parachors, $[P]^*$, calculated from Equation E.15 using a scaling exponent of $k = 3.55$ and $k = 3.91$, respectively. Reduced parachors $[P]^*$ were calculated at each scaling exponent varying (ω^*) from zero to one and T_r from 0.58 to 0.9999.

The reduced parachors shown in Tables XXXIX and XL were used to obtain constant values for $[P]^*$ at $\omega^* = 0.00$ and $\omega^* = 1.0$ ($\omega = 0.49$, n-decane) at scaling exponents of $k = 3.55$ and $k = 3.91$. These values were used in Equations E.17 and E.19 to obtain equations for the reduced parachor as a function of reduced acentric factor ω^* , without any temperature dependence. Next, the information in Tables XXXIX and XL used to obtain linear equations for $[P]^*$ as a function of reduced temperature T_r at $\omega^* = 0.00$ and $\omega^* = 1.0$ ($\omega = 0.49$, n-decane) and scaling exponents of $k = 3.55$ and 3.91 . These two equations were used in Equations E.18 and E.20 to obtain equations for the reduced parachor as a function of reduced acentric factor ω^* and reduced temperature T_r .

As mentioned above, Equations E.17 and E.19 require values of the reduced parachor $[P]^*$ at $\omega^* = 0.00$ and $\omega^* = 1.0$ ($\omega = 0.49$, n-decane) and independent of temperature. For Equation E.17 ($k = 3.55$), reduced parachor values of:

$$[P]^*_{(0)} = 1.14 \times 10^{-4}$$

TABLE XXXIX

PRESENT WORK REDUCED PARACHORS WITH K = 3.55

TR	W*=0.0	W*=0.1	W*=0.2	W*=0.3	W*=0.4	W*=0.5	W*=0.6	W*=0.7	W*=0.8	W*=0.9	W*=1.0
0.9999	0.1047D-04	0.2429D-04	0.3757D-04	0.5037D-04	0.6273D-04	0.7468D-04	0.8625D-04	0.9744D-04	0.1083D-03	0.1188D-03	0.1290D-03
0.9995	0.3185D-04	0.4315D-04	0.5400D-04	0.6443D-04	0.7448D-04	0.8417D-04	0.9351D-04	0.1025D-03	0.1112D-03	0.1197D-03	0.1278D-03
0.9992	0.4012D-04	0.5047D-04	0.6040D-04	0.6995D-04	0.7913D-04	0.8797D-04	0.9649D-04	0.1047D-03	0.1126D-03	0.1203D-03	0.1277D-03
0.9990	0.4435D-04	0.5422D-04	0.6369D-04	0.7279D-04	0.8154D-04	0.8996D-04	0.9806D-04	0.1059D-03	0.1134D-03	0.1207D-03	0.1277D-03
0.9970	0.6737D-04	0.7473D-04	0.8178D-04	0.8854D-04	0.9503D-04	0.1013D-03	0.1073D-03	0.1130D-03	0.1186D-03	0.1239D-03	0.1291D-03
0.9950	0.7848D-04	0.8473D-04	0.9071D-04	0.9644D-04	0.1019D-03	0.1072D-03	0.1123D-03	0.1172D-03	0.1218D-03	0.1264D-03	0.1307D-03
0.9900	0.9237D-04	0.9740D-04	0.1022D-03	0.1068D-03	0.1113D-03	0.1155D-03	0.1196D-03	0.1235D-03	0.1273D-03	0.1310D-03	0.1345D-03
0.9800	0.1030D-03	0.1075D-03	0.1117D-03	0.1158D-03	0.1197D-03	0.1235D-03	0.1271D-03	0.1306D-03	0.1339D-03	0.1371D-03	0.1403D-03
0.9700	0.1072D-03	0.1116D-03	0.1159D-03	0.1199D-03	0.1239D-03	0.1277D-03	0.1313D-03	0.1348D-03	0.1382D-03	0.1414D-03	0.1446D-03
0.9600	0.1092D-03	0.1137D-03	0.1181D-03	0.1224D-03	0.1264D-03	0.1304D-03	0.1341D-03	0.1378D-03	0.1413D-03	0.1447D-03	0.1480D-03
0.9500	0.1102D-03	0.1150D-03	0.1195D-03	0.1240D-03	0.1282D-03	0.1323D-03	0.1363D-03	0.1401D-03	0.1438D-03	0.1473D-03	0.1508D-03
0.9400	0.1108D-03	0.1157D-03	0.1205D-03	0.1251D-03	0.1295D-03	0.1338D-03	0.1379D-03	0.1419D-03	0.1458D-03	0.1495D-03	0.1531D-03
0.9200	0.1114D-03	0.1167D-03	0.1218D-03	0.1267D-03	0.1314D-03	0.1360D-03	0.1404D-03	0.1447D-03	0.1489D-03	0.1529D-03	0.1568D-03
0.9000	0.1118D-03	0.1174D-03	0.1227D-03	0.1279D-03	0.1328D-03	0.1377D-03	0.1423D-03	0.1469D-03	0.1513D-03	0.1555D-03	0.1596D-03
0.8800	0.1122D-03	0.1179D-03	0.1234D-03	0.1288D-03	0.1340D-03	0.1390D-03	0.1439D-03	0.1486D-03	0.1532D-03	0.1576D-03	0.1619D-03
0.8600	0.1126D-03	0.1184D-03	0.1241D-03	0.1296D-03	0.1350D-03	0.1402D-03	0.1452D-03	0.1501D-03	0.1548D-03	0.1594D-03	0.1639D-03
0.8400	0.1129D-03	0.1189D-03	0.1247D-03	0.1304D-03	0.1359D-03	0.1412D-03	0.1463D-03	0.1513D-03	0.1562D-03	0.1609D-03	0.1655D-03
0.8200	0.1133D-03	0.1194D-03	0.1253D-03	0.1311D-03	0.1367D-03	0.1421D-03	0.1473D-03	0.1525D-03	0.1575D-03	0.1623D-03	0.1670D-03
0.8000	0.1137D-03	0.1199D-03	0.1259D-03	0.1317D-03	0.1374D-03	0.1429D-03	0.1483D-03	0.1535D-03	0.1586D-03	0.1636D-03	0.1684D-03
0.7800	0.1140D-03	0.1203D-03	0.1264D-03	0.1323D-03	0.1381D-03	0.1437D-03	0.1491D-03	0.1545D-03	0.1597D-03	0.1647D-03	0.1696D-03
0.7600	0.1143D-03	0.1207D-03	0.1268D-03	0.1328D-03	0.1387D-03	0.1444D-03	0.1499D-03	0.1554D-03	0.1606D-03	0.1658D-03	0.1708D-03
0.7400	0.1145D-03	0.1210D-03	0.1272D-03	0.1333D-03	0.1393D-03	0.1450D-03	0.1507D-03	0.1562D-03	0.1616D-03	0.1668D-03	0.1719D-03
0.7200	0.1147D-03	0.1212D-03	0.1276D-03	0.1338D-03	0.1398D-03	0.1456D-03	0.1514D-03	0.1570D-03	0.1624D-03	0.1677D-03	0.1729D-03
0.7000	0.1149D-03	0.1215D-03	0.1279D-03	0.1341D-03	0.1402D-03	0.1462D-03	0.1520D-03	0.1577D-03	0.1632D-03	0.1686D-03	0.1739D-03
0.6800	0.1150D-03	0.1216D-03	0.1281D-03	0.1345D-03	0.1407D-03	0.1467D-03	0.1526D-03	0.1583D-03	0.1640D-03	0.1695D-03	0.1748D-03
0.6600	0.1150D-03	0.1218D-03	0.1283D-03	0.1348D-03	0.1410D-03	0.1471D-03	0.1531D-03	0.1590D-03	0.1647D-03	0.1702D-03	0.1757D-03
0.6400	0.1150D-03	0.1219D-03	0.1285D-03	0.1350D-03	0.1413D-03	0.1475D-03	0.1536D-03	0.1595D-03	0.1653D-03	0.1709D-03	0.1765D-03
0.6200	0.1150D-03	0.1219D-03	0.1286D-03	0.1352D-03	0.1416D-03	0.1479D-03	0.1540D-03	0.1600D-03	0.1659D-03	0.1716D-03	0.1772D-03
0.6000	0.1150D-03	0.1219D-03	0.1287D-03	0.1354D-03	0.1419D-03	0.1482D-03	0.1544D-03	0.1604D-03	0.1664D-03	0.1721D-03	0.1778D-03
0.5800	0.1149D-03	0.1219D-03	0.1288D-03	0.1355D-03	0.1421D-03	0.1485D-03	0.1547D-03	0.1608D-03	0.1668D-03	0.1726D-03	0.1783D-03

TABLE XL

PRESENT WORK REDUCED PARACHORS WITH K = 3.91

TR	W*-0.0	W*-0.1	W*-0.2	W*-0.3	W*-0.4	W*-0.5	W*-0.6	W*-0.7	W*-0.8	W*-0.9	W*-1.0
0 9999	0 3537D-04	0 7584D-04	0 1125D-03	0 1466D-03	0 1787D-03	0 2090D-03	0 2379D-03	0 2654D-03	0 2917D-03	0 3170D-03	0 3411D-03
0 9995	0 9272D-04	0 1219D-03	0 1492D-03	0 1749D-03	0 1992D-03	0 2222D-03	0 2441D-03	0 2650D-03	0 2849D-03	0 3040D-03	0 3223D-03
0 9992	0 1128D-03	0 1387D-03	0 1630D-03	0 1859D-03	0 2076D-03	0 2282D-03	0 2477D-03	0 2664D-03	0 2842D-03	0 3012D-03	0 3175D-03
0 9990	0 1228D-03	0 1471D-03	0 1699D-03	0 1915D-03	0 2119D-03	0 2313D-03	0 2498D-03	0 2673D-03	0 2841D-03	0 3001D-03	0 3155D-03
0 9970	0 1738D-03	0 1906D-03	0 2065D-03	0 2216D-03	0 2358D-03	0 2494D-03	0 2623D-03	0 2746D-03	0 2863D-03	0 2975D-03	0 3082D-03
0 9950	0 1967D-03	0 2105D-03	0 2235D-03	0 2358D-03	0 2475D-03	0 2587D-03	0 2693D-03	0 2794D-03	0 2890D-03	0 2982D-03	0 3071D-03
0 9900	0 2234D-03	0 2339D-03	0 2439D-03	0 2535D-03	0 2625D-03	0 2711D-03	0 2793D-03	0 2871D-03	0 2946D-03	0 3017D-03	0 3085D-03
0 9800	0 2414D-03	0 2504D-03	0 2588D-03	0 2669D-03	0 2746D-03	0 2819D-03	0 2889D-03	0 2956D-03	0 3019D-03	0 3080D-03	0 3139D-03
0 9700	0 2470D-03	0 2558D-03	0 2642D-03	0 2721D-03	0 2797D-03	0 2869D-03	0 2939D-03	0 3005D-03	0 3068D-03	0 3129D-03	0 3187D-03
0 9600	0 2488D-03	0 2578D-03	0 2664D-03	0 2746D-03	0 2824D-03	0 2898D-03	0 2970D-03	0 3038D-03	0 3104D-03	0 3166D-03	0 3227D-03
0 9500	0 2492D-03	0 2585D-03	0 2674D-03	0 2759D-03	0 2840D-03	0 2917D-03	0 2991D-03	0 3063D-03	0 3131D-03	0 3196D-03	0 3259D-03
0 9400	0 2489D-03	0 2586D-03	0 2678D-03	0 2766D-03	0 2850D-03	0 2930D-03	0 3007D-03	0 3082D-03	0 3153D-03	0 3221D-03	0 3287D-03
0 9200	0 2479D-03	0 2581D-03	0 2679D-03	0 2772D-03	0 2862D-03	0 2948D-03	0 3030D-03	0 3110D-03	0 3186D-03	0 3259D-03	0 3330D-03
0 9000	0 2470D-03	0 2576D-03	0 2678D-03	0 2776D-03	0 2870D-03	0 2960D-03	0 3047D-03	0 3130D-03	0 3210D-03	0 3288D-03	0 3362D-03
0 8800	0 2462D-03	0 2572D-03	0 2678D-03	0 2779D-03	0 2876D-03	0 2970D-03	0 3060D-03	0 3146D-03	0 3230D-03	0 3311D-03	0 3388D-03
0 8600	0 2458D-03	0 2570D-03	0 2678D-03	0 2782D-03	0 2882D-03	0 2978D-03	0 3071D-03	0 3160D-03	0 3246D-03	0 3330D-03	0 3410D-03
0 8400	0 2455D-03	0 2569D-03	0 2679D-03	0 2785D-03	0 2887D-03	0 2986D-03	0 3081D-03	0 3172D-03	0 3261D-03	0 3346D-03	0 3429D-03
0 8200	0 2453D-03	0 2569D-03	0 2681D-03	0 2789D-03	0 2893D-03	0 2993D-03	0 3090D-03	0 3183D-03	0 3274D-03	0 3361D-03	0 3446D-03
0 8000	0 2452D-03	0 2570D-03	0 2683D-03	0 2793D-03	0 2898D-03	0 3000D-03	0 3098D-03	0 3193D-03	0 3286D-03	0 3375D-03	0 3461D-03
0 7800	0 2452D-03	0 2571D-03	0 2685D-03	0 2796D-03	0 2903D-03	0 3006D-03	0 3106D-03	0 3203D-03	0 3297D-03	0 3387D-03	0 3475D-03
0 7600	0 2451D-03	0 2571D-03	0 2687D-03	0 2799D-03	0 2908D-03	0 3012D-03	0 3114D-03	0 3212D-03	0 3307D-03	0 3400D-03	0 3489D-03
0 7400	0 2450D-03	0 2571D-03	0 2689D-03	0 2802D-03	0 2912D-03	0 3018D-03	0 3121D-03	0 3221D-03	0 3317D-03	0 3411D-03	0 3502D-03
0 7200	0 2448D-03	0 2571D-03	0 2690D-03	0 2804D-03	0 2915D-03	0 3023D-03	0 3127D-03	0 3228D-03	0 3327D-03	0 3422D-03	0 3515D-03
0 7000	0 2446D-03	0 2570D-03	0 2690D-03	0 2806D-03	0 2919D-03	0 3028D-03	0 3133D-03	0 3236D-03	0 3335D-03	0 3432D-03	0 3526D-03
0 6800	0 2443D-03	0 2569D-03	0 2690D-03	0 2807D-03	0 2921D-03	0 3031D-03	0 3139D-03	0 3243D-03	0 3344D-03	0 3442D-03	0 3537D-03
0 6600	0 2440D-03	0 2567D-03	0 2689D-03	0 2808D-03	0 2923D-03	0 3035D-03	0 3143D-03	0 3249D-03	0 3351D-03	0 3450D-03	0 3547D-03
0 6400	0 2436D-03	0 2564D-03	0 2688D-03	0 2808D-03	0 2924D-03	0 3037D-03	0 3147D-03	0 3254D-03	0 3357D-03	0 3458D-03	0 3556D-03
0 6200	0 2432D-03	0 2561D-03	0 2686D-03	0 2808D-03	0 2925D-03	0 3039D-03	0 3150D-03	0 3258D-03	0 3363D-03	0 3465D-03	0 3564D-03
0 6000	0 2428D-03	0 2558D-03	0 2684D-03	0 2807D-03	0 2926D-03	0 3041D-03	0 3153D-03	0 3261D-03	0 3367D-03	0 3470D-03	0 3570D-03
0 5800	0 2423D-03	0 2555D-03	0 2682D-03	0 2806D-03	0 2925D-03	0 3041D-03	0 3154D-03	0 3264D-03	0 3370D-03	0 3473D-03	0 3574D-03

$$[P]^*_{(\omega = 0.49)} = 1.69 \times 10^{-4}$$

were obtained from Table XXXIX at $Tr = 0.78$ ($Tr = 0.78$ was the mid-range of the reduced temperatures). The value of $[P]^*_{(0)}$ was essentially constant over the range of reduced temperatures, but the values of $[P]^*_{(\omega = 0.49)}$ indicated a slight variation, however the mid-range value indicated above was selected. For Equation E.19 ($k = 3.91$), reduced parachor values of:

$$[P]^*_{(0)} = 2.452 \times 10^{-4}$$

$$[P]^*_{(\omega = 0.49)} = 3.50 \times 10^{-4}$$

were obtained from Table XL. The value of $[P]^*_{(0)}$ at $Tr = 0.78$ was essentially constant over the range of reduced temperatures. Again, the value of $[P]^*_{(\omega = 0.49)}$ indicated a slight variation with reduced temperature, however, an average value at $Tr = 0.74$ was selected.

Since the reduced parachors in Tables XXXIX and XL indicated a slight variation with reduced temperature, a linear function in reduced temperature (Tr) was obtained for $[P]^*_{(0)}$ and $[P]^*_{(\omega = 0.49)}$ using the data in Tables XXXIX and XL. For Equation E.18 ($k = 3.55$), the following two equations for $[P]^*_{(0)}$ and $[P]^*_{(\omega = 0.49)}$ as a function of reduced temperature were obtained from a linear least squares fit of the data in Table XXXIX.

$$[P]^*_{(0)} = 1.22 \times 10^{-4} + 1.01 \times 10^{-5} Tr \quad (B.1)$$

$$[P]^*_{(\omega = 0.49)} = 2.13 \times 10^{-4} + -5.70 \times 10^{-5} \text{ Tr} \quad (\text{B.2})$$

For Equation E.20 ($k = 3.91$), the following two equations for $[P]^*_{(0)}$ and $[P]^*_{(\omega = 0.49)}$ as a function of reduced temperature were obtained from a linear least squares fit of the data in Table XL.

$$[P]^*_{(0)} = 2.36 \times 10^{-4} + 1.18 \times 10^{-5} \text{ Tr} \quad (\text{B.3})$$

$$[P]^*_{(\omega = 0.49)} = 3.93 \times 10^{-4} + -5.91 \times 10^{-5} \text{ Tr} \quad (\text{B.4})$$

The values of $[P]^*_{(0)}$ and $[P]^*_{(\omega = 0.49)}$ at the four combinations of ($k = 3.55$ and 3.91) and (with and without temperature dependence) were used in Appendix E, Equations E.17 - E.20 to calculate parachors based on the correlations developed in this work. The results of these calculations for the six pure components studied in this work are shown in Chapter V.

APPENDIX C

COMPARISON OF IFTS PREDICTED BY CORRELATIONS

STUDIED IN THIS WORK

The true value of the interfacial tension (IFT) correlations evaluated in this work lies in their ability to predict the IFTs of multicomponent systems. The results presented below show this predictive ability for the W-K, L-C and "this work" IFT correlations. The experimental data for the five CO₂ + hydrocarbon binary systems, Appendix A, was used in this evaluation.

For all correlations, the experimental data on phase densities and compositions for the five binary systems were used in the evaluations. As mentioned earlier, appropriate equations of state (EOS) could be used to predict these properties if experimental data are not available (which is generally the case).

Results for the W-K correlation (Equation 2.7) are presented using pure component parachors predicted by the three parachor correlations evaluated in this work (e.g., L-C = Equation 2.16, H-VW = Equation 5.2, "this work" = Equation E.17 - E.20). Results for the L-C mixed parachor IFT correlation (Equation 2.15) and the IFT correlation proposed in this work (Equation 5.4) are also presented. The results are indicated in Tables XLI through LXXII. Tables XLI through XLVIII show the results for the five binary systems using a scaling exponent of $k = 3.55$ in the W-K, L-C and "this work mixed" IFT correlations. Equation E.17 (developed with $k = 3.55$ and no temperature dependence) was used to

predict the pure component parachors used in the W-K correlation results labeled "W-K this work". Equation E-17 was also used to predict the mixed liquid and vapor parachors for Equation 5.4. The results of Equation 5.4 are labeled "this work mixed". Tables IL through LVI show the same comparisons as Tables XLI through XLVIII except Equation E.18 (developed with $k = 3.55$ and temperature dependence) instead of Equation E.17 was used to predict the pure component and mixed liquid and vapor parachors. Tables LVII through LXIV show the same comparisons as Tables XLI through XLVIII except Equation E.19 (developed with $k = 3.91$ and no temperature dependence) was used to predict the pure component and mixed liquid and vapor parachors for the results labeled "this work". Also, the scaling exponent of $k = 3.91$ was used in the W-K, L-C, and "this work mixed" IFT correlations. The last set of comparisons is shown in Tables LXV through LXXII. These results were obtained in the same manner as those shown in Tables LVII through LXIV except Equation E.20 (developed with $k = 3.91$ and temperature dependence) was used to predict the pure component and mixed liquid and vapor parachors.

Table LXXIII shows the results in average absolute percent deviation (AAPD) and root mean square error (RMSE) for the five methods used to predict IFT. These results are based on the entire data set of 130 data points. The W-K correlation, using the H-VW parachor correlation and a scaling exponent $k = 3.55$, predicted the IFTs of the five binary systems studied with the best results (AAPD = 10.46 and RMSE = 0.1699 mN/m). Based on the above results and the favorable outcome from the optimization regressions discussed earlier in Chapter V, again the W-K correlation is recommended for the prediction of the interfacial

tension of multicomponent systems, specifically CO_2 + hydrocarbon systems similar to the ones studied in this work.

TABLE XLI

COMPARISON OF PREDICTED IFTS FOR CO₂ + N-BUTANE AT 319.3 K (115 °F),
K = 3.55, "THIS WORK" PARACHOR EQUATION E.17

TEMP F	PRES PSIA	EXPERIMENTAL IFT M N/M	PREDICTED									
			W-K (L-C) IFT %ERROR K = 3.55		W-K THIS WORK IFT %ERROR K = 3.55		W-K (H-VW) IFT %ERROR K = 3.55		L-C MIXED IFT %ERROR K = 3.55		THIS WORK MIXED IFT %ERROR K = 3.55	
115.00	316.00	5.7510	5.5313	-3.82	7.2596	26.23	5.8921	2.45	5.9645	3.71	5.8708	2.08
115.00	375.00	5.3662	5.1183	-4.62	6.7364	25.53	5.4333	1.25	5.6070	4.49	5.2275	-2.58
115.00	497.00	4.4082	4.2636	-3.28	5.6582	28.36	4.4795	1.62	4.8213	9.37	4.0596	-7.91
115.00	514.00	4.2650	4.1782	-2.03	5.5504	30.14	4.3842	2.80	4.7387	11.11	3.9548	-7.27
115.00	610.00	3.5490	3.3870	-4.56	4.5318	27.69	3.5222	-0.75	3.9170	10.37	3.0898	-12.94
115.00	710.00	2.6321	2.5007	-4.99	3.3760	28.26	2.5713	-2.31	2.9350	11.51	2.2363	-15.04
115.00	794.00	1.9280	1.7744	-7.97	2.4190	25.47	1.8021	-6.53	2.0976	8.80	1.5890	-17.59
115.00	875.00	1.4148	1.1748	-16.97	1.6197	14.48	1.1761	-16.88	1.3890	-1.83	1.0745	-24.05
115.00	906.00	1.0980	0.9439	-14.03	1.3070	19.04	0.9397	-14.41	1.1145	1.50	0.8733	-20.46
115.00	958.00	0.7290	0.6083	-16.56	0.8486	16.40	0.5998	-17.72	0.7154	-1.86	0.5759	-21.01
115.00	975.00	0.5980	0.5056	-15.45	0.7072	18.26	0.4968	-16.92	0.5935	-0.75	0.4832	-19.20
115.00	1010.00	0.4119	0.3499	-15.05	0.4925	19.54	0.3412	-17.17	0.4085	-0.85	0.3425	-16.87
115.00	1038.00	0.2547	0.2097	-17.65	0.2964	16.36	0.2034	-20.14	0.2438	-4.27	0.2087	-18.07
115.00	1053.00	0.1771	0.1468	-17.10	0.2078	17.37	0.1420	-19.81	0.1703	-3.83	0.1472	-16.85
115.00	1067.00	0.1159	0.0948	-18.19	0.1346	16.13	0.0914	-21.13	0.1097	-5.37	0.0962	-17.02
115.00	1078.00	0.0711	0.0651	-8.42	0.0927	30.45	0.0625	-12.11	0.0749	5.41	0.0671	-5.54
115.00	1088.00	0.0480	0.0385	-19.76	0.0549	14.46	0.0369	-23.13	0.0442	-7.81	0.0399	-16.71
115.00	1095.00	0.0255	0.0192	-24.83	0.0273	7.22	0.0184	-27.98	0.0220	-13.57	0.0199	-22.07
					RMSE		% AVE ABS DEV					
					W-K WITH LEE-CHIEN PARACHOR	0.13274	11.96					
					W-K WITH THIS WORK PARACHOR	0.71687	21.19					
					W-K WITH H-VW PARACHOR	0.10074	12.51					
					LEE-CHIEN MIXED	0.20493	5.91					
					THIS WORK MIXED	0.22913	14.63					

W-K (L-C) : W-K CORRELATION WITH PURE PARACHOR CALCULATED FROM L-C CORRELATION
W-K THIS WORK : W-K CORRELATION WITH PURE PARACHOR CALCULATED FROM THIS WORK CORRELATION
W-K (H-VW) : W-K CORRELATION WITH PURE PARACHOR CALCULATED FROM H-VW CORRELATION
L-C MIXED : L-C IFT CORRELATION USING MIXED PARACHORS
THIS WORK MIXED : IFT CORRELATION DEVELOPED IN THIS WORK

TABLE XLII

COMPARISON OF PREDICTED IFTS FOR CO₂ + N-BUTANE AT 344.3 K (160 °F),
K = 3.55, "THIS WORK" PARACHOR EQUATION E.17

TEMP F	PRES PSIA	EXPERIMENTAL IFT M N/M	PREDICTED									
			W-K (L-C) IFT %ERROR K = 3.55		W-K THIS WORK IFT %ERROR K = 3.55		W-K (H-VW) IFT %ERROR K = 3.55		L-C MIXED IFT %ERROR K = 3.55		THIS WORK MIXED IFT %ERROR K = 3.55	
160.00	465.00	4.2200	3.4952	-17.18	4.5872	8.70	3.7233	-11.77	3.7833	-10.35	3.6672	-13.10
160.00	610.00	3.1599	2.6916	-14.82	3.5509	12.37	2.8489	-9.84	3.0010	-5.03	2.6303	-16.76
160.00	699.00	2.4799	2.1705	-12.48	2.8735	15.87	2.2873	-7.77	2.4590	-0.84	2.0466	-17.47
160.00	802.00	1.8497	1.6216	-12.33	2.1576	16.65	1.6982	-8.19	1.8674	0.96	1.4794	-20.02
160.00	906.00	1.2859	1.0834	-15.75	1.4494	12.72	1.1267	-12.38	1.2650	-1.62	0.9644	-25.00
160.00	995.00	0.7031	0.6578	-6.44	0.8849	25.85	0.6795	-3.36	0.7751	10.24	0.5787	-17.70
160.00	1059.00	0.3970	0.3721	-6.28	0.5026	26.59	0.3823	-3.70	0.4406	10.99	0.3259	-17.91
160.00	1104.00	0.2259	0.1990	-11.93	0.2695	19.28	0.2038	-9.81	0.2363	4.61	0.1740	-22.99
160.00	1127.00	0.1289	0.1193	-7.46	0.1618	25.46	0.1220	-5.35	0.1420	10.10	0.1042	-19.22
160.00	1142.00	0.0899	0.0790	-12.21	0.1071	19.09	0.0807	-10.28	0.0940	4.54	0.0689	-23.45
160.00	1152.00	0.0570	0.0502	-11.93	0.0682	19.53	0.0513	-10.05	0.0598	4.93	0.0438	-23.22
160.00	1155.00	0.0470	0.0434	-7.75	0.0589	25.21	0.0443	-5.79	0.0517	9.95	0.0378	-19.63
			RMSE		% AVE ABS DEV							
			W-K WITH LEE-CHIEN PARACHOR		0.27946		11.38					
			W-K WITH THIS WORK PARACHOR		0.22580		18.94					
			W-K WITH H-VW PARACHOR		0.18936		8.19					
			LEE-CHIEN MIXED		0.13681		6.18					
			THIS WORK MIXED		0.29424		19.71					

W-K (L-C) : W-K CORRELATION WITH PURE PARACHOR CALCULATED FROM L-C CORRELATION
W-K THIS WORK : W-K CORRELATION WITH PURE PARACHOR CALCULATED FROM THIS WORK CORRELATION
W-K (H-VW) : W-K CORRELATION WITH PURE PARACHOR CALCULATED FROM H-VW CORRELATION
L-C MIXED : L-C IFT CORRELATION USING MIXED PARACHORS
THIS WORK MIXED : IFT CORRELATION DEVELOPED IN THIS WORK

TABLE XLIII

COMPARISON OF PREDICTED IFTS FOR CO₂ + N-BUTANE AT 377.6 K (220 °F),
K = 3.55, "THIS WORK" PARACHOR EQUATION E.17

TEMP F	PRES PSIA	EXPERIMENTAL IFT M N/M	W-K (L-C)		W-K THIS WORK		PREDICTED W-K (H-VW)		L-C MIXED		THIS WORK MIXED	
			IFT	%ERROR K = 3.55	IFT	%ERROR K = 3.55	IFT	%ERROR K = 3.55	IFT	%ERROR K = 3.55	IFT	%ERROR K = 3.55
220.00	418.00	2.6657	2.2256	-16.51	2.9011	8.83	2.3908	-10.31	2.2863	-14.23	2.6754	0.37
220.00	498.00	2.2393	1.9105	-14.68	2.4945	11.40	2.0484	-8.52	1.9917	-11.06	2.2052	-1.52
220.00	604.00	1.7298	1.4922	-13.74	1.9519	12.84	1.5961	-7.73	1.5834	-8.46	1.6416	-5.10
220.00	702.00	1.3324	1.1228	-15.73	1.4717	10.46	1.1981	-10.08	1.2111	-9.10	1.1837	-11.16
220.00	804.00	0.8870	0.7559	-14.78	0.9927	11.92	0.8045	-9.30	0.8284	-6.60	0.7654	-13.71
220.00	863.00	0.6464	0.5629	-12.93	0.7404	14.53	0.5980	-7.50	0.6223	-3.74	0.5581	-13.66
220.00	909.00	0.4961	0.4169	-15.96	0.5489	10.65	0.4424	-10.82	0.4639	-6.48	0.4070	-17.96
220.00	957.00	0.3160	0.2816	-10.89	0.3711	17.42	0.2985	-5.56	0.3154	-0.21	0.2707	-14.36
220.00	1003.00	0.1703	0.1627	-4.43	0.2147	26.11	0.1722	1.13	0.1834	7.70	0.1542	-9.43
220.00	1018.00	0.1375	0.1373	-0.16	0.1812	31.78	0.1452	5.61	0.1549	12.69	0.1296	-5.73
220.00	1041.00	0.0956	0.0888	-7.12	0.1173	22.66	0.0938	-1.84	0.1005	5.14	0.0833	-12.89
220.00	1058.00	0.0548	0.0555	1.27	0.0733	33.69	0.0587	7.09	0.0629	14.80	0.0518	-5.43
			RMSE		% AVE ABS DEV							
W-K WITH LEE-CHIEN PARACHOR			0.19014		10.68							
W-K WITH THIS WORK PARACHOR			0.13535		17.69							
W-K WITH H-VW PARACHOR			0.11559		7.12							
LEE-CHIEN MIXED			0.14346		8.35							
THIS WORK MIXED			0.07314		9.28							

W-K (L-C) : W-K CORRELATION WITH PURE PARACHOR CALCULATED FROM L-C CORRELATION
W-K THIS WORK : W-K CORRELATION WITH PURE PARACHOR CALCULATED FROM THIS WORK CORRELATION
W-K (H-VW) : W-K CORRELATION WITH PURE PARACHOR CALCULATED FROM H-VW CORRELATION
L-C MIXED : L-C IFT CORRELATION USING MIXED PARACHORS
THIS WORK MIXED : IFT CORRELATION DEVELOPED IN THIS WORK

TABLE XLIV

COMPARISON OF PREDICTED IFTS FOR CO₂ + N-DECANE AT 344.3 K (160 °F),
K = 3.55, "THIS WORK" PARACHOR EQUATION E.17

TEMP F	PRES PSIA	EXPERIMENTAL IFT M N/M	W-K (L-C)		W-K THIS WORK		PREDICTED W-K (H-VW)		L-C MIXED		THIS WORK MIXED	
			IFT	%ERROR K = 3.55	IFT	%ERROR K = 3.55	IFT	%ERROR K = 3.55	IFT	%ERROR K = 3.55	IFT	%ERROR K = 3.55
160.00	1007.00	7.8139	6.2218	-20.38	7.4315	-4.89	7.1135	-8.96	9.5382	22.07	1.4381	-81.59
160.00	1104.00	6.6539	5.4987	-17.36	6.5837	-1.06	6.2714	-5.75	8.6143	29.46	1.1808	-82.25
160.00	1210.00	5.6712	4.7315	-16.57	5.6656	-0.10	5.3958	-4.86	7.5691	33.47	0.9380	-83.46
160.00	1300.00	4.6121	4.0212	-12.81	4.8213	4.54	4.5797	-0.70	6.5431	41.87	0.7506	-83.73
160.00	1400.00	3.5410	3.2286	-8.82	3.8756	9.45	3.6727	3.72	5.3450	50.95	0.5664	-84.01
160.00	1500.00	2.5330	2.4123	-4.76	2.9025	14.59	2.7375	8.08	4.0520	59.97	0.4040	-84.05
160.00	1533.00	1.7132	1.5953	-6.88	1.9278	12.53	1.8023	5.20	2.7116	58.28	0.2601	-84.82
160.00	1650.00	1.2918	1.2419	-3.87	1.5021	16.28	1.4017	8.50	2.1235	64.38	0.1986	-84.62
160.00	1701.00	0.8483	0.8342	-1.67	1.0116	19.24	0.9391	10.70	1.4333	68.96	0.1324	-84.39
160.00	1726.00	0.6649	0.6676	0.40	0.8091	21.68	0.7520	13.09	1.1525	73.32	0.1037	-84.41
160.00	1751.00	0.5289	0.4867	-7.98	0.5921	11.95	0.5460	3.24	0.8385	58.53	0.0776	-85.32
160.00	1772.00	0.3561	0.3536	-0.72	0.4311	21.04	0.3958	11.15	0.6088	70.96	0.0570	-83.98
160.00	1799.00	0.2447	0.1963	-19.79	0.2398	-2.02	0.2193	-10.39	0.3381	38.18	0.0319	-86.97
160.00	1811.00	0.1422	0.1280	-9.94	0.1569	10.37	0.1426	0.28	0.2197	54.52	0.0215	-84.90
160.00	1821.00	0.1009	0.0895	-11.30	0.1096	8.60	0.0998	-1.14	0.1541	52.65	0.0148	-85.37
160.00	1830.00	0.0592	0.0587	-0.95	0.0715	20.67	0.0657	10.97	0.1020	72.20	0.0091	-84.68
160.00	1835.00	0.0293	0.0286	-2.56	0.0346	18.08	0.0322	9.78	0.0503	71.51	0.0041	-86.05
160.00	1842.00	0.0126	0.0143	13.81	0.0171	36.05	0.0163	30.02	0.0259	106.23	0.0017	-86.56

RMSE

% AVE ABS DEV

W-K WITH LEE-CHIEN PARACHOR	0.53928	8.92
W-K WITH THIS WORK PARACHOR	0.18124	12.95
W-K WITH H-VW PARACHOR	0.21230	8.14
LEE-CHIEN MIXED	1.10949	57.08
THIS WORK MIXED	2.64362	84.51

W-K (L-C) : W-K CORRELATION WITH PURE PARACHOR CALCULATED FROM L-C CORRELATION
W-K THIS WORK : W-K CORRELATION WITH PURE PARACHOR CALCULATED FROM THIS WORK CORRELATION
W-K (H-VW) : W-K CORRELATION WITH PURE PARACHOR CALCULATED FROM H-VW CORRELATION
L-C MIXED : L-C IFT CORRELATION USING MIXED PARACHORS
THIS WORK MIXED : IFT CORRELATION DEVELOPED IN THIS WORK

TABLE XLV

COMPARISON OF PREDICTED IFTS FOR CO₂ + N-DECANE AT 377.6 K (220 °F),
K = 3.55, "THIS WORK" PARACHOR EQUATION E.17

TEMP F	PRES PSIA	EXPERIMENTAL IFT M N/M	W-K (L-C)		W-K THIS WORK		PREDICTED W-K (H-VW)		L-C MIXED		THIS WORK MIXED	
			IFT	%ERROR K = 3.55	IFT	%ERROR K = 3.55	IFT	%ERROR K = 3.55	IFT	%ERROR K = 3.55	IFT	%ERROR K = 3.55
220.00	1500.00	4.3922	3.4633	-21.15	4.1097	-6.43	3.9862	-9.24	5.5852	27.16	0.6405	-85.42
220.00	1601.00	3.7258	2.9828	-19.94	3.5402	-4.98	3.4323	-7.88	4.8820	31.03	0.5206	-86.03
220.00	1705.00	3.0770	2.4674	-19.81	2.9257	-4.92	2.8422	-7.63	4.1064	33.45	0.4010	-86.97
220.00	1801.00	2.5399	1.9960	-21.42	2.3673	-6.80	2.2984	-9.51	3.3655	32.50	0.3080	-87.87
220.00	1903.00	1.9831	1.5672	-20.97	1.8602	-6.20	1.8033	-9.07	2.6772	35.00	0.2301	-88.40
220.00	2001.00	1.4230	1.1553	-18.81	1.3708	-3.67	1.3299	-6.54	1.9994	40.51	0.1604	-88.73
220.00	2053.00	1.2370	0.9663	-21.88	1.1464	-7.32	1.1124	-10.07	1.6819	35.97	0.1309	-89.42
220.00	2100.00	0.9501	0.7820	-17.69	0.9261	-2.53	0.9019	-5.08	1.3722	44.43	0.1015	-89.32
220.00	2151.00	0.7920	0.6363	-19.66	0.7516	-5.11	0.7358	-7.10	1.1265	42.23	0.0784	-90.10
220.00	2201.00	0.6336	0.4691	-25.96	0.5541	-12.54	0.5424	-14.39	0.8357	31.90	0.0563	-91.12
220.00	2226.00	0.4817	0.3903	-18.97	0.4605	-4.40	0.4519	-6.18	0.6990	45.11	0.0455	-90.56
220.00	2250.00	0.3903	0.3157	-19.13	0.3726	-4.55	0.3653	-6.42	0.5664	45.11	0.0365	-90.64
220.00	2276.00	0.3140	0.2388	-23.96	0.2819	-10.21	0.2762	-12.03	0.4299	36.93	0.0273	-91.32
220.00	2299.00	0.2210	0.1795	-18.76	0.2121	-4.05	0.2076	-6.06	0.3238	46.54	0.0204	-90.78
220.00	2315.00	0.1715	0.1398	-18.46	0.1648	-3.90	0.1621	-5.49	0.2536	47.90	0.0153	-91.07
220.00	2331.00	0.1271	0.1020	-19.77	0.1201	-5.47	0.1182	-6.98	0.1854	45.88	0.0110	-91.33
220.00	2341.00	0.1000	0.0806	-19.41	0.0951	-4.91	0.0933	-6.70	0.1465	46.41	0.0088	-91.19
220.00	2353.00	0.0691	0.0567	-17.89	0.0668	-3.26	0.0657	-4.81	0.1034	49.72	0.0061	-91.24
220.00	2362.00	0.0510	0.0412	-19.25	0.0484	-5.16	0.0479	-6.10	0.0757	48.20	0.0042	-91.77
220.00	2371.00	0.0330	0.0259	-21.61	0.0304	-7.86	0.0301	-8.90	0.0475	43.93	0.0026	-92.00
220.00	2376.00	0.0200	0.0180	-10.29	0.0210	4.68	0.0210	5.03	0.0335	67.04	0.0017	-91.75
220.00	2381.00	0.0120	0.0124	3.68	0.0145	21.15	0.0145	21.20	0.0231	92.52	0.0012	-90.27
220.00	2386.00	0.0080	0.0083	3.78	0.0097	21.98	0.0096	20.61	0.0152	90.63	0.0008	-89.42
			RMSE				% AVE ABS DEV					
W-K WITH LEE-CHIEN PARACHOR			0.32992				18.36					
W-K WITH THIS WORK PARACHOR			0.09406				7.05					
W-K WITH H-VW PARACHOR			0.13802				8.83					
LEE-CHIEN MIXED			0.50910				46.09					
THIS WORK MIXED			1.38995				89.86					

W-K (L-C) : W-K CORRELATION WITH PURE PARACHOR CALCULATED FROM L-C CORRELATION
W-K THIS WORK : W-K CORRELATION WITH PURE PARACHOR CALCULATED FROM THIS WORK CORRELATION
W-K (H-VW) : W-K CORRELATION WITH PURE PARACHOR CALCULATED FROM H-VW CORRELATION
L-C MIXED : L-C IFT CORRELATION USING MIXED PARACHORS
THIS WORK MIXED : IFT CORRELATION DEVELOPED IN THIS WORK

TABLE XLVI

COMPARISON OF PREDICTED IFTS FOR CO₂ + N-TETRADECANE AT 344.3 K (160 °F),
K = 3.55, "THIS WORK" PARACHOR EQUATION E.17

TEMP F	PRES PSIA	EXPERIMENTAL IFT M N/M	W-K (L-C)		W-K THIS WORK		PREDICTED W-K (H-VW)		L-C MIXED		THIS WORK MIXED	
			IFT	%ERROR K = 3.55	IFT	%ERROR K = 3.55	IFT	%ERROR K = 3.55	IFT	%ERROR K = 3.55	IFT	%ERROR K = 3.55
160.00	1600.00	4.0324	2.4865	-38.34	3.6650	-9.11	3.8128	-5.45	5.3654	33.06	0.1672	-95.85
160.00	1700.00	3.2310	1.9147	-40.74	2.8196	-12.73	2.9702	-8.07	4.2705	32.17	0.1055	-96.74
160.00	1800.00	2.4865	1.3956	-43.87	2.0528	-17.44	2.1976	-11.62	3.2283	29.83	0.0603	-97.57
160.00	1900.00	1.8076	0.9521	-47.33	1.3979	-22.66	1.5337	-15.15	2.3047	27.51	0.0290	-98.40
160.00	2000.00	1.2150	0.5934	-51.16	0.8691	-28.47	0.9857	-18.88	1.5176	24.90	0.0110	-99.10
160.00	2100.00	0.7275	0.3315	-54.44	0.4839	-33.49	0.5741	-21.09	0.9094	25.00	0.0028	-99.62
160.00	2200.00	0.3604	0.1556	-56.82	0.2264	-37.20	0.2819	-21.78	0.4603	27.70	0.0004	-99.88
160.00	2300.00	0.1131	0.0508	-55.07	0.0737	-34.82	0.0951	-15.89	0.1593	40.83	0.0000	-99.96
160.00	2310.00	0.0943	0.0425	-54.99	0.0616	-34.70	0.0793	-15.90	0.1329	40.87	0.0000	-99.96
160.00	2320.00	0.0765	0.0360	-52.93	0.0522	-31.74	0.0677	-11.56	0.1137	48.65	0.0000	-99.97
160.00	2330.00	0.0597	0.0294	-50.81	0.0426	-28.69	0.0554	-7.26	0.0933	56.18	0.0000	-99.97
160.00	2340.00	0.0439	0.0228	-48.08	0.0330	-24.75	0.0431	-1.75	0.0729	65.92	0.0000	-99.98
160.00	2350.00	0.0292	0.0163	-44.19	0.0236	-19.15	0.0310	6.16	0.0525	79.76	0.0000	-99.98
160.00	2352.00	0.0264	0.0152	-42.30	0.0221	-16.44	0.0291	10.23	0.0494	87.08	0.0000	-99.98
160.00	2354.50	0.0237	0.0141	-40.45	0.0204	-13.79	0.0271	14.18	0.0460	93.94	0.0000	-99.98
160.00	2356.50	0.0210	0.0127	-39.43	0.0184	-12.32	0.0244	16.24	0.0415	97.50	0.0000	-99.99
160.00	2358.00	0.0184	0.0117	-36.38	0.0170	-7.95	0.0227	22.88	0.0386	109.46	0.0000	-99.99
160.00	2360.00	0.0159	0.0104	-34.51	0.0151	-5.27	0.0202	26.85	0.0344	116.46	0.0000	-99.99

	RMSE	% AVE ABS DEV
W-K WITH LEE-CHIEN PARACHOR	0.60734	46.21
W-K WITH THIS WORK PARACHOR	0.21868	21.71
W-K WITH H-VW PARACHOR	0.14096	13.94
LEE-CHIEN MIXED	0.45943	57.60
THIS WORK MIXED	1.41223	99.27

W-K (L-C) : W-K CORRELATION WITH PURE PARACHOR CALCULATED FROM L-C CORRELATION
W-K THIS WORK : W-K CORRELATION WITH PURE PARACHOR CALCULATED FROM THIS WORK CORRELATION
W-K (H-VW) : W-K CORRELATION WITH PURE PARACHOR CALCULATED FROM H-VW CORRELATION
L-C MIXED : L-C IFT CORRELATION USING MIXED PARACHORS
THIS WORK MIXED : IFT CORRELATION DEVELOPED IN THIS WORK

TABLE XLVII

COMPARISON OF PREDICTED IFTS FOR CO₂ + BENZENE AT 344.3 K (160 °F),
K = 3.55, "THIS WORK" PARACHOR EQUATION E.17

TEMP F	PRES PSIA	EXPERIMENTAL IFT M N/M	PREDICTED									
			W-K (L-C) IFT %ERROR K = 3.55		W-K THIS WORK IFT %ERROR K = 3.55		W-K (H-VW) IFT %ERROR K = 3.55		L-C MIXED IFT %ERROR K = 3.55		THIS WORK MIXED IFT %ERROR K = 3.55	
160.00	1000.00	6.6038	5.8169	-11.92	8.3271	26.10	6.3523	-3.81	6.3983	-3.11	6.4102	-2.93
160.00	1101.00	4.9625	4.8155	-2.96	6.9093	39.23	5.2214	5.22	5.3328	7.46	5.2259	5.31
160.00	1201.00	3.7180	3.7518	0.91	5.3964	45.15	4.0362	8.56	4.1785	12.39	4.0224	8.19
160.00	1300.00	2.4821	2.6580	7.09	3.8359	54.55	2.8296	14.00	2.9716	19.73	2.8335	14.16
160.00	1399.00	1.3856	1.5769	13.80	2.2857	64.95	1.6553	19.46	1.7646	27.35	1.6867	21.73
160.00	1430.00	0.9377	1.1505	22.69	1.6680	77.88	1.2070	28.72	1.2900	37.57	1.2245	30.59
160.00	1475.00	0.7094	0.8078	13.86	1.1753	65.66	0.8378	18.10	0.9028	27.26	0.8715	22.84
160.00	1500.00	0.5078	0.5716	12.57	0.8325	63.95	0.5908	16.35	0.6385	25.75	0.6183	21.78
160.00	1520.00	0.3635	0.4140	13.91	0.6029	65.87	0.4283	17.85	0.4637	27.59	0.4446	22.33
160.00	1535.00	0.2624	0.2891	10.17	0.4220	60.82	0.2967	13.06	0.3224	22.85	0.3153	20.15
160.00	1550.00	0.1722	0.1923	11.68	0.2810	63.16	0.1969	14.32	0.2143	24.45	0.2104	22.17
160.00	1559.00	0.1227	0.1322	7.73	0.1933	57.53	0.1349	9.92	0.1471	19.89	0.1452	18.39
160.00	1571.00	0.0653	0.0688	5.30	0.1007	54.13	0.0700	7.11	0.0765	17.05	0.0759	16.23
160.00	1580.00	0.0255	0.0299	17.19	0.0438	71.67	0.0303	18.92	0.0332	30.16	0.0331	29.80
160.00	1584.00	0.0114	0.0146	27.95	0.0213	87.21	0.0148	30.32	0.0162	42.47	0.0160	40.53

	RMSE	% AVE ABS DEV
W-K WITH LEE-CHIEN PARACHOR	0.22693	11.98
W-K WITH THIS WORK PARACHOR	0.93728	59.86
W-K WITH H-VW PARACHOR	0.18747	15.05
LEE-CHIEN MIXED	0.25426	23.01
THIS WORK MIXED	0.19079	19.81

W-K (L-C) : W-K CORRELATION WITH PURE PARACHOR CALCULATED FROM L-C CORRELATION
W-K THIS WORK : W-K CORRELATION WITH PURE PARACHOR CALCULATED FROM THIS WORK CORRELATION
W-K (H-VW) : W-K CORRELATION WITH PURE PARACHOR CALCULATED FROM H-VW CORRELATION
L-C MIXED : L-C IFT CORRELATION USING MIXED PARACHORS
THIS WORK MIXED : IFT CORRELATION DEVELOPED IN THIS WORK

TABLE XLVIII

COMPARISON OF PREDICTED IFTS FOR CO₂ + CYCLOHEXANE AT 344.3 K (160 °F),
K = 3.55, "THIS WORK" PARACHOR EQUATION E.17

TEMP F	PRES PSIA	EXPERIMENTAL IFT M N/M	W-K (L-C)		W-K THIS WORK		PREDICTED W-K (H-VW)		L-C MIXED		THIS WORK MIXED	
			IFT	%ERROR	IFT	%ERROR	IFT	%ERROR	IFT	%ERROR	IFT	%ERROR
			K = 3.55		K = 3.55		K = 3.55		K = 3.55		K = 3.55	
160.00	997.00	6.3492	5.1227	-19.32	6.2132	-2.14	5.5962	-11.86	5.9236	-6.70	4.0489	-36.23
160.00	1101.00	4.9844	4.1646	-16.45	5.0761	1.84	4.5292	-9.13	4.8746	-2.20	3.2014	35.77
160.00	1200.00	3.7106	3.2729	-11.79	4.0071	7.99	3.5449	-4.46	3.8741	4.41	2.4534	-33.88
160.00	1300.00	2.6203	2.4142	-7.87	2.9826	13.83	2.5931	-1.04	2.8818	9.98	1.7911	-31.65
160.00	1400.00	1.3908	1.4515	4.37	1.8117	30.27	1.5444	11.04	1.7442	25.41	1.0737	-22.80
160.00	1450.00	0.9467	0.9998	5.61	1.2582	32.90	1.0557	11.52	1.2022	26.99	0.7475	-21.04
160.00	1500.00	0.5193	0.5581	7.48	0.7092	36.57	0.5840	12.46	0.6702	29.07	0.4250	-18.16
160.00	1525.00	0.3652	0.3710	1.59	0.4728	29.48	0.3870	5.99	0.4455	22.01	0.2837	-22.31
160.00	1540.00	0.2537	0.2627	3.57	0.3359	32.40	0.2734	7.76	0.3154	24.31	0.2022	-20.30
160.00	1550.00	0.1802	0.1924	6.76	0.2467	36.87	0.1997	10.79	0.2307	27.99	0.1492	-17.22
160.00	1560.00	0.1349	0.1356	0.52	0.1742	29.14	0.1404	4.10	0.1625	20.43	0.1057	-21.68
160.00	1570.00	0.0807	0.0798	-1.08	0.1029	27.46	0.0825	2.16	0.0955	18.34	0.0627	-22.29
160.00	1579.00	0.0362	0.0394	8.62	0.0507	39.98	0.0406	12.17	0.0471	30.04	0.0309	-14.79
160.00	1586.00	0.0094	0.0108	15.32	0.0138	47.70	0.0112	19.78	0.0130	39.04	0.0082	-12.05
			RMSE		% AVE ABS DEV							
			W-K WITH LEE-CHIEN PARACHOR		0.41565		7.88					
			W-K WITH THIS WORK PARACHOR		0.20379		26.33					
			W-K WITH H-VW PARACHOR		0.24543		8.88					
			LEE-CHIEN MIXED		0.19183		20.49					
			THIS WORK MIXED		0.88233		23.58					

W-K (L-C) : W-K CORRELATION WITH PURE PARACHOR CALCULATED FROM L-C CORRELATION
W-K THIS WORK : W-K CORRELATION WITH PURE PARACHOR CALCULATED FROM THIS WORK CORRELATION
W-K (H-VW) : W-K CORRELATION WITH PURE PARACHOR CALCULATED FROM H-VW CORRELATION
L-C MIXED : L-C IFT CORRELATION USING MIXED PARACHORS
THIS WORK MIXED : IFT CORRELATION DEVELOPED IN THIS WORK

TABLE II

COMPARISON OF PREDICTED IFTS FOR CO₂ + N-BUTANE AT 319.3 K (115 °F),
K = 3.55, "THIS WORK" PARACHOR EQUATION E.18

TEMP F	PRES PSIA	EXPERIMENTAL IFT M N/M	W-K (L-C) K = 3.55		W-K THIS WORK K = 3.55		PREDICTED W-K (H-VW) K = 3.55		L-C MIXED K = 3.55		THIS WORK MIXED K = 3.55	
			IFT	%ERROR	IFT	%ERROR	IFT	%ERROR	IFT	%ERROR	IFT	%ERROR
115.00	316.00	5.7510	5.5313	-3.82	9.1740	59.52	5.8921	2.45	5.9645	3.71	7.3685	28.12
115.00	375.00	5.3662	5.1183	-4.62	8.4882	58.18	5.4333	1.25	5.6070	4.49	6.5320	21.72
115.00	497.00	4.4082	4.2636	-3.28	7.0683	60.35	4.4795	1.62	4.8213	9.37	5.0115	13.69
115.00	514.00	4.2650	4.1782	-2.03	6.9265	62.40	4.3842	2.80	4.7387	11.11	4.8752	14.31
115.00	610.00	3.5490	3.3870	-4.56	5.6132	58.16	3.5222	-0.75	3.9170	10.37	3.7710	6.26
115.00	710.00	2.6321	2.5007	-4.99	4.1427	57.39	2.5713	-2.31	2.9350	11.51	2.6975	2.49
115.00	794.00	1.9280	1.7744	-7.97	2.9384	52.41	1.8021	-6.53	2.0976	8.80	1.8940	-1.76
115.00	875.00	1.4148	1.1748	-16.97	1.9445	37.44	1.1761	-16.88	1.3890	-1.83	1.2644	-10.63
115.00	906.00	1.0980	0.9439	-14.03	1.5621	42.27	0.9397	-14.41	1.1145	1.50	1.0228	-6.85
115.00	958.00	0.7290	0.6083	-16.56	1.0064	38.05	0.5998	-17.72	0.7154	-1.86	0.6691	-8.21
115.00	975.00	0.5980	0.5056	-15.45	0.8364	39.86	0.4968	-16.92	0.5935	-0.75	0.5109	-6.38
115.00	1010.00	0.4119	0.3499	-15.05	0.5787	40.49	0.3412	-17.17	0.4085	-0.85	0.3944	-4.25
115.00	1038.00	0.2547	0.2097	-17.65	0.3468	36.16	0.2034	-20.14	0.2438	-4.27	0.2394	-6.02
115.00	1053.00	0.1771	0.1468	-17.10	0.2427	37.06	0.1420	-19.81	0.1703	-3.83	0.1686	-4.81
115.00	1067.00	0.1159	0.0948	-18.19	0.1568	35.25	0.0914	-21.13	0.1097	-5.37	0.1098	-5.23
115.00	1078.00	0.0711	0.0651	-8.42	0.1076	51.38	0.0625	-12.11	0.0749	5.41	0.0764	7.53
115.00	1088.00	0.0480	0.0385	-19.76	0.0636	32.63	0.0369	-23.13	0.0442	-7.81	0.0454	-5.31
115.00	1095.00	0.0255	0.0192	-24.83	0.0317	24.25	0.0184	-27.98	0.0220	-13.57	0.0226	-11.41
			RMSE		% AVE ABS DEV							
W-K WITH LEE-CHIEN PARACHOR			0.13274		11.96							
W-K WITH THIS WORK PARACHOR			1.56101		45.74							
W-K WITH H-VW PARACHOR			0.10074		12.51							
LEE-CHIEN MIXED			0.20493		5.91							
THIS WORK MIXED			0.51642		9.17							

W-K (L-C) : W-K CORRELATION WITH PURE PARACHOR CALCULATED FROM L-C CORRELATION
W-K THIS WORK : W-K CORRELATION WITH PURE PARACHOR CALCULATED FROM THIS WORK CORRELATION
W-K (H-VW) : W-K CORRELATION WITH PURE PARACHOR CALCULATED FROM H-VW CORRELATION
L-C MIXED : L-C IFT CORRELATION USING MIXED PARACHORS
THIS WORK MIXED : IFT CORRELATION DEVELOPED IN THIS WORK

TABLE L

COMPARISON OF PREDICTED IFTS FOR CO₂ + N-BUTANE AT 344.3 K (160 °F),
K = 3.55, "THIS WORK" PARACHOR EQUATION E.18

TEMP F	PRES PSIA	EXPERIMENTAL IFT M N/M	W-K (L-C)		W-K THIS WORK		PREDICTED W-K (H-VW)		L-C MIXED		THIS WORK MIXED	
			IFT	%ERROR K = 3.55	IFT	%ERROR K = 3.55	IFT	%ERROR K = 3.55	IFT	%ERROR K = 3.55	IFT	%ERROR K = 3.55
160.00	465.00	4.2200	3.4952	-17.18	5.6492	33.87	3.7233	-11.77	3.7833	-10.35	4.4800	6.16
160.00	610.00	3.1599	2.6916	-14.82	4.3470	37.57	2.8489	-9.84	3.0010	-5.03	3.1838	0.75
160.00	699.00	2.4799	2.1705	-12.48	3.5036	41.28	2.2873	-7.77	2.4590	-0.84	2.4625	-0.70
160.00	802.00	1.8497	1.6216	-12.33	2.6157	41.41	1.6982	-8.19	1.8674	0.96	1.7659	-4.53
160.00	906.00	1.2859	1.0834	-15.75	1.7461	35.79	1.1267	-12.38	1.2650	-1.62	1.1415	-11.22
160.00	995.00	0.7031	0.6578	-6.44	1.0594	50.67	0.6795	-3.36	0.7751	10.24	0.6796	-3.34
160.00	1059.00	0.3970	0.3721	-6.28	0.5988	50.83	0.3823	-3.70	0.4406	10.99	0.3805	-4.15
160.00	1104.00	0.2259	0.1990	-11.93	0.3201	41.69	0.2038	-9.81	0.2363	4.61	0.2024	-10.42
160.00	1127.00	0.1289	0.1193	-7.46	0.1919	48.86	0.1220	-5.35	0.1420	10.10	0.1210	-6.18
160.00	1142.00	0.0899	0.0790	-12.21	0.1270	41.20	0.0807	-10.28	0.0940	4.54	0.0799	-11.16
160.00	1152.00	0.0570	0.0502	-11.93	0.0808	41.64	0.0513	-10.05	0.0598	4.93	0.0508	-10.95
160.00	1157.00	0.0470	0.0434	-7.75	0.0698	48.36	0.0443	-5.79	0.0517	9.95	0.0438	-6.80
			RMSE		% AVE ABS DEV							
W-K WITH LEE-CHIEN PARACHOR			0.27946		11.38							
W-K WITH THIS WORK PARACHOR			0.67584		42.76							
W-K WITH H-VW PARACHOR			0.18936		8.19							
LEE-CHIEN MIXED			0.13681		6.18							
THIS WORK MIXED			0.09034		6.37							

W-K (L-C) : W-K CORRELATION WITH PURE PARACHOR CALCULATED FROM L-C CORRELATION
W-K THIS WORK : W-K CORRELATION WITH PURE PARACHOR CALCULATED FROM THIS WORK CORRELATION
W-K (H-VW) : W-K CORRELATION WITH PURE PARACHOR CALCULATED FROM H-VW CORRELATION
L-C MIXED : L-C IFT CORRELATION USING MIXED PARACHORS
THIS WORK MIXED : IFT CORRELATION DEVELOPED IN THIS WORK

TABLE LI

COMPARISON OF PREDICTED IFTS FOR CO₂ + N-BUTANE AT 377.6 K (220 °F),
K = 3.55, "THIS WORK" PARACHOR EQUATION E.18

TEMP F	PRES PSIA	EXPERIMENTAL IFT M N/M	PREDICTED									
			W-K (L-C) IFT %ERROR K = 3.55		W-K THIS WORK IFT %ERROR K = 3.55		W-K (H-VW) IFT %ERROR K = 3.55		L-C MIXED IFT %ERROR K = 3.55		THIS WORK MIXED IFT %ERROR K = 3.55	
220.00	418.00	2.6657	2.2256	-16.51	3.4787	30.50	2.3908	-10.31	2.2863	-14.23	3.1996	20.03
220.00	498.00	2.2393	1.9105	-14.68	2.9849	33.30	2.0484	-8.52	1.9917	-11.06	2.6276	17.34
220.00	604.00	1.7298	1.4922	-13.74	2.3300	34.70	1.5961	-7.73	1.5834	-8.46	1.9475	12.58
220.00	702.00	1.3324	1.1228	-15.73	1.7522	31.51	1.1981	-10.08	1.2111	-9.10	1.3980	4.93
220.00	804.00	0.8870	0.7559	-14.78	1.1789	32.91	0.8045	-9.30	0.8284	-6.60	0.8999	1.45
220.00	863.00	0.6464	0.5629	-12.93	0.8775	35.74	0.5980	-7.50	0.6223	-3.74	0.6542	1.20
220.00	909.00	0.4961	0.4169	-15.96	0.6498	30.98	0.4424	-10.82	0.4639	-6.48	0.4761	-4.03
220.00	957.00	0.3160	0.2816	-10.89	0.4388	38.84	0.2985	-5.56	0.3154	-0.21	0.3160	-0.03
220.00	1003.00	0.1703	0.1627	-4.43	0.2534	48.85	0.1722	1.13	0.1834	7.70	0.1796	5.46
220.00	1018.00	0.1375	0.1373	-0.16	0.2138	55.49	0.1452	5.61	0.1549	12.69	0.1508	9.70
220.00	1041.00	0.0956	0.0888	-7.12	0.1383	44.61	0.0938	-1.84	0.1005	5.14	0.0968	1.25
220.00	1058.00	0.0548	0.0555	1.27	0.0864	57.70	0.0587	7.09	0.0629	14.80	0.0603	9.96
			RMSE		% AVE ABS DEV							
			W-K WITH LEE-CHIEN PARACHOR		0.19014		10.68					
			W-K WITH THIS WORK PARACHOR		0.40273		39.59					
			W-K WITH H-VW PARACHOR		0.11559		7.12					
			LEE-CHIEN MIXED		0.14346		8.35					
			THIS WORK MIXED		0.20177		7.33					

W-K (L-C) : W-K CORRELATION WITH PURE PARACHOR CALCULATED FROM L-C CORRELATION
W-K THIS WORK : W-K CORRELATION WITH PURE PARACHOR CALCULATED FROM THIS WORK CORRELATION
W-K (H-VW) : W-K CORRELATION WITH PURE PARACHOR CALCULATED FROM H-VW CORRELATION
L-C MIXED : L-C IFT CORRELATION USING MIXED PARACHORS
THIS WORK MIXED : IFT CORRELATION DEVELOPED IN THIS WORK

TABLE LII

COMPARISON OF PREDICTED IFTS FOR CO₂ + N-DECANE AT 344.3 K (160 °F),
K = 3.55, "THIS WORK" PARACHOR EQUATION E.18

TEMP F	PRES PSIA	EXPERIMENTAL IFT M N/M	PREDICTED									
			W-K (L-C) IFT %ERROR K = 3.55		W-K THIS WORK IFT %ERROR K = 3.55		W-K (H-VW) IFT %ERROR K = 3.55		L-C MIXED IFT %ERROR K = 3.55		THIS WORK MIXED IFT %ERROR K = 3.55	
160.00	1007.00	7.8139	6.2218	-20.38	9.4847	21.38	7.1135	-8.96	9.5382	22.07	1.6653	-78.69
160.00	1104.00	6.6539	5.4987	-17.36	8.3852	26.02	6.2714	-5.75	8.6143	29.46	1.3536	-79.66
160.00	1210.00	5.6712	4.7315	-16.57	7.2153	27.23	5.3958	-4.86	7.5691	33.47	1.0673	-81.18
160.00	1300.00	4.6121	4.0212	-12.81	6.1332	32.98	4.5797	-0.70	6.5431	41.87	0.8474	-81.63
160.00	1400.00	3.5410	3.2286	-8.82	4.9251	39.09	3.6727	3.72	5.3450	50.95	0.6343	-82.09
160.00	1500.00	2.5330	2.4123	-4.76	3.6811	45.33	2.7375	8.08	4.0520	59.97	0.4485	-82.29
160.00	1599.00	1.7132	1.5953	-6.88	2.4358	42.18	1.8023	5.20	2.7116	58.28	0.2856	-83.33
160.00	1650.00	1.2918	1.2419	-3.87	1.8964	46.80	1.4017	8.50	2.1235	64.38	0.2173	-83.18
160.00	1701.00	0.8483	0.8342	-1.67	1.2743	50.21	0.9391	10.70	1.4333	68.96	0.1440	-83.02
160.00	1726.00	0.6649	0.6676	0.40	1.0197	53.35	0.7520	13.09	1.1525	73.32	0.1126	-83.06
160.00	1751.00	0.5289	0.4867	-7.98	0.7438	40.63	0.5460	3.24	0.8385	58.53	0.0840	-84.13
160.00	1772.00	0.3561	0.3536	-0.72	0.5405	51.77	0.3958	11.15	0.6088	70.96	0.0615	-82.72
160.00	1799.00	0.2447	0.1963	-19.79	0.3001	22.64	0.2193	-10.39	0.3381	38.18	0.0343	-85.98
160.00	1811.00	0.1422	0.1280	-9.94	0.1958	37.77	0.1426	0.28	0.2197	54.52	0.0230	-83.80
160.00	1821.00	0.1009	0.0895	-11.30	0.1369	35.67	0.0998	-1.14	0.1541	52.65	0.0158	-84.31
160.00	1830.00	0.0592	0.0587	-0.95	0.0897	51.40	0.0657	10.97	0.1020	72.20	0.0098	-83.54
160.00	1835.00	0.0293	0.0286	-2.56	0.0437	48.84	0.0322	9.78	0.0503	71.51	0.0044	-84.98
160.00	1842.00	0.0126	0.0143	13.81	0.0218	73.52	0.0163	30.02	0.0259	106.23	0.0018	-85.46
					RMSE		% AVE ABS DEV					
					W-K WITH LEE-CHIEN PARACHOR		0.53928		8.92			
					W-K WITH THIS WORK PARACHOR		0.91301		41.49			
					W-K WITH H-VW PARACHOR		0.21230		8.14			
					LEE-CHIEN MIXED		1.10949		57.08			
					THIS WORK MIXED		2.56480		82.95			

W-K (L-C) : W-K CORRELATION WITH PURE PARACHOR CALCULATED FROM L-C CORRELATION
W-K THIS WORK : W-K CORRELATION WITH PURE PARACHOR CALCULATED FROM THIS WORK CORRELATION
W-K (H-VW) : W-K CORRELATION WITH PURE PARACHOR CALCULATED FROM H-VW CORRELATION
L-C MIXED : L-C IFT CORRELATION USING MIXED PARACHORS
THIS WORK MIXED : IFT CORRELATION DEVELOPED IN THIS WORK

TABLE LIII

COMPARISON OF PREDICTED IFTS FOR CO₂ + N-DECANE AT 377.6 K (220 °F),
K = 3.55, "THIS WORK" PARACHOR EQUATION E.18

TEMP F	PRES PSIA	EXPERIMENTAL IFT M N/M	PREDICTED									
			W-K (L-C) IFT %ERROR K = 3.55		W-K THIS WORK IFT %ERROR K = 3.55		W-K (H-VW) IFT %ERROR K = 3.55		L-C MIXED IFT %ERROR K = 3.55		THIS WORK MIXED IFT %ERROR K = 3.55	
220.00	1500.00	4.3922	3.4633	-21.15	4.9586	12.90	3.9862	-9.24	5.5852	27.16	0.6891	-84.31
220.00	1601.00	3.7258	2.9828	-19.94	4.2707	14.62	3.4323	-7.88	4.8820	31.03	0.5568	-85.05
220.00	1705.00	3.0770	2.4674	-19.81	3.5324	14.80	2.8422	-7.63	4.1064	33.45	0.4267	-86.13
220.00	1801.00	2.5399	1.9960	-21.42	2.8575	12.50	2.2984	-9.51	3.3655	32.50	0.3259	-87.17
220.00	1903.00	1.9831	1.5672	-20.97	2.2439	13.15	1.8033	-9.07	2.6772	35.00	0.2418	-87.80
220.00	2001.00	1.4230	1.1553	-18.81	1.6541	16.24	1.3299	-6.54	1.9994	40.51	0.1678	-88.21
220.00	2053.00	1.2370	0.9663	-21.88	1.3834	11.84	1.1124	-10.07	1.6819	35.97	0.1366	-88.96
220.00	2100.00	0.9501	0.7820	-17.69	1.1193	17.81	0.9019	-5.08	1.3722	44.43	0.1057	-88.87
220.00	2151.00	0.7920	0.6363	-19.66	0.9104	14.95	0.7358	-7.10	1.1265	42.23	0.0817	-89.68
220.00	2201.00	0.6336	0.4691	-25.96	0.6712	5.94	0.5424	-14.39	0.8357	31.90	0.0585	-90.77
220.00	2226.00	0.4817	0.3903	-18.97	0.5584	15.92	0.4519	-6.18	0.6990	45.11	0.0472	-90.20
220.00	2250.00	0.3903	0.3157	-19.13	0.4516	15.69	0.3653	-6.42	0.5664	45.11	0.0379	-90.30
220.00	2276.00	0.3140	0.2388	-23.96	0.3416	8.80	0.2762	-12.03	0.4299	36.93	0.0282	-91.02
220.00	2299.00	0.2210	0.1795	-18.76	0.2569	16.23	0.2076	-6.06	0.3238	46.54	0.0210	-90.48
220.00	2315.00	0.1715	0.1398	-18.46	0.2000	16.63	0.1621	-5.49	0.2536	47.90	0.0158	-90.78
220.00	2331.00	0.1271	0.1020	-19.77	0.1458	14.75	0.1182	-6.98	0.1854	45.88	0.0114	-91.05
220.00	2341.00	0.1000	0.0806	-19.41	0.1153	15.29	0.0933	-6.70	0.1465	46.41	0.0091	-90.92
220.00	2353.00	0.0691	0.0567	-17.89	0.0811	17.44	0.0657	-4.81	0.1034	49.72	0.0062	-90.97
220.00	2362.00	0.0510	0.0412	-19.25	0.0589	15.44	0.0479	-6.10	0.0757	48.20	0.0043	-91.51
220.00	2371.00	0.0330	0.0259	-21.61	0.0370	12.08	0.0301	-8.90	0.0475	43.93	0.0027	-91.75
220.00	2376.00	0.0200	0.0180	-10.29	0.0257	28.14	0.0210	5.03	0.0335	67.04	0.0017	-91.47
220.00	2381.00	0.0120	0.0124	3.68	0.0177	48.11	0.0145	21.20	0.0231	92.52	0.0012	-89.94
220.00	2386.00	0.0080	0.0083	3.78	0.0119	48.39	0.0096	20.61	0.0152	90.63	0.0009	-89.10
			RMSE		% AVE ABS DEV							
W-K WITH LEE-CHIEN PARACHOR			0.32992		18.36							
W-K WITH THIS WORK PARACHOR			0.22130		17.72							
W-K WITH H-VW PARACHOR			0.13802		8.83							
LEE-CHIEN MIXED			0.50910		46.09							
THIS WORK MIXED			1.37582		89.41							

W-K (L-C) : W-K CORRELATION WITH PURE PARACHOR CALCULATED FROM L-C CORRELATION
W-K THIS WORK : W-K CORRELATION WITH PURE PARACHOR CALCULATED FROM THIS WORK CORRELATION
W-K (H-VW) : W-K CORRELATION WITH PURE PARACHOR CALCULATED FROM H-VW CORRELATION
L-C MIXED : L-C IFT CORRELATION USING MIXED PARACHORS
THIS WORK MIXED : IFT CORRELATION DEVELOPED IN THIS WORK

TABLE LIV

COMPARISON OF PREDICTED IFTS FOR CO₂ + N-TETRADECANE AT 344.3 K (160 °F),
K = 3.55, "THIS WORK" PARACHOR EQUATION E.18

TEMP F	PRES PSIA	EXPERIMENTAL IFT M N/M	W-K (L-C)		W-K THIS WORK		PREDICTED W-K (H-VW)		L-C MIXED		THIS WORK MIXED	
			IFT	%ERROR K = 3.55	IFT	%ERROR K = 3.55	IFT	%ERROR K = 3.55	IFT	%ERROR K = 3.55	IFT	%ERROR K = 3.55
160.00	1600.00	4.0324	2.4865	-38.34	5.0366	24.90	3.8128	-5.45	5.3654	33.06	0.1861	-95.39
160.00	1700.00	3.2310	1.9147	-40.74	3.8990	20.67	2.9702	-8.07	4.2705	32.17	0.1166	-96.39
160.00	1800.00	2.4865	1.3956	-43.87	2.8616	15.09	2.1976	-11.62	3.2283	29.83	0.0663	-97.33
160.00	1900.00	1.8076	0.9521	-47.33	1.9727	9.14	1.5337	-15.15	2.3047	27.51	0.0317	-98.24
160.00	2000.00	1.2150	0.5934	-51.16	1.2470	2.64	0.9857	-18.88	1.5176	24.90	0.0120	-99.01
160.00	2100.00	0.7275	0.3315	-54.44	0.7103	-2.37	0.5741	-21.09	0.9094	25.00	0.0031	-99.58
160.00	2200.00	0.3604	0.1556	-56.82	0.3406	-5.51	0.2819	-21.78	0.4603	27.70	0.0005	-99.87
160.00	2300.00	0.1131	0.0508	-55.07	0.1129	-0.14	0.0951	-15.89	0.1593	40.83	0.0000	-99.96
160.00	2310.00	0.0943	0.0425	-54.99	0.0943	-0.06	0.0793	-15.90	0.1329	40.87	0.0000	-99.96
160.00	2320.00	0.0765	0.0360	-52.93	0.0802	4.79	0.0677	-11.56	0.1137	48.65	0.0000	-99.96
160.00	2330.00	0.0597	0.0294	-50.81	0.0655	9.69	0.0554	-7.26	0.0933	56.18	0.0000	-99.97
160.00	2340.00	0.0439	0.0228	-48.08	0.0509	15.98	0.0431	-1.75	0.0729	65.92	0.0000	-99.97
160.00	2350.00	0.0292	0.0163	-44.19	0.0365	24.98	0.0310	6.16	0.0525	79.76	0.0000	-99.98
160.00	2352.00	0.0264	0.0152	-42.30	0.0342	29.47	0.0291	10.23	0.0494	87.08	0.0000	-99.98
160.00	2354.50	0.0237	0.0141	-40.45	0.0317	33.85	0.0271	14.18	0.0460	93.94	0.0000	-99.98
160.00	2356.50	0.0210	0.0127	-39.43	0.0286	36.20	0.0244	16.24	0.0415	97.50	0.0000	-99.98
160.00	2358.00	0.0184	0.0117	-36.38	0.0265	43.50	0.0227	22.88	0.0386	109.46	0.0000	-99.99
160.00	2360.00	0.0159	0.0104	-34.51	0.0235	47.92	0.0202	26.85	0.0344	116.46	0.0000	-99.99
			RMSE				% AVE ABS DEV					
W-K WITH LEE-CHIEN PARACHOR			0.60734				46.21					
W-K WITH THIS WORK PARACHOR			0.30044				18.16					
W-K WITH H-VW PARACHOR			0.14096				13.94					
LEE-CHIEN MIXED			0.45943				57.60					
THIS WORK MIXED			1.40716				99.20					

W-K (L-C) : W-K CORRELATION WITH PURE PARACHOR CALCULATED FROM L-C CORRELATION
W-K THIS WORK : W-K CORRELATION WITH PURE PARACHOR CALCULATED FROM THIS WORK CORRELATION
W-K (H-VW) : W-K CORRELATION WITH PURE PARACHOR CALCULATED FROM H-VW CORRELATION
L-C MIXED : L-C IFT CORRELATION USING MIXED PARACHORS
THIS WORK MIXED : IFT CORRELATION DEVELOPED IN THIS WORK

TABLE LV

COMPARISON OF PREDICTED IFTS FOR CO₂ + BENZENE AT 344.3 K (160 °F),
K = 3.55, "THIS WORK" PARACHOR EQUATION E.18

TEMP F	PRES PSIA	EXPERIMENTAL IFT M N/M	PREDICTED									
			W-K (L-C) IFT %ERROR K = 3.55		W-K THIS WORK IFT %ERROR K = 3.55		W-K (H-VW) IFT %ERROR K = 3.55		L-C MIXED IFT %ERROR K = 3.55		THIS WORK MIXED IFT %ERROR K = 3.55	
160.00	1000.00	6.6038	5.8169	-11.92	10.8033	63.59	6.3523	-3.81	6.3983	-3.11	8.2072	24.28
160.00	1101.00	4.9625	4.8155	-2.96	8.8981	79.31	5.2214	5.22	5.3328	7.46	6.6313	33.63
160.00	1201.00	3.7180	3.7518	0.91	6.8938	85.42	4.0362	8.56	4.1785	12.39	5.0551	35.97
160.00	1300.00	2.4821	2.6580	7.09	4.8475	95.30	2.8296	14.00	2.9716	19.73	3.5170	41.70
160.00	1399.00	1.3856	1.5769	13.80	2.8472	105.48	1.6553	19.46	1.7646	27.35	2.0607	48.72
160.00	1430.00	0.9377	1.1505	22.69	2.0764	121.44	1.2070	28.72	1.2900	37.57	1.4945	59.37
160.00	1475.00	0.7094	0.8078	13.86	1.4461	103.84	0.8378	18.10	0.9028	27.26	1.0507	48.11
160.00	1500.00	0.5078	0.5716	12.57	1.0207	101.03	0.5908	16.35	0.6385	25.75	0.7427	46.28
160.00	1520.00	0.3635	0.4140	13.91	0.7398	103.56	0.4283	17.85	0.4637	27.59	0.5343	47.00
160.00	1535.00	0.2624	0.2891	10.17	0.5136	95.74	0.2967	13.06	0.3224	22.85	0.3758	43.21
160.00	1550.00	0.1722	0.1923	11.68	0.3411	98.06	0.1969	14.32	0.2143	24.45	0.2501	45.23
160.00	1559.00	0.1227	0.1322	7.73	0.2339	90.63	0.1349	9.92	0.1471	19.89	0.1721	40.29
160.00	1571.00	0.0653	0.0688	5.30	0.1215	85.92	0.0700	7.11	0.0765	17.05	0.0897	37.29
160.00	1580.00	0.0255	0.0299	17.19	0.0527	106.56	0.0303	18.92	0.0332	30.16	0.0390	52.94
160.00	1584.00	0.0114	0.0146	27.95	0.0257	126.11	0.0148	30.32	0.0162	42.47	0.0189	66.17
			RMSE		% AVE ABS DEV							
W-K WITH LEE-CHIEN PARACHOR			0.22693		11.98							
W-K WITH THIS WORK PARACHOR			1.88493		97.46							
W-K WITH H-VW PARACHOR			0.18747		15.05							
LEE-CHIEN MIXED			0.25426		23.01							
THIS WORK MIXED			0.78331		44.68							

W-K (L-C) : W-K CORRELATION WITH PURE PARACHOR CALCULATED FROM L-C CORRELATION
W-K THIS WORK : W-K CORRELATION WITH PURE PARACHOR CALCULATED FROM THIS WORK CORRELATION
W-K (H-VW) : W-K CORRELATION WITH PURE PARACHOR CALCULATED FROM H-VW CORRELATION
L-C MIXED : L-C IFT CORRELATION USING MIXED PARACHORS
THIS WORK MIXED : IFT CORRELATION DEVELOPED IN THIS WORK

TABLE LVI

COMPARISON OF PREDICTED IFTS FOR CO₂ + CYCLOHEXANE AT 344.3 K (160 °F),
K = 3.55, "THIS WORK" PARACHOR EQUATION E.18

TEMP F	PRES PSIA	EXPERIMENTAL IFT M N/M	PREDICTED									
			W-K (L-C) IFT %ERROR K = 3.55		W-K THIS WORK IFT %ERROR K = 3.55		W-K (H-VW) IFT %ERROR K = 3.55		L-C MIXED IFT %ERROR K = 3.55		THIS WORK MIXED IFT %ERROR K = 3.55	
160.00	997.00	6.3492	5.1227	-19.32	8.1392	28.19	5.5962	-11.86	5.9236	-6.70	5.2185	-17.81
160.00	1101.00	4.9844	4.1646	-16.45	6.6161	32.74	4.5292	-9.13	4.8746	-2.20	4.0973	-17.80
160.00	1200.00	3.7106	3.2729	-11.79	5.1989	40.11	3.5449	-4.46	3.8741	4.41	3.1196	-15.93
160.00	1300.00	2.6203	2.4142	-7.87	3.8339	46.31	2.5931	-1.04	2.8818	9.98	2.2511	-14.09
160.00	1400.00	1.3908	1.4515	4.37	2.3045	65.70	1.5444	-11.04	1.7442	25.41	1.3322	-4.21
160.00	1450.00	0.9467	0.9998	5.61	1.5870	67.64	1.0557	11.52	1.2022	26.99	0.9186	-2.96
160.00	1500.00	0.5193	0.5581	7.48	0.8857	70.56	0.5840	12.46	0.6702	29.07	0.5165	-0.54
160.00	1525.00	0.3652	0.3710	1.59	0.5886	61.20	0.3870	5.99	0.4455	22.01	0.3435	-5.92
160.00	1540.00	0.2537	0.2627	3.57	0.4169	64.33	0.2734	7.76	0.3154	24.31	0.2440	-3.80
160.00	1550.00	0.1802	0.1924	6.76	0.3053	69.38	0.1997	10.79	0.2307	27.99	0.1795	-0.40
160.00	1560.00	0.1349	0.1356	0.52	0.2151	59.47	0.1404	4.10	0.1625	20.43	0.1268	-5.98
160.00	1570.00	0.0807	0.0798	-1.08	0.1266	56.91	0.0825	2.16	0.0955	18.34	0.0751	-7.01
160.00	1579.00	0.0362	0.0394	8.62	0.0624	72.31	0.0406	12.17	0.0471	30.04	0.0369	1.94
160.00	1586.00	0.0094	0.0108	15.32	0.0171	82.97	0.0112	19.78	0.0130	39.04	0.0099	5.85
			RMSE		% AVE ABS DEV							
			W-K WITH LEE-CHIEN PARACHOR		0.41565		7.88					
			W-K WITH THIS WORK PARACHOR		0.88783		58.41					
			W-K WITH H-VW PARACHOR		0.24543		8.88					
			LEE-CHIEN MIXED		0.19183		20.49					
			THIS WORK MIXED		0.42726		7.45					

W-K (L-C) : W-K CORRELATION WITH PURE PARACHOR CALCULATED FROM L-C CORRELATION
W-K THIS WORK : W-K CORRELATION WITH PURE PARACHOR CALCULATED FROM THIS WORK CORRELATION
W-K (H-VW) : W-K CORRELATION WITH PURE PARACHOR CALCULATED FROM H-VW CORRELATION
L-C MIXED : L-C IFT CORRELATION USING MIXED PARACHORS
THIS WORK MIXED : IFT CORRELATION DEVELOPED IN THIS WORK

TABLE LVII

COMPARISON OF PREDICTED IFTS FOR CO₂ + N-BUTANE AT 319.3 K (115 °F),
K = 3.91, "THIS WORK" PARACHOR EQUATION E.19

TEMP F	PRES PSIA	EXPERIMENTAL IFT M N/M	W-K (L-C)		W-K THIS WORK		PREDICTED W-K (H-VW)		L-C MIXED		THIS WORK MIXED	
			IFT	%ERROR K = 3.911	IFT	%ERROR K = 3.91	IFT	%ERROR K = 3.91	IFT	%ERROR K = 3.91	IFT	%ERROR K = 3.91
115.00	316.00	5.7510	6.5821	14.45	7.2366	25.83	7.0566	22.70	7.1522	24.36	5.6678	-1.45
115.00	375.00	5.3662	6.0428	12.61	6.6564	24.04	6.4537	20.27	6.6815	24.51	4.9714	-7.36
115.00	497.00	4.4082	4.9410	12.09	5.4735	24.17	5.2174	18.36	5.6576	28.34	3.7343	-15.29
115.00	514.00	4.2650	4.8321	13.30	5.3565	25.59	5.0953	19.47	5.5509	30.15	3.6253	-15.00
115.00	610.00	3.5490	3.8344	8.04	4.2713	20.35	4.0034	12.80	4.5004	26.81	2.7473	-22.59
115.00	710.00	2.6321	2.7449	4.29	3.0764	16.88	2.8304	7.54	3.2746	24.41	1.9135	-27.30
115.00	794.00	1.9280	1.8810	-2.44	2.1222	10.07	1.9133	-0.76	2.2617	17.31	1.3068	-32.22
115.00	875.00	1.4148	1.1942	-15.60	1.3578	-4.04	1.1956	-15.49	1.4362	1.51	0.8454	-40.25
115.00	906.00	1.0980	0.9384	-14.54	1.0701	-2.54	0.9338	-14.95	1.1268	2.63	0.6717	-38.83
115.00	958.00	0.7290	0.5783	-20.67	0.6628	-9.08	0.5695	-21.89	0.6915	-5.15	0.4235	-41.91
115.00	975.00	0.5980	0.4717	-21.12	0.5416	-9.42	0.4627	-22.62	0.5628	-5.88	0.3487	-41.68
115.00	1010.00	0.4119	0.3145	-23.65	0.3626	-11.97	0.3059	-25.75	0.3729	-9.48	0.2383	-42.16
115.00	1038.00	0.2547	0.1789	-29.75	0.2069	-18.77	0.1730	-32.08	0.2112	-17.07	0.1379	-45.86
115.00	1053.00	0.1771	0.1208	-31.80	0.1398	-21.04	0.1164	-34.25	0.1422	-19.67	0.0938	-47.00
115.00	1067.00	0.1159	0.0746	-35.62	0.0866	-25.33	0.0717	-38.16	0.0876	-24.42	0.0587	-49.38
115.00	1078.00	0.0711	0.0493	-30.64	0.0573	-19.36	0.0471	-33.71	0.0576	-19.01	0.0394	-44.49
115.00	1088.00	0.0480	0.0276	-42.39	0.0322	-32.95	0.0264	-45.05	0.0322	-32.86	0.0223	-53.59
115.00	1095.00	0.0255	0.0128	-49.72	0.0149	-41.49	0.0122	-52.04	0.0150	-41.36	0.0103	-59.55

	RMSE	% AVE ABS DEV
W-K WITH LEE-CHIEN PARACHOR	0.33203	21.26
W-K WITH THIS WORK PARACHOR	0.62245	19.05
W-K WITH H-VW PARACHOR	0.50668	24.33
LEE-CHIEN MIXED	0.68098	19.72
THIS WORK MIXED	0.42743	34.77

W-K (L-C) : W-K CORRELATION WITH PURE PARACHOR CALCULATED FROM L-C CORRELATION
W-K THIS WORK : W-K CORRELATION WITH PURE PARACHOR CALCULATED FROM THIS WORK CORRELATION
W-K (H-VW) : W-K CORRELATION WITH PURE PARACHOR CALCULATED FROM H-VW CORRELATION
L-C MIXED : L-C IFT CORRELATION USING MIXED PARACHORS
THIS WORK MIXED : IFT CORRELATION DEVELOPED IN THIS WORK

TABLE LVIII

COMPARISON OF PREDICTED IFTS FOR CO₂ + N-BUTANE AT 344.3 K (160 °F),
K = 3.91, "THIS WORK" PARACHOR EQUATION E.19

TEMP F	PRES PSIA	EXPERIMENTAL IFT M N/M	W-K (L-C)		W-K THIS WORK		PREDICTED W-K (H-VW)		L-C MIXED		THIS WORK MIXED	
			IFT	%ERROR K = 3.911	IFT	%ERROR K = 3.91	IFT	%ERROR K = 3.91	IFT	%ERROR K = 3.91	IFT	%ERROR K = 3.91
160.00	465.00	4.2200	3.9695	-5.94	4.3642	3.42	4.2558	0.85	4.3314	2.64	3.3730	-20.07
160.00	610.00	3.1599	2.9767	-5.80	3.2842	3.93	3.1689	0.28	3.3558	6.20	2.3248	-26.43
160.00	699.00	2.4799	2.3485	-5.30	2.5973	4.73	2.4881	0.33	2.6946	8.66	1.7571	-29.14
160.00	802.00	1.8497	1.7033	-7.91	1.8902	2.19	1.7921	-3.11	1.9899	7.58	1.2239	-33.83
160.00	906.00	1.2859	1.0922	-15.06	1.2166	-5.39	1.1405	-11.31	1.2957	0.76	0.7608	-40.83
160.00	995.00	0.7031	0.6304	-10.34	0.7048	0.24	0.6533	-7.08	0.7553	7.42	0.4320	-38.56
160.00	1059.00	0.3970	0.3365	-15.25	0.3773	-4.98	0.3467	-12.67	0.4054	2.11	0.2290	-42.33
160.00	1104.00	0.2259	0.1688	-25.26	0.1897	-16.06	0.1733	-23.28	0.2041	-9.66	0.1145	-49.32
160.00	1127.00	0.1289	0.0961	-25.45	0.1080	-16.21	0.0985	-23.58	0.1164	-9.73	0.0650	-49.57
160.00	1142.00	0.0899	0.0610	-32.19	0.0686	-23.75	0.0625	-30.54	0.0739	-17.80	0.0412	-54.19
160.00	1152.00	0.0570	0.0371	-35.03	0.0417	-26.92	0.0379	-33.50	0.0449	-21.20	0.0250	-56.13
160.00	1155.00	0.0470	0.0315	-32.95	0.0355	-24.57	0.0323	-31.37	0.0383	-18.65	0.0213	-54.77
			RMSE		% AVE ABS DEV							
W-K WITH LEE-CHIEN PARACHOR			0.12493		18.04							
W-K WITH THIS WORK PARACHOR			0.07037		11.03							
W-K WITH H-VW PARACHOR			0.05472		14.83							
LEE-CHIEN MIXED			0.10021		9.37							
THIS WORK MIXED			0.47669		41.27							

W-K (L-C) : W-K CORRELATION WITH PURE PARACHOR CALCULATED FROM L-C CORRELATION
W-K THIS WORK : W-K CORRELATION WITH PURE PARACHOR CALCULATED FROM THIS WORK CORRELATION
W-K (H-VW) : W-K CORRELATION WITH PURE PARACHOR CALCULATED FROM H-VW CORRELATION
L-C MIXED : L-C IFT CORRELATION USING MIXED PARACHORS
THIS WORK MIXED : IFT CORRELATION DEVELOPED IN THIS WORK

TABLE LIX

COMPARISON OF PREDICTED IFTS FOR CO₂ + N-BUTANE AT 377.6 K (220 °F),
K = 3.91, "THIS WORK" PARACHOR EQUATION E.19

TEMP F	PRES PSIA	EXPERIMENTAL IFT M N/M	W-K (L-C)		W-K THIS WORK		PREDICTED W-K (H-VW)		L-C MIXED		THIS WORK MIXED	
			IFT	%ERROR K = 3.911	IFT	%ERROR K = 3.91	IFT	%ERROR K = 3.91	IFT	%ERROR K = 3.91	IFT	%ERROR K = 3.91
220.00	418.00	2.6657	2.4142	-9.43	2.6420	-0.89	2.6124	-2.00	2.4868	-6.71	2.4068	-9.71
220.00	498.00	2.2393	2.0405	-8.87	2.2355	-0.17	2.2033	-1.61	2.1362	-4.60	1.9398	-13.37
220.00	604.00	1.7298	1.5542	-10.15	1.7049	-1.44	1.6738	-3.24	1.6592	-4.08	1.3968	-19.25
220.00	702.00	1.3324	1.1361	-14.73	1.2480	-6.33	1.2203	-8.41	1.2350	-7.31	0.9713	-27.10
220.00	804.00	0.8870	0.7347	-17.17	0.8081	-8.89	0.7869	-11.28	0.8127	-8.37	0.5990	-32.47
220.00	863.00	0.6464	0.5309	-17.87	0.5846	-9.57	0.5675	-12.21	0.5930	-8.27	0.4222	-34.68
220.00	909.00	0.4961	0.3814	-23.11	0.4203	-15.28	0.4072	-17.92	0.4291	-13.51	0.2978	-39.97
220.00	957.00	0.3160	0.2476	-21.67	0.2729	-13.64	0.2639	-16.48	0.2805	-11.26	0.1898	-39.95
220.00	1003.00	0.1703	0.1353	-20.54	0.1493	-12.32	0.1440	-15.44	0.1543	-9.36	0.1020	-40.11
220.00	1018.00	0.1375	0.1122	-18.42	0.1238	-9.96	0.1193	-13.21	0.1282	-6.77	0.0842	-38.78
220.00	1041.00	0.0956	0.0694	-27.40	0.0766	-19.83	0.0738	-22.83	0.0796	-16.76	0.0517	-45.95
220.00	1058.00	0.0548	0.0414	-24.53	0.0457	-16.69	0.0440	-19.73	0.0475	-13.34	0.0307	-44.08
			RMSE		% AVE ABS DEV							
W-K WITH LEE-CHIEN PARACHOR			0.13820		17.82							
W-K WITH THIS WORK PARACHOR			0.04747		9.58							
W-K WITH H-VW PARACHOR			0.06345		12.03							
LEE-CHIEN MIXED			0.07738		9.20							
THIS WORK MIXED			0.22293		32.12							

W-K (L-C) : W-K CORRELATION WITH PURE PARACHOR CALCULATED FROM L-C CORRELATION
W-K THIS WORK : W-K CORRELATION WITH PURE PARACHOR CALCULATED FROM THIS WORK CORRELATION
W-K (H-VW) : W-K CORRELATION WITH PURE PARACHOR CALCULATED FROM H-VW CORRELATION
L-C MIXED : L-C IFT CORRELATION USING MIXED PARACHORS
THIS WORK MIXED : IFT CORRELATION DEVELOPED IN THIS WORK

TABLE LX

COMPARISON OF PREDICTED IFTS FOR CO₂ + N-DECANE AT 344.3 K (160 °F),
K = 3.91, "THIS WORK" PARACHOR EQUATION E.19

TEMP F	PRES PSIA	EXPERIMENTAL IFT M N/M	W-K (L-C) IFT %ERROR K = 3.911		W-K THIS WORK IFT %ERROR K = 3.91		PREDICTED W-K (H-VW) IFT %ERROR K = 3.91		L-C MIXED IFT %ERROR K = 3.91		THIS WORK MIXED IFT %ERROR K = 3.91	
			IFT	%ERROR	IFT	%ERROR	IFT	%ERROR	IFT	%ERROR	IFT	%ERROR
160.00	1007.00	7.8139	7.4929	-4.11	7.7393	-0.95	8.6843	11.14	11.9969	53.53	1.2042	-84.59
160.00	1104.00	6.6539	6.5394	-1.72	6.7653	1.67	7.5587	13.60	10.7232	61.16	0.9662	-85.48
160.00	1210.00	5.6712	5.5416	-2.28	5.7334	1.10	6.4047	12.93	9.2990	63.97	0.7485	-86.80
160.00	1300.00	4.6121	4.6324	0.44	4.7969	4.01	5.3461	15.92	7.9203	71.73	0.5844	-87.33
160.00	1400.00	3.5410	3.6373	2.72	3.7694	6.45	4.1921	18.39	6.3382	79.00	0.4278	-87.92
160.00	1500.00	2.5330	2.6383	4.16	2.7384	8.11	3.0327	19.73	4.6715	84.43	0.2943	-88.38
160.00	1550.00	1.7132	1.6729	-2.35	1.7414	1.65	1.9136	11.70	3.0011	75.18	0.1807	-89.45
160.00	1650.00	1.2918	1.2695	-1.73	1.3224	2.36	1.4506	12.29	2.2925	77.46	0.1342	-89.61
160.00	1701.00	0.8483	0.8189	-3.46	0.8545	0.73	0.9331	9.99	1.4868	75.26	0.0857	-89.89
160.00	1726.00	0.6649	0.6407	-3.64	0.6682	0.50	0.7305	9.86	1.1693	75.84	0.0655	-90.15
160.00	1751.00	0.5289	0.4523	-14.48	0.4730	-10.57	0.5135	-2.92	0.8236	55.71	0.0475	-91.01
160.00	1772.00	0.3561	0.3181	-10.68	0.3331	-6.47	0.3602	1.15	0.5789	62.55	0.0338	-90.50
160.00	1799.00	0.2447	0.1663	-32.03	0.1744	-28.73	0.1879	-23.20	0.3028	23.76	0.0178	-92.72
160.00	1811.00	0.1422	0.1039	-26.93	0.1091	-23.22	0.1169	-17.74	0.1883	32.45	0.0115	-91.90
160.00	1821.00	0.1009	0.0700	-30.61	0.0736	-27.13	0.0789	-21.79	0.1274	26.21	0.0076	-92.45
160.00	1830.00	0.0592	0.0440	-25.77	0.0460	-22.30	0.0498	-15.86	0.0809	36.53	0.0045	-92.46
160.00	1835.00	0.0293	0.0199	-32.12	0.0208	-29.21	0.0227	-22.59	0.0371	26.55	0.0019	-93.66
160.00	1842.00	0.0126	0.0093	-26.11	0.0096	-23.64	0.0107	-14.44	0.0179	42.24	0.0007	-94.39

	RMSE	% AVE ABS DEV
W-K WITH LEE-CHIEN PARACHOR	0.09818	12.52
W-K WITH THIS WORK PARACHOR	0.09512	11.04
W-K WITH H-VW PARACHOR	0.43516	14.18
LEE-CHIEN MIXED	2.02794	56.86
THIS WORK MIXED	2.75118	89.93

W-K (L-C) : W-K CORRELATION WITH PURE PARACHOR CALCULATED FROM L-C CORRELATION
W-K THIS WORK : W-K CORRELATION WITH PURE PARACHOR CALCULATED FROM THIS WORK CORRELATION
W-K (H-VW) : W-K CORRELATION WITH PURE PARACHOR CALCULATED FROM H-VW CORRELATION
L-C MIXED : L-C IFT CORRELATION USING MIXED PARACHORS
THIS WORK MIXED : IFT CORRELATION DEVELOPED IN THIS WORK

TABLE LXI

COMPARISON OF PREDICTED IFTS FOR CO₂ + N-DECANE AT 377.6 K (220 °F),
K = 3.91, "THIS WORK" PARACHOR EQUATION E.19

TEMP F	PRES PSIA	EXPERIMENTAL IFT M N/M	W-K (L-C)		W-K THIS WORK		PREDICTED W-K (H-VW)		L-C MIXED		THIS WORK MIXED	
			IFT	%ERROR K = 3.911	IFT	%ERROR K = 3.91	IFT	%ERROR K = 3.91	IFT	%ERROR K = 3.91	IFT	%ERROR K = 3.91
220.00	1500.00	4.3922	3.9297	-10.53	4.0412	-7.99	4.5880	4.46	6.6529	51.47	0.4935	-88.76
220.00	1601.00	3.7258	3.3334	-10.53	3.4285	-7.98	3.8909	4.43	5.7361	53.96	0.3923	-89.47
220.00	1705.00	3.0770	2.7048	-12.10	2.7801	-9.65	3.1607	2.72	4.7407	54.07	0.2940	-90.44
220.00	1801.00	2.5399	2.1413	-15.69	2.2013	-13.33	2.5014	-1.51	3.8075	49.91	0.2196	-91.35
220.00	1903.00	1.9831	1.6404	-17.28	1.6873	-14.92	1.9147	-3.45	2.9592	49.22	0.1591	-91.98
220.00	2001.00	1.4230	1.1724	-17.61	1.2056	-15.28	1.3691	-3.79	2.1454	50.76	0.1068	-92.49
220.00	2053.00	1.2370	0.9629	-22.16	0.9901	-19.96	1.1245	-9.09	1.7733	43.36	0.0854	-93.10
220.00	2100.00	0.9501	0.7627	-19.73	0.7833	-17.56	0.8924	-6.07	1.4171	49.15	0.0645	-93.21
220.00	2151.00	0.7920	0.6077	-23.27	0.6230	-21.34	0.7132	-9.96	1.1402	43.96	0.0486	-93.86
220.00	2201.00	0.6336	0.4343	-31.45	0.4453	-29.71	0.5097	-19.55	0.8206	29.52	0.0337	-94.68
220.00	2226.00	0.4817	0.3547	-26.36	0.3634	-24.56	0.4169	-13.46	0.6740	39.92	0.0267	-94.46
220.00	2250.00	0.3903	0.2807	-28.08	0.2877	-26.30	0.3297	-15.53	0.5346	36.96	0.0210	-94.63
220.00	2276.00	0.3140	0.2064	-34.26	0.2116	-32.62	0.2423	-22.82	0.3946	25.66	0.0152	-95.17
220.00	2299.00	0.2210	0.1508	-31.78	0.1546	-30.06	0.1769	-19.94	0.2888	30.66	0.0110	-95.02
220.00	2315.00	0.1715	0.1145	-33.24	0.1172	-31.66	0.1347	-21.46	0.2206	28.64	0.0080	-95.31
220.00	2331.00	0.1271	0.0808	-36.39	0.0827	-34.90	0.0951	-25.14	0.1562	22.91	0.0056	-95.60
220.00	2341.00	0.1000	0.0624	-37.61	0.0639	-36.09	0.0733	-26.70	0.1205	20.43	0.0044	-95.63
220.00	2353.00	0.0691	0.0424	-38.67	0.0434	-37.23	0.0498	-27.83	0.0821	18.87	0.0029	-95.81
220.00	2362.00	0.0510	0.0298	-41.62	0.0304	-40.37	0.0352	-31.06	0.0582	13.98	0.0019	-96.21
220.00	2371.00	0.0330	0.0179	-45.94	0.0182	-44.76	0.0211	-36.21	0.0349	5.59	0.0012	-96.48
220.00	2376.00	0.0200	0.0119	-40.38	0.0121	-39.38	0.0142	-29.08	0.0237	18.24	0.0007	-96.53
220.00	2381.00	0.0120	0.0080	-33.64	0.0081	-32.45	0.0094	-21.19	0.0157	31.22	0.0005	-96.05
220.00	2386.00	0.0080	0.0051	-36.25	0.0052	-34.86	0.0060	-24.78	0.0100	24.56	0.0003	-95.86

	RMSE	% AVE ABS DEV
W-K WITH LEE-CHIEN PARACHOR	0.21694	28.03
W-K WITH THIS WORK PARACHOR	0.18045	26.22
W-K WITH H-VW PARACHOR	0.07748	16.53
LEE-CHIEN MIXED	0.82715	34.48
THIS WORK MIXED	1.44551	94.00

W-K (L-C) : W-K CORRELATION WITH PURE PARACHOR CALCULATED FROM L-C CORRELATION
W-K THIS WORK : W-K CORRELATION WITH PURE PARACHOR CALCULATED FROM THIS WORK CORRELATION
W-K (H-VW) : W-K CORRELATION WITH PURE PARACHOR CALCULATED FROM H-VW CORRELATION
L-C MIXED : L-C IFT CORRELATION USING MIXED PARACHORS
THIS WORK MIXED : IFT CORRELATION DEVELOPED IN THIS WORK

TABLE LXII

COMPARISON OF PREDICTED IFTS FOR CO₂ + N-TETRADECANE AT 344.3 K (160 °F),
K = 3.91, "THIS WORK" PARACHOR EQUATION E.19

TEMP F	PRES PSIA	EXPERIMENTAL IFT M N/M	PREDICTED									
			W-K (L-C) IFT %ERROR K = 3.911		W-K THIS WORK IFT %ERROR K = 3.91		W-K (H-VW) IFT %ERROR K = 3.91		L-C MIXED IFT %ERROR K = 3.91		THIS WORK MIXED IFT %ERROR K = 3.91	
160.00	1600.00	4.0324	2.7279	-32.35	3.6669	-9.06	4.3687	8.34	6.3649	57.85	0.1137	-97.18
160.00	1700.00	3.2310	2.0454	-36.69	2.7551	-14.73	3.3180	2.69	4.9499	53.20	0.0687	-97.87
160.00	1800.00	2.4865	1.4437	-41.94	1.9498	-21.58	2.3808	-4.25	3.6369	46.27	0.0373	-98.50
160.00	1900.00	1.8076	0.9473	-47.59	1.2846	-28.93	1.6019	-11.38	2.5090	38.80	0.0168	-99.07
160.00	2000.00	1.2150	0.5627	-53.69	0.7672	-36.85	0.9842	-19.00	1.5833	30.31	0.0059	-99.52
160.00	2100.00	0.7275	0.2963	-59.28	0.4070	-44.06	0.5426	-25.42	0.9006	23.79	0.0013	-99.82
160.00	2200.00	0.3604	0.1288	-64.26	0.1784	-50.50	0.2478	-31.23	0.4253	18.01	0.0002	-99.95
160.00	2300.00	0.1131	0.0375	-66.81	0.0523	-53.76	0.0749	-33.79	0.1321	16.83	0.0000	-99.99
160.00	2310.00	0.0943	0.0308	-67.36	0.0429	-54.53	0.0613	-35.01	0.1082	14.73	0.0000	-99.99
160.00	2320.00	0.0765	0.0257	-66.43	0.0358	-53.19	0.0515	-32.75	0.0912	19.17	0.0000	-99.99
160.00	2330.00	0.0597	0.0205	-65.64	0.0286	-52.05	0.0413	-30.90	0.0733	22.70	0.0000	-99.99
160.00	2340.00	0.0439	0.0155	-64.65	0.0217	-50.65	0.0313	-28.63	0.0558	27.12	0.0000	-99.99
160.00	2350.00	0.0292	0.0107	-63.28	0.0150	-48.68	0.0218	-25.43	0.0389	33.21	0.0000	-99.99
160.00	2352.00	0.0264	0.0100	-62.29	0.0139	-47.26	0.0203	-23.06	0.0364	37.79	0.0000	-99.99
160.00	2354.50	0.0237	0.0092	-61.39	0.0128	-45.96	0.0188	-20.90	0.0336	41.80	0.0000	*****
160.00	2356.50	0.0210	0.0082	-61.13	0.0114	-45.59	0.0168	-20.30	0.0301	42.92	0.0000	*****
160.00	2358.00	0.0184	0.0075	-59.51	0.0105	-43.26	0.0154	-16.39	0.0278	50.46	0.0000	*****
160.00	2360.00	0.0159	0.0065	-58.83	0.0092	-42.26	0.0136	-14.71	0.0244	53.68	0.0000	*****
					RMSE			% AVE ABS DEV				
					W-K WITH LEE-CHIEN PARACHOR			57.40				
					W-K WITH THIS WORK PARACHOR			41.27				
					W-K WITH H-VW PARACHOR			21.34				
					LEE-CHIEN MIXED			34.93				
					THIS WORK MIXED			99.55				

W-K (L-C) : W-K CORRELATION WITH PURE PARACHOR CALCULATED FROM L-C CORRELATION
W-K THIS WORK : W-K CORRELATION WITH PURE PARACHOR CALCULATED FROM THIS WORK CORRELATION
W-K (H-VW) : W-K CORRELATION WITH PURE PARACHOR CALCULATED FROM H-VW CORRELATION
L-C MIXED : L-C IFT CORRELATION USING MIXED PARACHORS
THIS WORK MIXED : IFT CORRELATION DEVELOPED IN THIS WORK

TABLE LXIII

COMPARISON OF PREDICTED IFTS FOR CO₂ + BENZENE AT 344.3 K (160 °F),
K = 3.91, "THIS WORK" PARACHOR EQUATION E.19

TEMP F	PRES PSIA	EXPERIMENTAL IFT M N/M	PREDICTED									
			W-K (L-C) IFT %ERROR K = 3.911		W-K THIS WORK IFT %ERROR K = 3.91		W-K (H-VW) IFT %ERROR K = 3.91		L-C MIXED IFT %ERROR K = 3.91		THIS WORK MIXED IFT %ERROR K = 3.91	
160.00	1000.00	6.6038	6.9574	5.35	8.1731	23.76	7.6663	16.09	7.7274	17.01	6.0515	-8.36
160.00	1101.00	4.9625	5.6502	13.86	6.6462	33.93	6.1771	24.48	6.3223	27.40	4.8221	-2.83
160.00	1201.00	3.7180	4.2917	15.43	5.0556	35.98	4.6515	25.11	4.8326	29.98	3.6068	-2.99
160.00	1300.00	2.4821	2.9359	18.28	3.4652	39.61	3.1453	26.72	3.3197	33.75	2.4464	-1.44
160.00	1399.00	1.3856	1.6516	19.19	1.9544	41.05	1.7424	25.74	1.8696	34.92	1.3781	-0.54
160.00	1430.00	0.9377	1.1670	24.45	1.3811	47.29	1.2303	31.20	1.3239	41.18	0.9681	3.24
160.00	1475.00	0.7094	0.7904	11.42	0.9374	32.13	0.8229	15.99	0.8935	25.95	0.6646	-6.32
160.00	1500.00	0.5078	0.5400	6.34	0.6408	26.20	0.5600	10.29	0.6100	20.15	0.4552	-10.36
160.00	1520.00	0.3635	0.3785	4.14	0.4491	23.57	0.3929	8.11	0.4289	18.00	0.3164	-12.94
160.00	1535.00	0.2624	0.2548	-2.89	0.3028	15.39	0.2622	-0.09	0.2873	9.49	0.2165	-17.49
160.00	1550.00	0.1722	0.1626	-5.55	0.1934	12.28	0.1669	-3.10	0.1832	6.41	0.1386	-19.51
160.00	1559.00	0.1227	0.1076	-12.31	0.1280	4.30	0.1100	-10.34	0.1210	-1.34	0.0921	-24.91
160.00	1571.00	0.0653	0.0524	-19.79	0.0624	-4.54	0.0534	-18.27	0.0589	-9.88	0.0451	-31.01
160.00	1580.00	0.0255	0.0209	-17.99	0.0249	-2.35	0.0213	-16.65	0.0235	-7.94	0.0181	-29.21
160.00	1584.00	0.0114	0.0095	-16.78	0.0113	-0.98	0.0097	-15.08	0.0107	-6.32	0.0081	-28.81
					RMSE		% AVE ABS DEV					
					W-K WITH LEE-CHIEN PARACHOR		0.29039		12.92			
					W-K WITH THIS WORK PARACHOR		0.75951		22.89			
					W-K WITH H-VW PARACHOR		0.52568		16.48			
					LEE-CHIEN MIXED		0.60488		19.31			
					THIS WORK MIXED		0.15298		13.33			

W-K (L-C) : W-K CORRELATION WITH PURE PARACHOR CALCULATED FROM L-C CORRELATION
W-K THIS WORK : W-K CORRELATION WITH PURE PARACHOR CALCULATED FROM THIS WORK CORRELATION
W-K (H-VW) : W-K CORRELATION WITH PURE PARACHOR CALCULATED FROM H-VW CORRELATION
L-C MIXED : L-C IFT CORRELATION USING MIXED PARACHORS
THIS WORK MIXED : IFT CORRELATION DEVELOPED IN THIS WORK

TABLE LXIV

COMPARISON OF PREDICTED IFTS FOR CO₂ + CYCLOHEXANE AT 344.3 K (160 °F),
K = 3.91, "THIS WORK" PARACHOR EQUATION E.19

TEMP F	PRES PSIA	EXPERIMENTAL IFT M N/M	W-K (L-C)		W-K THIS WORK		PREDICTED W-K (H-VW)		L-C MIXED		THIS WORK MIXED	
			IFT	%ERROR K = 3.911	IFT	%ERROR K = 3.91	IFT	%ERROR K = 3.91	IFT	%ERROR K = 3.91	IFT	%ERROR K = 3.91
160.00	997.00	6.3492	6.0485	-4.74	6.0857	-4.15	6.6673	5.01	7.0982	11.80	3.7200	-41.41
160.00	1101.00	4.9844	4.8148	-3.40	4.8641	-2.41	5.2812	5.95	5.7266	14.89	2.8632	-42.56
160.00	1200.00	3.7106	3.6923	-0.49	3.7439	0.90	4.0317	8.66	4.4461	19.82	2.1297	-42.60
160.00	1300.00	2.6203	2.6405	0.77	2.6976	2.95	2.8569	9.03	3.2093	22.48	1.5003	-42.74
160.00	1400.00	1.3908	1.5076	8.40	1.5532	11.68	1.6141	16.06	1.8457	32.71	0.8506	-38.84
160.00	1450.00	0.9467	0.9998	5.61	1.0370	9.55	1.0616	12.14	1.2249	29.39	0.5694	-39.85
160.00	1500.00	0.5193	0.5260	1.29	0.5500	5.91	0.5529	6.48	0.6435	23.92	0.3049	-41.29
160.00	1525.00	0.3652	0.3354	-8.16	0.3516	-3.72	0.3514	-3.76	0.4104	12.38	0.1952	-46.55
160.00	1540.00	0.2537	0.2294	-9.59	0.2410	-4.99	0.2396	-5.55	0.2804	10.54	0.1343	-47.06
160.00	1550.00	0.1802	0.1627	-9.71	0.1714	-4.90	0.1695	-5.95	0.1987	10.26	0.0960	-46.72
160.00	1560.00	0.1349	0.1107	-17.96	0.1168	-13.44	0.1150	-14.74	0.1350	0.11	0.0656	-51.35
160.00	1570.00	0.0807	0.0617	-23.51	0.0653	-19.09	0.0640	-20.74	0.0752	-6.80	0.0369	-54.25
160.00	1579.00	0.0362	0.0283	-21.83	0.0300	-17.30	0.0293	-19.01	0.0345	-4.69	0.0169	-53.33
160.00	1586.00	0.0094	0.0068	-27.23	0.0072	-23.41	0.0071	-24.13	0.0084	-10.58	0.0039	-57.86
			RMSE				% AVE ABS DEV					
W-K WITH LEE-CHIEN PARACHOR			0.09972				10.19					
W-K WITH THIS WORK PARACHOR			0.09543				8.89					
W-K WITH H-VW PARACHOR			0.17193				11.23					
LEE-CHIEN MIXED			0.40556				15.03					
THIS WORK MIXED			1.05907				46.17					

W-K (L-C) : W-K CORRELATION WITH PURE PARACHOR CALCULATED FROM L-C CORRELATION
W-K THIS WORK : W-K CORRELATION WITH PURE PARACHOR CALCULATED FROM THIS WORK CORRELATION
W-K (H-VW) : W-K CORRELATION WITH PURE PARACHOR CALCULATED FROM H-VW CORRELATION
L-C MIXED : L-C IFT CORRELATION USING MIXED PARACHORS
THIS WORK MIXED : IFT CORRELATION DEVELOPED IN THIS WORK

TABLE LXV

COMPARISON OF PREDICTED IFTS FOR CO₂ + N-BUTANE AT 319.3 K (115 °F),
K = 3.91, "THIS WORK" PARACHOR EQUATION E.20

TEMP F	PRES PSIA	EXPERIMENTAL IFT M N/M	PREDICTED									
			W-K (L-C) IFT %ERROR K = 3.911		W-K THIS WORK IFT %ERROR K = 3.91		W-K (H-VW) IFT %ERROR K = 3.91		L-C MIXED IFT %ERROR K = 3.91		THIS WORK MIXED IFT %ERROR K = 3.91	
115.00	316.00	5.7510	6.5821	14.45	7.1284	23.95	7.0566	22.70	7.1522	24.36	5.5677	-3.19
115.00	375.00	5.3662	6.0428	12.61	6.5476	22.02	6.4537	20.27	6.6815	24.51	4.8736	-9.18
115.00	497.00	4.4082	4.9410	12.09	5.3616	21.63	5.2174	18.36	5.6576	28.34	3.6403	-17.42
115.00	514.00	4.2650	4.8321	13.30	5.2443	22.96	5.0953	19.47	5.5509	30.15	3.5317	-17.19
115.00	610.00	3.5490	3.8344	8.04	4.1667	17.41	4.0034	12.80	4.5004	26.81	2.6637	-24.94
115.00	710.00	2.6321	2.7449	4.29	2.9876	13.51	2.8304	7.54	3.2746	24.41	1.8449	-29.91
115.00	794.00	1.9280	1.8810	-2.44	2.0508	6.37	1.9133	-0.76	2.2617	17.31	1.2527	-35.02
115.00	875.00	1.4148	1.1942	-15.60	1.3046	-7.79	1.1956	-15.49	1.4362	1.51	0.8053	-43.08
115.00	906.00	1.0980	0.9384	-14.54	1.0259	-6.56	0.9338	-14.95	1.1268	2.63	0.6384	-41.86
115.00	958.00	0.7290	0.5783	-20.67	0.6331	-13.16	0.5695	-21.89	0.6915	-5.15	0.4009	-45.01
115.00	975.00	0.5980	0.4717	-21.12	0.5166	-13.60	0.4627	-22.62	0.5628	-5.88	0.3297	-44.87
115.00	1010.00	0.4119	0.3145	-23.65	0.3448	-16.29	0.3059	-25.75	0.3729	-9.48	0.2246	-45.48
115.00	1038.00	0.2547	0.1789	-29.75	0.1963	-22.91	0.1730	-32.08	0.2112	-17.07	0.1297	-49.07
115.00	1053.00	0.1771	0.1208	-31.80	0.1326	-25.14	0.1164	-34.25	0.1422	-19.67	0.0882	-50.19
115.00	1067.00	0.1159	0.0746	-35.62	0.0819	-29.30	0.0717	-38.16	0.0876	-24.42	0.0551	-52.48
115.00	1078.00	0.0711	0.0493	-30.64	0.0542	-23.78	0.0471	-33.71	0.0576	-19.01	0.0370	-47.98
115.00	1088.00	0.0480	0.0276	-42.39	0.0304	-36.68	0.0264	-45.05	0.0322	-32.86	0.0208	-56.53
115.00	1095.00	0.0255	0.0128	-49.72	0.0141	-44.73	0.0122	-52.04	0.0150	-41.36	0.0097	-62.12

	RMSE	% AVE ABS DEV
W-K WITH LEE-CHIEN PARACHOR	0.33203	21.26
W-K WITH THIS WORK PARACHOR	0.56416	20.43
W-K WITH H-VW PARACHOR	0.50668	24.33
LEE-CHIEN MIXED	0.68098	19.72
THIS WORK MIXED	0.47667	37.53

W-K (L-C) : W-K CORRELATION WITH PURE PARACHOR CALCULATED FROM L-C CORRELATION
W-K THIS WORK : W-K CORRELATION WITH PURE PARACHOR CALCULATED FROM THIS WORK CORRELATION
W-K (H-VW) : W-K CORRELATION WITH PURE PARACHOR CALCULATED FROM H-VW CORRELATION
L-C MIXED : L-C IFT CORRELATION USING MIXED PARACHORS
THIS WORK MIXED : IFT CORRELATION DEVELOPED IN THIS WORK

TABLE LXVI

COMPARISON OF PREDICTED IFTS FOR CO₂ + N-BUTANE AT 344.3 K (160 °F),
K = 3.91, "THIS WORK" PARACHOR EQUATION E.20

TEMP F	PRES PSIA	EXPERIMENTAL IFT M N/M	W-K (L-C)		W-K THIS WORK		PREDICTED W-K (H-VW)		L-C MIXED		THIS WORK MIXED	
			IFT	%ERROR K = 3.911	IFT	%ERROR K = 3.91	IFT	%ERROR K = 3.91	IFT	%ERROR K = 3.91	IFT	%ERROR K = 3.91
160.00	465.00	4.2200	3.9695	-5.94	4.2378	0.42	4.2558	0.85	4.3314	2.64	3.2644	-22.65
160.00	610.00	3.1599	2.9767	-5.80	3.1799	0.63	3.1689	0.28	3.3558	6.20	2.2403	-29.10
160.00	699.00	2.4799	2.3485	-5.30	2.5098	1.21	2.4881	0.33	2.6946	8.66	1.6885	-31.91
160.00	802.00	1.8497	1.7033	-7.91	1.8214	-1.53	1.7921	-3.11	1.9899	7.58	1.1716	-36.66
160.00	906.00	1.2859	1.0922	-15.06	1.1687	-9.11	1.1405	-11.31	1.2957	0.76	0.7254	-43.59
160.00	995.00	0.7031	0.6304	-10.34	0.6750	-4.00	0.6533	-7.08	0.7553	7.42	0.4103	-41.64
160.00	1059.00	0.3970	0.3365	-15.25	0.3605	-9.21	0.3467	-12.67	0.4054	2.11	0.2169	-45.38
160.00	1104.00	0.2259	0.1688	-25.26	0.1809	-19.91	0.1733	-23.28	0.2041	-9.66	0.1082	-52.09
160.00	1127.00	0.1289	0.0961	-25.45	0.1030	-20.10	0.0985	-23.58	0.1164	-9.73	0.0614	-52.36
160.00	1142.00	0.0899	0.0610	-32.19	0.0654	-27.32	0.0625	-30.54	0.0739	-17.80	0.0389	-56.74
160.00	1152.00	0.0570	0.0371	-35.03	0.0397	-30.36	0.0379	-33.50	0.0449	-21.20	0.0236	-58.59
160.00	1155.00	0.0470	0.0315	-32.95	0.0338	-28.13	0.0323	-31.37	0.0383	-18.65	0.0201	-57.30
			RMSE		% AVE ABS DEV							
W-K WITH LEE-CHIEN PARACHOR			0.12493		18.04							
W-K WITH THIS WORK PARACHOR			0.04285		12.66							
W-K WITH H-VW PARACHOR			0.05472		14.83							
LEE-CHIEN MIXED			0.10021		9.37							
THIS WORK MIXED			0.52444		44.00							

W-K (L-C) : W-K CORRELATION WITH PURE PARACHOR CALCULATED FROM L-C CORRELATION
W-K THIS WORK : W-K CORRELATION WITH PURE PARACHOR CALCULATED FROM THIS WORK CORRELATION
W-K (H-VW) : W-K CORRELATION WITH PURE PARACHOR CALCULATED FROM H-VW CORRELATION
L-C MIXED : L-C IFT CORRELATION USING MIXED PARACHORS
THIS WORK MIXED : IFT CORRELATION DEVELOPED IN THIS WORK

TABLE LXVII

COMPARISON OF PREDICTED IFTS FOR CO₂ + N-BUTANE AT 377.6 K (220 °F),
K = 3.91, "THIS WORK" PARACHOR EQUATION E.20

TEMP F	PRES PSIA	EXPERIMENTAL IFT M N/M	W-K (L-C)		W-K THIS WORK		PREDICTED W-K (H-VW)		L-C MIXED		THIS WORK MIXED	
			IFT	%ERROR K = 3.911	IFT	%ERROR K = 3.91	IFT	%ERROR K = 3.91	IFT	%ERROR K = 3.91	IFT	%ERROR K = 3.91
220.00	41 ^o OC	2.6657	2.4142	-9.43	2.5267	-5.21	2.6124	-2.00	2.4868	-6.71	2.2993	-13.74
220.00	49 ^o .00	2.2393	2.0405	-8.87	2.1358	-4.62	2.2033	-1.61	2.1362	-4.60	1.8500	-17.38
220.00	604.00	1.7298	1.5542	-10.15	1.6269	-5.95	1.6738	-3.24	1.6592	-4.08	1.3294	-23.15
220.00	702.00	1.3324	1.1361	-14.73	1.1893	-10.73	1.2203	-8.41	1.2350	-7.31	0.9225	-30.76
220.00	804.00	0.8870	0.7347	-17.17	0.7692	-13.28	0.7869	-11.28	0.8127	-8.37	0.5677	-36.00
220.00	863.00	0.6464	0.5309	-17.87	0.5559	-14.01	0.5675	-12.21	0.5930	-8.27	0.3996	-38.19
220.00	909.00	0.4961	0.3814	-23.11	0.3994	-19.49	0.4072	-17.92	0.4291	-13.51	0.2816	-43.24
220.00	957.00	0.3160	0.2476	-21.67	0.2592	-17.98	0.2639	-16.48	0.2805	-11.26	0.1792	-43.28
220.00	1003.00	0.1703	0.1353	-20.54	0.1417	-16.80	0.1440	-15.44	0.1543	-9.36	0.0962	-43.50
220.00	1018.00	0.1375	0.1122	-18.42	0.1175	-14.57	0.1193	-13.21	0.1282	-6.77	0.0794	-42.26
220.00	1041.00	0.0956	0.0694	-27.40	0.0727	-23.97	0.0738	-22.83	0.0796	-16.76	0.0487	-49.05
220.00	1058.00	0.0548	0.0414	-24.53	0.0433	-20.97	0.0440	-19.73	0.0475	-13.34	0.0289	-47.28
			RMSE		% AVE ABS DEV							
W-K WITH LEE-CHIEN PARACHOR			0.13820		17.82							
W-K WITH THIS WORK PARACHOR			0.09019		13.97							
W-K WITH H-VW PARACHOR			0.06345		12.03							
LEE-CHIEN MIXED			0.07738		9.20							
THIS WORK MIXED			0.26668		35.65							

W-K (L-C) : W-K CORRELATION WITH PURE PARACHOR CALCULATED FROM L-C CORRELATION
W-K THIS WORK : W-K CORRELATION WITH PURE PARACHOR CALCULATED FROM THIS WORK CORRELATION
W-K (H-VW) : W-K CORRELATION WITH PURE PARACHOR CALCULATED FROM H-VW CORRELATION
L-C MIXED : L-C IFT CORRELATION USING MIXED PARACHORS
THIS WORK MIXED : IFT CORRELATION DEVELOPED IN THIS WORK

TABLE LXVIII

COMPARISON OF PREDICTED IFTS FOR CO₂ + N-DECANE AT 344.3 K (160 °F),
K = 3.91, "THIS WORK" PARACHOR EQUATION E.20

TEMP F	PRES PSIA	EXPERIMENTAL IFT M N/M	W-K (L-C)		W-K THIS WORK		PREDICTED W-K (H-VW)		L-C MIXED		THIS WORK MIXED	
			IFT	%ERROR K = 3.911	IFT	%ERROR K = 3.91	IFT	%ERROR K = 3.91	IFT	%ERROR K = 3.91	IFT	%ERROR K = 3.91
160.00	1007.00	7.8139	7.4929	-4.11	8.6037	10.11	8.6843	11.14	11.9969	53.53	1.2280	-84.28
160.00	1104.00	6.6539	6.5394	-1.72	7.5052	12.79	7.5587	13.60	10.7232	61.16	0.9761	-85.33
160.00	1210.00	5.6712	5.5416	-2.28	6.3599	12.14	6.4047	12.93	9.2990	63.97	0.7514	-86.75
160.00	1300.00	4.6121	4.6324	0.44	5.3150	15.24	5.3461	15.92	7.9203	71.73	0.5826	-87.37
160.00	1400.00	3.5410	3.6373	2.72	4.1722	17.83	4.1921	18.39	6.3382	79.00	0.4234	-88.04
160.00	1500.00	2.5330	2.6383	4.16	3.0249	19.42	3.0327	19.73	4.6715	84.43	0.2889	-88.59
160.00	1599.00	1.7132	1.6729	-2.35	1.9163	11.85	1.9136	11.70	3.0011	75.18	0.1756	-89.75
160.00	1650.00	1.2918	1.2695	-1.73	1.4540	12.55	1.4506	12.29	2.2925	77.46	0.1299	-89.94
160.00	1701.00	0.8483	0.8189	-3.46	0.9374	10.50	0.9331	9.99	1.4868	75.26	0.0826	-90.27
160.00	1726.00	0.6649	0.6407	-3.64	0.7335	10.31	0.7305	9.86	1.1693	75.84	0.0630	-90.52
160.00	1751.00	0.5289	0.4523	-14.48	0.5174	-2.17	0.5135	-2.92	0.8236	55.71	0.0455	-91.39
160.00	1772.00	0.3561	0.3181	-10.68	0.3637	2.13	0.3602	1.15	0.5789	62.55	0.0323	-90.93
160.00	1799.00	0.2447	0.1663	-32.03	0.1901	-22.32	0.1879	-23.20	0.3028	23.76	0.0170	-93.07
160.00	1811.00	0.1422	0.1039	-26.93	0.1186	-16.54	0.1169	-17.74	0.1883	32.45	0.0109	-92.31
160.00	1821.00	0.1009	0.0700	-30.61	0.0800	-20.72	0.0789	-21.79	0.1274	26.21	0.0072	-92.83
160.00	1830.00	0.0592	0.0440	-25.77	0.0503	-15.11	0.0498	-15.86	0.0809	36.53	0.0043	-92.82
160.00	1835.00	0.0293	0.0199	-32.12	0.0228	-22.29	0.0227	-22.59	0.0371	26.55	0.0018	-93.94
160.00	1842.00	0.0126	0.0093	-26.11	0.0107	-15.17	0.0107	-14.44	0.0179	42.24	0.0007	-94.60

RMSE

% AVE ABS DEV

W-K WITH LEE-CHIEN PARACHOR	0.09818	12.52
W-K WITH THIS WORK PARACHOR	0.41109	13.84
W-K WITH H-VW PARACHOR	0.43516	14.18
LEE-CHIEN MIXED	2.02794	56.86
THIS WORK MIXED	2.74763	90.15

W-K (L-C) : W-K CORRELATION WITH PURE PARACHOR CALCULATED FROM L-C CORRELATION
W-K THIS WORK : W-K CORRELATION WITH PURE PARACHOR CALCULATED FROM THIS WORK CORRELATION
W-K (H-VW) : W-K CORRELATION WITH PURE PARACHOR CALCULATED FROM H-VW CORRELATION
L-C MIXED : L-C IFT CORRELATION USING MIXED PARACHORS
THIS WORK MIXED : IFT CORRELATION DEVELOPED IN THIS WORK

TABLE LXIX

COMPARISON OF PREDICTED IFTS FOR CO₂ + N-DECANE AT 377.6 K (220 °F),
K = 3.91, "THIS WORK" PARACHOR EQUATION E.20

TEMP F	PRES PSIA	EXPERIMENTAL IFT M N/M	W-K (L-C) IFT %ERROR K = 3.911		W-K THIS WORK IFT %ERROR K = 3.91		PREDICTED W-K (H-VW) IFT %ERROR K = 3.91		L-C MIXED IFT %ERROR K = 3.91		THIS WORK MIXED IFT %ERROR K = 3.91	
			IFT	%ERROR	IFT	%ERROR	IFT	%ERROR	IFT	%ERROR	IFT	%ERROR
220.00	1500.00	4.3922	3.9297	-10.53	4.3611	-0.71	4.5880	4.46	6.6529	51.47	0.4822	-89.02
220.00	1601.00	3.7258	3.3334	-10.53	3.6992	-0.72	3.8909	4.43	5.7361	53.96	0.3814	-89.76
220.00	1705.00	3.0770	2.7048	-12.10	3.0022	-2.43	3.1607	2.72	4.7407	54.07	0.2848	-90.74
220.00	1801.00	2.5399	2.1413	-15.69	2.3766	-6.43	2.5014	-1.51	3.8075	49.91	0.2117	-91.67
220.00	1903.00	1.9831	1.6404	-17.28	1.8204	-8.20	1.9147	-3.45	2.9592	49.22	0.1525	-92.31
220.00	2001.00	1.4230	1.1724	-17.61	1.3012	-8.56	1.3691	-3.79	2.1454	50.76	0.1020	-92.83
220.00	2053.00	1.2370	0.9629	-22.16	1.0687	-13.61	1.1245	-9.09	1.7733	43.36	0.0814	-93.42
220.00	2100.00	0.9501	0.7627	-19.73	0.8467	-10.88	0.8924	-6.07	1.4171	49.15	0.0614	-93.53
220.00	2151.00	0.7920	0.6077	-23.27	0.6750	-14.77	0.7132	-9.96	1.1402	43.96	0.0463	-94.15
220.00	2201.00	0.6336	0.4343	-31.45	0.4825	-23.85	0.5097	-19.55	0.8206	29.52	0.0321	-94.94
220.00	2226.00	0.4817	0.3547	-26.36	0.3941	-18.18	0.4169	-13.46	0.6740	39.92	0.0254	-94.74
220.00	2250.00	0.3903	0.2807	-28.08	0.3119	-20.10	0.3297	-15.53	0.5346	36.96	0.0199	-94.90
220.00	2276.00	0.3140	0.2064	-34.26	0.2293	-26.98	0.2423	-22.82	0.3946	25.66	0.0144	-95.42
220.00	2299.00	0.2210	0.1508	-31.78	0.1675	-24.22	0.1769	-19.94	0.2888	30.66	0.0104	-95.29
220.00	2315.00	0.1715	0.1145	-33.24	0.1272	-25.81	0.1347	-21.46	0.2206	28.64	0.0076	-95.56
220.00	2331.00	0.1271	0.0808	-36.39	0.0898	-29.31	0.0951	-25.14	0.1562	22.91	0.0053	-95.83
220.00	2341.00	0.1000	0.0624	-37.61	0.0693	-30.69	0.0733	-26.70	0.1205	20.43	0.0041	-95.87
220.00	2353.00	0.0691	0.0424	-38.67	0.0471	-31.85	0.0498	-27.83	0.0821	18.87	0.0027	-96.04
220.00	2362.00	0.0510	0.0298	-41.62	0.0331	-35.08	0.0352	-31.06	0.0582	13.98	0.0018	-96.41
220.00	2371.00	0.0330	0.0179	-45.94	0.0199	-39.89	0.0211	-36.21	0.0349	5.59	0.0011	-96.67
220.00	2376.00	0.0200	0.0119	-40.38	0.0133	-33.62	0.0142	-29.08	0.0237	18.24	0.0007	-96.70
220.00	2381.00	0.0120	0.0080	-33.64	0.0089	-26.14	0.0094	-21.19	0.0157	31.22	0.0004	-96.25
220.00	2386.00	0.0080	0.0051	-36.25	0.0057	-29.12	0.0060	-24.78	0.0100	24.56	0.0003	-96.08
			RMSE		% AVE ABS DEV							
W-K WITH LEE-CHIEN PARACHOR			0.21694		28.03							
W-K WITH THIS WORK PARACHOR			0.08846		20.05							
W-K WITH H-VW PARACHOR			0.07748		16.53							
LEE-CHIEN MIXED			0.82715		34.48							
THIS WORK MIXED			1.45015		94.27							

W-K (L-C) : W-K CORRELATION WITH PURE PARACHOR CALCULATED FROM L-C CORRELATION
W-K THIS WORK : W-K CORRELATION WITH PURE PARACHOR CALCULATED FROM THIS WORK CORRELATION
W-K (H-VW) : W-K CORRELATION WITH PURE PARACHOR CALCULATED FROM H-VW CORRELATION
L-C MIXED : L-C IFT CORRELATION USING MIXED PARACHORS
THIS WORK MIXED : IFT CORRELATION DEVELOPED IN THIS WORK

TABLE LXX

COMPARISON OF PREDICTED IFTS FOR CO₂ + N-TETRADECANE AT 344.3 K (160 °F),
K = 3.91, "THIS WORK" PARACHOR EQUATION E.20

TEMP F	PRES PSIA	EXPERIMENTAL IFT M N/M	PREDICTED									
			W-K (L-C) IFT %ERROR K = 3.911		W-K THIS WORK IFT %ERROR K = 3.91		W-K (H-VW) IFT %ERROR K = 3.91		L-C MIXED IFT %ERROR K = 3.91		THIS WORK MIXED IFT %ERROR K = 3.91	
160.00	1600.00	4.0324	2.7279	-32.35	4.5080	11.80	4.3687	8.34	6.3649	57.85	0.1176	-97.08
160.00	1700.00	3.2310	2.0454	-36.69	3.4100	5.54	3.3180	2.69	4.9499	53.20	0.0711	-97.80
160.00	1800.00	2.4865	1.4437	-41.94	2.4342	-2.10	2.3808	-4.25	3.6369	46.27	0.0387	-98.44
160.00	1900.00	1.8076	0.9473	-47.59	1.6250	-10.10	1.6019	-11.38	2.5090	38.80	0.0176	-99.03
160.00	2000.00	1.2150	0.5627	-53.69	0.9880	-18.69	0.9842	-19.00	1.5833	30.31	0.0063	-99.48
160.00	2100.00	0.7275	0.2963	-59.28	0.5369	-26.19	0.5426	-25.42	0.9006	23.79	0.0015	-99.79
160.00	2200.00	0.3604	0.1288	-64.26	0.2416	-32.97	0.2478	-31.23	0.4253	18.01	0.0002	-99.94
160.00	2300.00	0.1131	0.0375	-66.81	0.0722	-36.17	0.0749	-33.79	0.1321	16.83	0.0000	-99.98
160.00	2310.00	0.0943	0.0308	-67.36	0.0591	-37.30	0.0613	-35.01	0.1082	14.73	0.0000	-99.98
160.00	2320.00	0.0765	0.0257	-66.43	0.0495	-35.24	0.0515	-32.75	0.0912	19.17	0.0000	-99.98
160.00	2330.00	0.0597	0.0205	-65.64	0.0397	-33.54	0.0413	-30.90	0.0733	22.70	0.0000	-99.99
160.00	2340.00	0.0439	0.0155	-64.65	0.0301	-31.44	0.0313	-28.63	0.0558	27.12	0.0000	-99.99
160.00	2350.00	0.0292	0.0107	-63.28	0.0209	-28.49	0.0218	-25.43	0.0389	33.21	0.0000	-99.99
160.00	2352.00	0.0264	0.0100	-62.29	0.0195	-26.33	0.0203	-23.06	0.0364	37.79	0.0000	-99.99
160.00	2354.50	0.0237	0.0092	-61.39	0.0179	-24.35	0.0188	-20.90	0.0336	41.80	0.0000	-99.99
160.00	2356.50	0.0210	0.0082	-61.13	0.0160	-23.80	0.0168	-20.30	0.0301	42.92	0.0000	-99.99
160.00	2358.00	0.0184	0.0075	-59.51	0.0147	-20.23	0.0154	-16.39	0.0278	50.46	0.0000	-99.99
160.00	2360.00	0.0159	0.0065	-58.83	0.0129	-18.70	0.0136	-14.71	0.0244	53.68	0.0000	*****

	RMSE	% AVE ABS DEV
W-K WITH LEE-CHIEN PARACHOR	0.55855	57.40
W-K WITH THIS WORK PARACHOR	0.14921	23.50
W-K WITH H-VW PARACHOR	0.12429	21.34
LEE-CHIEN MIXED	0.75947	34.93
THIS WORK MIXED	1.42712	99.53

W-K (L-C) : W-K CORRELATION WITH PURE PARACHOR CALCULATED FROM L-C CORRELATION
W-K THIS WORK : W-K CORRELATION WITH PURE PARACHOR CALCULATED FROM THIS WORK CORRELATION
W-K (H-VW) : W-K CORRELATION WITH PURE PARACHOR CALCULATED FROM H-VW CORRELATION
L-C MIXED : L-C IFT CORRELATION USING MIXED PARACHORS
THIS WORK MIXED : IFT CORRELATION DEVELOPED IN THIS WORK

TABLE LXXI

COMPARISON OF PREDICTED IFTS FOR CO₂ + BENZENE AT 344.3 K (160 °F),
K = 3.91, "THIS WORK" PARACHOR EQUATION E.20

TEMP F	PRES PSIA	EXPERIMENTAL IFT M N/M	PREDICTED									
			W-K (L-C) IFT %ERROR K = 3.911		W-K THIS WORK IFT %ERROR K = 3.91		W-K (H-VW) IFT %ERROR K = 3.91		L-C MIXED IFT %ERROR K = 3.91		THIS WORK MIXED IFT %ERROR K = 3.91	
160.00	1000.00	6.6038	6.9574	5.35	8.2174	24.43	7.6663	16.09	7.7274	17.01	6.0473	-8.43
160.00	1101.00	4.9625	5.6502	13.86	6.6560	34.13	6.1771	24.48	6.3223	27.40	4.7961	-3.35
160.00	1201.00	3.7180	4.2917	15.43	5.0413	35.59	4.6515	25.11	4.8326	29.98	3.5691	-4.00
160.00	1300.00	2.4821	2.9359	18.28	3.4354	38.41	3.1453	26.72	3.3197	33.75	2.4049	-3.11
160.00	1399.00	1.3856	1.6516	19.19	1.9228	38.77	1.7424	25.74	1.8696	34.92	1.3434	-3.05
160.00	1430.00	0.9377	1.1670	24.45	1.3584	44.86	1.2303	31.20	1.3239	41.18	0.9432	0.58
160.00	1475.00	0.7094	0.7904	11.42	0.9162	29.15	0.8229	15.99	0.8935	25.95	0.6433	-9.33
160.00	1500.00	0.5078	0.5400	6.34	0.6251	23.11	0.5600	10.29	0.6100	20.15	0.4397	-13.41
160.00	1520.00	0.3635	0.3785	4.14	0.4383	20.60	0.3929	8.11	0.4289	18.00	0.3057	-15.88
160.00	1535.00	0.2624	0.2548	-2.89	0.2942	12.13	0.2622	-0.09	0.2873	9.49	0.2083	-20.63
160.00	1550.00	0.1722	0.1626	-5.55	0.1876	8.96	0.1669	-3.10	0.1832	6.41	0.1331	-22.68
160.00	1559.00	0.1227	0.1076	-12.31	0.1240	1.05	0.1100	-10.34	0.1210	-1.34	0.0883	-27.99
160.00	1571.00	0.0653	0.0524	-19.79	0.0603	-7.68	0.0534	-18.27	0.0589	-9.88	0.0432	-33.95
160.00	1580.00	0.0255	0.0209	-17.99	0.0241	-5.68	0.0213	-16.65	0.0235	-7.94	0.0073	32.32
160.00	1584.00	0.0114	0.0095	-16.78	0.0109	-4.17	0.0097	-15.08	0.0107	-6.32	0.0078	-31.81
			RMSE		% AVE ABS DEV							
W-K WITH LEE-CHIEN PARACHOR			0.29039		12.92							
W-K WITH THIS WORK PARACHOR			0.75985		21.91							
W-K WITH H-VW PARACHOR			0.52568		16.48							
LEE-CHIEN MIXED			0.60488		19.31							
THIS WORK MIXED			0.16040		15.37							

W-K (L-C) : W-K CORRELATION WITH PURE PARACHOR CALCULATED FROM L-C CORRELATION
W-K THIS WORK : W-K CORRELATION WITH PURE PARACHOR CALCULATED FROM THIS WORK CORRELATION
W-K (H-VW) : W-K CORRELATION WITH PURE PARACHOR CALCULATED FROM H-VW CORRELATION
L-C MIXED : L-C IFT CORRELATION USING MIXED PARACHORS
THIS WORK MIXED : IFT CORRELATION DEVELOPED IN THIS WORK

TABLE LXXII

COMPARISON OF PREDICTED IFTS FOR CO₂ + CYCLOHEXANE AT 344.3 K (160 °F),
K = 3.91, "THIS WORK" PARACHOR EQUATION E.20

TEMP F	PRES PSIA	EXPERIMENTAL IFT M N/M	W-K (L-C)		W-K THIS WORK		PREDICTED W-K (H-VW)		L-C MIXED		THIS WORK MIXED	
			IFT	%ERROR K = 3.911	IFT	%ERROR K = 3.91	IFT	%ERROR K = 3.91	IFT	%ERROR K = 3.91	IFT	%ERROR K = 3.91
160.00	997.00	6.3492	6.0485	-4.74	6.1503	-3.13	6.6673	5.01	7.0982	11.80	3.7299	-41.25
160.00	1101.00	4.9844	4.8148	-3.40	4.9026	-1.64	5.2812	5.95	5.7266	14.89	2.8603	-42.61
160.00	1200.00	3.7106	3.6923	-0.49	3.7644	1.45	4.0317	8.66	4.4461	19.82	2.1204	-42.86
160.00	1300.00	2.6203	2.6405	0.77	2.6989	3.00	2.8569	9.03	3.2093	22.48	1.4845	-43.35
160.00	1400.00	1.3908	1.5076	8.40	1.5453	11.11	1.6141	16.06	1.8457	32.71	0.8359	-39.90
160.00	1450.00	0.9467	0.9998	5.61	1.0272	8.51	1.0616	12.14	1.2249	29.39	0.5568	-41.19
160.00	1500.00	0.5193	0.5260	1.29	0.5419	4.35	0.5529	6.48	0.6435	23.92	0.2964	-42.93
160.00	1525.00	0.3652	0.3354	-8.16	0.3458	-5.30	0.3514	-3.76	0.4104	12.38	0.1893	-48.15
160.00	1540.00	0.2537	0.2294	-9.59	0.2367	-6.70	0.2396	-5.55	0.2804	10.54	0.1301	-48.74
160.00	1550.00	0.1802	0.1627	-9.71	0.1681	-6.75	0.1695	-5.95	0.1987	10.26	0.0928	-48.50
160.00	1560.00	0.1349	0.1107	-17.96	0.1144	-15.22	0.1150	-14.74	0.1350	0.11	0.0634	-53.03
160.00	1570.00	0.0807	0.0617	-23.51	0.0639	-20.88	0.0640	-20.74	0.0752	-6.80	0.0356	-55.91
160.00	1579.00	0.0362	0.0283	-21.83	0.0293	-19.14	0.0293	-19.01	0.0345	-4.69	0.0163	-55.02
160.00	1586.00	0.0094	0.0068	-27.23	0.0070	-24.86	0.0071	-24.13	0.0084	-10.58	0.0038	-59.25
			RMSE				% AVE ABS DEV					
W-K WITH LEE-CHIEN PARACHOR			0.09972				10.19					
W-K WITH THIS WORK PARACHOR			0.07918				9.43					
W-K WITH H-VW PARACHOR			0.17193				11.23					
LEE-CHIEN MIXED			0.40556				15.03					
THIS WORK MIXED			1.06106				47.33					

W-K (L-C) : W-K CORRELATION WITH PURE PARACHOR CALCULATED FROM L-C CORRELATION
W-K THIS WORK : W-K CORRELATION WITH PURE PARACHOR CALCULATED FROM THIS WORK CORRELATION
W-K (H-VW) : W-K CORRELATION WITH PURE PARACHOR CALCULATED FROM H-VW CORRELATION
L-C MIXED : L-C IFT CORRELATION USING MIXED PARACHORS
THIS WORK MIXED : IFT CORRELATION DEVELOPED IN THIS WORK

TABLE LXXIII

COMPARISON OF THE ACCURACY OF PREDICTED IFTS BASED ON ALL DATA POINTS

IFT Correlation	k = 3.55				k = 3.91			
	Temp. Independent Error in Predicted IFTs		Temp. Dependent Error in Predicted IFTs		Temp. Independent Error in Predicted IFTs		Temp. Dependent Error in Predicted IFTs	
	RMSE mN/m	AAPD %	RMSE mN/m	AAPD %	RMSE mN/m	AAPD %	RMSE mN/m	AAPD %
W-K with L-C parachor	0.385	16.8	--	--	0.287	23.5	--	--
W-K with "this Work" parachor	0.443	22.1	1.013	42.9	0.372	20.0	0.374	17.6
W-K with H-VW parachor	0.170	10.5	--	--	0.317	16.8	--	--
L-C - Equation 2.15	0.516	31.1	--	--	0.947	27.1	--	--
"This Work" - Equation 5.4	1.30	50.9	1.285	49.5	1.369	61.0	1.374	62.4

Note: The blanks indicate parachor correlations without any dependence on temperature.

APPENDIX D

NATIONAL BUREAU OF STANDARDS (NBS) DATA SET

Table LXXIV shows the pure component physical properties of critical pressure (P_c), critical volume (V_c), critical temperature (T_c), acentric factor, molecular weight, and normal boiling point temperature for the six components studied in the present work.

TABLE LXXIV

PHYSICAL PROPERTY DATA SET FROM THE NATIONAL BUREAU OF STANDARDS

	P_c , atm	V_c , cc/gmol	T_c , K	ω	MW	T_B , K
CO ₂	71.905	94.430	304.21	0.2251	44.010	194.60
n-Butane	36.974	256.410	425.160	0.20038	58.124	272.65
n-Decane	20.422	607.530	617.550	0.48847	142.287	447.30
n-Tetradecane	15.322	827.13	692.950	0.64416	198.395	526.73
Benzene	47.707	259.00	562.16	0.212	78.110	353.24
Cyclohexane	39.642	308.00	553.5	0.212	84.160	353.88

APPENDIX E

PARACHOR CORRELATION FROM THE PRESENT WORK

A parachor correlation was developed as part of the present work and is discussed below. The correlation was derived from a modified form of the Macleod form of the parachor equation:

$$[P] = M \gamma^{1/k} / \Delta\rho \quad (\text{E.1})$$

[P] = parachor

M = molecular weight

γ = interfacial tension, nM/m

k = scaling exponent, (Macleod used k = 4)

$\Delta\rho = (\rho^L - \rho^V)$, gm/cc

The parachor equation proposed was formulated by combining three equations: one for the IFT (γ), one for the liquid phase density (ρ^L), and one for the vapor phase density (ρ^V). Each of these properties were represented by a power series expansion in acentric factor, similar to that proposed by Pitzer (30). The IFT correlation was presented by Kobayashi (31) in the reduced form:

$$\ln \gamma^* = (\ln L^* - \ln A)/N \quad (\text{E.2})$$

$\gamma^* = \gamma / (R T_c P_c / M C)$, reduced dimensionless
interfacial tension

$R = 8.3145 \text{ J mol}^{-1} \text{ K}^{-1}$, $T_c - \text{K}$, $P_c - \text{atm}$,

$M = \text{molecular weight}$, and $C = 9.78387 \cdot 10^{-11}$

$L^* = L^*(0) + \omega^* L^*(1)$, reduced dimensionless latent heat of
vaporization

$\omega^* = \omega / \omega_1$, reduced acentric factor $\omega_1 = \text{acentric factor}$
of reference compound, n-decane, $\omega_1 = 0.49$

$$L^*(0) = A_1 \epsilon^\beta + A_2 \epsilon^{\beta+\Delta} + A_3 \epsilon^{1-\alpha+\beta} + A_4 \epsilon + A_5 \epsilon^2 + A_6 \epsilon^3 \quad (\text{E.3})$$

$$L^*(1) = B_1 \epsilon^\beta + B_2 \epsilon^{\beta+\Delta} + B_3 \epsilon^{1-\alpha-\beta} + B_4 \epsilon + B_5 \epsilon^2 + B_6 \epsilon^3 \quad (\text{E.4})$$

$A = 18877.66$; $N = 0.2852$, system independent constants

where $\epsilon = (T_c - T) / T_c = 1 - T_r$ and α , β , and Δ are scaling exponents given by $\alpha = 1/8$, $\beta = 1/3$, $\Delta = 1/2$ (Wegner's first gap exponent). A_1 , A_2 , A_3 , A_4 , A_5 , and A_6 , in Equation E.3 and B_1 , B_2 , B_3 , B_4 , B_5 , and B_6 in Equation E.4 are system independent constants and are shown in Table LXXV (taken from the work of Kobayashi).

The liquid density correlation proposed by Sivanaman and Kobayashi (32) was a reduced dimensionless corresponding-states correlation:

$$\Delta \rho^{L^*} = (\rho^L / \rho_c) - 1 = \Delta \rho^{L^*}(0) + \omega^* \Delta \rho^{L^*}(1) \quad (\text{E.5})$$

TABLE LXXV

SYSTEM INDEPENDENT CONSTANTS FOR EQUATIONS
E.3, E.4, E.6, E.7, E.9, E.10, AND E.12

Equation E.3 - $L^*(0)$		Equation E.4 - $L^*(1)$	
A ₁	-0.93298	B ₁	10.49454
A ₂	275.55325	B ₂	-351.09761
A ₃	416.64687	B ₃	-617.13917
A ₄	-617.76799	B ₄	854.73145
A ₅	-94.43886	B ₅	155.93484
A ₆	29.55731	B ₆	-50.59250
Equation E.6 - $\Delta\rho^{L^*}(0)$		Equation E.7 - $\Delta\rho^{L^*}(1)$	
C ₁	1.94825	D ₁	0.35447
C ₂	-68.80545	D ₂	13.16141
C ₃	99.18809	D ₃	-20.95529
C ₄	-31.62733	D ₄	9.15210
C ₅	3.27455	D ₅	-3.96241
C ₆	-1.96593	D ₆	4.23403
Equation E.9 - $\Delta\rho^{V^*}(0)$		Equation E.10 - $\Delta\rho^{V^*}(\omega=0.49)$	
E ₁	1.98377	F ₁	2.12552
E ₂	-107.76000	F ₂	-18.67319
E ₃	154.73000	F ₃	27.21436
E ₄	-50.30259	F ₄	-10.40200
E ₅	3.39973	F ₅	0.22753
E ₆	-1.34125	F ₆	0.80185
Equation E.12 - $\Delta\rho^{V^*}(1)$			
	G ₁		0.14175
	G ₂		89.08681
	G ₃		-127.51564
	G ₄		39.90059
	G ₅		-3.17220
	G ₆		2.14310

$$\Delta\rho_{(0)}^{L*} = C_1 \varepsilon^\beta + C_2 \varepsilon^{\beta+\Delta} + C_3 \varepsilon^{1-\alpha} + C_4 \varepsilon + C_5 \varepsilon^2 + C_6 \varepsilon^3 \quad (\text{E.6})$$

$$\Delta\rho_{(1)}^{L*} = D_1 \varepsilon^\beta + D_2 \varepsilon^{\beta+\Delta} + D_3 \varepsilon^{1-\alpha} + D_4 \varepsilon + D_5 \varepsilon^2 + D_6 \varepsilon^3 \quad (\text{E.7})$$

where $C_1, C_2, C_3, C_4, C_5, C_6$ in Equation E.6 and $D_1, D_2, D_3, D_4, D_5,$ and D_6 in Equation E.7 are system independent constants indicated in Table LXXV.

The saturated vapor density correlation was developed in the present work from data published by Pitzer-Curl (30). A power series expansion in acentric factor, similar in form to Equation E.5, was used to determine the reduced dimensionless vapor density. It consists of two terms, one representing a simple fluid ($\omega = 0.0$), $\Delta\rho_{(0)}^{V*}$, and another representing a complex fluid ($\omega \neq 0.0$); $\Delta\rho_{(1)}^{V*}$, (n-decane, $\omega = 0.49$, selected as complex fluid). In order to obtain equations for $\Delta\rho_{(0)}^{V*}$ and $\Delta\rho_{(1)}^{V*}$ the Pitzer-Curl tabulation of saturated vapor compressibility factors (Z) and reduced pressures (P_r) were used in a SAS regression analysis to determine parameters for equations similar to E.6 and E.7 for $\Delta\rho_{(0)}^{V*}$ and $\Delta\rho_{(1)}^{V*}$. The following approach was used.

$$\Delta\rho^{V*} = 1 - (\rho^V/\rho_c) = 1 - \left(\frac{P_r Z_c}{Tr Z}\right) = \Delta\rho_{(0)}^{V*} + \omega^* \Delta\rho_{(1)}^{V*} \quad (\text{E.8})$$

where

$P_r \sim f(\omega, Tr)$ and $Z \sim f(\omega, Tr)$ are obtained from Pitzer-Curl

$Z_c = 0.291 - \omega 0.08$, from Pitzer-Curl

Tr = reduced temperature (Tr varied from 0.58 = 1.0)

$\omega^* = (\omega_i/\omega_1)$, reduced acentric factor, $\omega_1 = 0.49$ (n-decane)

Using Equation E.8 and the Pitzer-Curl information, values for $\Delta\rho^{V*}$ at $\omega = 0.0$ and $\omega = 0.49$ (n-decane) and $\Delta\rho^{V*}$ were obtained for Tr from 0.58 to 1.0. The values for $\Delta\rho^{V*}(\omega = 0.0)$ and $\Delta\rho^{V*}(\omega = 0.49)$ were next used in a SAS regression analysis to determine the E and F parameters in the following equations.

$$\Delta\rho^{V*}(\omega = 0.0) = \Delta\rho^{V*}(0) = E_1\varepsilon^\beta + E_2\varepsilon^{\beta+\Delta} + E_3\varepsilon^{1-\alpha} + E_4\varepsilon + E_5\varepsilon^2 + E_6\varepsilon^3 \quad (\text{E.9})$$

$$\begin{aligned} \Delta\rho^{V*}(\omega = 0.49) &= \Delta\rho^{V*}(0) + (\omega^* = 1.0) \Delta\rho^{V*}(1) \\ &= F_1\varepsilon^\beta + F_2\varepsilon^{\beta+\Delta} + F_3\varepsilon^{1-\alpha} + F_4\varepsilon + F_5\varepsilon^2 + F_6\varepsilon^3 \end{aligned} \quad (\text{E.10})$$

where $E_1, E_2, E_3, E_4, E_5, E_6$, and $F_1, F_2, F_3, F_4, F_5, F_6$, are system independent constants indicated in Table LXXV.

Using the following form of Equation E.8

$$\Delta\rho^{V*} = \Delta\rho^{V*}(0) + \omega^* \Delta\rho^{V*}(1) \quad (\text{E.11})$$

and solving for $\Delta\rho^{V*}(1)$, an equation for $\Delta\rho^{V*}(1)$ in terms of $\Delta\rho^{V*}(0)$ and $\Delta\rho^{V*}(\omega=0.49)$ results

$$\begin{aligned} \Delta\rho^{V*}(1) &= \Delta\rho^{V*}(\omega = 0.49) - \Delta\rho^{V*}(0) = G_1\varepsilon^\beta + G_2\varepsilon^{\beta+\Delta} + G_3\varepsilon^{1-\alpha} \\ &\quad + G_4\varepsilon + G_5\varepsilon^2 + G_6\varepsilon^3 \end{aligned} \quad (\text{E.12})$$

where the parameter $G_i = (F_i - E_i)$ and $i = 1 \dots 6$ and the values are indicated in Table LXXV.

Substituting Equations E.12 and E.9 into Equation E.11 results in the desired equation for the reduced dimensionless vapor density in terms of the parameters $E_1, E_2, E_3, E_4, E_5, E_6$, and $G_1, G_2, G_3, G_4, G_5, G_6$.

$$\Delta\rho^{V*} = (\Delta\rho^{V*})_{(0)} \sim E) + \omega^* (\Delta\rho^{V*})_{(1)} \sim G) \quad (\text{E.13})$$

Using Equations E.5 and E.13, an equation for the reduced density difference was obtained:

$$\Delta\rho^* = \left(\frac{\rho^L - \rho^V}{\rho_c}\right) = \left(\frac{\rho^L}{\rho_c} - 1\right) + \left(1 - \frac{\rho^V}{\rho_c}\right) = \Delta\rho^{L*} + \Delta\rho^{V*} \quad (\text{E.14})$$

The next step in the development of the parachor correlation was to write the parachor Equation E.1 in reduced dimensionless form as are the equations for interfacial tension and density difference. The following equation presents the relationship.

$$[P]^* = \gamma^{*1/k} / \Delta\rho^* = [P] \rho_c \left[\frac{1}{(R T_c P_c / M C)^{1/k}} \right] \quad (\text{E.15})$$

where

$[P]^*$ = reduced parachor

$R = 8.3145 \text{ J mol}^{-1} \text{ K}^{-1}$, T_c - K, P_c - atm

M = molecular weight, and $C = 9.678387 \cdot 10^{-11}$

$\rho_c = 1/V_c = 1/[(0.291 - 0.08 \omega)(R T_c/P_c)]$,

for consistent units, $R = 82.06$ in the expression for ρ_c .

Reduced parachors are obtained by substituting Equations E.2 and E.14 into Equation E.15 and using the system independent parameter in Table LXXV. Reduced parachors were calculated varying ω^* from 0.0 to 1.0 and Tr from 0.58 to 0.9999 at scaling exponents of $k = 3.55$ and $k = 3.91$. The resulting reduced parachors are shown in Tables XXXIX and XL, Appendix B. The scaling exponent value of $k = 3.55$ was selected because it represents the lower acceptable range. The value of $k = 3.91$ was the scaling exponent used in the L-C work and represents an upper acceptable value close to the Macleod value of $k = 4.0$. The two scaling exponents covered the acceptable range (46) and indicate the dependence of the reduced parachor on scaling exponent. The reduced parachor information from Appendix B and Equation E.16 below were used to find expressions for the reduced parachor ($k = 3.55$ or $k = 3.91$) as either a function of reduced acentric factor $[P]^* \sim f(\omega^*)$ or as a function of reduced acentric factor and reduced temperature $[P]^* \sim f(\omega^*, Tr)$.

$$[P]^* = [P]^*_{(0)} + \omega^* ([P]^*_{(\omega = 0.49)} - [P]^*_{(0)}) \quad (E.16)$$

for $k = 3.55$ the following two equations resulted:

first with $[P]^* \sim f(\omega^*)$; the following values were obtained from Appendix B.

$$[P]^*_{(0)} = 1.14 \times 10^{-4}$$

$$[P]^*_{(\omega = 0.49)} = 1.69 \times 10^{-4}$$

substituting $[P]^*(0)$ and $[P]^*(\omega = 0.49)$ into Equation E.16 results in:

$$[P]^* = 1.14 \times 10^{-4} + \omega^* (1.69 \times 10^{-4} - 1.14 \times 10^{-4}) \quad (\text{E.17})$$

second with $[P]^* \sim f(\omega^*, \text{Tr})$; the following values were obtained from Appendix B.

$$[P]^*_{(0)} = 1.22 \times 10^{-4} + 1.01 \times 10^{-5} \text{Tr}$$

$$[P]^*_{(\omega = 0.49)} = 2.13 \times 10^{-4} + -5.70 \times 10^{-5} \text{Tr}$$

substituting $[P]^*_{(0)}$ and $[P]^*_{(\omega = 0.49)}$ into Equation E.16 results in:

$$[P]^* = 1.22 \times 10^{-4} + 1.01 \times 10^{-5} \text{Tr} \\ + \omega^* (9.10 \times 10^{-5} - 6.71 \times 10^{-5} \text{Tr}) \quad (\text{E.18})$$

The reduced parachors predicted by Equations E.17 and E.18 are converted to non-reduced form by Equation E.15.

Next, the same procedure indicated above was performed with a scaling exponent of $k = 3.91$. The comparable equations to E.17 and E.18 are indicated below:

first with $[P]^* \sim f(\omega^*)$ and information in Appendix B:

$$[P]^*(0) = 2.452 \times 10^{-4}$$

$$[P]^*(\omega = 0.49) = 3.50 \times 10^{-4}$$

substituting $[P]^*(0)$ and $[P]^*(\omega = 0.49)$ into Equation E.16 results in:

$$[P]^* = 2.452 \times 10^{-4} + \omega^* (3.50 \times 10^{-4} - 2.452 \times 10^{-4}) \quad (\text{E.19})$$

second with $[P]^* \sim (\omega^*, \text{Tr})$, and information in Appendix B:

$$[P]^*(0) = 2.36 \times 10^{-4} + 1.18 \times 10^{-5} \text{Tr}$$

$$[P]^*(\omega = 0.49) = 3.93 \times 10^{-4} + -5.91 \times 10^{-5} \text{Tr}$$

substituting $[P]^*(0)$ and $[P]^*(\omega^* = 0.49)$ into Equation E.16 results in:

$$[P]^* = 2.36 \times 10^{-4} + 1.18 \times 10^{-5} \text{Tr} \\ + \omega^* (1.57 \times 10^{-4} - 7.09 \times 10^{-5} \text{Tr}) \quad (\text{E.20})$$

The above work resulted in the development of four different reduced parachor correlations. Equation E.17 calculates the reduced parachor (E.15) with $k = 3.55$ and a function of reduced acentric factor

only. Equation E.18 calculates the reduced parachor (E.15) with $k = 3.55$ and a function of reduced acentric factor and reduced temperature, only. Equation E.19 calculates the reduced parachor (E.15) with $k = 3.91$ and a function of reduced acentric factor only. Equation E.20 calculates the reduced parachor (E.15) with $k = 3.91$ and a function of reduced acentric factor and reduced temperature.

VITA

KENNETH BAYARD DICKSON

Candidate for the Degree of

Master of Science

Thesis: INTERFACIAL TENSIONS IN CARBON DIOXIDE + HYDROCARBON SYSTEMS:
EXPERIMENTAL DATA AND CORRELATIONS

Major Field: Chemical Engineering

Biographical:

Personal Data: Born December 17, 1955, in Tucson, Arizona to Mr.
and Mrs. John B. Dickson.

Education: Graduate from Clovis High School, Clovis, New Mexico,
in May 1973; received Bachelor of Science Degree in Chemical
Engineering from New Mexico State University in May, 1978;
completed requirements for Master of Science Degree at
Oklahoma State University in May, 1987.

Professional Experience: Project engineer for El Paso Natural Gas
from June, 1978 until February, 1981. Process design engineer
for Phillips Petroleum from March, 1981 until January, 1985.